THE UNIVERSITY
of EDINBURGH

Proteomics of spindle checkpoint complexes and characterisation of novel interactors

Sjaak JA van der Sar

Dissertation presented for the degree of Doctor of Philosophy

Wellcome Trust Centre for Cell Biology, University of Edinburgh

2013

THE UNIVERSITY
of EDINBURGH

Declaration

I declare that the research presented here and this dissertation is all my own work, except where I acknowledge otherwise, and has not been submitted for any other degree or professional qualification.

Sjaak JA van der Sar

2013

Summary

The eukaryotic cell cycle is governed by molecular checkpoints that ensure genomic integrity and the faithful transmission of chromosomes to daughter cells. They inhibit the cycle until conditions prevail that guarantee accurate DNA duplication and chromosome segregation. Two major mechanisms are the 'spindle assembly checkpoint' and the 'DNA damage checkpoint'.

During pro-metaphase, the spindle checkpoint monitors the orientation process of chromatid pairs on the bipolar microtubule array nucleated by spindle pole bodies. In the yeasts *Schizosaccharomyces pombe* and *Saccharomyces cerevisiae*, six proteins are at the heart of spindle checkpoint function: Mad1, Mad2, Mad3, Bub1, Bub3 and Mph1/Mps1. The formation of spindle checkpoint complexes signals the presence of incorrect spindle microtubule attachments to kinetochores. These complexes cooperate to suppress the activity of the anaphase promoting complex (APC) and inhibit the onset of anaphase. By isolating these distinct complexes and analysing their composition by mass-spectrometry (MS) this work revealed several intriguing disparities between the two yeast species, and the way in which the Bub and Mad proteins cooperate to achieve inhibition. The 'mitotic checkpoint complex', which in *S.cerevisiae* consists of Mad2, Mad3, Bub3 and the APC activator Cdc20, was found to lack Bub3 in *S.pombe*. The *S.pombe* complex was shown to interact with the APC, but no stable interaction was found to be required in *S.cerevisiae* cells. And whereas Bub1 and Bub3 were found to form a complex with Mad1 in *S.cerevisiae*, in *S.pombe* they were shown to associate with Mad3 to form the 'BUB+ spindle checkpoint complex'.

In addition, MS analysis uncovered TAPAS: a novel *S.pombe* complex that was found to interact with the BUB+ complex and revealed to consist of Tfg3, Abo1 (gene product of *SPAC31G5.19*), Pob3 and Spt16. TAPAS mutant cells were shown to lose viability as a result of genotoxic stress, a phenotype that was surprisingly shared with *bub1*Δ and $bub1^{kd}$ 'kinase dead' mutants. Sensitivity of cells deficient in TAPAS or Bub1 did not appear to be due to the loss of DNA damage checkpoint or DNA replication checkpoint functions. Further examination revealed that Bub1 functions in the repair of DNA double strand breaks.

Taken together, this work demonstrates that even though the molecular components of the spindle checkpoint pathway are conserved, their regulatory connections have to some extent diverged through molecular evolution. This process not only rewired, but entwined two molecular processes that together safeguard the genetic heritage of cells.

Table of contents

Index of tables

Index of figures

List of abbreviations, including genes and protein complexes

A (‘DNA sequence’) ..... adenine
A (‘SI unit’) ..... Ampère
Å ..... Ångström
AAA (‘protein chemistry’) ..... ATPases associated with diverse cellular activities
ADE (‘ADE genes’) ..... adenine
ABO (‘ABO1 and 2 gene’) ..... ATPase bromodomain orthologue
ALP (‘ALP genes’) ..... altered polarity
ANCCA (‘ANCCA genes’) ..... AAA nuclear coregulator cancer-associated
AP (‘AP sites’) ..... apyrimidinic or apurinic
APC (‘APC genes and complex’) ..... anaphase promoting complex
ARK (‘ARK1 gene’) ..... aurora kinase
ATAD (‘ATAD genes’) ..... ATPase family, AAA domain containing
ATM (‘gene product’) ..... ataxia telangiectasia mutated
ATP ..... adenosine triphosphate
ATR (‘gene product’) ..... ataxia telangiectasia and Rad3-related protein
ATRIP (‘gene product’) ..... ATR interacting protein
B3i (‘protein chemistry’) ..... Bub3-interaction motif
BBC (‘protein complex’) ..... BubR1, Bub3 and Cdc20
BER (‘DNA damage repair’) ..... base excision repair
BRCA (‘BRCA genes’) ..... breast cancer
BRCT (‘protein chemistry’) ..... BRCA1 carboxy terminus
BSA ..... bovine serum albumin
BUB (‘BUB genes’) ..... budding uninhibited by benomyl
BUB (‘protein complex’) ..... Bub1 and Bub3
BUB+ (‘protein complex’) ..... Bub1, Bub3 and Mad3
BUBR (‘BUBR1 gene’) ..... BUB1 related
C (‘DNA sequence’) ..... cytosine
C (‘organic chemistry’) ..... carbon
C (‘°C’) ..... celcius
c (‘metric prefix’) ..... centi
CAK (‘CAK genes’) ..... CDK activating kinase
cal (‘thermodynamics’) ..... calories
CCT (‘CCT genes or protein complex’) ..... chaperonin containing T-complex
CDC (‘CDC genes’) ..... cell division cycle
CDH (‘CDH1 gene’) ..... CDC homologue
CDK (‘CDK genes’) ..... cyclin-dependent kinase
CDS (‘CDS1 gene’) ..... checking DNA synthesis
CHK (‘CHK genes’) ..... checkpoint
CKI (‘CKI genes’) ..... CDK inhibitor
CLB (‘CLB genes’) ..... cyclin B
CLN (‘CLN genes’) ..... cyclin
CPT (‘chemical compound’) ..... camptothecin
CRB (‘CRB2 gene’) ..... cut5-repeat binding
CSK (‘CSK genes’) ..... C-Src kinase

CUE (‘protein chemistry’).....coupling of ubiquitin conjugation to endoplasmatic reticulum degradation
CUEDC (‘CUEDC2 gene’).....CUE domain-containing
CUT (‘CUT genes’) ..... cut phenotype
D (‘D box, protein chemistry)..... destruction
Da.....Dalton
DAM (‘DAM1 gene’)..... Duo1 and Mps1 binding
DAPI (‘chemical compound’) .....4′,6-diamidino-2-phenylindole
DASH (‘protein complex’) .....Dad1, Dad3, Dam1, Duo1, Ask1, Spc19, Spc34 and Hsk1
DIS (‘DIS genes’)..... defective in sister chromatid disjoining
DNA.....deoxyribonucleic acid
dATP.....deoxyadenosine triphosphate
dCTP.....deoxycytidine triphosphate
dGTP .....deoxyguanosine triphosphate
dNTP ..... dATP, dTTP, dGTP and dCTP deoxyribonucleotides
dTTP .....deoxythymidine triphosphate
DSB (‘DNA damage’) ..... double strand break
DTT (‘chemical compound’)..... dithiothreitol
EB (‘EB1 gene’).....end binding
EDTA (‘chemical compound’).....ethylene diamine tetraacetic acid
EGTA (‘chemical compound’).....ethylene glycol tetraacetic acid
ESP (‘ESP1 gene’) ..... extra spindle poles
FACT (‘protein complex’) .....facilitates chromatin transcription
FHA (‘protein chemistry).....forkhead-associated
FOA (‘chemical compound’) .....5-fluoroorotic acid
FRAP (‘technique’) ..... fluorescence recovery after photobleaching
g (‘centrifugation’).....standard gravity
g (‘SI unit’)..... gramme
G (‘DNA sequence’).....guanine
G (‘G1 and G2 phase’).....gap
G (‘thermodynamics) .....Gibbs energy
GAL (‘GAL genes’) .....galactose
GFP.....green fluorescent protein
GLC (‘GLC7 gene’) ..... glycogen
GLEBS (‘protein chemistry’)..... GLE2-binding sequence
Gy (‘SI unit’) ..... Gray
H (‘organic chemistry’)..... hydrogen
HEPES (‘chemical compound’).....2-[4-(2-hydroxyethyl)piperazin-1-yl]ethanesulfonic acid
H (‘H1, H2A, H2B, H3 and H4’).....histone
HIS (‘HIS genes’).....histidine
HPLC (‘technique’) .....high-performance liquid chromatography
hr..... hour(s)
HU (‘chemical compound’) ..... hydroxyurea
IgG.....immunoglobulin G
IPL (‘IPL1 gene’).....increase in ploidy
J (‘thermodynamics’) ..... Joule
k (‘metric prefix’) .....kilo

KAP (‘KAP genes’) ..... karyopherin
kb ..... kilobase
K_d ..... dissociation constant
KEN (‘KEN box, protein chemistry’) ..... lysine, glutamate & asparagine
KLP (‘KLP genes’) ..... kinesin-like protein
KMN ..... KNL1, MIS12 and NDC80
KNL (‘KNL1 gene’) ..... kinetochore null
L (‘SI unit’) ..... litre
LEU (‘LEU genes’) ..... leucine
LID (‘LID1 gene’) ..... lethal in *dim1-35*
m (‘metric prefix’) ..... milli
m (‘SI unit’) ..... metre
M (‘SI unit’) ..... molar
M (‘M phase’) ..... mitotic
µ (‘metric prefix’) ..... micro
MAD (‘MAD genes’) ..... mitotic arrest-deficient
MAD (‘protein complex’) ..... Mad1 and Mad2
Mb ..... megabase
MBB (‘protein complex’) ..... Mad1, Bub1 and Bub3
MCC (‘protein complex’) ..... mitotic checkpoint complex
MEC (‘MEC1 gene’) ..... mitosis entry checkpoint
MLP (‘MLP genes’) ..... myosin-like protein
MMS (‘chemical compound’) ..... methyl methanesulfonate
MND (‘MND2 gene’) ..... meiotic nuclear division
MPH (‘MPH1 gene’) ..... MPS1 pombe homologue
MPF ..... maturation promoting factor
MPS (‘MPS1 gene) ..... monopolar spindles
MRC (‘MRC1 gene’) ..... mediator of the replication checkpoint
MRN (‘protein complex’) ..... Mre1, Rad50 and Nbs1
MS (‘technique’) ..... mass-spectrometry
MudPIT (‘technique’) ..... multidimensional protein identification technology
MVA ..... mosaic variegated aneuploidy
N (‘organic chemistry’) ..... nitrogen
n (‘metric prefix’) ..... nano
NDA (‘NDA3 gene’) ..... nuclear division arrest
NDC (‘NDC genes and complex’) ..... nuclear division cycle
NER (‘DNA damage repair’) ..... nucleotide excision repair
NHEJ (‘DNA damage repair’) ..... non-homologous end joining
NMR (‘technique’) ..... nuclear magnetic resonance
nmt (‘nmt promoters’) ..... no messenger in thyamine
NUF (‘NUF2 gene’) ..... nuclear filament containing
NUP (‘NUP genes’) ..... nuclear pore
O (‘organic chemistry’) ..... oxygen
OD (‘OD_{600}’) ..... optical density
P (‘organic chemistry’) ..... phosphorus
P (‘protein phosphorylation’) ..... phosphate group

PAGE (‘technique’) ..... polyacrylamide gel electrophoresis
PAR ..... poly-ADP-ribosylation
PBS ..... phosphate buffered saline
PCNA (‘protein complex’) ..... proliferating cell nuclear antigen
PCR (‘technique’) ..... polymerase chain reaction
PDS (‘PDS1 gene’) ..... precocious dissociation of sisters
PEG (‘chemical compound’) ..... polyethylene glycol
PIKK (‘protein chemistry’) ..... phosphatidyl inositol 3-kinase-related (PI3K) kinase
PLK (‘PLK1 gene’) ..... polo-like kinase
PLO (PLO1 gene’) ..... polo kinase
PMG (‘medium’) ..... pombe minimal growth
POB (‘POB3 gene’) ..... polymerase one binding
PP (‘PP1 and PP2 phosphatase complexes’) ..... protein phosphatase
PRR (‘DNA damage repair’) ..... post-replication repair
R (‘thermodynamics’) ..... gas constant
RAD (‘RAD genes’) ..... radiation
RC (‘protein complex’) ..... replication complex
RFC (‘RFC genes and complex’) ..... replication fork complex
RFP ..... red fluorescent protein
RHP (‘RHP genes’) ..... RAD homologue pombe
RNA ..... ribonucleic acid
RNR (‘RNR genes and complex’) ..... ribonucleotide reductase
RPA (‘RPA genes and complex’) ..... replication protein A
rRNA ..... ribosomal RNA
RTT (‘RTT genes’) ..... regulation of Ty1 transposition
RZZ (‘protein complex’) ..... Rod, Zwilch and Zw10
S (‘organic chemistry’) ..... sulphur
S (‘S phase’) ..... synthesis
s ..... seconds
SCF (‘protein complex’) ..... Skp, Cullin and F-box
SDS (‘chemical compound’) ..... sodium dodecyl sulfate
SILAC (‘technique’) ..... stable isotope labeling by amino acids in cell culture
SGO (‘SGO genes’) ..... shugoshin
SKA (‘SKA genes and complex’) ..... spindle and kinetochore-associated
SLP (‘SLP1 gene’) ..... sleepy
SPA (‘medium’) ..... synthetic sporulation agar
SPC (‘SPC genes’) ..... spindle pole component
SPD (‘SPD1 gene’) ..... S phase delayed
SPT (‘SPT16 gene’) ..... suppressor of Ty
SRW (‘SRW1 gene’) ..... suppressor of rad/wee1
SSB (‘DNA damage’) ..... single strand break
STY (‘protein phosphorylation’) ..... serine, threonine, tyrosine
T (‘DNA sequence’) ..... thymine
T ..... temperature
t ..... time
TAF (‘TAF genes’) ..... TBP-associated factors

TAPAS (‘protein complex’) ..... Tfg3, Abo1, Pob3 and Spt16
TBP (‘gene product’) ..... TATA-binding protein
TE ..... TRIS-EDTA
TEL (‘TEL1 gene’) ..... telomere
TFG (‘TFG3 gene’) ..... transcription factor g
TPR (‘protein chemistry’) ..... tetratricopeptide repeat
TRIS (‘chemical compound’) ..... tris(hydroxymethyl)aminomethane
TRP (‘TRP genes’) ..... tryptophan
TUB (‘TUB genes’) ..... tubulin
U (‘DNA sequence’) ..... uracil
Ub (‘Ub moiety’) ..... ubiquitin
URA (‘URA genes’) ..... uracil
UTR ..... untranslated region
UV ..... ultra violet
V (‘SI unit’) ..... Volt
WD (‘WD40 fold, protein chemistry) ..... tryptophan aspartic acid
XP (‘XP genes’) ..... xeroderma pigmentosum
YEATS (‘protein biochemistry’) ..... YAF9, ENL, AF9, TAF14, SAS5
YES (‘medium’) ..... yeast extract supplemented
YPDA (‘medium’) ..... yeast peptone dextrose adenine
YTA (‘YTA genes’) ..... yeast Tat-binding analogue

Foreword and acknowledgements

The two pictures on this page illustrate, in at least one aspect, the very extremities of the Eukaryota domain of life. The worker ant of the Australian species *Myrmecia pilosula* is a sterile and haploid male, whose cells contain only a single chromosome (Crosland & Crozier 1986). On the other hand, diploid cells of the adder's tongue fern *Ophioglossum reticulatum* encompass no fewer than 1,260 chromosomes, the highest count of any known living eukaryote (Britton 1974). During mitosis, despite the huge difference in chromosome numbers cells of both species segregate their chromosomes with equal high fidelity. This remarkable feat of nature is attributed to the spindle checkpoint, a molecular device that is extremely well-conserved from yeast to man. It is this mechanism that is the very topic of my doctoral research.

Each cell of every organism represents offspring safeguarding an unbroken lineage of ancestral DNA. Through the course of early evolution molecular mechanisms evolved that drive cellular proliferation (the Cdk^{cyclin} oscillator), preserve genomic integrity (the DNA damage response) and ensure accurate chromosome replication (the DNA replication checkpoint) and segregation (the spindle checkpoint).

The biological cell is under continuous assault of both endogenous and exogenous insults that interfere with cellular processes. Many species produce chemical compounds to contest rival organisms in their competition for natural resources. Thus "chemical warfare" has given rise to potent poisons and sophisticated toxins that are at the same time a rich source for pharmacological discovery. Some of these naturally occurring substances directly target the cell's ability to reproduce by for instance inhibiting Cdk^{cyclin} (Fischer & Lane 2000), by

interfering with chromosome segregation (Fojo & Giannakakou 2000) or by tampering with its genetic information (Clark 1976).

Simultaneously, the unremitting process of molecular evolution and adaptation actively shapes and moulds the molecular mechanisms in place to combat chemical interference that best serves a species survival to uniquely suit its habitat and niche. For this reasons molecular mechanisms diverge in the face of novel challenges and can take upon them new tasks or even provide redundancy if other mechanisms fail. This work presented here provides compelling evidence that the spindle checkpoint mechanism, too, is marked by the process of divergent evolution.

My research work into spindle checkpoint functioning utilises two of the most formidable model-organisms: the fission yeast *Schizosaccharomyces pombe* and the budding 'bread and beer' yeast *Saccharomyces cerevisiae*. They are generally considered as closely related species, even though their last common ancestor is estimated to have lived over a billion years ago (Hedges 2002), well into the Precambrian and quite some time before multicellular organisms emerged. However, many genes are functionally conserved between these two yeast species. When this is the case, this report will mention orthologous gene products 'in one go': proteins from the former yeast are given first followed by a forward slash and its closest orthologue in the latter yeast (i.e. the APC activator Slp1/Cdc20).

I would like to take this opportunity to thank Kevin Hardwick for his substantial support and advice in my PhD studies, my committee members Robin Allshire, Peter Fantes and Juri Rappsilber for their help and patience in achieving my aims and lab members past and present for their valuable input. I am especially indebted to Kostas Paraskevopoulos and Victor Bolanos-Garcia for their help and insight with protein structure modelling, Alicja Sochaj for creating Mad3 mutants and Karen May for advice and assistance with fluorescent microscopy.

This work could not have come to fruition without the cherished company and support from my family and loved-ones and I dedicate this work to the memory of Marina Jacomina Vos-Wesdorp (1919-2010).

Sjaak van der Sar

1 Introduction

1.1 The eukaryotic cell cycle

The proliferation of cells is a testament and fundamental to the success of life on Earth. A eukaryotic cell reproduces through a sequence of events commonly known as the mitotic cell cycle (Morgan 2006). It enables the transmission of genomic information that is contained in the nucleus by duplicating all chromosomes and distributing them equally to two daughter cells. The two major phases of the canonical cell cycle are S and M phase, which are preceded respectively by G1 and G2 when cells grow and prepare for entry into the next phase. S phase endows a cell with two identical sets of chromosomes, each chromosome and its faithful duplicate existing as a pair of sister-chromatids tightly bound by cohesin ring molecules as well as DNA catenation (Uhlmann 2003, Toyoda & Yanagida 2006). The actual nuclear and cellular division takes place in M phase, which encompasses both mitosis and cytokinesis: sister-chromatid cohesion is lost, and individual chromosomes are equally divided over the two daughter nuclei ahead of cell cleavage.

Mitosis is generally divided into five consecutive stages: prophase, prometaphase, metaphase, anaphase and telophase[1]. The spindle pole, which in a metazoan cell exists as a pair of centrioles called the centrosome, duplicates in S phase whilst DNA replication takes place or later in G2. In the case of metazoan mitosis the firmly paired sister-chromatids condense during prophase. At this time, the spindle poles begin to separate and nucleate microtubules; the bipolar microtubule array of the mitotic spindle starts to take shape (Adams & Kilmartin 2000, Tanaka *et al.* 2005a). The nuclear envelope breaks down in prometaphase and spindle microtubules at random seek out and capture each sister-chromatid by attaching to its kinetochore, a large protein structure that assembles on chromatin of centromeric DNA (Figure 1).

Chromosome biorientation is accomplished in metaphase: both kinetochores of each chromatid pair will have formed spindle attachments to opposite spindle poles, which results in chromosome alignment along the metaphase plate, a central region between the two poles (Tanaka 2005). As at this stage DNA decatenation has taken place, cleavage of the cohesin rings by separase during anaphase leads to the complete loss of sister-chromatid cohesion

[1] In many species strict distinctions are often difficult to make owing inevitably to genetic divergence in the course of eukaryotic evolution over several billions of years. For this reason, several – unsuccessful – attempts have been made to redefine mitotic phase terminology within molecular rather than cellular and nuclear morphological constraints (Pines & Rieder 2001).

(Nasmyth 1999). Chromosome dissolution (or 'disjunction') is followed by segregation: the identical genomic complements move towards the poles, one in each of the two halves of the dividing cell. Once the spindle apparatus disassembles and the contractile actomyosin ring begins to form in telophase the nuclear membranes are rebuilt around the decondensing chromosomes and will eventually envelope each of the two new nuclei. Finally, during cytokinesis the contractile ring will cleave the cell in two (Green *et al.* 2012, Howell & Lew 2012), so that each daughter cell will contain one nucleus and one spindle pole.

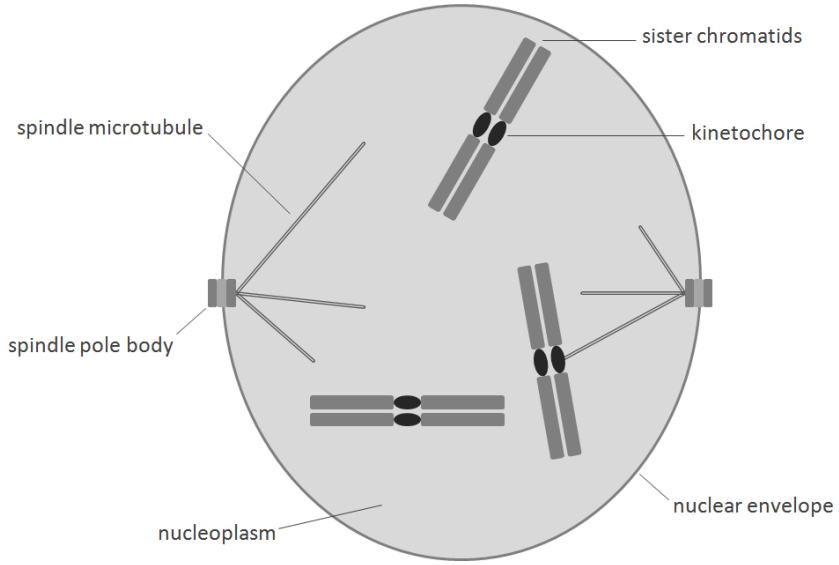

Figure 1: A highly schematic diagram of a yeast prometaphase nucleus with three chromosomes and mitotic structures as indicated. Each chromosome consists of a cohesed sister-chromatid pair with 'arms' extending from its centromeres on which the kinetochore is assembled. The mitotic spindle starts to form as the tripartite spindle pole bodies (the fungal equivalent of the metazoan centrosome) nucleate novel microtubules and seek out kinetochores. Note that the yeast mitotic spindle apparatus forms inside the nucleus as the nuclear envelope remains intact throughout cell division.

Although the nuclear envelope fully dismantles in vertebrate cells undergoing mitosis, in other metazoan cells this happens only partially and not at all in some fungal cells. Genomic DNA analysis of *Ascomycota* species provides evidence for a common ancestor of *Saccharomyces cerevisiae* and *Schizosaccharomyces pombe* that could have lived as long ago as 1.1 billion years in Precambrian times (Heckman *et al.* 2001, Hedges 2002), although a conservative estimate points to a Carboniferous ancestor of some 330 million years ago[2] (Sipiczki 2000).

[2] Species related to *Saccharomyces cerevisiae* in order of distance: *Candida albicans* < *Yarrowia lipolytica* < *Neurospora crassa* & *Aspergillus nidulans* < *Schizosaccharomyces pombe* < *Agaricus bisporus* < animals < plants (Hedges 2002).

Both yeast undergo ‘closed mitosis’ i.e. the nuclear membrane remains intact throughout the cell cycle (De Souza & Osmani 2007).

The mitotic spindle poles, named spindle pole bodies in yeast, are physiologically distinct but functionally equivalent to metazoan centrosomes (Adams & Kilmartin 2000). They accumulate γ-tubulin ring complexes and organise nuclear and cytoplasmic microtubule formation (Sawin & Tran 2006). In *S.cerevisiae*, the ‘microtubule organising centre’ is a tripartite structure consisting of an inner, central and outer plaque adjacent to a half-bridge that assembles the new spindle pole body. Throughout its cell cycle, the spindle pole body remains embedded in the nuclear membrane. There, it closely associates with kinetochores, which suggests the existence of persistent microtubule connections that are only temporarily interrupted to allow replication of centromeric DNA and the assembly of functional kinetochores (Winey & O'Toole 2001, Indjeian *et al.* 2005, Kitamura *et al.* 2007, Liu *et al.* 2008). Spindle pole duplication is completed in late G1 and separation starts to take place in S phase. Detailed microscopy studies of *S.pombe* interphase pole bodies suggest that they are largely bipartite assemblies: a filamentous, trans-nuclear envelope structure connects a central cytoplasmic domain with a much smaller nuclear component (Ding *et al.* 1997, Tamm *et al.* 2011). It duplicates when cells enter S phase and following maturation and separation complete nuclear membrane fenestration takes place when cells enter mitosis (Ding *et al.* 1997, Uzawa *et al.* 2004).

The ovoid-shaped cells of *S.cerevisiae* divide by bud formation (hence also known as ‘budding yeast’), have a relatively long G1, and, unlike all other studied eukaryotes, lack a clearly defined G2 phase as DNA replication has not yet fully completed when cells enter mitosis. Whereas a haploid *S.cerevisiae* cell contains 16 chromosomes (approximately 12.5 Mb with around 5,770 protein encoding genes), *S.pombe* genes are laid out on just three chromosomes (13.8 Mb, 4,970 genes). The latter yeast is rod-shaped, grows by elongation at the two tips and divides by septation and medial fission (i.e. ‘fission yeast’). It exhibits a characteristically short G1 and does not complete cytokinesis until S phase of the following cell cycle (Russell & Nurse 1986b, Forsburg & Nurse 1991). Control of cell size occurs in *S.cerevisiae* G1 and *S.pombe* G2 (Turner *et al.* 2012).

1.2 Cdk and APC activities control the eukaryotic cell cycle

The purpose of each mitotic cell division is to provide viable and healthy progeny and for that reason the eukaryotic cell cycle is a highly orchestrated sequence of discrete yet interdependent molecular events that are exceptionally well-conserved. Comparative

genomics and a wide variety of model organisms have greatly expanded knowledge of cell cycle regulation since the original isolation and characterisation of key regulators of the eukaryotic cell cycle in the 1970s through the Nobel prize-winning work of Lee Hartwell (in the yeast *S.cerevisiae*) (Hartwell *et al.* 1974), Paul Nurse (in the yeast *S.pombe*) (Nurse & Thuriaux 1980) and Tim Hunt (in eggs of the sea urchin *Arbacia punctulata* and bivalve mollusc *Spisula solidissima*) (Evans *et al.* 1983).

The mitotic cell cycle is characterised by the rise and fall of two activities that are carefully regulated (Figure 2): that of the cyclin dependent kinase (Cdk) and the anaphase promoting complex (APC). Both yeast species contain a single Cdk responsible for controlling cell cycle progression. Named Cdc2/Cdc28[3], they were discovered in the Nurse and Hartwell laboratories in screens for temperature-sensitive mutants affecting the cell division cycle (hence termed 'cdc' mutants) (Humphrey & Pearce 2005, Bloom & Cross 2007). They are remarkably well-conserved proteins, illustrated by the fact that yeast cells proliferate as normal when the Cdk-coding gene is replaced with their human counterpart (Lee & Nurse 1987).

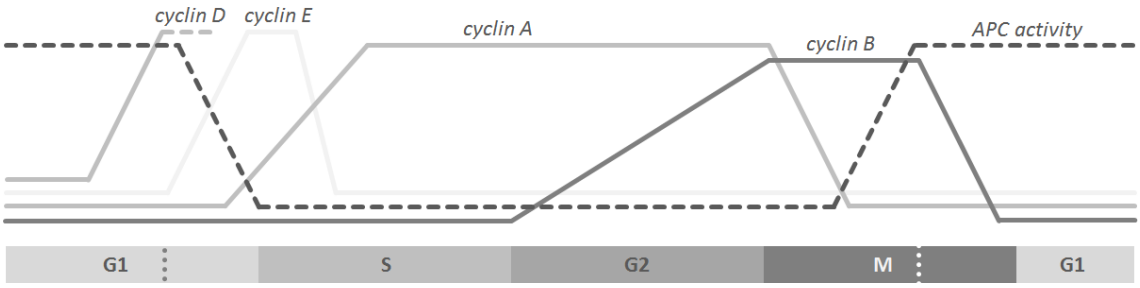

Figure 2: Schematic diagram of the levels of the cyclin Cdk-activators and APC activity during a general metazoan cell cycle. Molecular levels of the three major cyclins oscillate and the 'cyclin dependent kinase' Cdk is active as long as one cyclin is present. In M phase, the rising activity of the APC ubiquitin E3 ligase complex will first target cyclin A and, at the onset of anaphase, cyclin B for destruction. Cdk activity ceases when the latter cyclin is degraded and will not return until the cell commits to a new round of cell division (termed 'restriction point' in metazoa and 'start' in yeast) in G1 that coincides with diminishing APC activities and increase in cyclin D levels. Note that in metazoa, the S phase cyclins E and A are bound to Cdk2, whereas the mitotic cyclins A and B associate with Cdk1. In *S.pombe* and *S.cerevisiae*, Cdc2/Cdc28 Cdk binds the B-type cyclins that characterise both S and M phase. Freely adapted from 'The cell cycle: principles of control' (Morgan 2006).

The importance of Cdk activity oscillation is neatly illustrated by the assembly of prereplicative complexes onto DNA in a process termed 'licensing', which can only occur in the absence of Cdk activity. Cdk activation inhibits the formation of these complexes, but stimulates

[3] In this work, orthologous gene products from *S.pombe* and *S.cerevisiae* are noted as Cdc2/Cdc28, where the former is the *S.pombe* homologue and the latter that of *S.cerevisiae*.

downstream processes such as the recruitment of replication enzymes. Thus a single round of genome replication is determined by a period of low Cdk activity in G1 followed by a period of high activity in S phase (Zachariae & Nasmyth 1999).

As the cell cycle progresses Cdk activity is modulated by positive regulators called cyclins that crucially confer Cdk substrate specificity. Generally, each stage of the cell cycle is governed by a unique cyclin in complex with Cdk (denoted here as Cdk^{cyclin}) as different cyclins are produced at different cell cycle stages (Bloom & Cross 2007, Jackson 2008). When a cell cycle event is successfully accomplished the timely degradation of phase-specific cyclins promotes new Cdk^{cyclin} activities. These cyclin oscillations effectively make each phase a discrete and irreversible event (Murray & Kirschner 1989, Tyson & Novak 2008).

Environmental or physiological cues regulate G1 Cdk activity of cells by modulating cyclin (metazoan cyclin D, yeast Puc1/Cln3) levels. If nutrients are abundant and other conditions are favourable, the rising Cdk^{cyclin} activity drives cells past a point of no return, called the metazoan 'restriction point' or simply 'start' in yeast, when they commit to a new cell cycle (Morgan 2006). Cdk inhibitors such as Rum1/Sic1 are earmarked for proteolysis by the SCF complex, which consists of Skp1, cullin and a F box protein (Vodermaier 2004).

The SCF and APC complexes are the two major E3 ubiquitin ligases driving the cell cycle by targeting regulators for destruction (Figure 3). SCF ubiquitination is regulated by phosphorylation of its substrates that increases their affinity for the F box protein, whereas APC activity is positively regulated by co-factors called Slp1/Cdc20 and Srw1/Cdh1 (also called Ste9/Hct1) in yeast. These activators bind APC substrates directly through recognition of so-called destruction motifs or degrons. KEN box degrons are tri-peptide motifs that are preferentially but not exclusively targeted by the $APC^{Srw1/Cdh1}$ complex, whereas D box degrons (consensus amino acid sequence RxxLxxx[EDNQ], in which 'x' indicates any amino acid) are thought to be mainly targeted by $APC^{Slp1/Cdc20}$ (Pfleger & Kirschner 2000). Many APC substrates contain multiple degrons and both KEN and D box degrons are present in some M phase cyclins[4].

[4] Two other metazoan degrons have been identified: the A box identified in aurora A kinase (Littlepage & Ruderman 2002) and the GExN box of the Kid kinesin (Castro *et al.* 2003).

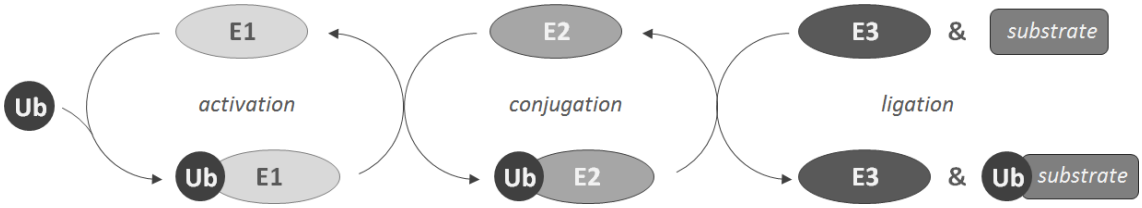

Figure 3: Ubiquitination of a substrate requires an E1 ubiquitin activating enzyme, an E2 ubiquitin conjugating enzyme and, finally, the activity of an E3 ubiquitin ligating enzyme that transfers the ubiquitin (Ub) moiety onto a substrate. The completion of one ubiquitination cycle results in a mono-ubiquitinated substrate and poly-ubiquitination can be achieved by numerous repetitions of the cycle.

Both the APC and Slp1/Cdc20 are substrates of Cdk^{cyclin} and their phosphorylation is essential priming the $APC^{Slp1/Cdc20}$ for activation (Peters 2002, Castro *et al.* 2005, Peters 2006, Barford 2011). Once activated at the metaphase to anaphase transition it ubiquitinates securin (Cut2/Pds1 in yeast), which, as a consequence, is degraded by the proteasome. This leads to activation of separase (Cut1/Esp1) cleaving the cohesin complexes and allowing sister-chromatid separation to take place (Figure 4). $APC^{Slp1/Cdc20}$ provides negative feedback by additionally targeting M phase cyclins (of which cyclin B is the most important), which eventually results in Cdk inactivation and the *de facto* dephosphorylation of Cdk^{cyclin} substrates by phosphatases such as Clp1 (or Flp1)/Cdc14 (Zachariae & Nasmyth 1999). As the Cdk activity diminishes, so will the activity of $APC^{Slp1/Cdc20}$, which is replaced by $APC^{Srw1/Cdh1}$ in late mitosis. Srw1/Cdh1 does not require Cdk^{cyclin} phosphorylation and $APC^{Srw1/Cdh1}$ thus ultimately targets Slp1/Cdc20 for destruction (Figure 5b on page 8).

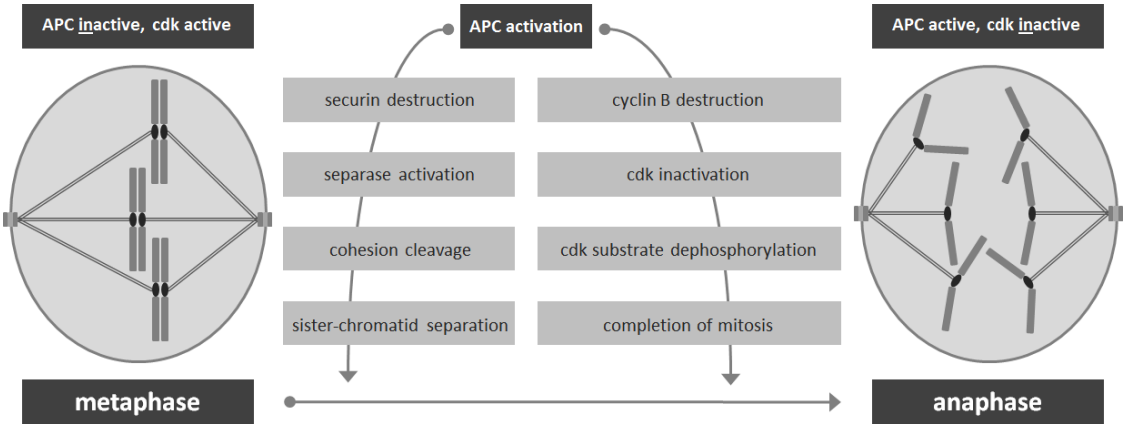

Figure 4: A diagram illustrating key molecular events at the transition of metaphase to anaphase. Refer to Figure 1 for a key to the yeast nucleus drawings. Freely adapted from 'The cell cycle: principles of control' (Morgan 2006).

Since the early 1970s, the biochemical dissection of oocyte maturation (Masui & Markert 1971) in the frogs *Xenopus laevis* and *Rana pipiens* has been particularly fruitful in shedding

light on the behaviour of the Cdk^{cyclin} oscillator that is driven by an irreversible, bistable[5] trigger or switch. *In vitro* micro-injection of some cytoplasm from meiotic metaphase II eggs into that of eggs arrested in G2 with low levels of Cdk activity triggers completion of meiosis I, a process that *in situ* would require exposure to progesterone hormones secreted by follicle cells. This cytoplasmic activity was termed 'maturation promoting factor' (MPF), eventually identified as an active Cdk^{cyclin} complex of Cdk1 (originally named Cdc2) and a mitotic cyclin (generically termed cyclin B) (Lohka *et al.* 1988, Gautier *et al.* 1990, Solomon *et al.* 1990).

The biochemical nature of this Cdk switch was uncovered using extracts of frog oocytes. The activity of Cdk1 is two-pronged: it can inhibit its inhibitors (the Wee1 kinases: Wee1/Swe1, Mik1, human Myt1) (Tang *et al.* 1993b) and activate its activator (the Cdc25/Mih1 phosphatase) (Kumagai & Dunphy 1992), but crucially it can also activate another inhibitor (the $APC^{Slp1/Cdc20}$) (Zachariae & Nasmyth 1999). Thus a powerful combination of positive and negative feedback results in bistability of Cdk activity that requires activation of $APC^{Slp1/Cdc20}$ to trigger the switch between states of high and low kinase activity (Murray *et al.* 1989, Felix *et al.* 1990, Thron 1996, Pomerening *et al.* 2003).

Studies in yeast revealed the finely tuned and multiplex nature of Cdk^{cyclin} (Figure 5a). The activity of the Cdk kinase Cdc2/Cdc28 is inhibited by the Wee1/Swe1 kinase that targets tyrosine residue 15 within the activation loop of the kinase domain and prevents entry into mitosis (Gould & Nurse 1989, Den Haese *et al.* 1995). This phosphorylated residue is a substrate of the Cdc25/Mih1 phosphatase that thus stimulates Cdk activity (Russell & Nurse 1986a), a remarkably well-conserved regulatory event for entry in mitosis. HeLa cell investigations provided evidence that the Cdc25 phosphatase activity is positively regulated by Cdk kinase activity itself (Galaktionov & Beach 1991, Millar & Russell 1992). In addition, experiments using *Xenopus* egg extracts showed that further Cdc25 activation is provided by the polo-like kinase activity of Plx1 (human Plk1 and Plo1/Cdc5 in yeast) (Kumagai & Dunphy 1996, van Vugt & Medema 2005). Activity of the *S.cerevisiae* polo kinase Cdc5 also may inhibit Wee1/Swe1 (Tang *et al.* 1993a, Bartholomew *et al.* 2001).

[5] A bistable system toggles between two discrete alternative states, e.g. 'on' and 'off', without being able to rest in intermediate states.

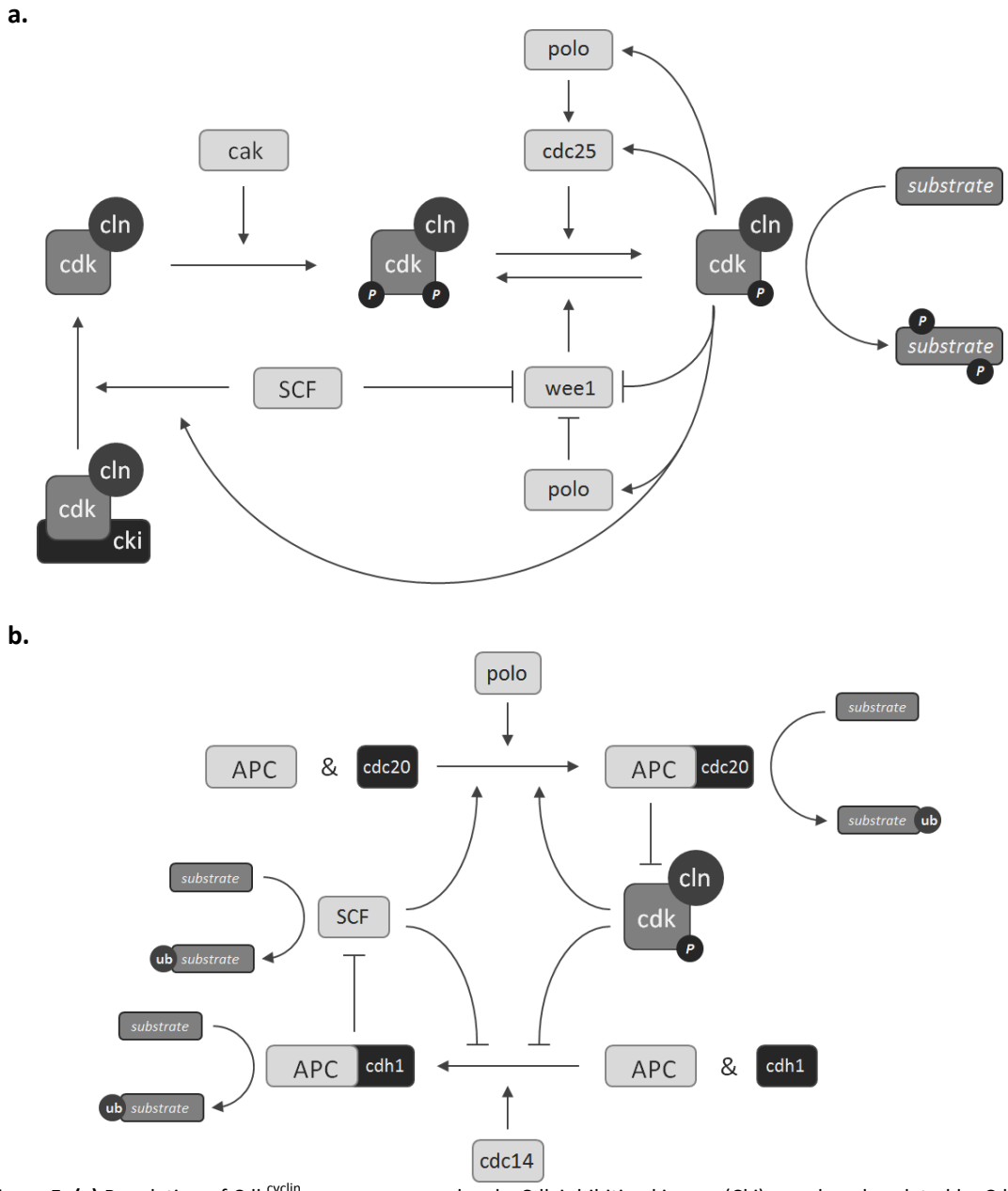

Figure 5: (a) Regulation of Cdk^{cyclin} occurs on many levels. Cdk inhibiting kinases (Cki) are phosphorylated by Cdk^{cyclin} and subsequently targeted for degradation by the SCF E3 ubiquitin ligase complex, after which Cak kinase phosphorylation is required for activation of Cdk^{cyclin}. However, phosphorylation of the catalytic centre by the Wee1 kinase inhibits Cdk^{cyclin}, an activity antagonised by the Cdc25 phosphatase. Further activation of Cdk^{cyclin} is achieved by positive feedback: its rising activity inhibits Wee1 and stimulates Cdc25, activities that are supported by polo kinase and SCF activities. **(b)** Multi-layered regulation of the APC and SCF E3 ubiquitin ligase complexes by polo-like kinase, Cdk^{cyclin} kinase and Cdc14 phosphatase action. For clarity, the mutual APC^{Cdc20} and APC^{Cdh1} inhibition and the Cdk^{cyclin} inhibition by the latter are not drawn.

The cyclins are described in four classes that are more or less specific to cell cycle phases (Morgan 2006). Cdk activity in S phase occurs through binding of cyclin A in metazoan cells, Clb5 and 6 in *S.cerevisiae* and Cig1 and 2 in *S.pombe*. The M phase Cdk binds cyclin B in

metazoa, Clb2 and 3 in *S.cerevisiae* and Cdc13 in *S.pombe*. The G1 cyclins are metazoan cyclin D, *S.cerevisiae* Cln3 and *S.pombe* Puc1. Lastly, the G1/S cyclins are metazoan cyclin E and *S.cerevisiae* Cln1 and Cln2.

Not surprisingly, Cdk kinases are regulated at many levels. In all eukaryotes, its phosphorylation by the 'Cdk activating kinase' (Cak) is essential for Cdk activity and results in displacement of the inhibitory T-loop from the kinase domain (Kaldis 1999). Some Cak proteins themselves possess Cdk activities that in turn depend on T-loop kinase activation. *S.pombe* has two partially redundant Cak factors, Csk1 and the Mcs6 Cdk complex, and *S.cerevisiae* Cak1 and the Kin28 Cdk complex (Liu & Kipreos 2000, Humphrey & Pearce 2005). Cdk kinase activity can be inhibited by the cyclin-dependent binding of Cdk inhibitor proteins (Cki), which are thought to act through active site substrate restriction (Pavletich 1999). In *S.pombe* Rum1 inhibits $Cdc2^{Cig2}$ and $Cdc2^{Cdc13}$ in G1 to prevent premature cell cycle progression (Forsburg & Nurse 1991, Humphrey & Pearce 2005). In *S.cerevisiae* Sic1 inhibits $Cdc28^{Clb2\&5}$ to prevent premature S phase entry and Far1 inhibits $Cdc28^{Cln2}$ in G1 during the α-factor pheromone response. Cdk substrate binding is promoted by Cks protein factors such as *S.pombe* Suc1 and *S.cerevisiae* Cks1 (Morris *et al.* 2003).

1.3 Checkpoints safeguard genome stability by governing transitions of cell cycle phases

Eukaryotic cells employ molecular mechanisms that prevent aneuploidy and promote high-fidelity transmission of the genetic material. Prior to cell cycle progression, the correct completion of critical events is assessed and a response is instigated when potentially detrimental problems arise. Until such liabilities are resolved, these 'checkpoints' are able to arrest the cell cycle by for instance inhibiting Cdk^{cyclin} or $APC^{Slp1/Cdc20}$ activity (Tyson & Novak 2008). Collectively, checkpoints ensure faithful DNA replication and equal chromosome segregation to daughter cells and are thus essential for the well-being of organisms and the long-term survival of a species.

The concept of checkpoints as cell cycle surveillance mechanisms was initially noted and described by Ted Weinert and Lee Hartwell (Hartwell & Weinert 1989). They studied radiation sensitive ('rad') *S.cerevisiae* Rad9 mutants that failed to block cell cycle progression when DNA damage occurs due to UV irradiation (Weinert & Hartwell 1988). This work led to the characterisation of the DNA damage checkpoint (see Figure 6; also called the 'DNA integrity checkpoint or 'DNA checkpoint' for short) that regulates the G1 to S and the G2 to M

transition[6] (Harrison & Haber 2006, Jeggo & Lobrich 2006). In general terms, this checkpoint inhibits cell cycle progression when DNA lesions are detected by preventing the Cdc25/Mih1 phosphatase from targeting the kinase activation loop of Cdc2/Cdc28 that is phosphorylated by the Cdk inhibitors Wee1/Swe1 and Mik1 (Rhind *et al.* 1997, Sanchez *et al.* 1997).

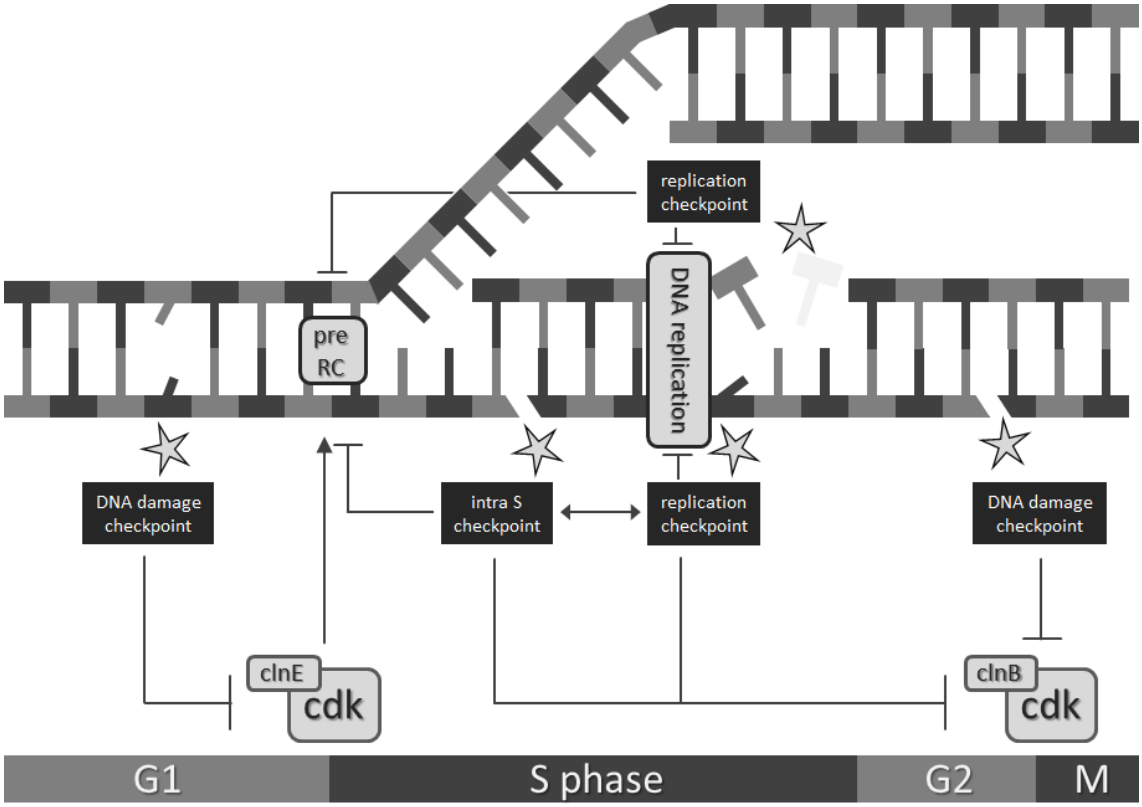

Figure 6: Several checkpoints ensure the integrity of DNA and faithful replication of genetic material. The DNA damage checkpoint acts to inhibit entry into S or M phase in the presence of DNA lesions by inhibiting Cdk^{cyclin} complexes. When such lesions occur during S phase, the replication-independent intra-S checkpoint slows DNA replication by preventing pre-replication complexes (pre RC) at origins from firing and slowing down replication forks. The replication checkpoint prevents mitosis in response to unreplicated DNA and forks that have stalled due to encountering replication blocks such as nucleotide insufficiencies and DNA damage. The intra-S checkpoint and replication checkpoint response partially overlap and numerous components are shared.

In S phase, the DNA damage checkpoint slows or prevents DNA replication in the presence of DNA lesions in a process that is referred to as the replication-independent 'intra-S checkpoint' (or 'S phase DNA damage checkpoint') (Bartek *et al.* 2004), which shares some of its molecular components with the 'DNA replication checkpoint' (sometimes referred to as the 'replication-

[6] *S.cerevisiae* is unique in that the S and M phase seem to overlap and the DNA damage checkpoint arrests cells in metaphase in response to DNA damage, not at the transition of G2 to M. In contrast, *S.pombe* cells spend most of their time in G2 phase, but their G1 is not a particularly well-defined molecular transition. Thus DNA lesions that either induce the intra-S or G2-M DNA damage checkpoint as the G1-S transition does not appear to be controlled by a damage checkpoint (Krohn *et al.* 2008).

dependent intra-S checkpoint') that acts when replication blocks are encountered. Finally, the 'S-M checkpoint' or 'G2-M checkpoint' ensures that cells do not attempt to divide in the presence of unreplicated DNA, but as this checkpoint effectively monitors replication progression it is generally labelled as the 'replication checkpoint'. The DNA damage checkpoints as part of the wider DNA damage response are discussed in section 1.5.4 in further detail.

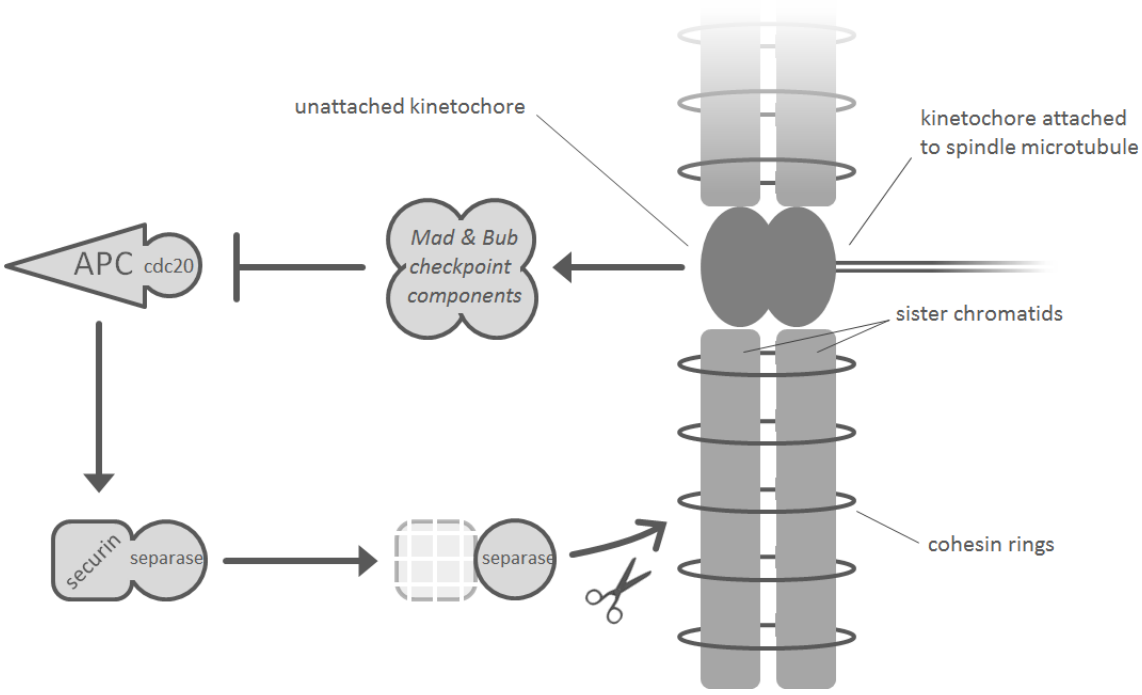

Figure 7: Schematic diagram of spindle checkpoint function. At the metaphase to anaphase transition securin is targeted for destruction by the E3 ubiquitin ligase complex APC. Its subsequent proteolysis by the proteasome releases separase, a protease that cleaves the cohesin ring molecules responsible for keeping sister-chromatids cohesed until anaphase onset. However, the presence of an unattached kinetochore inhibits $APC^{Slp1/Cdc20}$ activity through spindle checkpoint signalling that involves the Mad1, Mad2, Mad3 (BubR1 in metazoa), Bub1, Bub3 and Mps1 (Mph1 in *S.pombe*) proteins.

Equal distribution of the genomic content critically depends on each sister-chromatid pair establishing biorientation: every mitotic chromosome must attach its kinetochores in a bipolar fashion to plus-ends of spindle microtubules emanating from opposite spindle poles (Tanaka 2005, Tanaka *et al.* 2005b). This mitotic checkpoint, termed 'spindle assembly checkpoint' or spindle checkpoint in brief, guards the transition from metaphase to anaphase and accurately monitors the intricate process of biorientation during prometaphase (May & Hardwick 2006). The core of the spindle checkpoint consists of Mad1, Mad2, Mad3 (BubR1 in metazoa), Bub1, Bub3 and Mps1 (Mph1 in *S.pombe*) proteins. Premature chromosome segregation is prevented

because unattached or improperly attached kinetochores result in a checkpoint-dependent mitotic arrest through inhibition of mitotic $APC^{Slp1/Cdc20}$, and anaphase is delayed until all chromosomes achieve correct attachment (Rieder *et al.* 1995, Taylor *et al.* 2004, May & Hardwick 2006). A schematic drawing of the spindle checkpoint responding to an erroneous chromosome attachment is depicted in Figure 7 and discussed in further detail in section 1.4.

Not surprisingly, deficiencies in the spindle checkpoint or DNA damage checkpoint response contribute significantly to the onset of cancer in mammalian cells. Human hereditary syndromes associated with defective DNA maintenance and which predispose carriers to cancer are for instance: xeroderma pigmentosum (mutations in *XPA – XPG* and *XPV* genes), ataxia telangiectasia (*ATM*), seckel (*ATR*), Fanconi anaemia (*PALBP2*, *BRIP1*), ataxia-oculomotor apraxia 1 (*APTX*), nijmegen breakage (*NBS1*), cockayne (*CSA*, *CSB*), trichothiodystrophy (*XPB*, *XPD*, *TTDA*), bloom (*BLM*) and some forms of breast cancer (*BRCA1* and *2*) (Fuss & Cooper 2006, Caldecott 2008, Hartlerode & Scully 2009).

Unequal chromosome segregation is an inevitable consequence of cells that fail to monitor and achieve biorientation prior to sister-chromatid separation. Aneuploidy often results in cell death and in humans is a contributory factor in carcinogenesis and implicated in chromosomal disorders such as Down (trisomy of chromosome 21), Edward (trisomy 18), Patau (trisomy 13), Klinefelter (XXY) and Turner (monosomy X) syndrome (Cimini & Degrassi 2005, Kops *et al.* 2005, Michor *et al.* 2005, Holland & Cleveland 2009, Li & Zhang 2009).

Genetic germline mutations in the human *BUBR1* gene encoding a spindle checkpoint kinase have been associated with mosaic variegated aneuploidy (MVA) syndrome (Hanks *et al.* 2004, Suijkerbuijk *et al.* 2010). High rates of aneuploidy are observed in tissues and patients are predisposed to cancers from a young age and typically display physical impairments, cognitive disabilities and deficiencies in growth and development (Ganmore *et al.* 2009). Thus far, this is the only constitutional or structural aneuploidy syndrome that has been conclusively linked with a mutation in a spindle checkpoint gene. A germline mutation in another spindle checkpoint gene, *BUB1*, was recently identified in an individual with gastrointestinal cancer (de Voer *et al.* 2011) and mouse model experiments suggests that both BUBR1 and BUB1 haplo-insufficiencies can, in certain conditions, drive colon tumorigenesis (Rao *et al.* 2005, Baker *et al.* 2009).

Somatic aneuploidy is one of the hallmarks of tumorigenesis, and gene mutations have been identified in cancer tissues which appear to affect spindle checkpoint protein function as well

as abundance (Gemma *et al.* 2001, Tsukasaki *et al.* 2001, Grabsch *et al.* 2003, Kim *et al.* 2005, Bolanos-Garcia & Blundell 2011, Ryan *et al.* 2012). Disruption of *MAD* and *BUB* spindle checkpoint genes in a variety of metazoan tissue cultured cells leads to chromosomal instability and severely affects cell viability. Gene knockout studies in mice demonstrate that all *MAD* and *BUB* gene products are essential for normal cell proliferation. No homozygous null progeny is born from intercrosses between heterozygous knockout mice because development of such blastocysts is halted as a result of extensive apoptosis during the early stages of embryogenesis (Dobles *et al.* 2000, Kalitsis *et al.* 2000, Wang *et al.* 2004, Iwanaga *et al.* 2007, Jeganathan *et al.* 2007). Moreover, haploinsufficiencies of spindle checkpoint genes often lead to aneuploidy and tumorigenesis (Baker *et al.* 2004, Baker *et al.* 2006, Jeganathan *et al.* 2007, Baker *et al.* 2009).

The spindle checkpoint, the main focus of this work, is discussed in detail in the following section. In the course of this work, an additional function was identified for the Bub1 spindle checkpoint kinase that argues in favour of a role in the DNA damage response. This molecular pathway and the DNA damage checkpoint are therefore discussed in section 1.5.

1.4 The mitotic spindle checkpoint

1.4.1 The molecular components of the yeast spindle checkpoint

In 1991 two independent mutant screens identified six *S.cerevisiae* genes that are required for a cell cycle arrest in response to loss of microtubule function by exposure to the depolymerising drug benomyl (Hoyt *et al.* 1991, Li & Murray 1991). These genes were named *MAD* and *BUB* (acronyms for 'mitotic arrest-deficient' and 'budding uninhibited by benzimidazole', respectively). It soon became evident that the *MAD* and *BUB* genes are conserved from yeast to man indicating that they play an important role during cell division to merit evolutionary conservation (Hardwick 1998, Campbell *et al.* 2001). Five of these genes[7] and their protein products designated Mad1, Mad2, Mad3, Bub1 and Bub3 have since been shown to be required for a spindle checkpoint-mediated anaphase delay. A sixth gene was uncovered as an additional checkpoint component (Weiss & Winey 1996) and encodes the

[7] Cdc16/Bub2, the sixth gene product that was identified in the original screen, is unlike the Mad and other Bub proteins fundamental to a delay of late anaphase events. It specifically monitors the condition of non-nuclear astral microtubules (Pereira *et al.* 2000), which are nucleated by the outer plaque of the spindle pole bodies and are required for migration of the duplicated chromosomes into the newly formed bud in budding yeast and cytokinesis in fission yeast (Fankhauser *et al.* 1993, Bloecher *et al.* 2000). In the presence of impaired astral microtubules Cdc16/Bub2 associates with the spindle pole bodies (Fraschini *et al.* 1999) and its activity blocks exit from mitosis. This arrest upon spindle damage is therefore distinct from an arrest invoked by improper kinetochore-microtubule attachments and is functionally independent from Mad and other Bub proteins (Hardwick *et al.* 1996).

essential Mps1 protein kinase, which, unlike its *S.pombe* orthologue Mph1 (He *et al.* 1998), also functions in spindle pole body duplication (Winey *et al.* 1991).

BubR1 was identified as the metazoan Mad3 orthologue and is unlike its fungal counterpart endowed with a carboxy terminal protein kinase domain. The high sequence similarity of the amino termini of Mad3 and the Bub1 and BubR1 kinases (Roberts *et al.* 1994, Chen 2002) provides evidence for a common origin by means of a '*Mad3Bub(R)1*' proto-gene duplication event (Carvunis *et al.* 2012) and subsequent loss of the kinase domain that gave rise to *MAD3* genes (Kellis *et al.* 2004, Liti & Louis 2005). Bub1 and Mad3 (and Bub1 and BubR1) are therefore ancient paralogous gene products, although their function within the checkpoint has diverged to such an extent that these are not thought to overlap. Remarkably, nine independent gene duplication events can be discerned that were followed by parallel evolution (Suijkerbuijk *et al.* 2012a). Paralogous gene products that have arisen through genome duplication are sometimes referred to as 'ohnologues', a term coined by Kenneth Wolfe in reference to Susumo Ohno (Byrne & Wolfe 2005), one of the first researchers to study molecular evolution of diverging gene pairs.

Unlike their metazoan counterparts, all *MAD* and *BUB* genes in studied yeast cells are non-essential suggesting that under normal growth conditions, biorientation has completed some time before sister-chromatid disjunction takes place. In the absence of Mad and Bub proteins, however, perturbation of mitotic spindle stability by, for instance, benzimidazole fungicides, which interfere with microtubule polymerisation (Quinlan *et al.* 1980), leads to severe chromosome loss and lethality. Many natural toxins target microtubules (Fojo & Giannakakou 2000, Altmann & Gertsch 2007, Schmidt & Bastians 2007), such as taxanes (e.g. taxol), colchicines (e.g. colcemid) produced by plants of the *Taxus* (yew) and *Colchicum* (crocus) genus, respectively. Microtubules are also inherently cold-labile and can disassemble spontaneously when exposed to cold temperatures (Kerr & Carter 1990, Denarier *et al.* 1998). In the light of evolution this perhaps implies that the mitotic checkpoint initially evolved as a defence mechanism against harmful conditions and substances to delay anaphase until microtubule impairment is resolved. Eventually, as in metazoan cells, the checkpoint secured an absolute and vital control over completion of metaphase events. For instance, the Mph1/Mps1 and Bub1 kinases are known to directly promote biorientation (van der Waal *et al.* 2012) and cytosolic Mad2 and BubR1 (the metazoan orthologue of yeast Mad3) are implicated in the timing and duration of mitosis (Meraldi *et al.* 2004). The latter mechanism delays anaphase events even when microtubules are not perturbed and thereby provides extra

time to allow kinetochore assembly and the formation of proper and stable bipolar attachments.

1.4.2 Detecting deficiencies in chromosome biorientation

Chromosome biorientation generates tension across centromeres that stabilises microtubule attachments to kinetochores, whereas incorrect attachments exert minimal or no tension and are rendered unstable (Nezi & Musacchio 2009). The mechanism by which tension dictates the stability of kinetochore-microtubule attachments is becoming clearer. A contemporary model for 'tension sensing' is based on intra-kinetochore stretching of centromeric chromatin as a consequence of tension (Maresca & Salmon 2009, Joglekar *et al.* 2010) that ultimately results in the spatial separation of outer-kinetochore and inner-centromere components (Figure 8).

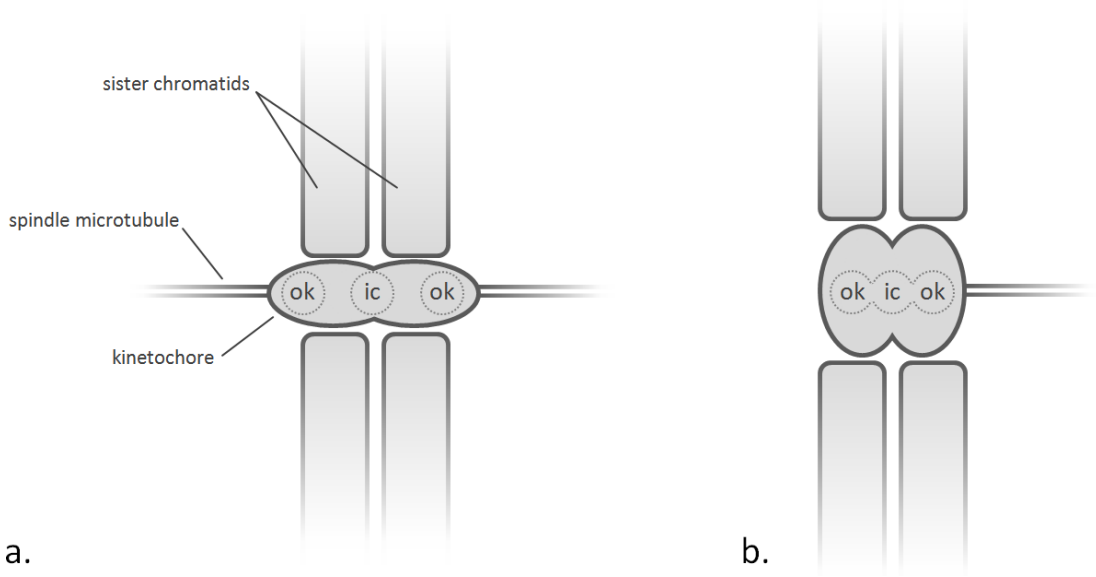

Figure 8: Diagram illustrating the intra-kinetochore tension-dependent spatial arrangement of the outer-kinetochore (ok) structure relative to the inner-centromere (ic) region in case of bioriented sister-chromatids **(a)** and mono-oriented sister-chromatids **(b)**. **(a)** Upon establishing biorientation the intra-kinetochore tension stretches the kinetochore and centromere structure resulting in separation of the inner-centromere and outer-kinetochore components. Note that cohesion of the sister-chromatid pair opposes the kinetochore pulling forces (not indicated). **(b)** Tension deficiency of a monopolar spindle microtubule attachment results in localisation of the inner-centromere chromatin proximate to outer-kinetochore components.

Since the mitotic aurora B kinase (Ark1/Ipl1 in yeast) localises to inner-centromeres and some of its substrates are present at the outer-kinetochore, it is reasoned that the application of tension leads to decreased phosphorylation of now distant aurora substrates (Cheeseman *et al.* 2002, Liu *et al.* 2009). Indeed, the aurora kinase activity is required for destabilising

microtubule-kinetochore attachments that do not generate tension (Biggins *et al.* 1999, Pinsky *et al.* 2006b, Gestaut *et al.* 2008).

1.4.3 Promoting chromosome biorientation

Kinetochore-microtubule attachments are thought to form by a process of 'trial and error' and the kinetochore interface is characterised by the highly dynamic presence of microtubules (Maiato *et al.* 2004). The stabilisation of attachments that are bipolar and destabilisation of those that are not will eventually ensure that all chromosomes are bioriented on the mitotic spindle apparatus (Tanaka 2005) (Figure 9).

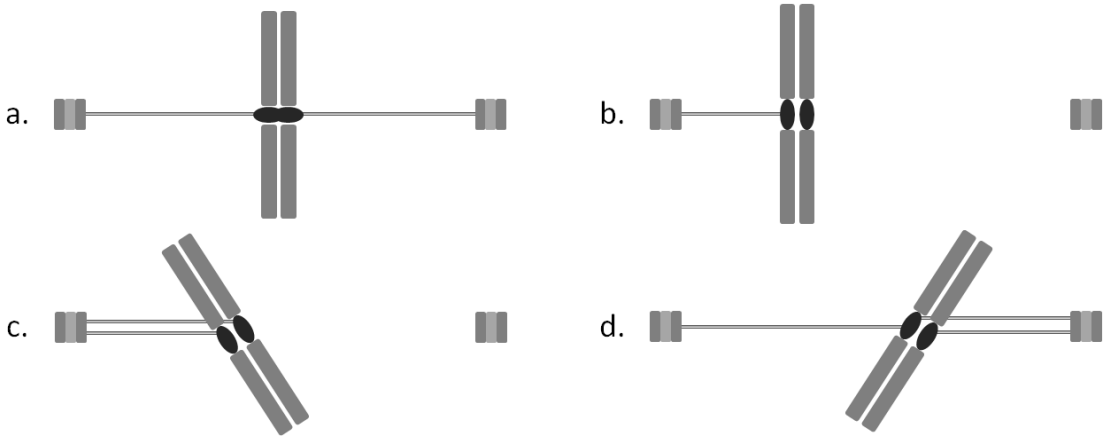

Figure 9: Schematic depiction of potential configurations of spindle microtubule attachments to kinetochores of sister-chromatids. **(a)** A bipolar or amphitelic attachment that properly biorients sister-chromatids on the bipolar mitotic spindle. **(b)** A monopolar or monotelic attachment. **(c)** A syntelic attachment, where both kinetochores are connected improperly to the same spindle pole. **(d)** A merotelic attachment, where one of the two kinetochores is incorrectly connected to both spindle poles. The latter situation cannot occur in *S.cerevisiae*, since its kinetochore architecture only allows a single microtubule attachment in contrast to the triple microtubule binding sites of a *S.pombe* kinetochore and 20-40 sites per kinetochore in metazoa.

Interestingly, apart from their role in delaying anaphase some spindle checkpoint proteins play an active role in promoting biorientation. The Mph1/Mps1 kinase is required to correct both non-bipolar attachments and biorient chromosomes in a tension-dependent manner (Jones *et al.* 2005, Maure *et al.* 2007, Meyer *et al.* 2013) and the Bub1 kinase performs a similar role that depends on Bub3, although by targeting different substrates (Fernius & Hardwick 2007, Logarinho & Bousbaa 2008, Windecker *et al.* 2009). In addition to the checkpoint kinases, the mitotic aurora B kinase Ark1/Ipl1 actively destabilises incorrect attachments (Pinsky *et al.* 2006b). Recent developments unravelled how these three kinases cooperate in promoting chromosome biorientation. Mph1/Mps1 phosphorylation of Spc7/Spc105 (orthologous to

human Blinkin and KNL1 in *Caenorhabditis elegans*) recruits Bub3 and Bub1 (London *et al.* 2012, Shepperd *et al.* 2012). In turn, Bub1 kinase action targets centromeric histone H2A and this histone mark is recognised by the shugoshin protein Sgo2 that recruits the aurora B kinase (Kawashima *et al.* 2010). Further aurora B kinase enrichment at centromeres occurs through Mph1/Mps1 phosphorylation of the chromosomal passenger borealin (Nbl1 in yeast) (Jelluma *et al.* 2008), positive feedback by aurora B-dependent Mph1/Mps1 recruitment (van der Waal *et al.* 2012) and histone H3 phosphorylation by haspin kinase action (Higgins 2010, Yamagishi *et al.* 2010).

Proteins that are implicated in attachment stabilisation and can directly counteract the aurora B destabilising activities are the polo-like kinase Plk1 (Plo1/Cdc5 in yeast) (Liu *et al.* 2012a) and TOG-XMAP family members (Garcia *et al.* 2002) that in yeast are Dis1/Stu2, Alp7/Slk19, Alp14 and the EB1 microtubule plus-end tracking proteins Mal3/Bim1 (Asakawa & Toda 2006). In yeast, the DASH (acronym for 'Dam1 and Duo1, Ask1, Spc34 and Spc19, Hsk1') complex serves an important role in the biorientation process as it is both a substrate of the polo-like kinase Plo1 (Buttrick *et al.* 2012) and its antagonist aurora B (Cheeseman *et al.* 2002, Keating *et al.* 2009). This complex holds onto the plus-end of microtubules perhaps by encirclement (Joglekar *et al.* 2006, Gao *et al.* 2010) and is essential in *S.cerevisiae* whereas *S.pombe* cells lacking DASH components are cold-sensitive (Miranda *et al.* 2007). It crucially functions during chromosome segregation to maintain attachments when microtubules depolymerise to pull apart the sister-chromatids (Westermann *et al.* 2005, Saitoh *et al.* 2008). The DASH complex has not been identified in metazoan cells, although the SKA complex is thought to serve an analogous role (Hanisch *et al.* 2006, Welburn *et al.* 2009, Chan *et al.* 2012, Jeyaprakash *et al.* 2012). In addition, the heterodimeric Klp5/Kip3 and Klp6 complex is thought to coordinate biorientation in *S.pombe* (Sanchez-Perez *et al.* 2005). They are kinesin-like proteins that possess motor activity (Grissom *et al.* 2009), are able to destabilise microtubules and facilitate kinetochore capture (Garcia *et al.* 2002).

1.4.4 Generating and propagating the 'wait anaphase' signal

The fundamental purpose of the spindle checkpoint is the generation of a molecular signal that delays cell cycle progression until all chromosomes have correctly bioriented. Clearly, a source of this 'wait anaphase' signal is the unattached kinetochore and the resultant lack of intra-kinetochore tension. It is evident that a single unattached kinetochore can delay anaphase as long as reasonably necessary (Rieder *et al.* 1994, Rieder *et al.* 1995).

One of the first important clues in unravelling the nature of the anaphase inhibitor came from yeast two-hybrid screens that provided evidence of APC function as a target for spindle checkpoint proteins. In two separate studies *S.cerevisiae* and *S.pombe* Mad2 were identified as a binding partner of Slp1/Cdc20 (Hwang *et al.* 1998, Kim *et al.* 1998), which had previously been identified as an APC activator (Visintin *et al.* 1997). Moreover, *S.pombe* cells with a *slp1-mr63* allele fail to arrest in metaphase even when Mad2 is over-expressed as the physical association of Mad2 with Slp1 is lost (Kim *et al.* 1998). The localisation of Mad2 in complex with Mad1 on an unattached mitotic kinetochore was observed in *X.laevis* egg extracts treated with the microtubule depolymerising drug nocodazole (Chen *et al.* 1996) and this was found to hold true in yeast and human cells (Campbell *et al.* 2001). Indeed, all checkpoint proteins, their target Slp1/Cdc20, and possibly the APC (Jorgensen *et al.* 1998, Acquaviva *et al.* 2004), have been shown to localise to kinetochores during prometaphase in response to improper microtubule attachment or the presence of microtubule (de)stabilising drugs (Chen *et al.* 1996, Li & Benezra 1996, Gorbsky *et al.* 1998, Taylor *et al.* 1998, Waters *et al.* 1998). The association of checkpoint components with kinetochores is abolished when microtubules attach (Mad1 and Mad2) or diminished once biorientation completes (Mad3 and Bub3).

The kinetochore component involved in Bub1, Bub3 and BubR1 anchoring has been revealed as Blinkin (Spc7/Spc105 in yeast) (Kiyomitsu *et al.* 2007), but the exact mode of engagement and the binding motifs involved are of topical interest and debate (Bolanos-Garcia *et al.* 2012, Krenn *et al.* 2012). Structural studies employing x-ray crystallography and nuclear magnetic resonance (NMR) show that 'tetratricopeptide repeat' (TPR) domains in both Bub1 and BubR1 are able to interact with Blinkin in a direct manner but at specific Bub1 and BubR1 binding sites (Bolanos-Garcia *et al.* 2011, Krenn *et al.* 2012). However, additional sites of interaction are anticipated, because the TPR domains and their binding sites on Blinkin are neither sufficient nor required (Lara-Gonzalez *et al.* 2011, Krenn *et al.* 2012). *S.pombe* cell studies recently identified the highly conserved MELT motifs of Spc7 as a binding site for Bub1 and Bub3 (Shepperd *et al.* 2012, Yamagishi *et al.* 2012). Moreover, association is stimulated by Mph1/Mps1 kinase activity targeting these motifs in the absence of microtubule attachments to kinetochores (London *et al.* 2012, Shepperd *et al.* 2012). It has been shown that ectopic targeting of Mph1 is sufficient for Bub1 but not Mad1 recruitment (Ito *et al.* 2012). However, the presence of Mph1 at kinetochores does seem to be a prerequisite for Mad1 enrichment (Heinrich *et al.* 2012). The exact identity of the Mad1 and Mad2 kinetochore binding site remains unclear (Martin-Lluesma *et al.* 2002).

It is Mad2 action that takes a key role in the so-called 'template model' that provides a molecular mechanism for amplifying the spindle checkpoint signal. NMR and x-ray studies revealed that Mad2 can assume two distinct conformations depending on the position of its flexible carboxy terminal 'safety belt' (i.e. seat belt) structure. Whereas monomeric Mad2 exists as an 'open' conformation, when 'strapped' onto a ligand such as Mad1 or Slp1/Cdc20 it will adopt the 'closed' conformation (Sironi *et al.* 2002, De Antoni *et al.* 2005). Fundamental to this model is the topological conversion of 'open' to 'closed' conformers catalysed by dimerisation of 'open' with 'closed' Mad2 either bound to Mad1 or Slp1/Cdc20 (Luo *et al.* 2004, Mapelli *et al.* 2007, Yang *et al.* 2008). This positive feedback mechanism results in a rapid increase of soluble Mad2 – Slp1/Cdc20 dimers (Simonetta *et al.* 2009).

Mitotic FRAP (for 'fluorescence recovery after photobleaching) microscopy experiments in PtK2 cells (Howell *et al.* 2004, Shah *et al.* 2004) and *in vitro* studies (Vink *et al.* 2006) reveal a relatively stable Mad1 association with Mad2 at unattached kinetochores that recruits an additional pool of Mad2 that rapidly exchanges. This biphasic behaviour of Mad2 can be seen in the light of the 'template model' as the production of diffusible Mad2 – Slp1/Cdc20 dimers catalysed on a Mad2 – Mad1 template stably bound to unattached kinetochores. This scenario provides the means for rapid amplification of the 'wait anaphase' signal away from a single unattached kinetochore with the potential to bring about a complete halt of the cell cycle machinery.

1.4.5 APC inhibition by the spindle checkpoint

The precise way in which the spindle checkpoint proteins inhibit the APC E3 ubiquitin ligase is a topic of ample debate. Early checkpoint studies in *S.cerevisiae* provided evidence of a larger spindle checkpoint complex that consists of Mad2, Mad3, Bub3 plus Cdc20 and is termed 'mitotic checkpoint complex' (MCC) (Hwang *et al.* 1998, Hardwick *et al.* 2000). This complex has since been found in the majority of eukaryotes studied so far and *in vitro* APC activity assays indicate that the MCC is a more potent $APC^{Slp1/Cdc20}$ inhibitor than Mad2 alone. Current checkpoint models therefore pose that the soluble 'wait anaphase' signal in the shape of a Mad2 – Slp1/Cdc20 complex develops into a mature $APC^{Slp1/Cdc20}$ inhibitor by binding Mad3 and Bub3 to form a MCC complex (Kulukian *et al.* 2009).

Exactly what conditions and additional factors drive this 'maturation' process are largely open questions. It is, however, likely that post-translational modifications of MCC components play an important role. In *S.pombe*, the sustained kinase activity of aurora B is essential, which

suggests that spindle checkpoint maintenance requires the continual production of anaphase inhibitors (Vanoosthuyse & Hardwick 2009a). Aurora B activity is indirectly implicated in delaying anaphase by generating unattached kinetochores from those microtubule attachments that do not generate tension (Pinsky *et al.* 2006b). However, a more direct role has been uncovered in *S.cerevisiae* in which the aurora B kinase Ipl1 was shown to phosphorylate Mad3 when kinetochore-microtubule attachments lack tension (King *et al.* 2007a). In addition to its phosphorylation by aurora B kinase, *S.cerevisiae* Mad3 and also its human orthologue BubR1 have been identified as a substrate of the polo kinase activity (Plo1/Cdc5 in yeast, Plk1 in human) (Rancati *et al.* 2005, Elowe *et al.* 2007). In *S.pombe*, Mph1 kinase phosphorylates both Mad2 (Zich *et al.* 2012) and Mad3 (Hardwick lab, unpublished observations) to facilitate APC inhibition. Figure 10 details the processes that are thought to form the basis of spindle checkpoint signalling to inhibit the APC.

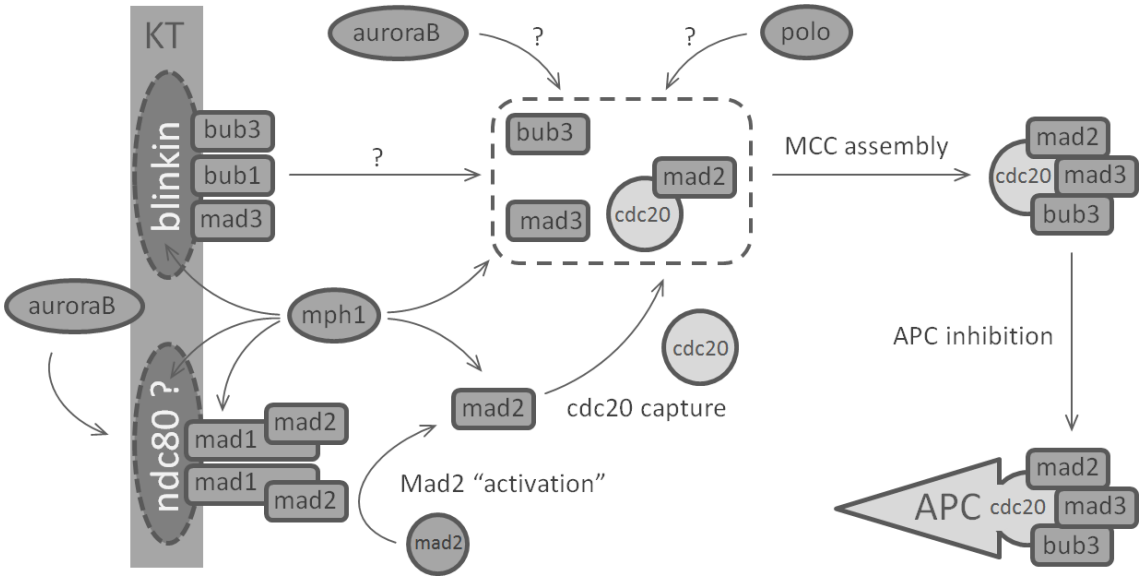

Figure 10: Molecular signalling of the spindle checkpoint pathway in the absence of a microtubule attachment to a kinetochore results in inhibition of the anaphase promoting complex (APC). The Mph1/Mps1 and aurora B (Ark1/Ipl1) kinase activities target Blinkin (Spc7/Spc105) and potentially other kinetochore components to direct enrichment of Mad and Bub proteins. As Mad2 molecules are activated (through a conformational change-over from 'open' to 'closed') the aurora and Mph1/Mps1 kinases (perhaps with cooperation of the polo-like kinase Plk1 in metazoan cells) prime the formation of MCC complexes that can target and inhibit the activity of the APC E3 ubiquitin ligase.

The ability of the MCC to stably bind mitotic APC to form APC^{MCC} complexes in *S.pombe* (Sczaniecka *et al.* 2008) and vertebrate cells (Morrow *et al.* 2005) implies a mechanism for spindle checkpoint action that cannot solely depend on Slp1/Cdc20 sequestration from the APC. Although it is currently unknown whether a direct association of the MCC with the APC is

required for APC inhibition, *in vitro* experiments using purified chromosomes and immuno-precipitated APC from colcemid treated HeLa cells show that the MCC can form on prior assembled APC^{Cdc20} and still inhibit its poly-ubiquitination activity (Kulukian *et al.* 2009). A stable association between the MCC and the APC is not observed in *S.cerevisiae* however (this work), and Mad2 alone is not able to inhibit preformed APC^{Cdc20} complexes *in vitro* (Foster & Morgan 2012).

In both *S.pombe* and *S.cerevisiae*, the MCC is formed each mitosis even in the absence of drugs that interfere with spindle formation (Poddar *et al.* 2005, Sczaniecka *et al.* 2008). Some studies have suggested the existence of MCC in HeLa interphase cells (Sudakin & Yen 2004) although in G1 the absence of Cdc20 would naturally prevents its formation. Both mitotic and unmodified (recombinant) MCC exert *in vitro* APC inhibition, but APC purified from a mitotic HeLa cell extract is profoundly more susceptible to MCC inhibition than that purified from interphase cells (Sudakin & Yen 2004). This strongly suggests that the APC can be 'sensitised' or primed to inhibition by the MCC. This mode of action is reminiscent of APC targeting of cyclin B that requires priming by $Cdk^{cyclin\ B}$ activity. Several lines of evidence suggest that the APC is subject to multiple levels of regulation. A prime example is of course the contrast in activities of APC^{Cdc20} and APC^{Cdh1}: only the former relies on the kinase activities of Cdc2/Cdc28 Cdk and polo-like kinase Plo1/Cdc5 (Rudner & Murray 2000, May *et al.* 2002). Furthermore, APC^{MCC} has no activity towards anaphase substrates such as cyclin B, but early mitotic substrates such as cyclin A in human cells are still processed in a Cdc20-dependent manner. For cyclin A degradation to occur it must bind a Cks protein to override checkpoint inhibition of the APC (Wolthuis *et al.* 2008).

Mad3 and metazoan BubR1 possess two evolutionary conserved KEN box degrons that are recognised by the mitotic APC activators Slp1/Cdc20 and Srw1/Cdh1 (Pfleger *et al.* 2001, Rape *et al.* 2006). Although *S.cerevisiae* Mad3 is indeed degraded during G1 in a KEN box and APC^{Cdh1}-dependent manner, it is evident that these degrons have an additional mitotic role in spindle checkpoint function as mutation of the amino terminal KEN box abrogates the checkpoint by preventing MCC formation and Cdc20 degradation in early mitosis (Burton & Solomon 2007, King *et al.* 2007b). This observation led to the proposition of the 'pseudo-substrate' model that posits that mitotically stable Mad3 competes with APC substrates, such as securin, for Cdc20 binding.

This model leaves unexplained the notion that over-expression of *S.pombe* and *S.cerevisiae* Mad2, but not Mad3 alone, leads to a checkpoint-dependent anaphase delay (He *et al.* 1997, Millband & Hardwick 2002, Mariani *et al.* 2012). In contrast to fusing Mad3 to Cdc20, *S.cerevisiae* Mad2 artificially tethered to either Mad3 or Cdc20 results in an anaphase delay (Lau & Murray 2012). Interestingly, these arrests neither depend on the presence of endogenous Mad and Bub proteins, nor on the kinase activities of Mps1 and Ipl1 or functional kinetochores. However, Cdc20 inhibition by Mad2 tethering does depend on the ability of the latter to form 'closed' conformers (Lau & Murray 2012). These experiments thus suggest that the main Mad3 function is in promoting Mad2 to inhibit Cdc20 and stabilisation of the MCC complex.

Peculiarly, in metazoan cells the observation has been made that although Mad2 is required for stimulating the BubR1 (Mad3 in yeast) interaction with Cdc20 and forming MCC complexes, Mad2 dissociates to create a final APC inhibitor (Nilsson *et al.* 2008, Kulukian *et al.* 2009). Recent work has shown that Mad2 is indeed able to catalytically convert the conformation of Cdc20 and promote its binding to BubR1 (Han *et al.* 2013). Mad2 extraction from the MCC to form a BBC complex (consisting of BubR1, Bub3 and Cdc20) is thought to be catalysed by P31 (see §1.4.6) (Westhorpe *et al.* 2011). This process has not been witnessed in yeast (Hardwick lab, unpublished observations), presumably as no functional P31 orthologues are present.

The recent elucidation of the *S.pombe* MCC structure by x-ray crystallography considerably clarifies its *modus operandi* in regards to APC inhibition (Chao *et al.* 2012). The interaction of Slp1 with Mad2 is primarily through the latter's 'safety belt' structure and Mad3 is thought to coordinate the overall structure of the MCC (Figure 11a). The Mad3 amino terminal KEN box degron blocks Slp1 substrate binding by engaging the receptor on Slp1 and this presumably stimulates the APC-mediated ubiquitination of the latter. The degron is positioned within a helix-loop-helix motif that interacts with Mad2 too, but only when the latter adopts its 'closed' conformation. The amino terminal TPR domain of Mad3 provides additional contacts with both Mad2 and Slp1 (Chao *et al.* 2012). Further insight was gained by *in silico* docking of the MCC structure onto a partial structural surface model of *S.cerevisiae* APC that was obtained by electron microscopy (Schreiber *et al.* 2011). Mad3 contacts Cut4/Apc1 within the central cavity of the APC, whereas Mad2 interacts with the Apc8/Cdc23 and Apc5 TPR subunits (Figure 11b). Its 'closed safety belt' conformation prohibits Slp1/Cdc20 from fully engaging the APC. Interestingly, this model indicates that whilst both the D and KEN box receptors of Slp1/Cdc20 are obstructed by Mad3, the D box receptor of Slp1/Cdc20 is also prevented from engaging the

D box co-receptor of Apc10/Doc1 (da Fonseca *et al.* 2011) and is instead tilted towards Apc5 (Herzog *et al.* 2009, Chao *et al.* 2012). In support of this finding, the second KEN box degron (downstream of the amino terminal first) of the metazoan Mad3 orthologue BubR1 has been shown to block APC substrate binding (Lara-Gonzalez *et al.* 2011). Mad2 and Mad3 thus cooperate to prevent APC stimulation by Slp1/Cdc20 and APC from recognising and ubiquitinating D box substrates at the same time as perhaps facilitating Slp1/Cdc20 ubiquitination.

Cdc20 is continuously synthesised during a mitotic arrest (Nilsson *et al.* 2008, Foster & Morgan 2012). Although over-expression of Cdc20 does not prematurely activate the APC in HeLa cells, the APC-dependent ubiquitination of Cdc20 and its consequent destruction by the proteasome is thought to be a contributing factor in spindle checkpoint maintenance (Nilsson *et al.* 2008, Mansfeld *et al.* 2011) and silencing (Uzunova *et al.* 2012). In *S.cerevisiae*, a spindle checkpoint-mediated anaphase delay was shown to destabilise Cdc20 in a similar manner and high levels of the APC activator can drive cells out of metaphase in the absence of spindle microtubules (Pan & Chen 2004). Its mitotic turnover is, however, not required for maintenance of a mitotic arrest, but rather for silencing the checkpoint (refer to §1.4.6) (Varetti *et al.* 2011, Foster & Morgan 2012).

Whereas recombinant *S.cerevisiae* Mad2 can inhibit APC-mediated ubiquitination of both securin and Cdc20 *in vitro*, Mad3 in combination with Bub3 only inhibits that of securin (Foster & Morgan 2012). Further evidence suggests that Mad3 and Bub3 promote the association between Cdc20 and the APC contrasting Mad2 activity that prevents Cdc20 from contacting the APC. Whereas substrates actively stimulate activators such as Cdc20 and Cdh1 to bind the APC in a manner dependent on Apc10/Doc1 (Matyskiela & Morgan 2009), the binding of Cdc20 in association with Mad3 and Bub3 does not depend on this particular APC subunit (Foster & Morgan 2012), corroborating the finding that Mad3 prevents Cdc20 from contacting Apc10/Doc1 (Herzog *et al.* 2009, Chao *et al.* 2012). Remarkably, mitotic Cdc20 turnover does not rely on its own degron motifs, but rather on those of Mad3 (King *et al.* 2007b). Indeed, the purpose of MCC formation in regards to its APC target is two-fold: to prevent ubiquitination of securin and also to promote ubiquitination of Cdc20. It is thus that the MCC is not an APC inhibitor *per se*, but rather a very potent APC modulator.

a.

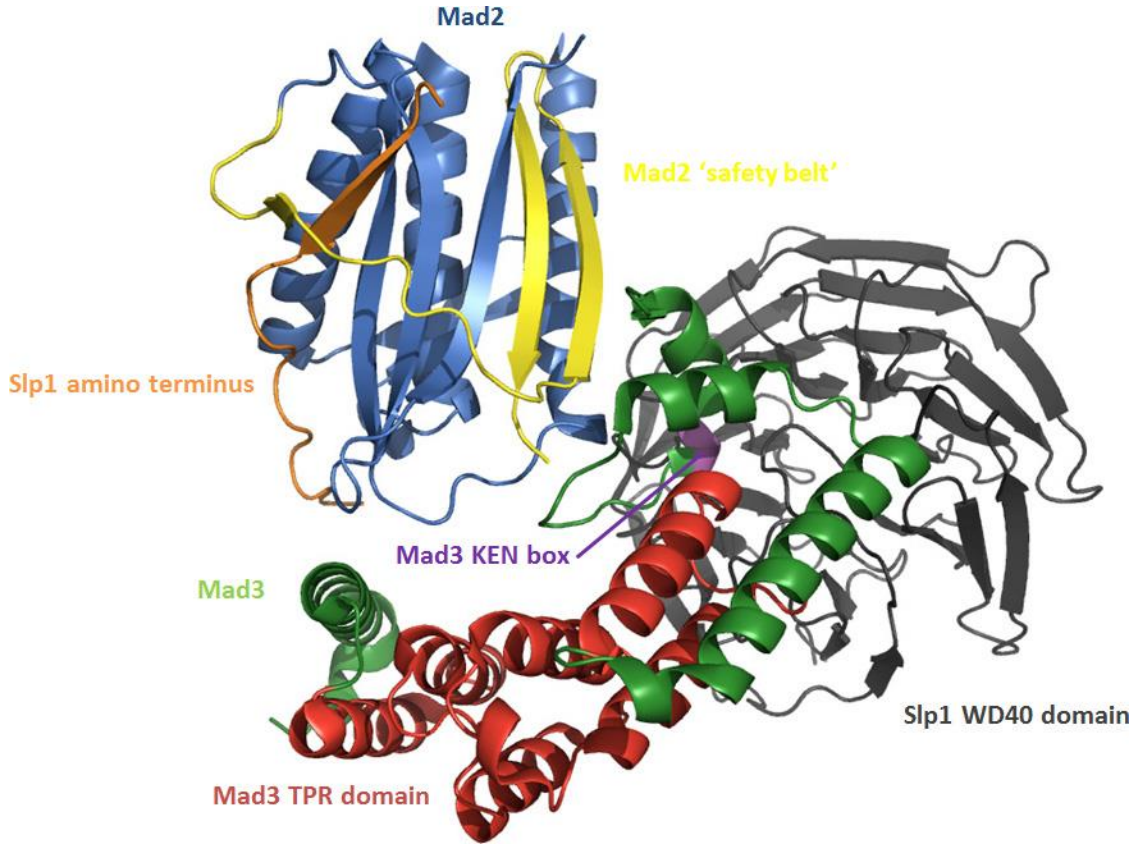

b.

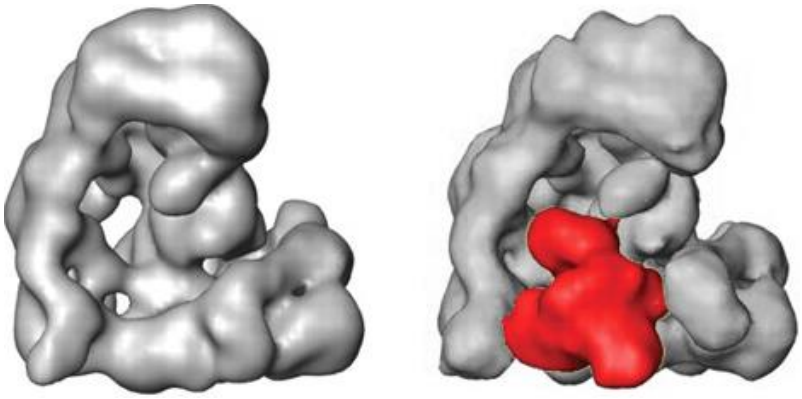

Figure 11: (a) Partial *S.pombe* MCC structure as revealed by x-ray diffraction crystallography (Chao *et al.* 2012). The 3D ribbon representation was prepared in PyMol (§2.5.3). **(b)** Surface model reconstruction of human APC (left) and APC^{MCC} (right; with MCC particle in red) obtained by single-particle electron microscopy (Herzog *et al.* 2009).

1.4.6 Silencing spindle checkpoint signalling

When all chromosomes are bioriented, the spindle checkpoint is satisfied and production of anaphase inhibitors must cease or, alternatively, the APC must be desensitised to MCC inhibition. Studies in both *S.pombe* and *S.cerevisiae* revealed that the Dis2/Glc7 catalytic subunit of protein phosphatase 1 (PP1) is essential for checkpoint silencing and directly binds the kinetochore component Spc7/Spc105 in the presence of microtubule attachment and

tension (Vanoosthuyse & Hardwick 2009a, Liu *et al.* 2010a, Meadows *et al.* 2011, London *et al.* 2012). As Spc7/Spc105 and its human orthologue Blinkin had previously been proposed as the kinetochore anchor for some of the Bub proteins (Kiyomitsu *et al.* 2007, Kiyomitsu *et al.* 2011) and that this targeting depends on the Mph1/Mps1 kinase activity, the identification of Spc105 as a $PP1^{Glc7}$ substrate to reverse Bub kinetochore recruitment was perhaps no surprise (London *et al.* 2012). In *S.pombe*, $PP1^{Dis2}$ that does not bind Spc7 can associate with the Klp5/Kip3 and Klp6 kinesin complex and this interaction is required for both biorientation and checkpoint silencing (Meadows *et al.* 2011).

The current 'checkpoint silencing' paradigm extends the tension sensing model (see §1.4.2) and poses that enzymatic activities at the inner-centromere antagonise activities on the outer-kinetochore and *vice versa*. Thus the application of tension moves kinetochore substrates further away from aurora B activity at the inner-centromere so that the more prominent activity is that of PP1 at the outer-kinetochore (Pinsky *et al.* 2006a, Maresca & Salmon 2009, Uchida *et al.* 2009) (refer to Figure 12b, page 27). As a consequence of the prevailing PP1 activity the checkpoint components are thought to be dislodged from their kinetochore anchor.

The core kinetochore protein Ndc80 (also termed Hec1 and Tid3 in *S.cerevisiae*) (DeLuca *et al.* 2006, Tooley & Stukenberg 2011) that regulates microtubule binding is a known substrate of both Ark1/Ipl1 aurora B and Mph1/Mps1 kinases (Kemmler *et al.* 2009). Its role in recruiting Mad1, Mad2 and Mph1/Mps1 to kinetochores is as yet unclear (Martin-Lluesma *et al.* 2002), but Ndc80 has been identified as a PP1 substrate (DeLuca *et al.* 2011, Wei *et al.* 2011) and Mps1 binding site (Kemmler *et al.* 2009).

Other factors whose phosphorylation is reduced when kinetochores come under tension are the Dam1 subunit of the yeast DASH microtubule ring complex (Keating *et al.* 2009) and the polo-like kinase Plk1 (Plo1/Cdc5 in yeast) (Liu *et al.* 2012a). Since some checkpoint proteins have been identified as *bona fide* Ark1/Ipl1 and Mph1/Mps1 substrates it remains to be investigated whether they can also serve as substrates of specific phosphatase such as PP1 (Visconti *et al.* 2010).

Interestingly, in the absence of bioriented chromosomes *S.pombe* cells that lack Bub3 are still able to delay anaphase in a checkpoint-dependent manner (Tange & Niwa 2008, Windecker *et al.* 2009). However, Bub3 deficiency prevents Mad3 and Bub1, but not Mph1, from stably associating with unattached kinetochores and cells fail to silence the spindle checkpoint

efficiently when biorientation is achieved (Chan *et al.* 2009, Daum *et al.* 2009, Vanoosthuyse *et al.* 2009, Heinrich *et al.* 2012). These findings suggest that the Mad and Bub checkpoint components do not need to be enriched on kinetochores for checkpoint activation to occur, but that silencing of the checkpoint is greatly enhanced by enrichment on kinetochores near the prevailing PP1 phosphatase activity. However, *S.pombe* Spc7 mutants that fail to bind Bub3 and Bub1 are not able to robustly delay anaphase, which suggest that Bub3 can modulate Bub1 activity (Shepperd *et al.* 2012, Yamagishi *et al.* 2012) or that Spc7 binding of other essential factors is disrupted. The mitotic interplay of checkpoint kinases and phosphatases targeting the Mad and Bub proteins to the kinetochore docking sites is schematically depicted in Figure 12 (page 27).

Much detail for the spindle checkpoint silencing model in regards to the dissolution of APC^{MCC}, especially in fungal model organisms, is however lacking (Vanoosthuyse & Hardwick 2009b, Hardwick & Shah 2010, Kops & Shah 2012). MCC disassembly is thought to be catalysed by the multi-ubiquitination of Cdc20 in an APC-dependent manner (Reddy *et al.* 2007). Opinions are however divided whether this process facilitates recycling of checkpoint components or heralds the proteasomal destruction of Cdc20. In other words, does disassembly of MCC serve checkpoint maintenance (Nilsson *et al.* 2008) or silencing (Reddy *et al.* 2007)? The release of checkpoint proteins was found to rely on the E2 ubiquitin ligase activities of UbcH10 and Ube2S that target Cdc20 (Reddy *et al.* 2007, Garnett *et al.* 2009), a process that is reversed by the antagonistic deubiquitinating activity of Usp44 (Stegmeier *et al.* 2007). Although these studies suggest that ubiquitinated Cdc20 is not necessarily targeted for destruction, APC-dependent proteolysis does seem to play a role in disabling the checkpoint signal and activating the APC in full (Visconti *et al.* 2010, Zeng *et al.* 2010, Ma & Poon 2011).

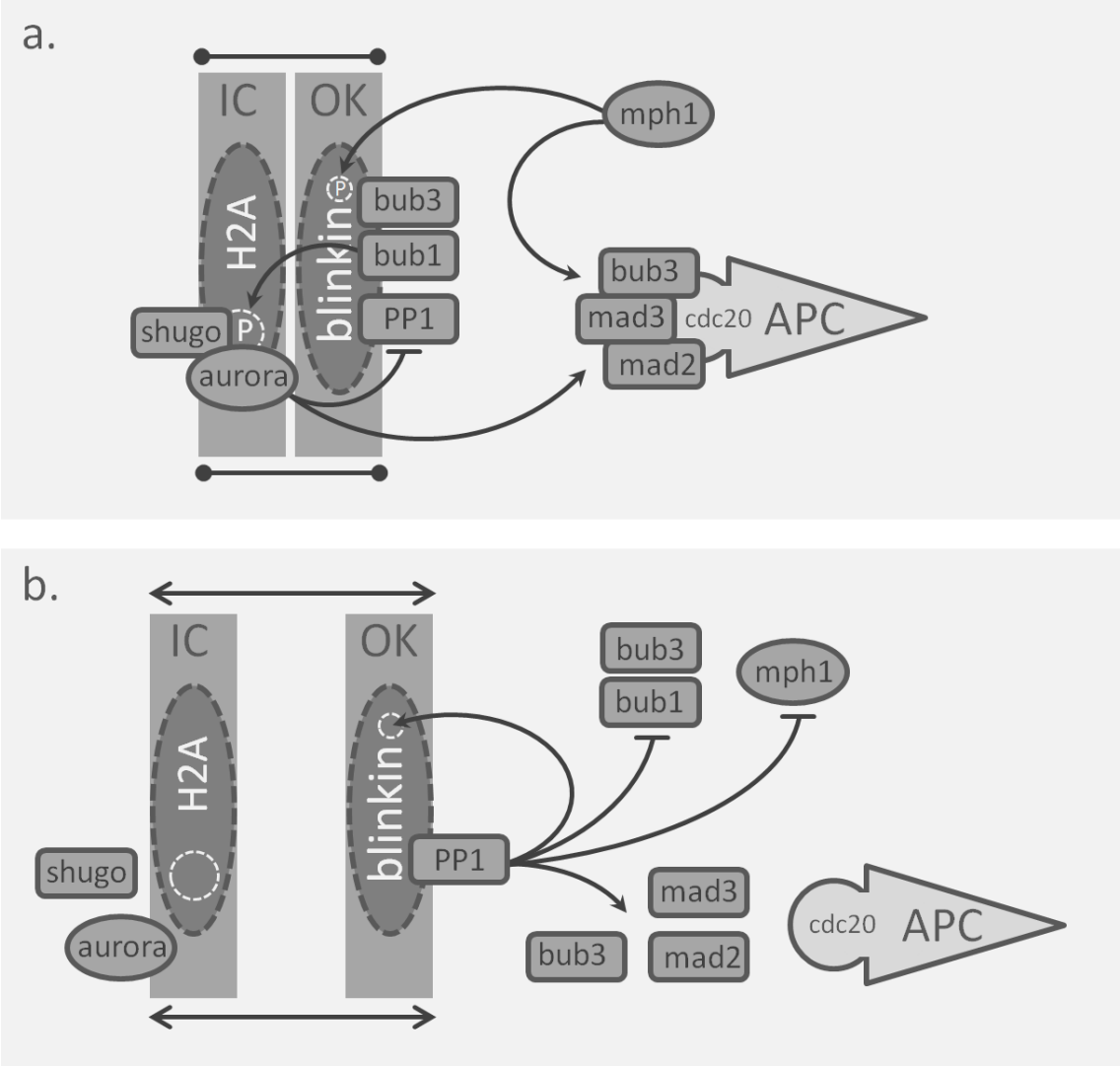

Figure 12: Schematic diagram illustrating the key role of Blinkin (Spc7/Spc105 in yeast). **(a)** In prometaphase, a spindle checkpoint response is triggered when kinetochores lack tension in the absence of microtubule attachments. **(b)** Tension is established at anaphase onset when microtubules have properly attached to kinetochores and satisfy the spindle checkpoint to silence the response. Note that in contrast to the situation depicted in **(b)** in the absence of tension **(a)** the inner-centromere (ic) structure is in close proximity to the outer-kinetochore (ok) – see also Figure 8 – so that Bub1 kinase can phosphorylate histone H2A and recruit shugoshin and aurora B. Activity of the latter in addition to that of Mph1/Mps1 antagonises the PP1 phosphatase and is essential in sustaining a spindle checkpoint-dependent anaphase delay by generating MCC complexes (Mad2, Mad3, Slp1/Cdc20 and, in other model organisms than *S.pombe*, Bub3) that inhibit the anaphase promoting complex (APC). When kinetochore tension is applied **(b)** aurora B substrates such as the checkpoint proteins are withdrawn from the kinase and rapidly dephosphorylated by the prevailing PP1 activity. As a consequence, MCC dissociation results in activation of the APC complex. Note that the Mph1/Mps1-dependent phosphorylation of the kinetochore component Blinkin regulates Bub1 and Bub3 binding and facilitates MCC formation.

In both human cells and *S.cerevisiae* the APC subunit Apc15 (Apc15/Mnd2 in yeast) is thought to play a crucial role in efficiently silencing the spindle checkpoint. Depletion of Apc15 in HeLa cells causes delay in anaphase onset and leads to accumulation of APC^{MCC} (Mansfeld *et al.* 2011, Uzunova *et al.* 2012). Here, Apc15 enables Cdc20 ubiquitination leading to MCC dissociation (Uzunova *et al.* 2012). Similarly, *S.cerevisiae* cells that lack Apc15 delay anaphase for longer when microtubule drugs are removed (Foster & Morgan 2012). These mutants are able to robustly arrest in metaphase but fail to ubiquitinate and degrade Cdc20 in contrast to an unchallenged cell cycle. This suggests that mitotic Cdc20 turnover is a requirement for checkpoint silencing and not for checkpoint maintenance. Strikingly, the *in vitro* APC ubiquitination of Cdc20 is not inhibited by the absence of Mnd2 or the presence of Mad3 and Bub3. However, Cdc20 ubiquitination in the presence of the two checkpoint proteins is Mnd2 dependent, which indicates that the positioning of Cdc20 onto the APC is greatly influenced by MCC binding (Chao *et al.* 2012).

Several key players of checkpoint silencing that are unique to metazoa have been discovered. In 2002 a mechanism was identified that targets 'closed' Mad2 conformers and could prevent Mad2 dimerisation or instruct MCC disassembly. P31 (also called Comet and originally CMT2) was uncovered as a Mad2 binding partner in a yeast two-hybrid assay (Habu *et al.* 2002). Whereas anaphase is delayed when P31 is depleted, over-expression of P31 causes HeLa cells to precociously degrade securin and exit mitosis early (Habu *et al.* 2002). Crucially, this work also revealed that Mad2 exchanges Cdc20 for P31 when cells enter anaphase. Subsequent structural studies showed that P31 specifically binds the 'closed' Mad2 conformers through conformational mimicry of Mad2 (Xia *et al.* 2004, Yang *et al.* 2007). The 'capping' model that was put forward proposed that in this manner P31 would prevent 'closed' Mad2 from catalysing 'open' to 'closed' species (Mapelli *et al.* 2006, Fava *et al.* 2011). Further studies indicated that P31 can directly act upon the MCC to evict and reset Mad2 to an 'open' conformation primarily to recycle Mad2 during a metaphase arrest as BBC (BubR1, Bub3 and Cdc20) complexes remain potent APC inhibitors (Teichner *et al.* 2011, Westhorpe *et al.* 2011). Moreover, the complete dissolution of MCC is mediated by P31 and has been implicated in APC activation and checkpoint silencing (Hagan *et al.* 2011, Teichner *et al.* 2011). This process is ATP dependent and stimulated by Cdk1 phosphorylation of Cdc20, which could decrease its affinity for BubR1 (Miniowitz-Shemtov *et al.* 2012).

The latest studies unify most of the available data and suggest that the P31 pathway acts in parallel and independent of Cdc20 ubiquitination and its proteasome-mediated degradation to

promote MCC dissociation and checkpoint silencing (Jia *et al.* 2011). In addition, CUEDC2, a putative novel metazoan checkpoint silencing factor, was recently identified as an interactor of Cdc20 regulated by Cdk1 kinase activity (Gao *et al.* 2011). Although its exact mode of action remains to be clarified, Mad2 binding is lost from the APC when CUEDC2 is over-expressed and cells are prematurely driven out of metaphase, whereas anaphase onset is delayed when CUEDC2 is depleted (Gao *et al.* 2011).

A distinct metazoan checkpoint silencing mechanism that is studied in *C.elegans*, *Drosophila* and human cells is known as 'dynein stripping' and requires a set of proteins called Spindly, Rough deal (Rod), Zeste-white 10 (Zw10) and Zwilch (Karess 2005, Chan *et al.* 2009, Bader & Vaughan 2010). The latter three form a complex called RZZ and none of these four proteins are thought to have functional orthologues in fungi. Spindly, in cooperation with RZZ, recruits dynactin and the dynein motor to kinetochores. Upon spindle microtubule attachment Mad1, Mad2, BubR1 and many other proteins including Spindly and RZZ are thought to be transported from the kinetochore via the spindle microtubule array to the spindle pole (Howell *et al.* 2001, Basto *et al.* 2004, Bader & Vaughan 2010, Barisic & Geley 2011). It is proposed that this ATP-dependent and dynein-mediated pathway withdraws the checkpoint proteins and RZZ from aurora B kinase action and thus prevents the formation of APC inhibitors (Barisic & Geley 2011).

1.5 The cellular responses to DNA damage

1.5.1 DNA molecules are under continuous assault

Biomolecules are continually at risk of damage from exogenous as well as endogenous genotoxic agents that affect the cell's genetic integrity. Whereas sources of the former are cosmic, natural, biological or man-made in origin and include environmental chemicals and certain types of radiation, the latter often are by-products from the cell's metabolism, such as reactive oxygen and nitrogen species and even water driving spontaneous hydrolysis. To combat the endogenous sources of DNA damage, cells evolved a battery of antioxidant defences that relies on the activities of catalases, ascorbate peroxidases, superoxide dismutases, metallothioneins, peroxiredoxins, glutathione reductases and glutathione peroxidases (Finkel & Holbrook 2000). Nonetheless, it has been estimated that mammalian

cells undergo up to 3,000 DNA lesions every hour[8] as a result of both endogenous and exogenous genotoxins (Lindahl 1993, Lindahl & Barnes 2000).

Examples of exogenous genotoxins (Ciccia & Elledge 2010) are many anti-tumour drugs used in chemotherapy, polycyclic aromatic hydrocarbons in overcooked foods or as atmospheric pollutants from petrochemical products and smoke, some organophosphorous pesticides, biological and industrial bromides, natural products with antibiotic, insecticidal, fungicidal or broader pesticidal properties, ionising radiation including the high intensity ultraviolet (UV) light emitted by the sun, γ-rays produced through the decay of naturally occurring radioisotopes such as radon gas and x-rays used in diagnostic medical procedures.

As a direct result of DNA damage and structure distortion, gene transcription and genome duplication can be disrupted, mutations can be introduced and, worst of all, breakage of the DNA double helix can take place. The consequences of improperly repaired or undetected DNA lesions attribute to genetic instability, which is often deleterious for the cell's well-being and in organisms can contribute to disease manifestations, such as the onset of cancer and premature aging (Hoeijmakers 2009, Ciccia & Elledge 2010).

The hereditary and long-lasting nature of DNA molecules in contrast to the transitory nature of for instance RNA species, proteins and lipids, necessitates a robust cellular response mechanism to its impairment (Ciccia & Elledge 2010). Cells evolved strategies to restore the original DNA sequence and structure upon detection of damage. Not surprisingly, the variety of damages that can occur to a long double-stranded DNA chain requires an exquisitely varied and regulated damage response. Its molecular basis is extremely well-conserved throughout eukaryote evolution and takes care of both small but undesirable DNA modifications and complicated events such as double strand breaks. In addition, mechanisms evolved for cells to cope with damage when DNA repair has failed (Su 2006), such as adaptation in unicellular organisms and programmed cell death in multicellular organisms.

[8] Quantitative data suggest that the number of DNA lesions that occur daily in a cell is quite staggering: for human beings estimates range from 50 – 80,000 lesions per cell per day (Lindahl 1993). In a cell that's undergoing active gene transcription and DNA replication, this includes up to 50,000 single strand DNA breaks, 10,000 depurination events, 600 depyrimidination events, 500 deamination events, 2000 damage events due to oxidation, 4500 due to alkylation, 10 due to cross-linking and 10 double strand breaks (Lindahl & Barnes 2000). Direct sunlight introduces around 100,000 lesions per hour per fully exposed cell (Hoeijmakers 2009).

1.5.2 DNA lesions can take many shapes and forms

In spite of their extreme mutagenic properties, subtle alterations of nucleotides in genomic DNA are remarkably common. Such incidences occur for instance through alkylation[9], oxidation and deamination that can dramatically transform base pairing properties. For example, methylation of guanine at its O(6) position or thymine at O(4) by chemical compounds such as methyl methanesulfonate (MMS) but also cellular S-adenosylmethionine lead to selective base pairing with thymine and guanine, respectively (Kondo *et al.* 2010). C(8)-hydroxyguanine is formed through oxidation[10] of guanine by reactive oxygen species and results in pairing with adenine (Evans *et al.* 2004). Deamination by spontaneous hydrolysis or exposure to nitrosative agents converts cytosine into uracil, C(5)-methylcytosine into thymine and adenine into hypoxanthine (Lee *et al.* 2011, Pang *et al.* 2012). Another remarkably frequent and spontaneous occurrence is the depyrimidination or depurination of nucleobases into abasic sites by hydrolysis of the N-glycosidic bond via base protonation by water (Boiteux & Guillet 2006, Ciccia & Elledge 2010). Apyrimidinic and apurinic (AP) sites are so-called non-instructional bases as no base pairing can be established.

Exposure to UV light and chemical compounds such as cisplatin (chemotherapy drug), mitomycin (produced by several *Streptomyces* bacterial species), nitrogen mustards, acreleins and furocoumarins (e.g. psoralen produced by several plant species) can lead to intrastrand or interstrand crosslinks of the DNA duplex, often linking the N(7) position of guanines. Other chemical compounds have the ability to indirectly damage DNA through structural distortion of the double helix or through interference with essential nuclear processes such as DNA replication, transcription, supercoiling and even repair. DNA intercalating agents like acridins, ethidiumbromide and actinomycin are often planar aromatic or heterocyclic compounds that insert within the nucleobase stack of the double helix or covalently bond to nucleobases. Intercalation can prevent the separation of the DNA duplex required for its transcription or replication, or can distort and stress the DNA double helix structure leading to base-pairing frame-shifts.

---

[9] Alkylating mutagens are often strong electrophiles that alkykate DNA at nucleophilic sites such as the ring nitrogens and oxygens of nucleobases (Motorin *et al.* 2010). Due to their strong nucleophilic character, the N(7) position of guanine and the N(3) position of adenine are particularly susceptible to alkylation. Spontaneous alkylation of cytosine at N(3) is not uncommon, but alkylation of its non-nucleophilic C(5) carbon atom only occurs through the catalytic activity of DNA methyltransferases that function in gene regulation by creating the C(5)-methylcytosine epigenetic marks.

[10] Curiously, a controlled DNA oxidation mechanism involving 8-hydroxyguanine evolved that regulates gene transcription (Perillo *et al.* 2008).

DNA replication and transcription can be blocked by nucleobase coupling of bulky adducts such as benzopyrenes and metabolites of aflatoxin, which is produced by some fungal *Aspergillus* species. Among the many other natural products that interfere with genome stability are camptothecin that is produced by the *Camptotheca acuminata* tree (Hsiang *et al.* 1985), staurosporine that is produced by some *Actinomyces* bacteria (Nakano & Omura 2009) and caffeine, which is produced by a variety of plant species. The latter directly inhibits the DNA damage response by targeting the ATM and ATR kinases (refer to §1.5.4), whereas the other two compounds inhibit the DNA topoisomerase II enzyme. Finally, nucleobase-analogues are mutagens as their chemical properties are sufficiently similar to any of the nucleobases to simulate pairing. For instance, the thymine analogue 5-bromouracil promotes erroneous DNA replication as pairing can be achieved with either adenine or guanine.

Ionising radiation in the form of γ and x-rays is perhaps one of the most potent genotoxins as it will give rise to an abundance of highly reactive free radicals (Finn *et al.* 2012). Three types of DNA damage have been observed as a result of radicals attacking the double helical structure: single strand breaks or nicks in the deoxyribose-phosphate backbone, complete double strand breakage and nucleobase modifications. DNA strand breaks can also be introduced by so-called radiomimetic chemicals, such as the zeocin and bleomycin compounds that are produced by several *Streptomyces* bacterial species.

Most types of DNA damage can indirectly lead to single-stranded breaks and in a few cases to complete double strand breaks: the former not only as intermediates of repair mechanisms but also as a result of chemical instability of impaired or absent nucleobases. Unintentional double-stranded breaks of the DNA duplex are every so often a consequence of DNA replication forks that stall and collapse when encountering lesions such as single strand breaks. The high prevalence of double strand breaks in cells exposed to DNA topoisomerase inhibitors is indicative of this process: they prevent the isomerase from re-joining the phosphodiester backbone of DNA after single strand cleavage and relaxation of supercoiling during transcription and replication (Pommier *et al.* 2003).

Besides, double strand breaks are deliberately generated during the establishment of cross-over events in meiotic cells, during V(D)J and immunoglobulin class switch recombination in lymphocytes (Masson & West 2001) and during mating type switching in fungi like the yeasts *S.cerevisiae* and *S.pombe* (Raji & Hartsuiker 2006).

1.5.3 Molecular pathways responding to DNA damage

The frequent occurrence of single-stranded DNA breaks necessitates efficient repair as they can be converted into double strand breaks by further insults as well as DNA replication. Not surprisingly, DNA double strand breaks are particularly mutagenic as one such break can lead to cell death (Resnick & Martin 1976), whilst gene conversion, mutations and chromosomal rearrangements are inadvertent and inherent to break repair mechanisms (Kasparek & Humphrey 2011). In both *S.pombe* and *S.cerevisiae*, repair of double strand breaks preferentially requires the homologous sequence of a sister-chromatid or chromosome homologue to serve as a template (Langerak & Russell 2011). In these instances, repair is achieved by 'homologous recombination' through non-crossover events (Krogh & Symington 2004, Wyman *et al.* 2004, Kasparek & Humphrey 2011). Remarkably, a mechanism exists that suppresses the use of homologues in the presence of identical sister-chromatids in diploid G2 cells, as break repair through the use of the former can lead to gene conversion and loss of gene heterozygosity (Kadyk & Hartwell 1992, Arbel *et al.* 1999, Krogh & Symington 2004, Langerak & Russell 2011). In the absence of homologous sequences, these breaks are repaired through the process of 'non-homologous end joining', which is the predominant repair mechanism in metazoan cells (Ira *et al.* 2004, Garber *et al.* 2005, Hartlerode & Scully 2009). In this process, the two broken ends are rapidly re-joined with relative ease, but this approach is not entirely foolproof (Finn *et al.* 2012). DNA degradation and resection by nucleases prior to fusion can result in large deletions or chromosome rearrangements can arise when ends from different chromosomes are mistakenly ligated (Raji & Hartsuiker 2006).

A subtle DNA lesion is either repaired relatively quickly or remains undetected until it is encountered by a replication fork during S phase. In contrast, if damage is extensive or not straightforward to repair, an immediate ATM or ATR[11] kinase-mediated damage response is triggered (Shiloh 2003, Smith *et al.* 2010). As a direct consequence, several signalling pathways are activated that result in the large scale induction of gene expression, a genome wide increase in chromosome cohesion levels and, crucially, inhibition of cell cycle progression (Melo & Toczyski 2002).

[11] ATR (Rad3/Mec1 in yeast) and ATM (Tel1) are by virtue of their structure phosphatidyl inositol 3-kinase-related (PI3K) kinases (PIKK). Individuals with 'ataxia telangiectasia mutations' (ATM) are hypersensitive to ionising radiation and are highly predisposed to manifestations of cancer (Zakian 1995, Lavin & Shiloh 1997). ATR is an acronym for 'ATM and Rad3 related'.

DNA strand break repair and other major molecular pathways that respond to the wide variety of genotoxic lesions that can affect the DNA double helix are listed in Table 1. The checkpoint response is discussed in further detail in the following section.

#	molecular pathway	function and characteristics	reference(s)
	Direct repair		(Yi & He 2013)
1	Alkyl guanine transferase	Specifically targets alkylated guanine.	(Gerson 2004)
2	DNA photolyase	Light activated reversal of UV induced thymine dimers. Not present in mammalian cells or *S.pombe*.	(Essen & Klar 2006)
	Repair by excision of lesions		
3	Base excision repair (BER):	Repair of subtle alterations that do not distort the DNA backbone or obstruct DNA transcription and replication, e.g. deaminated, oxidised and alkylated nucleobases.	(Robertson *et al.* 2009)
4	Short patch BER	Single nucleotide gap repair by DNA polymerase β.	(Caldecott 2003)
5	Long patch BER	Repair of gaps less than 10 nt by RFC^{Rfc1} loaded PCNA clamp and DNA polymerase δ or ε.	(Overmeer *et al.* 2010)
6	Nucleotide excision repair (NER):	Repair of distorting DNA lesions that obstruct replication or transcription.	(Lagerwerf *et al.* 2011)
7	Transcription coupled NER	NER by 'transcription factor II H' (TFIIH) complex.	(Sarker *et al.* 2005)
8	Global genome NER	Detection and repair by NER of lesions throughout the genome.	(Gillet & Scharer 2006)
9	Alternative excision repair	Excision repair of a variety of UV photoproducts. Present in *S.pombe*, absent in *S.cerevisiae*.	(McCready *et al.* 2000)
	Post-replication repair (PRR)	or 'DNA damage tolerance'	(Lehmann & Fuchs 2006) (Lee & Myung 2008)
10	Translesion DNA synthesis (TLS)	PRR by bypass of UV-induced replication-blocks followed by low-fidelity DNA polymerase gap repair.	(Diamant *et al.* 2012)
11	Template switching-dependent synthesis	Error-free repair of bypassed lesions by homologous recombination using the undamaged sister chromatid as a replication template.	(Zhang & Lawrence 2005)
	Repair of DNA strand breaks		(Ciccia & Elledge 2010)
12	Single-strand break repair	Efficient and rapid repair of single-strand gaps.	(Caldecott 2008)
13	Double-strand break (DSB) repair	Repair through homologous recombination: strand invasion and formation of double Holliday junctions with or without crossovers.	(Raji & Hartsuiker 2006) (Kasparek & Humphrey 2011)
14	Single-strand annealing	DSB repair by pairing of regions with microhomology after 5' to 3' exonuclease activity.	(Mansour *et al.* 2008)
15	Synthesis-dependent strand annealing	DSB repair through strand invasion, followed by displacement of resynthesized DNA.	(Miura *et al.* 2012)
16	Non-homologous end joining	DSB repair by processing and annealing of DNA ends.	(Symington & Gautier 2011)
	Checkpoint response		(Finn *et al.* 2012)
17	G1 DNA damage checkpoint	Arrest cells at Start/restriction point. Not in *S.pombe*.	(Bartek & Lukas 2001)
18	Intra-S DNA damage checkpoint	Replication independent. Slows replication by preventing new origins from firing.	(Bartek *et al.* 2004) (Willis & Rhind 2009)
19	G2 checkpoint	Prevents onset of mitosis by inhibiting $Cdk^{cyclinB}$. *S.cerevisiae* arrests in metaphase.	(O'Connell & Cimprich 2005) (Willis & Rhind 2011)
20	Replication checkpoint	Also called replication dependent 'S-M checkpoint'. Replication fork stabilisation during stress and encountering damage.	(Branzei & Foiani 2007)
	Other responses		
21	Cohesin enrichment	Promotes DNA repair and genomic stability. Essential for DSB repair by homologous recombination and rescues stalled replication forks.	(Caron *et al.* 2012) (Wu & Yu 2012)
22	Chromatin remodelling	Increase accessibility of repair complexes at chromatin dense sites. Histone modifications activate checkpoint response and facilitate repair.	(Dinant *et al.* 2008) (Luijsterburg & van Attikum 2011)

#	molecular pathway	function and characteristics	reference(s)
23	(Post-)transcriptional regulation	DNA damage induced gene repression and expression to facilitate repair.	(Rieger & Chu 2004) (Reinhardt *et al.* 2011) (Mannuss *et al.* 2012)
24	Cellular senescence	Preventing further division of cells exposed to genotoxins.	(d'Adda di Fagagna 2008)
25	Apoptosis	Multicellular organisms: Elimination of cells with damaged DNA.	(Borges *et al.* 2008)
26	Adaptation	Inactivation of the DNA damage checkpoint when DNA damage persists.	(Clemenson & Marsolier-Kergoat 2009)

Table 1: The main molecular pathways responding to DNA damage in eukaryotic cells.

1.5.4 The DNA damage response and cell cycle progression

The damage response can act to block cell division or halt DNA replication to prevent passing on damaged and mutated DNA content to progeny. The cell cycle is interrupted at crucial transition points and this control is referred to as the 'DNA damage', 'DNA integrity' or 'DNA structure' checkpoint, or more generally the 'DNA checkpoint' (Su 2006). Differences between organisms and cell types result in different outcomes, as for instance the major point of cell cycle control is the transition from G1 to S phase in metazoa, the transition from G2 to M phase in *S.pombe* (Humphrey 2000) and the metaphase to anaphase transition in *S.cerevisiae*. DNA damage that is detected during S phase generally leads to replication checkpoint-mediated stalling and stabilisation of replication forks that are not restarted until such lesions are repaired (discussed in §1.5.5). In addition, 'firing' of replication origins is blocked in a checkpoint-mediated manner in the presence of DNA damage. This particularly concerns replication origins that are known to fire late in normal S phase (Santocanale & Diffley 1998, Kumar & Huberman 2009).

Pivotal to the cell cycle responding to DNA damage in all organisms, however, are two unrelated protein kinases that transduce the DNA damage signal to the cell cycle machinery (Smith *et al.* 2010, Langerak & Russell 2011, Stolz *et al.* 2011). Chk1 that was originally identified in *S.pombe* (also referred to as Rad27) (Walworth *et al.* 1993), whilst Chk2 (Cds1/Rad53 in yeast) was identified in *S.cerevisiae* and is characterised by an amino terminal forkhead associated (FHA) protein-protein interaction domain (Allen *et al.* 1994). A cell cycle block is achieved through activated Chk1 and Chk2. They phosphorylate and inactivate Cdc25 phosphatase that in turn targets and activates Cdk (Furnari *et al.* 1999, Karlsson-Rosenthal & Millar 2006) to enforce inhibition of the G1 to S or G2 to M transition (see also §1.2). Their recruitment to sites of DNA damage is achieved by the so-called 911 complex and is crucial in establishing a cell cycle arrest.

The heterotrimeric 911 complex, consisting of Rad9/Ddc1, Hus1/Mec3 and Rad1/Rad17, is thought to play a principal role in conveying the DNA damage response to the cell cycle machinery (Eichinger & Jentsch 2011). In a similar fashion to RFC^{Rfc1} enabled loading of PCNA, the 911 clamp is loaded onto DNA by $RFC^{Rad17/Rad24}$ at junctions of single and double strand DNA that are exposed through damage or repair (Bermudez *et al.* 2003, Zou & Elledge 2003). There, 911 recruits ATRIP (Rad26/Ddc2) and the ATR kinase Rad3/Mec1, which sets off a cascade of events that includes phosphorylation of histone H2A and variants (denoted as γ species of H2A or H2AX in yeast and metazoan, respectively) (Barlow *et al.* 2008). This creates binding sites for BRCT (for 'BRCA1 carboxyl-terminal') domain containing adapter proteins, such as 53BP1 (Crb2 or Rhp9/Rad9), Claspin (Mrc1), BRCA1 and Rtt107 (Brc1/Rtt107) (Nakamura *et al.* 2004, Hammet *et al.* 2007, Wilson & Stern 2008). A second binding site that targets the tandem Tudor domain containing protein Crb2/Rad9 is created by methylation of histone H4 at lysine 20 in *S.pombe* or of histone H3 at lysine 79 in *S.cerevisiae* (Finn *et al.* 2012). Accumulation of Crb2/Rad9 is thought to be a crucial step in the activation of Chk1 in *S.pombe* (Saka *et al.* 1997, Mochida *et al.* 2004, Qu *et al.* 2012).

In metazoan cells, unprocessed DNA double strand breakages activate the ATR-related protein kinase ATM through localisation of the MRN complex that consists of the DNA nuclease Mre11, ATPase Rad50[12] and Nbs1 (respectively Rad32/Mre11, Rad50 and Nbs1/Xrs2 in yeast) (Lee & Paull 2005, Finn *et al.* 2012). But as double strand break repair by homologous recombination involves formation of single stranded DNA by resection and the consequent loading of 911, it involves ATR signalling too (Cuadrado *et al.* 2006, Hurley & Bunz 2007). In *S.pombe* and *S.cerevisiae*, however, the ATR kinase Rad3/Mec1 is involved in both single and double strand break detection and repair, whereas the ATM kinase Tel1 is primarily involved in the maintenance of telomere length (Sabourin & Zakian 2008).

Although many components of the DNA damage response pathway are conserved between species, the regulatory connections of ATM and ATR kinase orthologues with Chk1 and Chk2 kinase orthologues have diverged to some extent. ATR activates both Chk1 and Chk2 (Cds1/Rad53) in both *S.pombe* and *S.cerevisiae*. *S.pombe* Chk1 is primarily required for the DNA damage response, whereas the Chk2 kinase Cds1 functions during S phase halting DNA

[12] Rad50 belongs to the SMC ('structural maintenance of chromosomes') family of ATPases (Carter & Sjogren 2012). Other SMC ATPases are the cohesion molecules Smc1 and 3 (respectively Psm1 and Psm3 in *S.pombe*), the condensing molecules Smc2 and 4 (respectively Cut14 and Cut3 in *S.pombe*) and Smc5 and 6 (also known as respectively Spr18 and Rad18 in *S.pombe*) that are involved in DNA repair in association with Rad60/Esc2 (Murray & Carr 2008).

synthesis in the presence of replication stresses (Stewart & Enoch 1996, Furnari *et al.* 1997, Furnari *et al.* 1999, Humphrey 2000, Rhind & Russell 2000). However, activation of Chk1 in the presence of DNA damage during replication does not occur until late S phase and stalling of DNA replication is thus likely signalled through Cds1 (Martinho *et al.* 1998). Either way, Cds1 kinase function is redundant as loss of function is to some extent rescued by Chk1 (Furnari *et al.* 1999). The main target of Chk1 and Chk2 phosphorylation is the Cdc25 phosphatase that must remain inactive, thereby preventing activation of Cdk^{cyclin} complexes to advance the cell cycle (Rhind & Russell 2000).

As in *S.pombe*, the *S.cerevisiae* Chk1 kinase is required for the response to DNA damage and the Chk2 kinase Rad53 is thought to primarily function as a result of DNA replication blocks. As S and M phase partly overlap, *S.cerevisiae* cells enter mitosis in the presence of DNA damage and delay anaphase by targeting and stabilising securin in a Chk1-dependent manner (Cohen-Fix & Koshland 1997, Rhind & Russell 2000, Finn *et al.* 2012). Other pathways that target the mitotic spindle through inhibition of the polo-like kinase Cdc5 by Rad53 (Zhang *et al.* 2009). This ultimately prevents accumulation of the Cin8 and Kip1 kinesin motor proteins that are involved in spindle elongation (Zhang *et al.* 2009).

In metazoan cells ATR activates Chk1 primarily as a result of DNA replication stress, whereas Chk2 activation is a response to severe DNA damage and regulated through ATM activity (Niida & Nakanishi 2006). Phosphorylation of Chk1 or Chk2 in metazoa inhibits the Cdc25A phosphatase that targets Cdk^{cyclin} complexes. The predominant genotoxin-induced delay in metazoa is that of S phase: initiation of DNA replication by Cdc45 is prevented through inhibition of $Cdk2^{cyclin\ E}$ during G1 (Sancar *et al.* 2004). In the presence of permanent DNA damage metazoan cells possess a pathway that depends on the oncosuppressor p53 and can permanently arrest the cell cycle, known as senescence (Blagosklonny 2003), or initiate controlled cell death by apoptosis (Canman *et al.* 1998, Meek 2004).

1.5.5 The DNA damage response during S phase

Many minor forms of DNA damage are thought to remain undetected until they are encountered by DNA replication complexes during S phase. Proteins that can detect DNA damage such as the BRCT domain protein Claspin (Mrc1 in yeast) travel along with the replication fork (Bartek *et al.* 2004, Branzei & Foiani 2007, Labib & De Piccoli 2011, Liu *et al.* 2012b). A replicating DNA strand is particularly vulnerable as unwinding of the double strand exposes two naked single strands. Unintentionally, this process can also convert a single-

stranded break into a complete double strand break. Complexes consisting of RPA (for 'replication protein A') proteins quickly coat exposed single-stranded DNA to serve as a signal for fork stalling. Subsequent 911 loading by $RFC^{Rad17/Rad24}$ and the ATR kinase activity elicits a DNA damage response. In *S.pombe*, Mrc1 recruits the Chk2 kinase Cds1, which is activated by the ATR kinase Rad3 (Tanaka & Russell 2004). A complex signalling pathway (often termed the 'S phase DNA damage checkpoint' or 'intra S checkpoint') that involves metazoan Chk1 and yeast Chk2 (Cds1/Rad53) will stabilise the fork for the duration of the repair process, whilst other replication origins are prevented from firing (Lee *et al.* 2005). Stabilisation of replication forks is of vital importance, as fork collapse often leads to abnormal DNA structures resulting in large stretches of single stranded DNA that are extremely liable to breakage through nuclease activity (Branzei & Foiani 2005).

The ATR response is also elicited when replication forks stall due to causes other than DNA damage (Branzei & Foiani 2007). This can occur at chromosomal sites characterised by dense chromatin or when nucleotides are in short supply. Remarkably, two independent pathways have been identified that are able to sense replication stresses of either the lagging (via the 911 clamp complex) or leading (via DNA polymerase ε) strand (Puddu *et al.* 2011). The 'DNA replication checkpoint' thus responds to DNA replication stresses and subsequent studies revealed that its mechanism is not uniquely or entirely different from that responding to DNA damage during replication (Marchetti *et al.* 2002, Labib & De Piccoli 2011).

The supply of deoxyribonucleotides (dATP, dTTP, dGTP and dCTP) required for DNA replication and repair is strictly regulated as unbalanced dNTP pools can lead to nucleotide misincorporation during DNA synthesis and genomic instability as a consequence. The exceptionally well-conserved ribonucleotide reductase (RNR) is an enzyme that catalyses the reduction of ribonucleotides to their corresponding deoxyribonucleotides (Reichard 1988, Hofer *et al.* 2012). The activity of RNR, which consists of two subunits in *S.pombe* (Cdc22 and Suc22) and four subunits in *S.cerevisiae* (Rnr1, Rnr 2, Rnr 3 and Rnr 4), is tightly regulated (Moss *et al.* 2010). Its inhibition by chemical compounds such as hydroxyurea severely skews the availability of dNTP species hampering DNA synthesis. Prolonged exposure to RNR inhibitors can ultimately result in the creation of single and double strand breaks induced by malfunctioning replication forks (Petermann *et al.* 2010, Feng *et al.* 2011). In addition, ribonucleotides unintentionally incorporated into DNA can in certain cases lead to genomic instability (Dalgaard 2012). Remarkably, DNA repair in *S.cerevisiae* requires a higher concentration of deoxyribonucleotides than that present during normal DNA replication;

artificially increasing this level renders the cells more resistant to genotoxic insults (Chabes *et al.* 2003). The key role of RNR in DNA replication and repair makes it an interesting target for therapeutic drug development and is exploited by several toxic natural products, such as a quinol compound produced by the *Agaricus bisporus* mushroom (FitzGerald *et al.* 1984) and streptonigrin by *Streptomyces flocculus* (Tholander & Sjoberg 2012).

Aims of my study

Chapter 3

A large-scale purification procedure will be developed in conjunction with tandem mass spectrometry protein identification to explore the (1) network of physical interactions of the core spindle checkpoint proteins – Mad1, Mad2, Mad3, Bub1 and Bub3 – in the yeasts *S.pombe* and *S.cerevisiae*, (2) catalogue their phospho-modifications and (3) uncover novel interactors. The formation of distinct spindle checkpoint complexes during a mitotic arrest is an important part of checkpoint signalling. It is, however, anticipated that variations between species in complex formation exist, which sometimes makes the interpretation of cross-species checkpoint models a haphazard undertaking. In addition, the identification of novel spindle checkpoint protein interactors and phospho-modifications could provide mechanistic insights into spindle checkpoint function and the way in which cells monitor and promote chromosome biorientation.

Chapter 4

The interfaces of spindle checkpoint protein complex components will be mapped by identifying *in vitro* cross-linked intermolecular proximate residues by mass-spectrometry analysis. This relatively new and promising technology will allow insight into the manner in which spindle checkpoint protein interact with each other. Ultimately, it is hoped that this technology will provide the means to probe the association of checkpoint proteins with kinetochores and the APC ubiquitin ligase complex.

Chapter 5

The newly identified interactors of the *S.pombe* BUB+ (Bub1, Bub3 and Mad3) complex will be characterised. This concerns the gene product of *SPAC31G5.19* (here named Abo1), Tfg3, Pob3 and Spt16, that all function in the remodelling of chromatin. Insight will be provided into their functional relationship with the spindle checkpoint proteins and their molecular mechanism of action.

2 Material and methods

2.1 Relating to *S.pombe*

2.1.1 Growth and maintenance of *S.pombe*

Several excellent *S.pombe* resources have published over the last decades. In addition to the 'Fission Yeast Handbook' downloadable from Paul Nurse lab's website, the handbook 'Experiments with Fission Yeast' (Alfa 1993) and several papers by Susan Forsburg (Forsburg 2003, Gomez & Forsburg 2004, Forsburg & Rhind 2006) and Paul Nurse (Moreno *et al.* 1991) are of interest.

Generally, plates with yeast were incubated at 32°C or at 25°C in the case of temperature sensitive yeast strains. Liquid cultures of less than 250 mL were generally placed in a shaking water bath set at 32°C (or 25°C for temperature-sensitive yeast) and larger cultures in dry shaking incubators set at 30°C. Cells were typically harvested in mid-log phase (corresponding to an OD_{600} of approximately 0.5 and $5 \cdot 10^6$ cells per mL). The permissive and restrictive temperature for cold-sensitive yeast containing the β-tubulin mutant allele *nda3-KM311* was 32°C and 18°C respectively. Stock collections were maintained frozen at -80°C in YES with the addition of 30% glycerol.

2.1.2 *S.pombe* strains used in this study

#	name	genotype	source
1	SJ510	*abo1-szz::kanmx6 bub1-ha::ura4 bub3Δ::hphmx6 ura4-D18*	this study
2	SJ515	*tfg3-gfp ade6-216 ura4-D18 leu1- h-*	RIKEN, Japan
3	SJ516	*tfg3Δ::LEU2 ade6-216 ura4-D18 leu1- h-*	RIKEN, Japan
4	SJ521	*tfg3Δ::LEU2 abo1-szz::kanmx6 bub1-ha::ura4 ura4-D18*	this study
5	SJ522	*bub1$^{[K762R\ D900N]}$ ade6-216 ura4 h+*	Y.Watanabe
6	SJ543	*abo1::kanmx6 ade6-M210 ura4-D18 leu1-32 h+*	Bioneer v2
7	SJ544	*abo2::kanmx6 ade6-M210 ura4-D18 leu1-32 h+*	Bioneer v2
8	SJ574	*sgo2-cherry::hphmx6 tg3Δ::LEU2 nda3-km311 ura4-D18*	this study
9	SJ576	*sgo2-cherry::hphmx6 bub1$^{[K762R\ D900N]}$ nda3-km311 ura4-D18*	this study
10	SJ578	*bub1Δ::natmx6 nda3-km311 ura4 h+*	this study
11	SJ580	*mad3Δ::ura4 nda3-km311 ura4-D18*	this study
12	SJ581	*abo1Δ::natmx6 nda3-km311 ura4-D18 h-*	this study
13	SJ582	*tfg3Δ::LEU2 nda3-km311*	this study
14	SJ597	*bub1Δ::natmx6 leu1-32 ura4-D18 h-*	this study
15	SJ599	*bub1-camzz::ura4 abo1-gfp::kanmx6 ura4-D18 h+*	this study
16	SJ603	*bub1Δ::ura4 abo1Δ-natmx6 ura4-D18 h+*	this study

#	name	genotype	source
17	SJ604	*bub1Δ::natmx6 tfg3Δ::LEU2 leu1-32 ura4-D18 h+*	this study
18	SJ607	*bub1Δ::natmx6 abo2Δ::kanmx6 leu1-32 ura4-D18*	this study
19	SJ612	*pob3Δ::natmx6 ade6-210 arg3Δ4 his3Δ1 leu1-32*	R.Allshire
20	SJ613	*pob3Δ::natmx6 bub1Δ::ura4 ura4-D18*	this study
21	SJ614	*pob3Δ::natmx6 nda3-km311*	this study
22	SJ616	*bub1Δ::natmx6 mad3Δ::ura4 ura4-D18*	this study
23	SJ622	*bub1-rfp::kanmx6 pob3-gfp::kanmx6 nda3-km311*	this study
24	SJ623	*pob3-gfp::kanmx6*	R.Allshire
25	SJ634	*bub1$^{[1-324]}$-szz::kanmx6 ade6-210 leu1-32 ura4-D18 h-*	this study
26	SJ636	*bub1-szz::kanmx6 ade6-210 leu1-32 ura4-D18 h-*	this study
27	SJ650	*bub1-camzz::ura4 abo1-gfp::kanmx6 bub3Δ::hphmx6 ura4-D18*	this study
28	SJ658	*bub3-szz::kanmx6 abo1-gfp::kanmx6*	this study
29	SJ661	*bub3-szz::kanmx6 abo1-gfp::kanmx6 bub1Δ::natmx6*	this study
30	SJ673	*arp8Δ::kanmx6 ade6-M210 ura4-D18 leu1-32 h+*	Bioneer V2
31	SJ677	*mph1Δ::ura4 leu1-32 h+*	lab stock
32	SJ678	*rad3Δ::ura4 ade6-704 leu1-32 ura4-D18 h-*	A.Carr
33	SJ687	*bub1$^{[Δ264\ -299]}$ -szz::kanmx6*	this study
34	SJ698	*bub1$^{[1-324]}$-szz::kanmx6 abo1-gfp::kanmx6*	this study
35	SJ701	*fta3-tdt::natmx6 tfg3-gfp nda3-km311*	this study
36	SJ704	*fta3-tdt::natmx6 abo1-gfp::kanmx6*	this study
37	SJ707	*mad2Δ::ura4 bub1Δ::natmx6 ura4-D18*	this study
38	SJ723	*fta3-tdt::natmx6 pob3-gfp::kanmx6 nda3-km311*	this study
39	SJ725	*fta3-tdt::natmx6 tfg3-gfp*	this study
40	SJ730	*chk1Δ::ura4 ade6-704 leu1-32 ura4-D18 h-*	A.Carr
41	SJ739	*bub1Δ::natmx6 leu1-32 ura4-DS/E ade6-210 his1-102 ch16 [ade6-216 bub1Δ::ura4]*	this study
42	SJ740	*mph1Δ:: ? leu1-32 ura4-DS/E ade6-210 his1-102 ch16 [ade6-216 bub1Δ::ura4]*	lab stock
43	SJ742	*tfg3Δ::LEU2 leu1-32 ura4-DS/E ade6-210 his1-102 ch16 [ade6-216 bub1Δ::ura4]*	this study
44	SJ744	*abo1Δ::natmx6 leu1-32 ura4-DS/E ade6-210 his1-102 ch16 [ade6-216 bub1Δ::ura4]*	this study
45	SJ749	*pob3Δ::natmx6 leu1-32 ura4-DS/E ade6-210 his1-102 ch16 [ade6-216 bub1Δ::ura4]*	this study
46	SJ750	*abo1-gfp::kanmx6 bub1-rfp::kanmx6 nda3-km311*	this study
47	SJ751	*abo1-gfp::kanmx6 bub1-rfp::kanmx6 nda3-km311*	this study
48	SJ772	*abo1-gfp::kanmx6 bub1$^{[Δ264\ -299]}$ -szz::kanmx6*	this study
49	SJ774	*abo1-gfp::kanmx6 bub1$^{[Δ264\ -299]}$ bub3-szz::kanmx6*	this study
50	SJ776	*spd1Δ::ura4 ade6-704 ura4-D18 leu1 h-*	T.Humphrey
51	SJ777	*spd1Δ::ura4 bub1Δ::natmx6 ura4-D18*	this study
52	SJ778	*spd1Δ::ura4 abo1Δ::natmx6 ura4-D18*	this study
53	SJ790	*cds1Δ::ura4 leu1-32 ura4-D18 h-*	A.Carr
54	SJ793	*mph1Δ::natmx6 leu1-32 ura4-D18*	lab stock
55	SJ820	*abo1-szz::kanmx6 tfg3-gfp pob3Δ::natmx6*	this study

#	name	genotype	source
56	SJ821	*abo1-szz::kanmx6 tfg3-gfp bub1Δ::natmx6*	this study
57	SJ849	*fta3-gfp::kanmx6 sgo2-cherry::natmx6 nda3-km311*	this study
58	SJ851	*fta3-gfp::kanmx6 sgo2-cherry::hphmx6 abo1Δ::natmx6 nda3-km311*	this study
59	SJ881	*rad22Δ::ura4 ade6-210 his1-102 leu1-32 ura4-D18 h-*	R.Allshire
60	SJ882	*rhp54Δ::ura4 ade6-704 leu1-32 ura4-D18 h+*	A.Pastink
61	SJ906	*bub3Δ::ura4 mad3-szz::kanmx6 nda3-km311 ade6-210/216 leu1-32 ura4-D18*	this study
62	SJ961	*mad2-szz::kanmx6 ade6-210 leu1-32 ura4-D18 h-*	this study
63	SJ970	*abo1Δ::natmx6 ade6-210/216 leu1-32 ura4-D18*	this study
64	SJ977	*abo1-szz::kanmx6 ade6-210 leu1-32 ura4-D18 h+*	this study
65	SJ986	*abo1-gfp::kanmx6 ura4-D18 leu1-32 ade6-210/6*	this study
66	SJ987	*abo1Δ::natmx6 / abo1 ade6-M210 / ade6-M216 ura4-D18 / ura4-D18 leu1-32 / leu1-32 h+ / h-*	this study
67	SJ989	*abo1-szz::kanmx6 bub1-ha::ura4 ura4-D18*	this study
68	SJ993	*abo1-gfp::kanmx6 alp4-tdt::natmx6 nda3-km311*	this study
69	SJ996	*SPBPB2B2.06c-szz::kanmx6 ade6-210 leu1-32 ura4-D18 h-*	this study
70	SJ1060	*mad1-szz::kanmx6 nda3-km311 ade6-210 leu1-32 ura4-D18 h-*	this study
71	SJ1087	*fta3-gfp::kanmx6 sgo2-cherry::hphmx6 nda3-km311*	this study
72	SJ1101	*abo1Δ::natmx6 cdc13-gfp::LEU2 nda3-km311 ura4-D18 leu1-32*	this study
73	SJ1103	*tfg3Δ::LEU2 cdc13-gfp::natmx6 nda3-km311 ura4-D18*	this study
74	SJ1104	*bub1Δ::natmx6 cdc13-gfp::LEU2 nda3-km311 ura4-D18 leu1-32*	this study
75	SJ1106	*bub3Δ::ura4 cdc13-gfp::LEU2 nda3-km311 ura4-D18 leu1-32*	lab stock
76	SJ1107	*mad3Δ::ura4 cdc13-gfp::LEU2 nda3-km311 ura4-D18 leu1-32*	lab stock
77	SJ1110	*cdc13-gfp::LEU2 nda3-km311 ura4-D18 leu1-32*	this study
78	SJ1112	*abo1-szz::kanmx6 bub1-ha::ura4 mad3Δ::ura4 ura4-D18*	this study
79	SJ1113	*abo1-szz::kanmx6 bub1-ha::ura4 pob3Δ::natmx6 ura4-D18*	this study
80	SJ1114	*abo1-szz::kanmx6 tfg3-gfp*	this study
81	SJ1115	*abo1-szz::kanmx6 pob3-gfp::kanmx6*	this study
82	SJ1116	*abo1-szz::kanmx6 pob3-gfp::kanmx6 bub1Δ::ura4 ura4-D18*	this study
83	SJ1117	*abo1-szz::kanmx6 pob3-gfp::kanmx6 tfg3Δ::LEU2 ura4-D18*	this study
84	SJ1137	*spd1Δ::ura4 bub1$^{[K762R\ D900N]}$ ura4-D18*	this study
85	SJ1138	*spd1Δ::ura4 bub1$^{[\Delta 264\text{-}299]}$ ura4-D18*	this study
86	SJ1143	*bub1Δ::natmx6 mad1Δ::ura4 ura4-D18*	this study
87	SJ1165	*mad3Δ::ura4 leu1::mad3-gfp ura4-D18 h-*	this study
88	SJ1173	*bub1-szz::kanmx6 mad3Δ::ura4 leu1::mad3-gfp ura4-D18*	this study
89	SJ1174	*bub1-szz::kanmx6 mad3Δ::ura4 leu1::mad3$^{[D69AD79A]}$-gfp ura4-D18*	this study
90	SJ1175	*bub1-szz::kanmx6 mad3Δ::ura4 leu1::mad3$^{[G146V]}$-gfp ura4-D18*	this study
91	SJ1179	*rad22-gfp::kanmx6 bub1-rfp::kanmx6*	this study
92	SJ1182	*mad3Δ::ura4 leu1::mad3$^{[D69AD79A]}$-gfp ura4-D18*	A.Sochaj
93	SJ1184	*mad3Δ::ura4 leu1::mad3$^{[H144V]}$-gfp ura4-D18*	A.Sochaj
94	SJ1185	*mad3Δ::ura4 leu1::mad3$^{[H144V]}$-gfp ura4-D18*	A.Sochaj

#	name	genotype	source
95	SJ1187	*mad3Δ::ura4 leu1::mad3$^{[G146V]}$-gfp ura4-D18*	A.Sochaj
96	SJ1188	*mad3Δ::ura4 leu1::mad3$^{[G146V]}$-gfp ura4-D18*	A.Sochaj
97	KP64	*bub1Δ::ura4 ade6-210 leu1-32 ura4-D18 h-*	lab stock
98	KP105	*bub3Δ::ura4 leu1-32 ade6-210/6 ura4-D18 h+*	lab stock
99	KP106	*bub3Δ::ura4 leu1-32 ade6-210/6 ura4-D18 h-*	lab stock
100	KP114	*ade6-210 leu1-32 ura4-D18 h-*	lab stock
101	KP115	*ade6-210 leu1-32 ura4-D18 h+*	lab stock
102	KP116	*ade6-216 leu1-32 ura4-D18 h-*	lab stock
103	KP145	*bub1Δ::ura4 bub3Δ::ura4*	lab stock
104	KP146	*bub1Δ::ura4 bub3Δ::ura4*	lab stock
105	KP147	*mad1Δ::ura4 leu1*	T.Matsumoto
106	KP155	*bub3Δ::ura4 nda3-km311*	lab stock
107	KP177	*mad2Δ::ura4 h+*	lab stock
108	KP179	*mad3Δ::ura4 h+*	lab stock
109	KP209	*bub1-ha::ura4 leu1-32 ura4-D18*	J.Javerzat
110	KP261	*lid1-camzz::kanmx6 ade6-210 leu1-32 h-*	K.Gould
111	KP340	*nda3-km311 h-*	lab stock
112	KP379	*leu1-32 ura4-DS/E ade6-210 his1-102 ch16 [ade6-216 bub1Δ::ura4]*	lab stock
113	KP466	*hta1$^{[S121A]}$ hta2$^{[S121A]}$ ade6 leu1 ura4 h-*	Y.Watanabe
114	SP22	*mad3-szz::kanmx6 ade6-210 leu1-32 ura4-D18 h-*	lab stock
115	SP24	*bub3-szz::kanmx6 ade6-210 leu1-32 ura4-D18 h-*	lab stock
116	SP26	*mad1-szz::kanmx6 ade6-210 leu1-32 ura4-D18 h-*	lab stock
117	SP30	*bub3-szz::kanmx6 nda3-km311 ade6-210 leu1-32 ura4-D18 h-*	lab stock
118	SP32	*mad2-szz::kanmx6 nda3-km311 ade6-210 leu1-32 ura4-D18 h-*	lab stock
119	SP42	*mad3-szz::kanmx6 nda3-km311 ade6-210 leu1-32 ura4-D18 h-*	lab stock
120	VV96	*bub1-camzz::ura4 ura4-D18 h-*	J.Javerzat
121	VV97	*bub1-camzz::ura4 nda3-km311 ura4-D18 h+*	J.Javerzat
122	VV295	*sgo2Δ::natmx6 leu1-32 lys1-131*	lab stock
123	VV1492	*bub1$^{[Δ264\ -299]}$ leu1-32 ura4-DS/E his1-102 h-*	S.Hauf
124	YJB68	*lid1-camzz::kanmx6 nda3-km311 ade6-210 leu1-32 h-*	lab stock

Table 2: *S.pombe* yeast strains used in this study. Auxotrophic genetic markers and mating types are indicated where known.

2.1.3 *S.pombe* media recipes, supplements and additives

#	name	ingredients
1	YES (yeast extract supplemented)	5 g/L yeast extract, 30 g/L glucose, 1x supplements, 20 g/L agar for solid medium
2	PMG (pombe minimal growth)	3 g/L phtalic acid, 2.2 g/L Na_2HPO_4, 3.75 g/L L-glutamic acid, 20 g/L D-glucose, 1x vitamins, 1x minerals, 1x salts, 20 g/L agar for solid medium
3	SPA (synthetic sporulation agar)	10 g/L D-glucose, 1 g/L KH_2PO_4, 20 g/L agar, 1x vitamins, 1x supplements
4	50x supplement stock	3.75 g/L adenine, uracil, arginine, histidine and lysine, 7.5 g/L leucine
5	1,000x vitamin stock	4.20 mM pantothenic acid, 81.2 mM nicotinic acid, 55.5 mM inositol, 40.8 mM biotin
6	10,000x mineral stock	80.9 mM H_3BO_3, 23.7 mM $MnSO_4$, 13.9 mM $ZnSO_4$, 7.4 mM $FeCl_3$, 2.47 mM MoO_3, 6.02 mM KI, 1.6 mM $CuSO_4$, 47.6 mM citric acid
7	50x salt stock	260 mM $MgCl_2$, 5 mM $CaCl_2$, 670 mM KCl, 14.1 mM Na_2SO_4
8	G418	150 µg/mL G418 sulphate
9	ClonNAT	100 µg/mL nourseothricin
10	Hygromycin	100 µg/mL hygromycin B

Table 3: Recipes for *S.pombe* liquid and solid growth media. All stocks were filter sterilised; supplement stock and additives were added after autoclaving.

2.1.4 DNA transformation of *S.pombe* cells

A culture of 50 mL YES (§2.1.3) was inoculated to reach mid-log phase after overnight growth. About $1 \cdot 10^8$ cells were collected by centrifugation at 2,500g for 3 minutes and washed in sterile water. After resuspension in 100 µL pombe lithium buffer (§2.5.5) and incubation for 1 hour at 30°C, 290 µL pombe PEG buffer and DNA (8x50 µL PCR reactions precipitated and dissolved in 5 µL TE buffer; refer to §2.4.4 and 2.4.5) were added and carefully mixed. After 1 hour incubation at 30°C, cells were heat-shocked at 42°C for 15 minutes. Cells were plated onto YES or selective media plates and incubated at 32°C. Confirmation of locus targeting was obtained by PCR or Western blotting.

2.1.5 Setting up crosses

Cells were plated onto YES medium and the next day mated by mixing two strains of opposite mating type on a SPA plate in a drop of water. The formation and presence of tetraploid zygotes (or zygotic 'tetrads') was confirmed by light microscope after 1 or 2 days at 30°C.

2.1.6 Random spore analysis

A small amount of material containing tetrads was scraped from a SPA plate into 100 µL sterile water with 2 µL β-glucuronidase extract (MP Biomedicals LLC, CA, USA) and incubated for 1 or 2 days at 37°C to eliminate vegetative cells and digest ascus walls. The spores were washed three times in sterile water and plated onto YES medium. After incubation at 32°C for 3 days colonies were subsequently streaked onto appropriate selective media to select for the desired strain.

2.1.7 Tetrad dissection

Cells were sporulated on SPA medium (§2.1.5) and sparsely streaked onto a YES medium plate. Using a MSM micromanipulator (System 300; Singer Instruments Co. Ltd, UK), 10 zygotic (or azygotic spore asci depending on experiment) were selected and isolated and the plate was incubated for about 3 hours at 37°C to allow ascus walls to break down. The four spores were subsequently isolated and lined up using the manipulator. Spore germination and colony development took place by incubation at an appropriate temperature for at least 3 days.

2.1.8 Plate spot assay

Yeast strains were plated out onto YES medium and 10-fold serial dilutions were prepared the next day in a 96-well plate. Using a 48-pin replicator, yeast was spotted onto appropriate solid medium and incubated for a minimum of 3 days at 30°C unless stated otherwise.

2.1.9 Plate recovery assay

Cells from a mid-log phase overnight liquid culture were counted using a haemocytometer and approximately $4 \cdot 10^6$ cells per mL were exposed to genotoxic compounds supplemented to YES medium at the desired concentration. 200 µL culture volumes were incubated in a taped 96-well microplate and agitated at 32°C in a Sunrise microplate reader (Tecan Group Ltd, Switzerland). After the stated number of hours, 10 µL was taken and added to 990 µL of fresh medium, of which 50 µL was diluted 20-fold in sterile water. 200 µL was spread each onto 3 YES plates (plates 1 to 3, plates 4 to 6 for repeat experiment), which corresponds to 400 unexposed cells per plate and at least 2,000-fold dilution of the drug. The relative standard error of this procedure for plates 1 to 3 was typically less than 5% and 10% compared to plates 4 to 6. After 4 days of growth at 32°C, colonies were counted, viability for each strain and condition calculated and visualised by column or line graph.

2.1.10 Cold-sensitive microtubule recovery assay

The viability of mutant yeast in a wild-type and *nda3-KM311* cold-sensitive microtubule background was measured by plating approximately 400 cells from a mid-log phase culture on three warm (32°C) and three cold plates (10°C) each. The latter three plates were placed at 18°C for 10 hours after which they were moved to 32°C. All plates were incubated for 4 days at 32°C after which the number of colonies was counted and viability determined.

2.1.11 Plate irradiation assay

Cells from an overnight liquid culture in mid-log phase were counted using a haemocytometer and approximately 750 colony forming cells were plated out onto 6 plates containing solid YES medium. Three plates (plates 1 to 3, plates 4 to 6 for repeat experiment) were exposed to γ-rays at 6.9 Gy per minute sourced by caesium-137 (GSR-C1 irradiator; Gamma-Service Medical GmbH, Germany) or to 254 nm ultraviolet (UV) light (CX-2000 Crosslinker; UVP LLC, CA, USA). The relative standard error of this procedure for plates 1 to 3 was typically less than 5% and 10% compared to plates 4 to 6. After 4 days of growth at 32°C, colonies were counted, viability for each strain and condition calculated and visualised by column or line graph.

2.1.12 Chromosome loss assay

This method, also referred to as the half-sectoring assay, measures the loss of Ch16, a short linear mini-chromosome containing the *ade6-216* mutant allele that functionally complements the *ade6-210* allele on chromosome 3 and allows cells to grow on medium lacking adenine (Niwa *et al.* 1989, Allshire *et al.* 1995). Additionally, the mini-chromosome as used in this study was deleted for *bub1,* marked with *ura4*$^{+}$.

Cells containing Ch16 were grown overnight to mid-log phase in 3 mL cultures using PMG lacking adenine and uracil (§2.1.3). The cell concentration was determined using a haemocytometer and approximately 400 cells were plated on YES medium that was supplemented with 0.25 g/L adenine rather than 3.75 g/L (§2.1.3). Plates were incubated for 4 days at 32°C, after which the percentage of Ch16 loss was calculated by counting the number of half-sectored and completely white colonies. Partially segmented colonies were not taken into account. The incidence of half-sectored colonies infers the loss of a single chromosome in one cell division due to missegregation.

2.2 Relating to *S.cerevisiae*

2.2.1 Growth and maintenance of *S.cerevisiae*

Plates with yeast were incubated at 30°C. Liquid cultures were generally placed in shaking incubators set at 30°C and cells harvested in mid-log phase (corresponding to an OD_{600} of approximately 0.5). The permissive and restrictive temperature for cold-sensitive yeast bearing the β-tubulin mutant allele *tub2-401* was 30°C and 16°C respectively. Stock collections were maintained frozen at -80°C in YPDA with the addition of 30% glycerol.

2.2.2 *S.cerevisiae* strains used in this study

#	name	genotype	source
1	SJ108	*MAD3-SZZ::KanMX6 prb1-1122 pep4-3 prc1-407 leu2 trp1 ura3-52 MATa*	this study
2	SJ110	*MAD3-SZZ::KanMX6 tub2-401 prb1-1122 pep4-3 prc1-407 leu2 trp1 ura3-52 MATa*	this study
3	SJ123	*tub2-401 prb1-1122 pep4-3 prc1-407 leu2 trp1 ura3-52 MATa*	this study
4	SJ130	*MAD1-SZZ::KanMX6 tub2-423::URA3 prb1-1122 pep4-3 prc1-407 leu2 trp1 ura3-52 MATa*	this study
5	SJ148	*APC4-SZZ::KanMX6 tub2-401 prb1-1122 pep4-3 prc1-407 leu2 trp1 ura3-52 MATa*	this study
6	SJ177	*lys1Δ::NatMX6 prb1-1122 pep4-3 prc1-407 leu2 trp1 ura3-52 MATa*	this study
7	SJ180	*MAD1-SZZ::KanMX6 lys1Δ::NatMX6 prb1-1122 pep4-3 prc1-407 leu2 trp1 ura3-52 MATa*	this study
8	SJ184	*MAD2-SZZ::KanMX6 prb1-1122 pep4-3 prc1-407 leu2 trp1 ura3-52 MATa*	this study
9	SJ185	*BUB3-SZZ::KanMX6 prb1-1122 pep4-3 prc1-407 leu2 trp1 ura3-52 MATa*	this study
10	SJ186	*MAD2-SZZ::KanMX6 tub2-401 prb1-1122 pep4-3 prc1-407 leu2 trp1 ura3-52 MATa*	this study
11	SJ187	*BUB3-SZZ::KanMX6 tub2-401 prb1-1122 pep4-3 prc1-407 leu2 trp1 ura3-52 MATa*	this study
12	SJ192	*SPC25-ZZ lys1Δ::NatMX6 ade2-1 trp1-1 can1-100 leu2-3,112 his3-11,15 ura3 MATa*	this study (W303)
13	SJ206	*MAD1-SZZ::KanMX6 prb1-1122 pep4-3 prc1-407 leu2 trp1 ura3-52 MATa*	this study
14	SJ207	*APC4-SZZ::KanMX6 prb1-1122 pep4-3 prc1-407 leu2 trp1 ura3-52 MATa*	this study
15	SJ208	*YHR202W-SZZ::KanMX6 prb1-1122 pep4-3 prc1-407 leu2 trp1 ura3-52 MATa*	this study
16	SJ219	*prb1-1122 pep4-3 prc1-407 leu2 trp1 ura3-52 MATa*	lab stock JB811
17	JF60	*BUB1-SZZ::KanMX6 prb1-1122 pep4-3 prc1-407 leu2 trp1 ura3-52 MATa*	lab stock
18	JF74	*BUB1-SZZ::KanMX6 tub2-401 prb1-1122 pep4-3 prc1-407 leu2 trp1 ura3-52 MATa*	lab stock
19	KH288	*SPC25-ZZ ade2-1 trp1-1 can1-100 leu2-3,112 his3-11,15 ura3 MATa*	lab stock (W303)
20	PJ69-4	*trp1-901 leu2-3,112 ura3-52 his3-200 gal4Δ gal80Δ LYS2::GAL1-HIS3 GAL2-ADE2 met2::GAL7-lacZ MATa*	lab stock

Table 4: *S.cerevisiae* yeast strains used in this study. Unless stated otherwise, all strains are S288c background.

2.2.3 *S.cerevisiae* media recipes, supplements and additives

#	name	ingredients
1	YPDA	10 g/L yeast extract, 20 g/L Bacto peptone and D-glucose, 0.3 g/L adenine, 20 g/L agar for solid medium
2	minimal medium	7 g/L yeast nitrogen base without amino acids, 20 g/L D-glucose, 1x supplements, 20 g/L agar for solid medium
3	100x supplement stock	2 g/L methionine, 3 g/L uracil and lysine, 6 g/L adenine and histidine, 8 g/L tryptophan and leucine
4	SILAC	Minimal medium with 1x supplements but L-[$^{13}C_6$]-lysine or L-[$^{12}C_6$]-lysine at 1g/L
5	G418	300 µg/mL G418 sulphate
6	clonNAT	100 µg/mL nourseothricin
7	FOA	1 g/L 5-fluoroorotic acid
8	3AT	5 mM 3-amino-1,2,4-triazole

Table 5: Recipes for *S.cerevisiae* liquid and solid growth media. All stocks were filter sterilised; supplement stock and additives were added after autoclaving.

2.2.4 DNA transformation of *S.cerevisiae* cells

A 10 mL yeast culture in YPDA liquid medium was grown overnight at 30°C on a platform shaker to mid-log phase the next day. Cells were harvested by centrifugation at 2,500g for 3

minutes, washed twice in sterile water, once in lithium buffer and resuspended in 100 µL lithium buffer (§2.5.5). To this, 15 µL 10 mg/mL salmon sperm DNA was added, DNA of 8x50 µL PCR reactions precipitated and dissolved in 5 µL TE buffer (refer to §2.4.4 and 2.4.5) and 700 µL PEG buffer. After gentle mixing, incubation at 30°C for 30 minutes, the cells were heat shocked at 42°C for 15 minutes and plated onto YPDA or selective medium. Colonies were analysed by PCR or Western blotting after several days of growth at 30°C.

2.3 Relating to protein

2.3.1 Large-scale purifications of protein complexes

Yeast cells were grown at 30°C in 1.5 litres of 4x concentrated rich YES or YPDA medium (§2.1.3) to high densities that could still support active proliferation and mitotic arrests. Mitotically arrested cells (harbouring cold-sensitive β-tubulin alleles) were obtained by rapid cooling on ice and shifting cultures to 18°C (or 16°C in the case of *S.cerevisiae*) for 7 hours. Cells were harvested by centrifugation at 3,500g for 8 minutes under cold conditions. Pelleted cells were frozen into pea-sized drops using liquid nitrogen and stored at -80°C until further processing. Approximately 25 grammes of cell mass was disrupted using a mixing mill (MM 400; Retsch, Germany) with grinding balls under cryogenic conditions (5 cycles of 3 minutes at 30 Hz). Yeast lysates were reconstituted in 1 mL cold lysis buffer A (§2.5.5) per 1 gramme of milled yeast with the following additions: one tablet of 'complete EDTA-free protease inhibitors' per 50 mL, 1mM Pefabloc SC, 10 µg/mL leupeptin, pepstatin and chymostatin (all from Roche Applied Science, Germany), 5mM NaN_3, 0.4 mM Na_3VO_4, 2 µM microcystin-LR (Axxora Life Sciences, CA, USA), 20 mM β-glycerophosphate and 1% Triton X100. After five 30 second rounds of sonication in a Vibra-Cell (VCX500; Sonics & Materials Inc, CT, USA) cell debris was pelleted at 4,000g and 4°C for 5 minutes and supernatant was subsequently filtered through a Whatman 1.6 micron GD/X glass microfibre syringe filter (GE Healthcare, UK).

Bait proteins were isolated from prepared yeast extracts by a 20 minute incubation with 1 mg IgG-Dynabeads (§2.5.2) per 1 gramme of cell input at 4°C whilst mixing. Dynabeads and associated complexes were washed 4 times with cold buffer A (§2.5.5) and twice with buffer B (§2.5.5).

2.3.2 Elution and precipitation of protein complexes

Protein complexes were eluted from Dynabeads by two 5 minute incubations with 150 µL low-pH buffer D (§2.5.5) at room temperature and precipitated by mixing in 100 µL cold 100% (w/v) trichloroacetic acid and 30 minutes on ice. Protein material was pelleted by

centrifugation for 30 minutes in a cooled centrifuge at 22,000g. Supernatant was aspirated off and the pellet was washed twice in 500 µl of ice-cold acetone and spinning for 10 minutes at 22,000g. Finally, the pellet was air-dried in a sterile laminar flow cabinet.

2.3.3 Tandem mass spectrometry and peptide identification

At the Yates laboratory (Scripps Research Institute, CA, USA) peptide mixtures were generated from the eluted protein complexes through endoproteinase lys-C and trypsin digestion followed by multi-dimensional protein identification technology (MudPIT) analysis. HPLC (for 'high pressure liquid chromatography') was performed by loading the peptides onto a cation exchange column directly followed by a reverse phase column whilst a four-step elution procedure was devised using a solvent gradient of respectively increasing salt and hydrophobicity (Diop *et al.* 2008). Peptides were electro-sprayed into an in-line coupled LTQ 2D linear ion trap mass spectrometer (Thermo Fisher Scientific Inc, IL, USA) set so each step of the multi-dimensional cycle one full-scan mass spectrum of 400 to 2,000 m/z was followed by 5 data-dependent MS/MS spectra at a 35% normalised collision energy.

Mass spectrometry (MS) data were extracted from each raw data file using RawXtract software and peptides identified by the SEQUEST algorithm (Eng *et al.* 1994, Sadygov *et al.* 2002) and searching against a database consisting of the *S.cerevisiae* (SGD 19 August 2008) or *S.pombe* proteome (SGD 15 May 2007). This search allowed for semi-tryptic peptides, a maximum charge state of +3 and three phosphorylated residues per peptide specified as static modifications of +80 Da on serine, threonine and tyrosine residues in MS2 spectra and -18 Da on serine and threonine residues (corresponding to a -98 Da neutral loss of phosphoric acid or dehydration) for MS3 spectra. The resulting data set was filtered using the DTASelect programme (Tabb *et al.* 2002, Cociorva *et al.* 2007) with dynamic quality thresholds and parameters derived empirically using a default false-positive rate that was assessed using a decoy database of reversed protein sequences to maximise sensitivity and accuracy (MacCoss *et al.* 2002, Peng *et al.* 2003). The minimum filter criterion for protein hits was set at two peptides and, finally, data was uploaded to the YRC internet data servers http://depts.washington.edu/yeastrc hosted at the University of Washington (WA, USA).

2.3.4 On-bead cross-linking and tandem MS analysis

The following procedure was performed by Angel Zuo Chen in the Rappsilber lab at the Wellcome Trust Centre for Cell Biology in Edinburgh, UK. Protein complexes bound onto IgG-Dynabeads were cross-linked in buffer B (§2.5.5) using 10 µg BS2G or BS3 cross-linker (Thermo

Fisher Scientific Inc, IL, USA) per milligram Dynabeads on ice for 2 hours. Digestion was performed by adding 0.3 µg of trypsin per 10 µg of on-bead protein complexes in 25 mM ammonium bicarbonate at 37°C for 15 hours. Subsequently, peptides mixtures were fractionated using SCX-STAGE tips (Rappsilber *et al.* 2007, Bohn *et al.* 2010). Flow through was collected and peptides were fractionated by a step-wise salt gradient. Fraction 3 and 4, containing the cross-linked peptides, were desalted using C18-stage tips prior to mass spectrometric analysis (Rappsilber *et al.* 2003).

Peptides were separated on an analytical column packed with C18 material (3 µm ReproSil-Pur C18-AQ; Dr. Maisch GmbH, Ammerbuch-Entringen, Germany) employing a self-assembled particle frit in the spray emitter (Ishihama *et al.* 2006) and loaded at a flow rate of 0.7 µl/min and eluted at 0.3 µl/min into an LTQ Orbitrap (Thermo Fisher Scientific Inc, IL, USA) using a 90 minute linear gradient from 5% acetonitrile in 0.5% acetic acid to 23% acetonitrile in 0.5% acetic acid followed by a 5 minute linear increase from 23% to 80%. High-resolution spectra were acquired for both MS and MS2 scans and FTMS spectra were recorded at 100,000 resolution. The three most intense peaks with a charge state of three or higher were selected in each cycle for ion trap fragmentation and Orbitrap detection at 7,500 resolution.

The peak lists of MS2 spectra were extracted from MS raw files using MaxQuant (Cox & Mann 2008). The top 200 MS/MS peaks per 100 Da were added to the peak list, while all other parameters were kept at default setting. Xi, a software programme developed in-house, was used to search a database that only contained the respective target sequences that includes the ZZ tag sequence of the baited protein used to purify the complexes. Search parameters were: MS accuracy of 6 ppm, MS/MS accuracy of 20 ppm, fully tryptic trypsin enzyme specificity with a maximum of 4 missed cleavages, variable modifications that includes oxidation of methionines, BS2G or BS3 mono-link reacted with water or ammonia on lysines and protein amino termini. For SILAC labeled samples, the L-[$^{13}C_6$]-lysine label was also included as a variable modification.

2.3.5 Small scale purifications of protein complexes

A 100 mL yeast culture in YES medium was grown overnight at 30°C on a platform shaker to mid-log phase. Cells were harvested by centrifugation at 2,500g for 3 minutes, washed twice in sterile water and the cell pellet snap frozen in liquid nitrogen or dry ice. Cells were broken in three cycles of 20 seconds with a Mini-Beadbeater 8 (BioSpec Products Inc, OK, USA) in the presence of approximately 200 µL 0.5 mm zirconia-silica beads (BioSpec Products Inc, OK,

USA), 400 µL ice cold buffer C (§2.5.5) with 1mM Pefabloc SC, 10 µg/mL leupeptin, pepstatin and chymostatin (all from Roche Applied Science, Germany), 0.4 mM Na_3VO_4, 2 µM microcystin-LR (Axxora Life Sciences, CA, USA) and 20 mM β-glycerophosphate. The lysate was cleared by a 3 minute centrifugation at 10,000g and 4°C, transferred to a fresh tube, spun again at the same settings after which the tube was turned by 180° in the rotor and spun once again. Supernatant was transferred to a fresh tube and 100 µg IgG Dynabeads (§2.5.2) was added. After a 20 minute incubation on a rotating wheel, beads were collected by binding to a magnet, washed four times in ice cold buffer C (§2.5.5). Protein complexes were released from the Dynabeads by a 20 minute incubation in an appropriate volume of protein sample buffer (§2.5.5) without DTT. Supernatant was collected and DTT added to a final concentration of 100 mM.

2.3.6 Whole cell extract preparation for SDS-PAGE

Cells of 3 mL overnight cultures were collected by centrifugation at 2,500g for 3 minutes, washed in 1 mL sterile water and cell pellets snap frozen in liquid nitrogen or dry ice. Approximately 150 µL 0.5 mm zirconia-silica beads (BioSpec Products Inc, OK, USA) and 200 µL ice cold sample buffer (§2.5.5) with 1mM Pefabloc SC, 10 µg/mL leupeptin, pepstatin and chymostatin (all from Roche Applied Science, Germany) were added prior to cell disruption using a FastPrep ribolyser (FP120; Thermo Fisher Scientific Inc, IL, USA) at speed 4.0 for 20 seconds. Extract were once again snap frozen and subsequently boiled at 95°C for 5 minutes and spun at full speed in a table top centrifuge for 3 minutes. Supernatant was stored at -80°C or directly loaded onto gel.

2.3.7 Protein SDS-PAGE

Proteins were resolved on 50x185x1mm gels with 18 or 25 stacking wells by polyacrylamide gel electrophoresis (PAGE). Gels were prepared as indicated in Table 6 below and, after sample loading, run for a minimum of 1.5 hours at 150 V in PAGE buffer (§2.5.5).

#	name	10% (mL)	12.5% (mL)	15% (mL)	stacking gel (mL)
1	40% acrylamide	3.70	4.70	5.60	6.25
2	2% bis-acrylamide	0.98	0.75	0.64	3.33
3	1.5 M Tris-HCl (pH8.8)	3.75	3.75	3.75	-
4	1.0 M Tris-HCl (pH6.8)	-	-	-	6.25
5	H_2O	6.57	5.80	5.01	34.2
6	10% (w/v) APS	0.5%	0.5%	0.5%	1%
7	TEMED	0.5‰	0.5‰	0.5‰	1‰

Table 6: Three recipes for 15 mL resolving polyacrylamide gels and 50 mL stock solution for generic stacking gel to be kept at 4°C. Ammonium persulfate (APS) and tetramethylethylenediamine (TEMED) were added, volume to volume, immediately prior to *in situ* gel polymerisation.

2.3.8 Precast protein gel electrophoresis

Protein samples were prepared in NuPage LDS sample buffer (Life Technologies Corp, CA, USA) containing 100 mM dithiothreitol (DDT) and loaded onto NuPage Bis-Tris (Life Technologies Corp, CA, USA) mini gels prepared according to manufacturer's instructions. Gels were run in NuPAGE MOPS-SDS running buffer (Life Technologies Corp, CA, USA) for 50 minutes at a constant 200 V.

2.3.9 Western blotting and detection by ECL

Following SDS-PAGE, proteins were transferred onto 0.2 µm Protran nitrocellulose membrane (GE Healthcare, UK) by using a semi-dry transfer unit (Hoefer Inc, MA, USA) using 10 or 20% methanol buffer (§2.5.5) depending on protein-of-interest size. The membrane and PAGE gel were sandwiched between four pieces of 3MM Whatman paper (GE Healthcare, UK), all soaked in transfer buffer. Transfer was carried out for 1.5 hours at a constant 1.6 mA/cm^2, bound protein visualised using Ponceau S solution (§2.5.5) and the blot washed in PBS (§2.5.5).

The membrane was blocked in blotto (§2.5.5) for 15 minutes at room temperature with gentle shaking, after which binding of the primary antibody (Table 7) was done overnight at 4°C on a rocking platform. After 3 blotto washes of 10 min each, horseradish peroxidase (HRP) conjugated ('secondary') antibody (Table 7) incubation was done for a minimum of three hours at room temperature and the membrane washed 3 times for 10 minutes with blotto. The blot was rinsed with PBS and enhanced chemiluminescent (ECL) substrate was prepared by mixing equal volumes of SuperSignal West enhancer solution with peroxide solution (Thermo Fisher Scientific Inc, IL, USA). The membrane was immersed in this mixture for up to 3 minutes, excess substrate removed and the membrane laid onto a glass plate and covered in a single layer of cling film. Several exposures of the membrane to medical x-ray film (Agfa Healthcare

NV, Belgium) were done in the dark and film was processed by a SRX-101A medical film developer (Konica-Minolta Holdings Inc, Japan)

#	generic name	epitope	type	source	working concentration
1	α-HA	HA	mouse HA11 (16B12) ascites	Thermo Fisher Scientific, IL, USA	1:5,000
2	α-GFP	GFP	sheep; affinity purified	lab stock	1:500
3	α-S	S peptide	mouse mono-clonal	GE Healthcare, UK	1:5,000
4	α-peroxidase (PAP)	ZZ tag binding	rabbit IgG HRP conjugate	Sigma-Aldrich, MO, USA	1:5,000
5	α-mouse	mouse IgG	sheep IgG HRP conjugate	GE Healthcare, UK	1:5,000
6	α-sheep	sheep IgG	donkey IgG HRP conjugate	GE Healthcare, UK	1:5,000

Table 7: Primary and secondary antibodies used in this study. All antibodies were diluted in blotto buffer (§2.5.5).

2.3.10 Colloidal blue stain

SDS-PAGE gels were washed once for 5 minutes in sterile water and pre-fixed with a 50% methanol and 7% acetic acid solution for 15 minutes after which they were washed three times 5 minutes in water. GelCode Blue Stain (Thermo Fisher Scientific Inc, IL, USA) solution containing colloidal Coomassie Brilliant Blue G-250 dye was applied overnight and gels were scanned using a flat-bed scanner (Perfection 2450; Seiko-Epson Corp, Japan) after washing three times with water for one hour total.

2.4 Relating to DNA

2.4.1 DNA oligonucleotides used in this study

SJo	sequence	use
1	GAATCTATGGGTGGAAGATAGAGGTCAACTTCCGTGCTTTTTGGCAACAATAACATTGCGTCTGTGGGAACAGCGACAAGCCAAACGGATCCCCGGGTTAATTAA	F CT scMad1
2	AGGAATCATAAAAGGTCAATGATGAAGAAAGATAAAAGAATTTTGTGACCAACAATTATGTCAGCGGATAGGAGTTTATCGAATTCGAGCTCGTTTAAAC	R CT scMad1
11	TTTTTCTCAGTACACCACAGGCGGGTTCCAAACTTCTTCATAGTGCGCCATACAAAAGAAAAGTCTTGGGGAATTCGAGCTCGTTTAAAC	R CT scApc4
12	CATAGCATGCACCGCGAAGGTATCGGTGGATGGAAGAAGCGCATCCCTAGTGTTTCCAAAAGAAAAACAAAATGTTCGGATCCCCGGGTTAATTAA	F CT scApc4
25	ATAACAACGAAAACGCTTTATTTTTCACACAACCGCAAAACGGATCCCCGGGTTAATTAA	F Δ scLys1
26	AATGTCAGCGTAACGATAATGTATATACTTTAAATGTAAAGAATTCGAGCTCGTTTAAAC	R Δ scLys1
75	AATACGAAGTCCGAATGGAATAGAAACTCTGTGGTTGATGAATGCGAGCGAGCAGTAAAAGAGTTTATGATTAATGCACTACAACGGATCCCCGGGTTAATTAA	F CT spAbo1
76	TAATGTATTAAAAAAATTTCAGCTTAAGCGAATACTTTCGTCATTCTGTATCAAAAATATGTAGCAATTCTCGACCATTATTCAGAATTCGAGCTCGTTTAAAC	R CT/Δ spAbo1
77	TAGTACAGATGGCAATGTATTATCTAACGGTTATTCTCAACTACCGAACGAGGACGACGCTCAACATAGCGATAATGTTGAAATGCGGATCCCCGGGTTAATTAA	F Δ spAbo1
85	CCTGATGGTGAAGTAGTTCAATTCAAAACATTCTCTACCAACGATCATAAAGTTGGTGCGCAGGTCAGCTATAAATATCGGATCCCCGGGTTAATTAA	F CT scMad2
86	GTACGTAGTATAGTATAATATAGTTCATAAATCTATATTCTTTCTAAACATCGAAAACGAGATTTTTTTGGACTTCCGGAATTCGAGCTCGTTTAAAC	R CT scMad2
87	TCTCAAAGCAAAAATTCTGAGATCATTTCAGATGATGACAAGTCGAGTTCGTCTTTCATATCGTACCCACCACAGCGTCGGATCCCCGGGTTAATTAA	F CT scMad3
88	TCGTTAAATAATCATTATATCATCTGTGCTTTAAATAAAAAAGTCGGCCGCCGATGTGTTTACGATTGGCCAGTATACGAATTCGAGCTCGTTTAAAC	R CT scMad3
93	TTTCAAGACAAACGCCGCAATTGACCAAACTATTGAACTAAACGCAAGTTCAATATACATAATATTTGACTATGAGAACCGGATCCCCGGCTTAATTAA	F CT scBub3
94	GATGATTGATCTATATATAATTTTTCTAGCAGATCCTATTTACTTAATCTATGTATGTGATTTTTTCTTTATTCCTTAAGAATTCGAGCTCGTTTAAAC	R CT scBub3

SJo	sequence	use
172	GGGGACAAGTTTGTACAAAAAAGCAGGCTTCTCCGATTGGCGGCTTACAGAAAATG	F attB spBub1
173	GGGGACCACTTTGTACAAGAAAGCTGGGTCGGATGAAGATGAATCATGATGCAC	R attB spBub1a
174	GGGGACAAGTTTGTACAAAAAAGCAGGCTTCAATGTATCACCTATTTACAAGAACC	F attB spBub1b
175	GGGGACCACTTTGTACAAGAAAGCTGGGTCACTTCTTCGACGTCCAGGGCCAC	R attB spBub1b
176	GGGGACAAGTTTGTACAAAAAAGCAGGCTTCAGCAATCGACACTCTCTTGATGG	F attB spBub1c
177	GGGGACCACTTTGTACAAGAAAGCTGGGTCAATTTTTCTTTTTTCGATGCTTTTTAAT	R attB spBub1
205	CAATTGGCATCGAAAGCCATAGCCCTTGAACTCGCTTTG	F M spBub1$^{GIG>AIA}$
206	CAAAGCGAGTTCAAGGGCTATGGCTTTCGATGCCAATTG	R M spBub1$^{GIG>AIA}$
207	CAATTGGCATCGAAAGGCAACGGCCTTGAACTCGCTTTG	F M spBub1$^{GIG>GNG}$
208	CAAAGCGAGTTCAAGGCCGTTGCCTTTCGATGCCAATTG	R M spBub1$^{GIG>GNG}$
209	GGGGACAAGTTTGTACAAAAAAGCAGGCTTCAGTAAAGGAGAAGAACTTTTCACTGG	F attB GFP
210	GGGGACCACTTTGTACAAGAAAGCTGGGTCTTTGTATAGTTCATCCATGCC	R attB GFP
233	GGGGACAAGTTTGTACAAAAAAGCAGGCTTCGAACCATTAGATGCTGGCAAGA	F attB spMad3
238	GGGGACCACTTTGTACAAGAAAGCTGGGTCTTCTTTCGATACTTCCTCATCAC	R attB spMad3
346	TCTTTCTTGGCACATCATCATATTGTGCAGGAGTCCTCGATT	F M spMad3$^{HIG>HIV}$
347	AATCGAGGACTCCTGCACAATATGATGATGTGCCAAGAAAGA	R M spMad3$^{HIG>HIV}$
348	TCTTTCTTGGCACATCATGTGATTGGACAGGAGTCCTCGATT	F M spMad3$^{HIG>VIG}$
349	AATCGAGGACTCCTGTCCAATCACATGATGTGCCAAGAAAGA	R M spMad3$^{HIG>VIG}$
350	CGATCCAAACTTGTAGTGGAGCAGCAAGAGACTCGCTCGTCTC	F M spMad3$^{DDP>AAP}$
351	GAGACGAGCGAGTCTCTTGCTGCTCCACTACAAGTTTGGATCG	R M spMad3$^{DDP>AAP}$

Table 8: DNA oligonucleotide sequences (5' to 3') used in this study. All were ordered from Sigma-Genosys (Sigma-Aldrich, MO, USA) in desalted form or purified by reverse phase, reconstituted in sterile water to 100 µM on arrival and stored at -20°C. Key: M = mutagenesis primer, attB = Gateway cloning primer, Δ = deletion primer, CT = carboxy terminal tagging, F = forward sequence, R = reverse sequence, sc = *S.cerevisiae*, sp = *S.pombe*.

2.4.2 DNA plasmids used in this study

#	original name	description	source	reference
1	pTH18	*tub2-401* mutant allele; *Ura3* selection marker	Tim Huffaker Cornell University, USA	(Huffaker *et al.* 1988)
2	pKW804	C-terminal S-TEV-ZZ tag; KanMX selection marker	Karsten Weis University of California, USA	(Brune *et al.* 2005)
3	pFA6a-NatMX6	gene disruption cassette; NatMx selection marker	Anthony Carr University of Sussex, UK	(Hentges *et al.* 2005)
4	pFA6a-GFP-KanMX6	C-terminal GFP tag; KanMX selection marker	John Pringle; Stanford University, USA	(Longtine *et al.* 1998)
5	pDONR201	Gateway donor vector	Life Technologies Corp, USA	-
6	pDEST22	yeast two-hybrid GAL4 AD; *TRP1* selection marker	Life Technologies Corp, USA	-
7	pDEST32	yeast two-hybrid GAL4 DBD; *LEU2* selection marker	Life Technologies Corp, USA	-
8	pDONR201-GFP	GFP donor vector	this study	-
9	pDONR201-Bub1	*S.pombe* Bub1 full length	this study	-
10	pDONR201-Bub1a	*S.pombe* Bub1a fragment	this study	-
11	pDONR201-Bub1b	*S.pombe* Bub1b fragment	this study	-

#	original name	description	source	reference
12	pDONR201-Bub1c	*S.pombe* Bub1c fragment	this study	-
13	pDONR201-Bub1a$^{GIG>AIA}$	*S.pombe* Bub1 GIG mutant	this study	-
14	pDONR201-Bub1a$^{GIG>GNG}$	*S.pombe* Bub1 GIG mutant	this study	-
15	pDONR201-Mad3	*S.pombe* Mad3 full length	this study	-
16	pDONR201-Mad3$^{HIG>HIV}$	*S.pombe* Mad3 HIG mutant	this study	-
17	pDONR201-Mad3$^{HIG>VIG}$	*S.pombe* Mad3 HIG mutant	this study	-
18	pDONR201-Mad3$^{DDP>AAP}$	*S.pombe* Mad3 DDP mutant	this study	-
19	pDEST22-Bub1	two-hybrid prey vector	this study	-
20	pDEST22-GFP	two-hybrid prey vector	this study	-
21	pDEST22-Bub1a	two-hybrid prey vector	this study	-
22	pDEST22-Bub1b	two-hybrid prey vector	this study	-
23	pDEST22-Bub1c	two-hybrid prey vector	this study	-
24	pDEST22-Bub1a$^{GIG>AIA}$	two-hybrid prey vector	this study	-
25	pDEST22-Bub1a$^{GIG>GNG}$	two-hybrid prey vector	this study	-
26	pDEST32-GFP	two-hybrid bait vector	this study	-
27	pDEST32-Mad3	two-hybrid bait vector	this study	-
28	pDEST32-Mad3$^{DDP>AAP}$	two-hybrid bait vector	this study	-
29	pDEST32-Mad3$^{HIG>HIV}$	two-hybrid bait vector	this study	-
30	pDEST32-Mad3$^{HIG>VIG}$	two-hybrid bait vector	this study	-
31	pDEST32-Bub1a	two-hybrid bait vector	this study	-

Table 9: DNA plasmids used in this study.

2.4.3 Genomic DNA extraction from yeast

Cells from a 3 mL overnight culture were collected by centrifugation at 2,500g for 3 minutes and washed in sterile water. 200 µL of 0.1 mm glass beads (BioSpec Products Inc, OK, USA), 200 µL XSE buffer (§2.5.5) and 200 µL phenol chloroform mixture (§2.5.5) were added to the cell mass prior to vortexing for 5 minutes. 200 µL TE buffer was added and the phases separated by centrifugation at 18,000g for 10 minutes. The aqueous phase was transferred to a new tube and DNA precipitated according to the protocol in section 2.4.5.

2.4.4 DNA amplification by PCR

#	amount	component
	50 µL high-fidelity PCR reactions	
1	3.5 units	Expand HiFi DNA polymerase (Roche Applied Science, Germany)
2	5 µL	Expand Long Template PCR buffer #2 (Roche Applied Science, Germany)
	10 µL Taq PCR reactions	
1	1 µL	Taq polymerase (lab stock)
2	1 µL	Taq buffer (§2.5.5)
	other components	
3	0.5µM	forward primer (§2.4.1)
4	0.5µM	reverse primer (§2.4.1)
5	0.2mM	dATP, dTTP, dGTP and dCTP
6	*varying*	0.5 µg/mL plasmid DNA (§2.4.2) or 4 µg/mL genomic DNA
7	*varying*	sterile double-distilled water to final reaction volume

Table 10: Typical PCR reactions as performed in this study. Lab-made Taq polymerase was used for diagnostic purposes, whereas the high fidelity enzyme was used for DNA cloning or transformation purposes.

step	temperature (°C)	time (s)	remarks
1	95	180	initial denaturing temperature
2	95	20	denaturing temperature
3	52-60*	20	annealing temperature
4	72	60**	extension temperature
5	*cycle back to step one 29 times*		
6	72	300	final extension temperature
7	4	∞	cool reaction

Table 11: Typical PCR reaction conditions used in this study. All reactions were run in a DNA Engine thermal cycler (Bio-Rad Laboratories Inc, CA, USA). * Typically 54°C depending on primers, ** per kb.

2.4.5 DNA precipitation

DNA was precipitated by the addition of 1/10th volume of 3M NaOAc and 2.5 volumes of ice-cold 100% ethanol. After incubation on ice for 30 minutes, DNA was pelleted by centrifugation at 18,000g for 15 minutes, washed with an appropriate volume of 70% ethanol and once again pelleted by centrifugation. Supernatant was aspirated and the DNA air dried for 15-30 minutes. Finally, DNA was dissolved in an appropriate volume of TE buffer (§2.5.5).

2.4.6 DNA cloning by Gateway recombination technology

The Gateway DNA cloning technology (Life Technologies Corp, CA, USA) relies on the site-specific recombination of *attB* with *attP* and *attL* with *attR* short DNA sequences catalysed respectively by BP and LR clonase. It is based on integration of bacteriophage λ into the *E.coli*

chromosome and the switch between the lytic and lysogenic pathway. Gateway DNA cloning was carried out according to manufacturer's instructions. Briefly, oligonucleotides were designed that carry *attB* and gene-specific sequences to generate an *attB* flanked sequence of interest by PCR amplification (§2.4.4). BP clonase-mediated recombination into an *attP*-bearing 'donor vector' (pDONR vector range) to create an 'entry vector' was followed by transformation of DH5α cells (§2.4.9) that were sensitive to the lethal *ccdB* gene product. Selection takes place due to the presence of lethal *ccdB* sequence in 'donor vectors' that was replaced by the sequence of interest in 'entry vectors'. Subsequently, the final 'expression vector' was created by BP clonase-mediated recombination of the 'entry vector' with an appropriate 'destination vector' (pDEST series). Vectors used and created are listed in Table 9.

2.4.7 DNA restriction digests

Typically, around 200 ng of DNA was digested using appropriate restriction endonucleases and buffers from New England BioLabs Inc (MA, USA) in 10 µL volumes at 37°C for 2 hours. For double digests, the online 'NEB double digestion chart' was consulted. DNA was visualised using a UV light source set at 254 nm wavelength. Reactions were scaled up for DNA transformation purposes and typically performed overnight at 37°C with the inclusion of 100 µg/mL BSA, after which DNA was precipitated and dissolved in TE buffer (§2.4.5).

2.4.8 DNA gel electrophoresis

For diagnostic purposes, DNA was suspended in 1x DNA sample buffer (§2.5.5) and typically loaded onto 0.8% (w/v) agarose gels prepared in TBE buffer containing 0.25 mg/mL ethidiumbromide and run using TBE buffer (§2.5.5).

2.4.9 Bacterial plasmid DNA transformation and purification

For propagation and purification purposes DNA vectors were transformed into chemically competent *E.coli* DH5α (lab stock or 'Library Efficiency cells' from Life Technologies Corp, CA, USA) or XL1-Blue MRF' (Agilent Technologies Inc, CA, USA) cells. *E.coli* DB3.1 cells (Life Technologies Corp, CA, USA) were used for Gateway unmodified pDONR or pDEST vectors (§2.4.2) where the *gyrA462* mutation provides resistance to the *ccdB* gene (Table 12). Transformation typically involved thawing of the bacterial stock on ice, addition of DNA, incubation on ice for a further 30 minutes, a 45 second heat shock in a 37°C water bath, addition of 200 µL of SOC medium (Table 12) and incubation for 1 hour at 37°C whilst shaking. Finally, cells were plated on LB solid media containing the appropriate antibiotic (Table 12) and incubated overnight at 37°C.

#	item	details
1	DH5α genotype	*F- Φ80lacZΔM15 Δ(lacZYA-argF) U169 recA1 endA1 hsdR17(r_{k^-}, m_k+) phoA supE44 thi-1 gyrA96 relA1 λ-*
2	XL1-Blue MRF' genotype	*Δ(mcrA)183 Δ(mcrCB-hsdSMR-mrr)173 endA1 supE44 thi-1 recA1 gyrA96 relA1 lac [F' proAB $lacI^q$ZΔM15 Tn10 (Tet^r) Amy Cam^r]*
3	DB3.1 genotype	*F- gyrA462 endA1 glnV44 Δ(sr1-recA) mcrB mrr hsdS20(r_{B^-}, m_{B^-}) ara14 galK2 lacY1 proA2 rpsL20(Sm^r) xyl5 Δleu mtl1*
4	LB recipe	10 g/L tryptone, 5 g/L yeast extract, 5 g/L NaCl (pH7.2), 20 g/L agar for solid media
5	SOC recipe	20 g/L tryptone, 5 g/L yeast extract, 2.5 mM KCl, 10 mM $MgCl_2$, 20mM D-glucose, 5 g/L NaCl (pH7.2)
6	kanamycin	50 µg/mL working concentration
7	ampicillin	50 µg/mL working concentration
8	gentamycin	50 µg/mL working concentration

Table 12: Genotype of bacterial strains used in this study, recipes for bacterial media and antibiotic concentrations.

A single colony was picked to inoculate a 3 mL LB medium culture containing the appropriate antibiotic (Table 12) and incubated in a rotating wheel at 37°C. The next day, cells were harvested by centrifugation and plasmid DNA was purified using a GeneJet miniprep kit (Thermo Fisher Scientific Inc, IL, USA) according to manufacturer's instructions that are based on the alkaline lysis method developed by Birnboim and Doty (Birnboim & Doty 1979). DNA was stored in TE buffer (§2.5.5) at -20°C.

2.4.10 Site-directed mutagenesis of DNA vectors

In vitro site-directed mutagenesis on plasmid DNA was performed by using the QuikChange II kit (Agilent Technologies Inc, CA, USA), which relies on the extension of complementary mutagenic primers (§2.4.1) by high-fidelity PCR, digestion of methylated template DNA with *Dpn*I endonuclease and transformation of the mutated molecule into ultra-competent *E.coli* cells for nick repair. Plasmid DNA of several colonies was isolated (§2.4.9) and analysed by DNA sequencing (§2.4.11) using an appropriate oligonucleotide sequence.

2.4.11 DNA sequencing

Sequencing of DNA plasmids or fragments was carried out by Sanger dideoxy technology on an ABI 3730 capillary DNA electrophoresis instrument (Life Technologies Corp, CA, USA) at the GenePool facility (University of Edinburgh, UK). 10 µL sequencing reactions were set up using approximately 150 ng DNA, 1.5 µM DNA primer and 2 µL BigDye Terminator v3.1 mix (Life Technologies Corp, CA, USA). PCR cycling was carried out using an annealing temperature of 54°C and a 4 minute extension at 60°C (§2.4.4).

2.5 Miscellaneous

2.5.1 Yeast two-hybrid assay

Yeast two-hybrid vectors were created by Gateway recombination technology (§2.4.6) using low-copy pDEST22 and pDEST32 vectors (Life Technologies Corp, CA, USA) that provide *ADH1* promoter driven expression of the gene of interest fused to *GAL4* transcription activator or *GAL4* DNA binding domain sequences, respectively. *S.cerevisiae* strain PJ69-4 (§2.2.2) (James *et al.* 1996) was transformed using the appropriate combination of vectors and maintained on minimal medium lacking leucine and tryptophan (§2.2.3). Interactions were identified on minimal medium also lacking histidine or adenine. Increased sensitivity was obtained by adding 3-amino-1,2,4-triazole (3AT) to medium lacking histidine, leucine and tryptophan. 3AT is a competitive inhibitor of the *HIS3* gene product and thus titrates *HIS3* expression levels required for histidine prototrophic yeast.

2.5.2 IgG coupling to Dynabeads

Rabbit IgG antibodies (I5006; Sigma-Aldrich, MO, USA) were covalently coupled to Epoxy Dynabeads (M-270; Life Technologies Corp, CA, USA) following manufacturer's directions. Briefly, 300 mg Dynabeads were washed twice in phosphate buffer (§2.5.5) and incubated with 6 mg IgG for 24 hours at 37°C under gentle shaking in 15 mL PBS with 1.0 M $(NH_4)_2SO_4$. Following this, IgG-Dynabeads were washed twice with PBS (§2.5.5), twice with PBS with the inclusion of 0.5% (v/v) Triton X100, twice with PBS and stored in PBS at 20 mg/mL with the addition of 0.1% (w/v) NaN_3 at 4°C.

2.5.3 Bioinformatics tools, repositories, protein structure models and illustrations

The software and other tools used to generate 3D protein structure representations, sequence alignments and sequence analysis in this report are listed in Table 13. Table 14 contains detailed information on the PDB structure data used and, additionally, the workflow for homology models made in this work. PDB data files were downloaded from the RCSB Protein Data Bank, edited in WordPad (Microsoft Corp, USA) and viewed using PyMol software (Schrödinger LLC, USA). Electrostatic surface of molecules were calculated and presented from within Pymol using the APBS plugin tool. High resolution figures were rendered in CMYK colours using the 'ray' command, saved in PNG format and edited in Photoshop CS5 (Adobe Sytems Corp, USA).

#	software / database	version	URL	reference
1	ABPS	1.2	www.poissonboltzmann.org/apbs	(Baker *et al.* 2001)
2	Chiron	17.01.2013	dokhlab.unc.edu/tools/chiron	(Ramachandran *et al.* 2011)
3	ClustalΩ	1.1.0	www.ebi.ac.uk/Tools/msa/clustalo	(Sievers *et al.* 2011)
4	ClustalW2 phylogeny	2.1	www.ebi.ac.uk/Tools/phylogeny	(Goujon *et al.* 2010)
5	Conserved Domain Database (CDD)	3.10	www.ncbi.nlm.nih.gov/cdd	(Marchler-Bauer *et al.* 2011)
6	I-TASSER	2.1	zhanglab.ccmb.med.umich.edu/i-tasser	(Roy *et al.* 2010)
7	Image Studio Lite	3.1	www.licor.com/islite	-
8	Interactive Tree of Life (iTOL)	2.2.1	itol.embl.de	(Letunic & Bork 2011)
9	InterProScan	4.8	www.ebi.ac.uk/interp	(Quevillon *et al.* 2005)
10	NCBI	-	www.ncbi.nlm.nih.gov	-
11	OrthoDB	6	www.orthodb.org	(Waterhouse *et al.* 2013)
12	PDBePISA	1.41	www.ebi.ac.uk/pdbe/pisa	(Krissinel & Henrick 2007)
13	PhylomeDB	29.03.2013	www.phylomedb.org	(Huerta-Cepas *et al.* 2011)
14	PomBase	-	www.pombase.org	(Wood *et al.* 2012)
15	Protein Data Bank (PDB)	-	www.rcsb.org	(Berman *et al.* 2000)
16	PyMol	1.5.0.5	www.pymol.org	-
17	Sequence Identity And Similarity	18.2.13	imed.med.ucm.es/Tools/sias.html	-
18	*Schizosacch.* Comp. Genome Project	29.03.2013	www.broadinstitute.org	(Rhind *et al.* 2011)
19	TreeFam	8.0	www.treefam.org	(Ruan *et al.* 2008)
20	UniProt	2013_03	www.uniprot.org	(Magrane & Consortium 2011)

Table 13: Information on software and tools used for sequence analysis, database searches and protein structure modelling.

Homology models were created using I-TASSER software developed by the Yang Zhang lab at the University of Michigan (MI, USA). Structure alignments were made in PyMol using the 'align' command at default settings. The Chiron software used to refine dimerisation interfaces is developed by Nikolay Dokholyan group at the University of North Carolina (NC, USA) and contact residues determined using the PISA server hosted at the European Bioinformatics Institute (Cambridge, UK).

#	protein / complex	species	figure (page)	PDB id	comments & reference(s)
1	MCC	*S.pombe*	figure 11a (24)	4AEZ	Resolution: 2.3 Å. Crystal data: Mad3 (chain c): residues 9-223 of 310 (9-208 in diagram). Mad2 (chain h): 6-89, 93-106 and 115-210 of 203. Slp1 (chain a): 125-144, 162-467 of 488. Reference: (Chao *et al.* 2012)
2	Bub1	*S.pombe*	figure 18a (81)	-	Structure homology model of residues 21-184 generated in this work on PDB 3ESL.b using I-TASSER.
3	Bub1 homodimer	*S.cerevisiae*	figure 18b (81)	3ESL	Resolution: 1.74 Å. Crystal data: chain a: residues 31-199, 204-214 and 216-229 of 1021, chain b: 29-214, 216-230. In diagram: 54-171. Reference: (Bolanos-Garcia *et al.* 2009)
4	Bub1 – Mad3	*S.pombe*	figure 19 (84)	-	Complex modelled in this work upon PDB 3ESL by PyMol structural alignment and optimisation by Chiron. Bub1 residues 21-184, Mad3 residues 44-202.
5	Bub1 homodimer	*S.pombe*	figure 22 (90)	-	Dimer modelled in this work upon PDB 3ESL by PyMol structural alignment and optimisation by Chiron. Bub1 residues 21-184
6	NDC80 complex	human	figure 25b (121)	2VE7	Chimaeras: Ndc80 (80-286) – Spc25 (118-224) and Nuf2 (1-169) – Spc24 (122-197). Resolution: 2.88 Å. Crystal data: Ndc80 (chain b): residues 80-202 and 211-286 of 642, Spc25 (chain b): 118-188 and 193-223 of 224, Spc24 (chain d): 122-197 of 197, Nuf2 (chain d): 4-169 of 464. Reference: (Ciferri *et al.* 2008)
7	Bub1 – Blinkin	*S.pombe* / human	figure 23	3SI5 4A1G	Structural alignment of human BubR1 and Bub1 TPR domain in association with small Blinkin (also termed KNL1 or CASC5) fragments onto the homology model of *S.pombe* Bub1 TPR homodimer (see 5). 3SI5: Blinkin residues 234-251 of 2342 with BubR1 TPR. 4A1G: Blinkin residues 201-216 with Bub1 TPR. References: (Bolanos-Garcia *et al.* 2011, Krenn *et al.* 2012)
8	Mad1 – Mad2	human	figure 26b (123)	1GO4	Resolution: 2.05 Å. Crystal: Mad2 (chain a): Mad2: residues 8-203 of 205, Mad1 (chain g): 485-584 of 718. Reference: (Sironi *et al.* 2002)
9	Mad1	human	figure 26b (123)	4DZO	Resolution: 1.76 Å. Crystal: chain b: residues 597-668 and 672-718 of 718. Reference: (Kim *et al.* 2012)
10	Bub3 – Bub1	*S.cerevisiae*	figure 28b (125)	2I3S	Resolution: 1.90 Å. Crystal: Bub3 (chain a): residues 1-133 and 151-340 of 343. Bub1 (chain b): 315-350 of 1021 Reference: (Larsen *et al.* 2007)
11	Bub3 – Mad3	*S.cerevisiae*	figure 28b (125)	2I3T	Resolution: 2.80 Å. Crystal: Bub3 (chain a): residues 1-225 and 232-340 of 343. Mad3 (chain d): 354- 395 of 515. Reference: (Larsen *et al.* 2007)

Table 14: Details and references to protein structure illustrations in this report.

2.5.4 Fluorescence microscopy and sample preparation

Cells were collected by centrifugation at 4°C and 3,000g for 1 minute, fixed by adding excess ice-cold 100% methanol and stored at -20°C or -80°C. Cells were densely placed onto a clean glass slide and, after the methanol had evaporated, mounted using PBS containing 0.4 µg/mL DAPI (4',6-diamidino-2-phenylindole). To determine the proportion of cells with septa, cell walls were stained using calcofluor white at 25 µg/mL in PEM buffer (§2.5.5) for 15 minutes on a rotary wheel and washed three times in PEM prior to mounting. Analysis was done on a 3i Marianas system (3i Inc, CO, USA) consisting of a fully motorised Axiovert 200M inverted fluorescence microscope (Zeiss AG, Germany), a cooled CoolSnap HQ CCD camera (Photometrics, AZ, USA) and Slidebook image capture and analysis software (3i Inc, Co, USA).

2.5.5 Buffers and other solutions used in this study

#	name	ingredients
1	Blotto	40 g/L Marvel dried skimmed milk and 0.1% (v/v) Tween-20 in PBS
2	Buffer A	50mM Bis-Tris Propane-HCl (pH 7.6), 10% (v/v) glycerol, 100 mM KCl, 5 mM EGTA
3	Buffer B	50 mM HEPES-KOH (pH 7.0), 50 mM KCl
4	Buffer C	50 mM HEPES-KOH (pH 7.6), 75 mM KCl, 1 mM $MgCl_2$, 1mM EGTA, 0.1% (v/v) Triton X100
5	Buffer D	100 mM glycine-HCl (pH 2.5)
6	Cerevisiae lithium buffer	10 mM Tris-HCl (pH7.4), 100 mM LiOAc, 1 mM EDTA
7	Cerevisiae PEG buffer	40% (w/v) polyethylene glycol (MW 4000) in Cerevisiae lithium buffer
8	6x DNA loading buffer	1 g/L bromophenol blue, 250 g/L sucrose, 75 mM EDTA
9	PAGE buffer	25 mM Tris base, 250 mM glycine, 1 g/L SDS
10	PBS (phosphate buffered saline)	2.7 mM KCl, 10 mM Na_2PO_4, 2 mM KH_2PO_4 (pH7.4), 137 mM NaCl
11	PEM buffer	100 mM PIPES-NaOH (pH 6.9), 1 mM EGTA, 1 mM $MgSO_4$
12	Phenol chloroform mix	phenol:chloroform:isoamyl alcohol at 25:24:1 equilibrated with 10 mM Tris-HCl (pH8.0), 1 mM EDTA
13	Phosphate buffer	77.4 mM Na_2HPO_4, 22.6 mM $NaHPO_4$ (pH7.4)
14	Pombe lithium buffer	100 mM LiOAc (pH 4.9)
15	Pombe PEG buffer	50% (w/v) polyethylene glycol (PEG; MW 4000) in Pombe lithium buffer
16	Ponceau S	1 g/L ponceau S, 5% (v/v) acetic acid
17	2x Protein sample buffer	100 mM Tris-HCl (pH6.8), 40 g/L SDS, 2 g/L bromophenol blue, 20% (v/v) glycerol, 200 mM DTT
18	Semi-dry transfer buffer	25mM Tris base, 130 mM glycine, 10% or 20% (v/v) methanol
19	10x Taq buffer	100 mM Tris-HCl (pH8.3), 500 mM KCl, 20 mM $MgCl_2$, 1 g/L gelatin
20	TBE	89 mM Tris base, 89 mM H_3BO_4, 2 mM EDTA
21	TE	10 mM Tris-HCl (pH 8.0), 1 mM EDTA
22	XSE buffer	10 mM Tris-HCl (pH 8.0), 2% (v/v) Triton X100, 10 g/L SDS, 100 mM NaCl, 1mM EDTA

Table 15: All buffers and solutions were prepared in sterile water and filter sterilised or autoclaved where necessary.

3 Proteomic analysis of *S.pombe* and *S.cerevisiae* spindle checkpoint complexes

3.1 Summary

As a result of divergent molecular evolution, establishing conceptual analogies of molecular mechanisms can be a haphazard process in species that last shared a common ancestor many hundreds of millions of years ago. This chapter aims to explore and compare the network of physical interactions of the core spindle checkpoint proteins in the phylogenetically distant yeast species *S.pombe* and *S.cerevisiae*, both model organisms in fundamental biological research. Checkpoint complexes are purified from cell extracts using an improved and rapid protocol that optimised yield to identify, by means of mass spectrometry, their composition, novel interactors and residues modified by phosphorylation.

Using the outlined method, purification of APC and spindle checkpoint complexes indicated that the 'mitotic checkpoint complex' (MCC) of *S.cerevisiae* is of similar build as metazoan MCC and consists of the BubR1 orthologue Mad3 in addition to Mad2, Bub3 and Cdc20. Unlike *S.cerevisiae* MCC, the equivalent complex formed in *S.pombe* does not contain Bub3 as Mad3 is unique among its other eukaryotic orthologues by having lost its B3i (Bub3-interaction) motif through molecular evolution. The MCC did, however, stably interact with mitotic APC, in marked contrast with purified *S.cerevisiae* APC, which was devoid of any Mad or Bub proteins, indicating that the association is perhaps very fleeting.

Although *S.pombe* Mad3 did not interact with Bub3 in direct fashion, they are engaged through mediation of Bub1. This ternary so-called BUB+ complex is based on reciprocal association of evolutionary conserved and related sequence motifs within the TPR domains of Bub1 and Mad3. Mutation of these motifs rendered cells checkpoint-deficient, which suggest that the Bub1 – Mad3 interaction is important for checkpoint signalling. Although these motifs are present in *S.cerevisiae*, Bub1 and Mad3 were not found to interact. In *S.cerevisiae*, Mad1 was observed to associate with both Bub1 and Bub3 to form the MBB complex, but no evidence was forthcoming for its formation in *S.pombe* cells.

These findings indicate that a well-established molecular mechanism can be remodelled short of functional compromise to suit environmental or physiological constraints of evolving organisms. Despite overt similarities, remarkable differences render *S.pombe* and *S.cerevisiae* as complementary experimental model systems to study spindle checkpoint function.

3.2 Aims and background

Eukaryote cell division relies on the formation of a bipolar spindle to equally segregate replicated chromosomes during mitosis. Cells evolved the spindle checkpoint mechanism that oversees the precise execution of this process. Its core molecular components (the Mad, Bub and Mph1/Mps1 proteins) are highly conserved. However, molecular divergence of their structural domains (such as the kinase domain of metazoan BubR1 that is lacking in the Mad3 yeast orthologue) and evolution of additional components (e.g. the metazoan RZZ complex) has brought about species specific variances in regulating checkpoint function. This somewhat hinders the interpretation of checkpoint studies and models across a variety of organisms exploited in research. A methodological survey to explore the molecular basis of checkpoint functioning could further clarify findings and enhance current models. In addition, checkpoint components have been observed at the site of kinetochores, microtubules, spindle poles and the nuclear envelope by fluorescent microscopy. In many cases, the exact identity of their anchoring protein partners is unknown or has only been determined recently.

This study set out to explore and compare the physiological interactions of spindle checkpoint proteins from two of the most widely used model organisms. Tandem mass spectrometry (MS/MS) was employed to identify protein partners of each individual Mad and Bub checkpoint component purified from *S.pombe* and *S.cerevisiae* cell extracts. In addition, APC complexes were purified to analyse the APC^{MCC}, and all purifications were performed from both cycling ('interphase') cells and mitotically arrested cells. MS/MS employment has the additional advantage in its ability to resolve residues that are modified through phosphorylation. These modifications can be at the heart of spindle checkpoint functioning as has been exemplified by several studies (see §3.4.9). Although this study did not set out to investigate their functional significance, evidence of their presence will greatly facilitate future investigations.

This proteomic approach is a collaborative effort through the Yeast Resource Center[13] (YRC at the University of Washington, WA, USA) with the John Yates lab at the Scripps Research Institute (CA, USA). Protein digestion and subsequent tandem MS analysis as described (§2.3.3) were performed by researchers in the Yates lab.

[13] The Yeast Resource Center (YRC) is a Biomedical Technology Research Center supported by the National Institute of General Medical Studies (P41 GM103533: 'Comprehensive Biology: Exploiting the Yeast Genome') at the US National Institutes of Health (MD, USA). The YRC is located in the Department of Biochemistry and Department of Genome Sciences at the University of Washington (WA, USA) and the Department of Chemical Physiology at the Scripps Research Institute (CA, USA).

3.3 Results

3.3.1 Strains created for protein complex purifications

To purify complexes from mitotically arrested yeast cells, mutant β-tubulin coding alleles were used that render microtubules hypersensitive to cold. At restrictive temperatures, labile spindle microtubules depolymerise to such extent that cells undergo a spindle checkpoint-mediated metaphase arrest. The allele used in *S.pombe* was *nda3-km311* (Hiraoka *et al.* 1984). A cold-labile *S.cerevisiae* strain SJ123 (§2.2.2), deficient in several proteases to minimise degradation of bait complexes in cell extracts, was engineered by transforming strain SJ219 (§2.2.4) with *Kpn*I digested plasmid pTH18 (§2.4.2 and 2.4.7). In addition to a *URA3* coding sequence as a selectable marker, this DNA vector bears a partial *tub2-401* allele to direct integration at the chromosomal *TUB2* locus by homologous recombination (Huffaker *et al.* 1988). Transformants with a disrupted *tub2* and a wild-type *TUB2* sequence were selected for uracil prototrophy on minimal plates lacking uracil (§2.2.3) and these primary transformants were subsequently selected for loss of wild-type *TUB2* and *URA3* by counter-selection on rich plates containing FOA (§2.2.3).

S.pombe and *S.cerevisiae* strains containing the wild-type or cold-sensitive β-tubulin allele and with the protein of interest fused to a carboxy terminal ZZ tag (duplex protein A moieties encoded by an optimised sequence originally derived from the bacterium *Staphylococcus aureus* (Rigaut *et al.* 1999)) through manipulation of the endogenous gene locus were obtained or created as indicated (§2.1.2). The PCR template for PCR-based gene tagging strategies was pKW804 (§2.4.2) and oligonucleotides for this pFA6 derivative DNA vector were designed with around 80 nucleotides of gene specific sequence to target the genomic DNA of interest by homologous recombination, whilst care was taken not to disrupt UTR sequences of downstream genes (Bahler *et al.* 1998). The module was amplified by PCR (§2.4.4) and introduced into yeast by lithium acetate-mediated transformation (§2.1.4 and 2.2.4). Cells were plated on rich YES plates for overnight recovery after which selection of transformants was performed by replica-plating onto rich plates containing G418 (§2.1.3 and 2.2.3). Confirmation of the ZZ tag presence on the protein of interest was obtained by resolving yeast extracts (§2.3.6) by SDS-PAGE (§2.3.7), followed by Western blotting and ECL detection using PAP reagent (§2.3.9).

3.3.2 Development of a large-scale single-step protein co-purification procedure for yeast

The objective of this project was to map the 'interactome' and phospho-modifications of spindle checkpoint components in the two yeast species, *S.pombe* and *S.cerevisiae*. The

method for preparing protein complexes as detailed in section 2.3.1 relies on speed, efficiency and minimal handling, whilst their analysis by MS/MS relies on material of high quality, purity and quantity. The devised strategy thus boosts peptide counts and protein coverage by mass spectrometer analysis in order to maximise the detection rate of unstable interactors and phospho-modifications. Established co-purification procedures were adapted to reflect the requirement for maximal yield and minimal processing time. For instance, yeast cell breakage by automated 'ball mill' action was preferred over a manual 'mortar and pestle' procedure of lesser efficiency and reproducibility, and the need for a lengthy ultra-centrifugation step was dropped in favour of rapidly clearing lysates through a glass microfiber filter.

Bait proteins from *S.pombe* and *S.cerevisiae* were initially purified from reconstituted extracts by means of a tandem affinity strategy that involves binding of the ZZ tag to an IgG matrix, followed by overnight TEV protease cleavage and subsequent re-adsorption on S-protein agarose or calmodulin agarose. This two-step purification protocol, however, was dropped in favour of a single step protocol that utilises the strong adsorption of the ZZ tag to rabbit IgG covalently bonded through epoxy groups on paramagnetic Dynabeads (§2.5.2) that have a characteristic low non-specific protein binding. Although the single purification step generally results in a higher background protein hit count compared to the tandem protocol (data not shown) this is greatly compensated by high peptide counts and polypeptide coverage of the bait protein and its binding partners in combination with a rapid processing time that reduces protein degradation and leaves the weaker *in vivo* protein associations and modifications intact.

The complete procedure as developed for rapid and large-scale protein co-purifications from yeast is described in section 2.3.1. Processing of a sample typically takes upto 1 hour, from reconstituting the lysate to elution of protein complexes. The precipitated and dried preparations (§2.3.2) were sent by courier to the Scripps Research Institute (La Jolla, CA, USA) for MS/MS analysis (§2.3.3). Figure 13a and b are colloidal coomassie blue stains (§2.3.10) of purified protein complexes resolved on a 4-20% gradient gel (§2.3.8). Incubation of *S.cerevisiae* Mad1-SZZ cell-free extracts with varying amounts of IgG-Dynabeads (0 – 2 mg beads per gramme of cells; see Figure 13c), subsequent gel electrophoresis and immune-blotting with anti-S peptide antibody indicate an optimal concentration of 1mg IgG Dynabeads per gramme of cells. Approximately 10% of each sample corresponding to 3 mg of Dynabeads was run. An estimation of the number of protein complexes was performed using 10% of a Mad1 sample each from *S.cerevisiae* and *S.pombe* run alongside 100 ng bovine serum albumin (BSA) protein.

This indicated that a large-scale purification yields approximately 2 µg of tagged Mad1 protein, corresponding to roughly 120 pmols of bait protein. On the assumption that a single complex consists of two copies of the Mad1 – Mad2 dimer, 25 grammes of cell mass thus approximately yields 60 pmol or 13 µg of protein complexes.

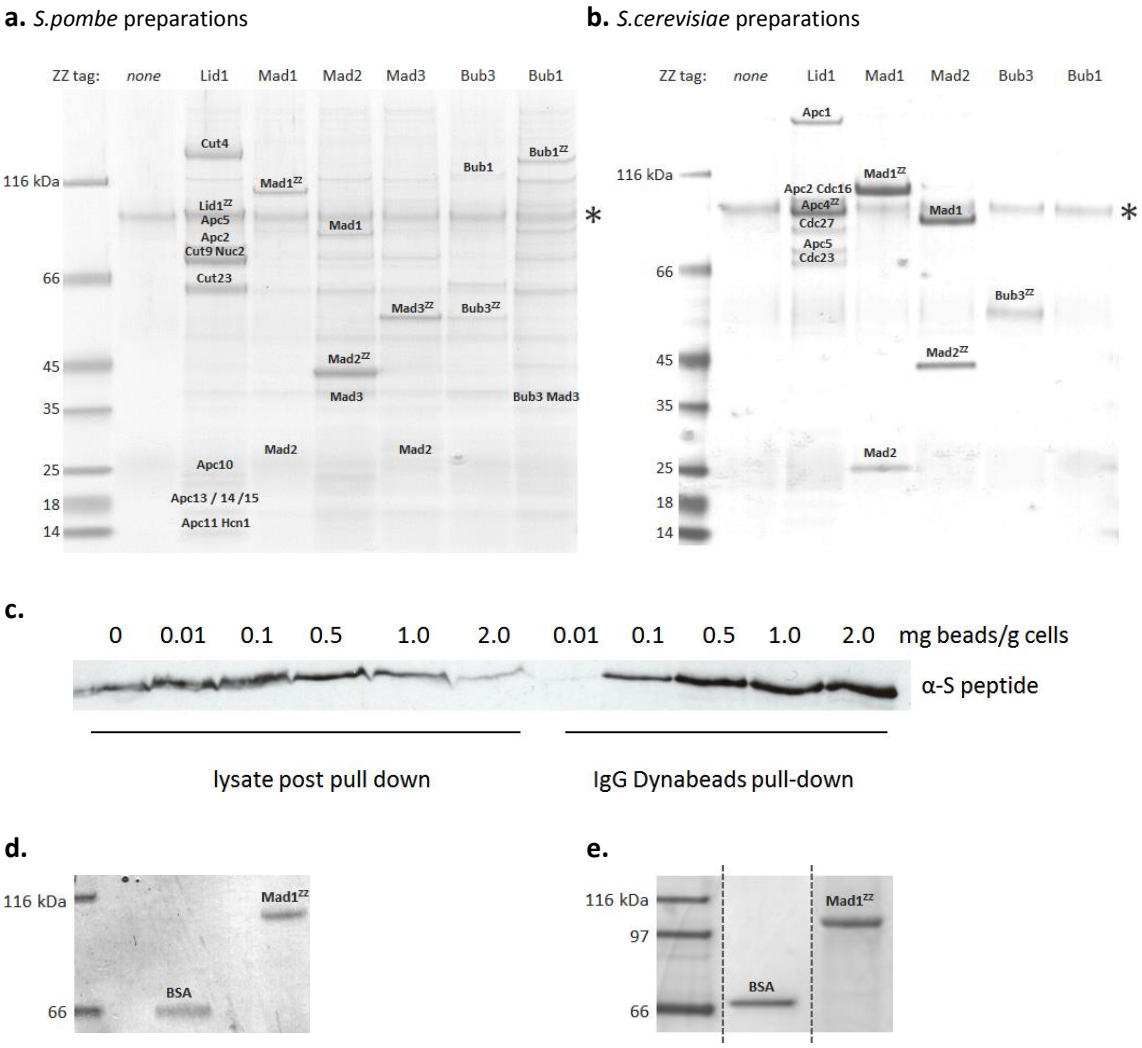

Figure 13: (a) Isolated ZZ tagged protein complexes from *S.pombe* and **(b)** *S.cerevisiae* resolved by PAGE alongside a protein molecular weight marker on a 4-20% gradient gel and dyed using colloidal coomassie. The asterisk indicates a background band. **(c)** Immuno-blot of *S.cerevisiae* Mad1-SZZ cell extracts incubated with different amounts of IgG Dynabeads. **(d)** Colloidal coomassie stain of PAGE gel containing purified *S.pombe* Mad1 protein preparations alongside 100 ng bovine serum albumin (BSA). **(e)** Colloidal coomassie stain of PAGE gel containing purified *S.cerevisiae* Mad1 protein preparations alongside 100 ng BSA.

3.3.3 MS data analysis

MS/MS data sets for all purifications were copied from the YRC repository and combined into a single Excel (Microsoft Corp, USA) workbook. Due to the larger number of protein hits in single-step affinity purifications compared to tandem purifications the challenge is to assign

each hit as a true or false positive in terms of binding partners of the bait proteins that are physiologically and biologically relevant. It was noted that the larger number of proteins that were assumed to belong to background (such as ribosomal proteins and chaperones with non-nuclear localisation that are common contaminants of predominantly nuclear localised bait proteins) were found in bait purifications rather than mock purifications (data not shown). It deserves mention that the observed issue of inherent 'stickiness' of a variety of proteins is especially true for *S.pombe* purifications for reasons that are currently unknown. To this end a negative control purification of a biologically and functionally unrelated bait protein (*S.pombe* SPBPB2B2.06c, predicted to be a nuclear phosphatase, and *S.cerevisiae* YHR202W, a putative cytosolic phospho-esterase) was performed to facilitate false-positive bait interaction analysis ('filter 1' in Table 16). In addition, proteins that were found right across the board in the vast majority of MS data sets in the Hardwick lab are considered to be of no particular interest, do not constitute a meaningful interaction or are the default background inherent to this particular experimental procedure ('filter 2' in Table 16). Thus proteins from this 'grey list' were therefore excluded in the final compilation that is the core data set (*S.pombe* MS data in section 7.1 and protein ontology in section 7.2, *S.cerevisiae* data in section 7.3 and 7.4).

Protein hits in these data sets were ranked according to the following calculation: Rank = $C \cdot N_T / N_U$. This equation takes into account the total number of peptides (N_T) that were assigned to a given protein during one single MS run; the number of peptides of these that are unique (thus non-identical; N_U); and the percentage coverage (C) of the protein's sequence that is represented by peptides identified in the MS run for that protein. Note that as larger proteins are more likely to have a high number of both total (N_T) and unique peptides (N_U), N_T / N_U is a good arbitrary approximate for the abundance of a protein of any size, assuming decent sequence coverage and little protein degradation. The percentage sequence coverage (C) is often high for proteins that are abundant and least prone to degradation by proteases during purification. Thus this ranking is a rough but useful measure of the abundance of a protein in the purified material, and a high ranking is good evidence of the detected protein interacting with the bait protein and thus occurring in a single complex.

Protein hits in section 7.1 and 7.3 are listed by their ranking and include the top 80 hits for *S.cerevisiae* and 80 protein hits of interest for *S.pombe*, including the top 57. Table 16 lists the total number of protein hits for each purification before and after filtering. With the exception of *S.cerevisiae* Bub1 preparations, the peptide coverage of all Mad and Bub bait proteins obtained by MS/MS analysis was uniform, indicating that they were stable and not liable to

degradation. Unfortunately, rapid but partial proteolysis of *S.cerevisiae* Bub1 did prevent a thorough analysis of its interactors and modifications.

#	bait	conditions	hits total	filter 1	filter 2	run ID	strain
	S.pombe						
1	Mad1	cycling	584	446	194	3437	SP26
2	Mad1	mitotic arrest	507	378	135	3418	SJ1060
3	Mad2	cycling	863	715	388	3395	SJ961
4	Mad2	mitotic arrest	127	57	18	3653	SP32
5	Mad3	cycling	752	601	314	3093	SP22
6	Mad3	mitotic arrest	192	115	51	3406	SP42
7	Mad3	*bub3Δ*; arrest	77	37	16	3392	SJ906
8	Bub1	cycling	411	289	133	3407	VV96
9	Bub1	mitotic arrest	765	613	324	3440	VV97
10	Bub3	cycling	807	655	355	3085	SP24
11	Bub3	mitotic arrest	434	300	109	3405	SP30
12	Lid1	cycling	939	796	461	3436	KP261
13	Lid1	mitotic arrest	683	537	277	3089	JB68
14	Abo1	cycling	79 / 270	22 / 183	10 / 75	3882 / 4850	SJ977
15	SPBPB2B2.06c	*control bait*	146	-	-	3896	SJ996
16	-	*mock*	65	-	-	3439	KP114
	S.cerevisiae						
17	Mad1	cycling	87	53	19	3541	SJ206
18	Mad1	mitotic arrest	25	15	10	3582	SJ130
19	Mad2	cycling	99	47	16	3536	SJ184
20	Mad2	mitotic arrest	31	15	11	3550	SJ186
21	Mad3	cycling	55	21	11	3539	SJ108
22	Mad3	mitotic arrest	116	62	25	3540	SJ110
23	Bub1	cycling	10	5	5	3548	JF60
24	Bub1	mitotic arrest	15	5	2	3549	JF74
25	Bub3	cycling	145	83	32	3537	SJ185
26	Bub3	mitotic arrest	11	5	4	3573	SJ187
27	Apc4	cycling	180	128	64	3538	SJ207
28	Apc4	mitotic arrest	147	114	42	3554	SJ148
29	YHR202W	*control bait*	236	-	-	4208	SJ208
30	-	*mock*	56	-	-	3895	SJ219

Table 16: Total number of protein hits for each *S.pombe* and *S.cerevisiae* purification performed in this study before and after filtering. 'Filter 1' designates the use of control bait and mock purification data, 'filter 2' are ubiquitous hits from a large set of different MS runs (see text). The run ID is a unique number for the MS run as part of project 1177 at the Yeast Resource Center.

3.3.4 Mad and Bub proteins form distinct and unique complexes

To facilitate analysis of spindle checkpoint complexes, line diagrams were drawn based on the presence of Mad and Bub proteins in addition to Slp1/Cdc20 and APC subunits in individual purifications from both interphase and mitotically arrested cells (Figure 14).

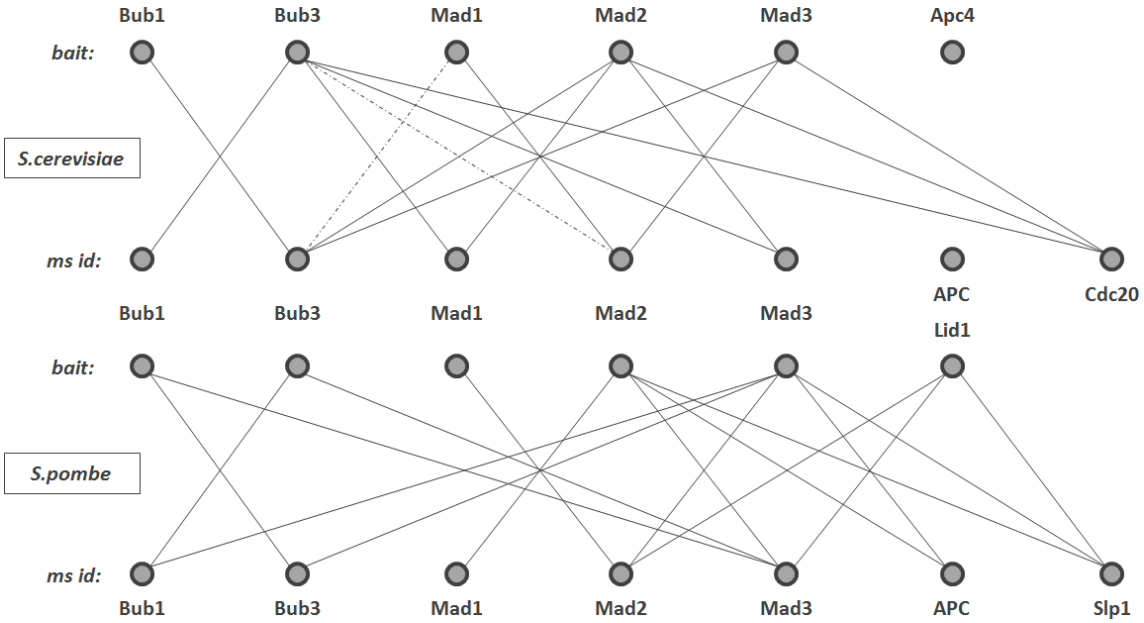

Figure 14: Diagram detailing interactions among spindle checkpoint proteins and the APC as identified by tandem MS ('ms id') from bait purifications ('bait') in the yeasts *S.cerevisiae* and *S.pombe*. APC bait purifications are Apc4 in *S.cerevisiae* and its orthologue Lid1 in *S.pombe*. 'APC ms id' indicates any of the APC subunits identified in bait preparations. For simplicity, bait identifications are not indicated. Interactions that were identified but are known to exist based on reciprocal bait purifications are shown with a dotted line.

Analysis of interactions among the spindle checkpoint proteins revealed that the Mad and Bub proteins form distinct complexes and that one protein factor can contribute to the composition of more than one unique complex. For instance, *S.cerevisiae* and *S.pombe* Mad2 was observed to interact with both Mad1 and Mad3, but Mad1 was not found in Mad3-containing complexes. Similarly, *S.cerevisiae* Bub3 was found in association with both Bub1 and Mad3, but the latter two were not shown to associate. And as *S.pombe* Mad3 was shown to bind both Bub3 and Mad2, Bub3 did not associate with Mad2. The distinct complexes that were identified in the two yeast species are listed in Table 17.

The MAD complex (consisting of Mad1 and Mad2) forms in both yeast species and represents the evolutionary conserved 'templating complex' on which 'open' Mad2 conformers are catalysed into 'closed' species to bind Slp1/Cdc20 (refer to §1.4.4). Strikingly, Mad1 did not

purify in association with Slp1/Cdc20, which suggests that Mad2 binds the latter after dissociating from the Mad1 – Mad2 'templating complex' (see Figure 10, page 20).

#	complex	composition	perceived function	reference(s)
	S.cerevisiae			
1	MCC	Mad2, Mad3, Bub3, Cdc20	APC inhibitor	(Hardwick *et al.* 2000)
2	MAD	Mad2, Mad1	Mad2 conformational catalysis	(Chen *et al.* 1999)
3	-	Mad2, Cdc20	primary checkpoint signal	(Hwang *et al.* 1998)
4	BUB	Bub3, Bub1	promotes biorientation	(Roberts *et al.* 1994)
5	MBB	Mad1, Bub1, Bub3	essential for checkpoint arrest	(Brady & Hardwick 2000)
	S.pombe			
6	MCC	Mad2, Mad3, Slp1	APC inhibitor	(Millband & Hardwick 2002)
7	MAD	Mad2, Mad1	Mad2 conformational catalysis	(Ikui *et al.* 2002)
8	-	Mad2, Slp1	primary checkpoint signal	(Kim *et al.* 1998)
9	BUB	Bub3, Bub1	promotes biorientation	(Vanoosthuyse *et al.* 2004)
10	BUB+	Bub3, Bub1, Mad3	essential for checkpoint arrest	(Vanoosthuyse *et al.* 2004); Hardwick lab, manuscript in preparation

Table 17: Spindle checkpoint functioning in *S.cerevisiae* and *S.pombe* relies on the formation of distinct protein complexes composed of the *MAD* and *BUB* gene products that target the APC E3 ubiquitin ligase activator Slp1/Cdc20. Note that the analysis performed in this study did not distinguish MCC from Mad2 – Slp1/Cdc20 complexes. References are to the first description of the complex.

3.3.5 Divergent associations among spindle checkpoint proteins in the two yeast species

Between the two yeast species some notable differences in regards to spindle checkpoint protein interactions were recognised that are summarised in two Venn diagrams (Figure 15 and see Table 17). Comparison of the yeast complexes identified showed that:

i. Unlike *S.cerevisiae*, *S.pombe* mitotic checkpoint complex (MCC) was found to interact stably with the APC E3 ubiquitin ligase. This finding is discussed in section 3.3.6.

ii. Unlike *S.cerevisiae*, *S.pombe* MCC was not observed to contain Bub3 (§3.3.7).

ii. Unlike *S.cerevisiae*, *S.pombe* Bub1 was shown to associate with both Mad3 and Bub3 to form the BUB+ complex (§3.3.8).

iii. Unlike *S.pombe*, *S.cerevisiae* Mad1 was found to stably associate with both Bub1 and Bub3 to form the MBB complex (§3.3.9).

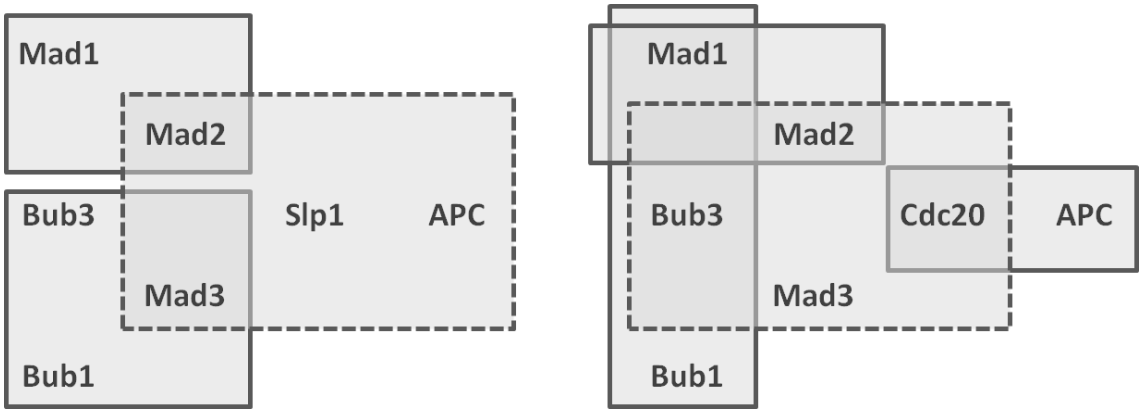

Figure 15: Venn diagrams summarising and illustrating dissimilar interactions identified by tandem MS between the spindle checkpoint proteins in *S.pombe* (left) and *S.cerevisiae* (right). The protein groupings with the dotted line are the checkpoint components and Slp1/Cdc20 that form mitotic checkpoint complexes (MCC) and inhibit the APC E3 ubiquitin ligase. The MCC interacts stably with the APC in *S.pombe*, but not so in *S.cerevisiae*.

3.3.6 The *S.cerevisiae* mitotic checkpoint complex does not stably interact with the APC complex

Unlike mitotic APC preparations from *S.pombe*, the *S.cerevisiae* APC did not readily purify in complex with the MCC, despite a number of efforts. The MS data for *S.pombe* Mad2 and Mad3 identified all 13 known subunits of the APC and reverse experiments showed both Mad2 and Mad3 in purifications of the APC subunit Lid1. No evidence for peptides of any APC subunit was forthcoming from *S.cerevisiae* Mad2, Mad3 and Bub3 purifications and no peptides for these checkpoint proteins were found in purifications of the *S.cerevisiae* Lid1 orthologue Apc4. The *S.cerevisiae* MCC, however, is subject to APC activities during mitosis, in which the Apc15/Mnd2-dependent Cdc20 ubiquitination determines the dynamic process of MCC (dis)assembly (Foster & Morgan 2012). The inability to detect *S.cerevisiae* APC^{MCC} complexes in mitotic MCC or APC preparations could indicate that the MCC associates with few APC complexes, that this interaction is perhaps very fleeting, or that the MCC is readily disassembled upon contacting the APC.

3.3.7 The *S.pombe* mitotic checkpoint complex does not contain Bub3

The MS data presented in Figure 14 and summarised in Figure 15 and Table 17 indicate that the MCC as formed in *S.cerevisiae* includes Bub3. Both Mad3 and Mad2 purifications did contain Bub3 and Cdc20 and *vice versa* Cdc20, Mad3 and Mad2 were detected in Bub3 purifications. The *S.pombe* Bub3 protein was not present in complexes purified through Mad2 or the Lid1 APC subunit, nor did Mad2, Lid1 and Slp1 co-purify with Bub3. This suggests that Bub3 does not associate with Mad3, Mad2 and Slp1 to form the MCC as occurs in *S.cerevisiae* (Figure 15 and Table 17) and other studied eukaryotes.

Genetic evidence for this difference is the lack of a conserved sequence motif in *S.pombe* Mad3 (refer to the multiple sequence alignment of Mad3 orthologous in section 7.5.3 on page 197) that permits association with Bub3. This approx. 35 amino acid Bub3-interaction motif is (re)named the B3i motif and is also known as the GLEBS (for 'Gle2-binding sequence') motif (Larsen *et al.* 2007). It was originally identified in the *S.cerevisiae* Nup116 nuclear pore protein (Bailer *et al.* 1998) and is represented in all other studied Mad3 orthologues as well as paralogues (Wang *et al.* 2001) where it provides binding with the seven-bladed β-propeller-like WD40 domain of Bub3 (Larsen *et al.* 2007). Apart from probably *Schizosaccharomyces japonicus* Mad3, all other known fission yeast orthologues lack the B3i motif (refer to Figure 27 on page 124).

3.3.8 *S.pombe* Bub1 can bind both Mad3 and Bub3 to form BUB+ complexes

The MS data presented here suggest that the interaction of *S.cerevisiae* Bub3 with Bub1 and Mad3 is mutually exclusive, as Bub1 purified with Bub3 but not Mad3, and Mad3 purified with Bub3 but not Bub1. As both Mad3 and Bub1 contain a single B3i motif, this finding implies that Bub3 allows engagement of only one single B3i motif. Indeed, crystallography studies of the B3i residues of *S.cerevisiae* Mad3 and Bub1 in association with Bub3 show that the seven WD40 repeats of the latter accommodate a single B3i interaction (see Figure 28b, page 125)(Larsen *et al.* 2007).

As *S.pombe* Mad3 (unlike its 'ohnologue' Bub1; refer to page 14) lacks the Bub3-interaction motif, the finding that it purified with Bub3 and *vice versa* is thus surprising. Analysis of both Mad3 and Bub3 purifications identified interactions with Bub1. Reciprocally, Bub1 preparations contained both Mad3 and Bub3. These MS data thus impart a Bub3 association with Mad3 that is likely to be indirect and facilitated through Bub1. Indeed, MS analysis of interactors from Mad3-containing complexes isolated from cells that lack Bub3 revealed the presence of Bub1 (Table 18). Besides, this experiment also revealed that *S.pombe* Bub3 is not required for Mad3 to associate with the APC E3 ubiquitin ligase complex as two subunits, namely Cut9 and Cut23, are identified. As discussed in §3.4.3, this corroborates the finding that *S.pombe* Bub3 is not required for a spindle checkpoint-mediated metaphase arrest (Tange & Niwa 2008, Vanoosthuyse *et al.* 2009).

#	interactor	number of unique peptides	total number of peptides	% polypeptide coverage
	Mad3-ZZ, *bub3Δ* cells			
1	Mad3	712	60	66
2	Bub1	57	21	15
3	Bub3	0	0	0
4	Mad2	16	7	15
5	Slp1	84	15	18
6	Cut9	4	4	5
7	Cut23	3	3	5

Table 18: Spindle checkpoint proteins and APC subunits that interact with *S.pombe* Mad3 in the absence of Bub3. Interactors were identified by tandem MS through analysis of Mad3-ZZ precipitations from cells deleted for the *bub3* coding sequence.

Evidence in favour of the direct nature of the Bub1 – Mad3 interaction was provided by yeast two-hybrid analysis (§2.5.1). The Mad3 interaction with Bub1 was studied in a split Gal4 transcription factor setup using the *GAL* promoter driven histidine (*GAL1-HIS3*) and adenine (*GAL2-ADE2*) reporter genes (James *et al.* 1996). Low-copy two-hybrid vectors carrying an *ARS4/CEN6* origin in addition to an *ADH1* promoter, which drives expression of a sequence encoding the Gal4 DNA binding domain (vector pDEST32 with *LEU2* gene for selection) or Gal4 transcription activator domain (vector pDEST22 with *TRP1* gene) sequences were prepared by Gateway recombinational cloning (§2.4.6) to fuse sequences of interest in-frame and downstream of the split *GAL4* gene. The yeast two-hybrid strain PJ69-4 was transformed with the combination of two-hybrid vectors to study the desired interaction and maintained on synthetic medium lacking leucine and tryptophan. A two-hybrid strain expressing Bub1 fused to the Gal4 activation domain and Mad3 fused to the Gal4 DNA binding domain exhibited growth on plates additionally lacking histidine or adenine (row 3 in Figure 16b). This two-hybrid positive confirmed a likely direct association of Bub1 with Mad3 and allowed mapping of the interaction domains involved. Three fragments (a, b and c; see Figure 16a) of the Bub1 protein were studied to delineate sequences that confer interaction with Mad3. A schematic diagram of structural and functional domain features of *S.pombe* Bub1 and Mad3 is given in Figure 16a.

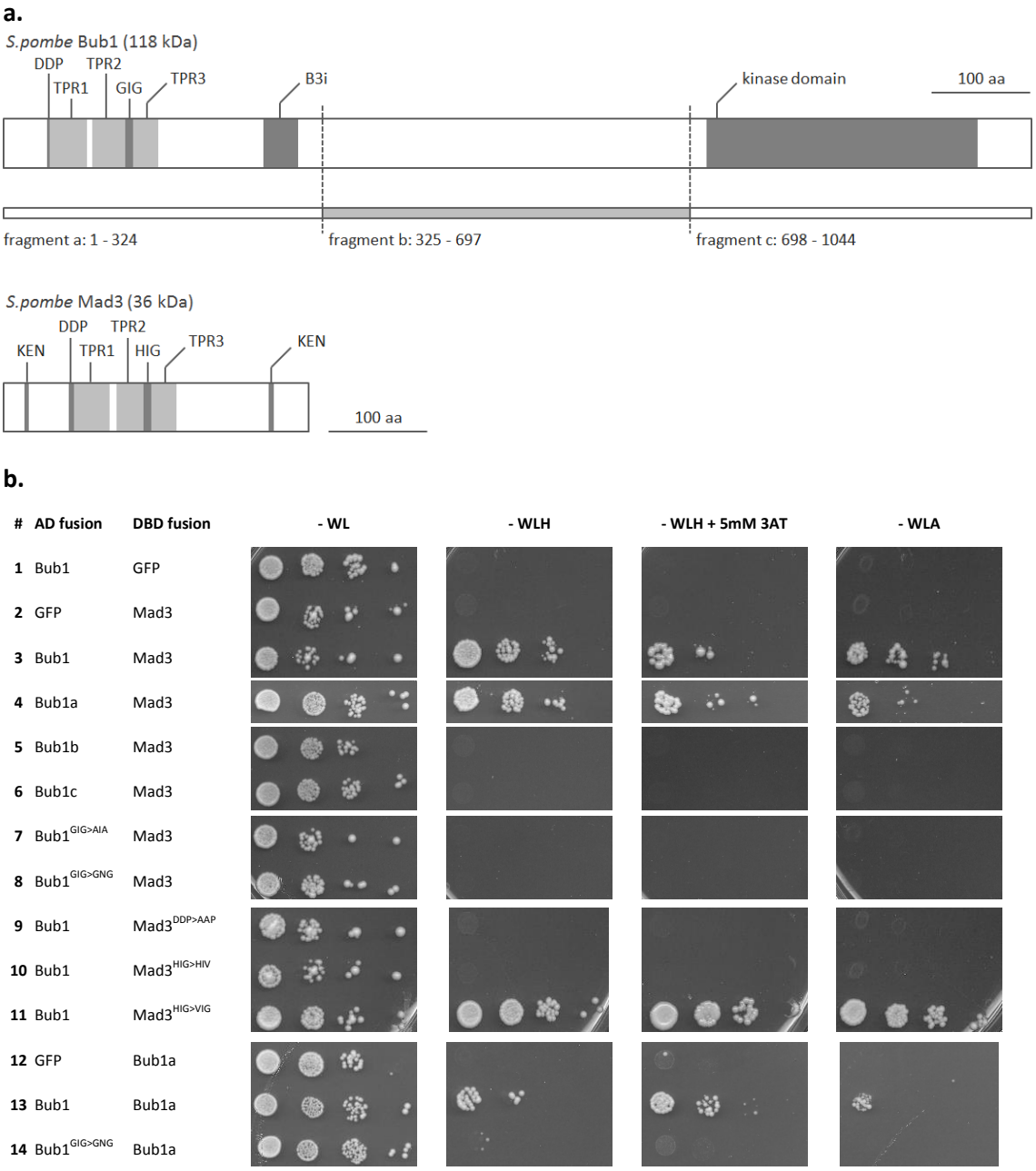

Figure 16: (a) Schematic representation of conserved domains and motifs in *S.pombe* Mad3 and Bub1. Fragments A, B and C of Bub1 are those used in the yeast two-hybrid assay. The amino terminal fragment 'a' counts 324 residues and is characterised by a TPR domain consisting of 3 TPR unit repeats, followed by a B3i sequence motif that confers interaction with Bub3. In both Bub1 and Mad3, the conserved DDP sequence motif precedes the first TPR unit and the conserved H/GIG motif precedes the third. **(b)** Yeast two-hybrid analysis using fusions to the Gal4 DNA binding domain (DBD) and activation domain (AD) revealed that the direct interaction of Mad3 with the 324 amino terminal residues of Bub1 (row 3 and 4) is facilitated by the HIG and DDP motifs of the former (row 9-11) and the related sequence motif GIG of the latter (row 7 and 8). Moreover, this assay did indicate that the Bub1 GIG motif is essential for homodimerisation (row 13 and 14).

The amino terminal Bub1 fragment ‘a’ comprising the first 324 residues was shown to uniquely associate with Mad3 (rows 4, 5 and 6 in Figure 16b). This fragment contains a region of approximately 200 amino acids in length that shares high sequence similarity with Mad3 (Figure 16a) and evidences their kinship through molecular evolution (Suijkerbuijk *et al.* 2012a). Its main feature is a ‘tetratricopeptide repeat’ (TPR) domain flanked by an α-helix on either side. Each individual TPR unit is 34 residues in length (Figure 17) and folds as antiparallel α-helices in a hairpin-like helix-turn-helix structural arrangement.

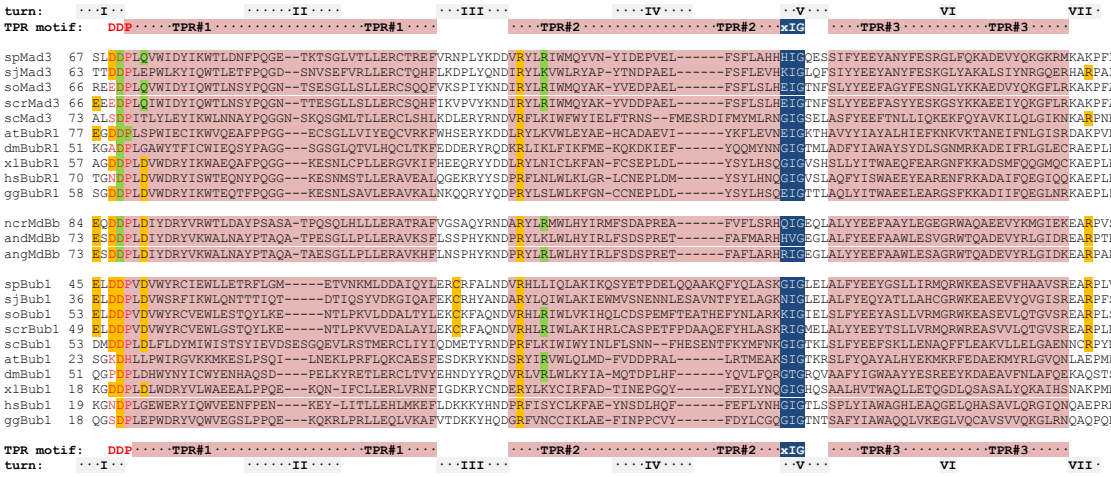

Figure 17: Multiple sequence alignment of TPR domain-containing Mad and Bub orthologous proteins prepared using Clustal Omega (v1.1.0). The six α-helices (in shaded red) that form three sequential TPR units (numbered 1, 2 and 3) are flanked by ‘tight turn’ regions (I - VII). Turn regions I and V comprise the characteristic and well-conserved DDP (red font colour) and H/GIG (in shaded blue) sequence motifs, respectively. *S.pombe* Bub1 and Mad3 conserved residues that are involved in (homo)dimerisation (see Table 20) are coloured in green and yellow respectively: Mad3 Asp70, Gln73, Arg121, Arg186 and Bub1 Glu45, Asp47, Cys85, Arg93, Arg164, Arg168. Note that Mad3 residues Asp70 and Arg186 correspond to the conserved Bub1 residues Asp48 and Arg168, respectively. Abbreviations used: *S.pombe* (sp), *Schizosaccharomyces japonicus* (sj), *Schizosaccharomyces octosporus* (so), *Schizosaccharomyces cryophilus* (scr), *S.cerevisiae* (sc), *Arabidopsis thaliana* (at), *Drosophila melanogaster* (dm), *X.laevis* (xl), *Homo sapiens* (hs), *Gallus gallus* (gg), *Neurospora crassa* (nc), *Aspergillus nidulans* (and) and *Aspergillus niger* (ang).

Analysis of the crystal structures of *S.cerevisiae* Bub1 (Bolanos-Garcia *et al.* 2009), human BubR1 (D'Arcy *et al.* 2010) and *S.pombe* Mad3 (Chao *et al.* 2012) reveal a similar arrangement for their amino termini with eight consecutive antiparallel α-helices folding into a right-handed superhelical structure with a convex and concave surface (*S.pombe* Mad3 representation in Figure 18a). Residues forming the ‘tight turns’ that link the three TPR units vary in length and local structure. Curiously, they are characterised by the presence of well-conserved amino acids (see for instance turn region III and IV in Figure 17) or are acidic in nature.

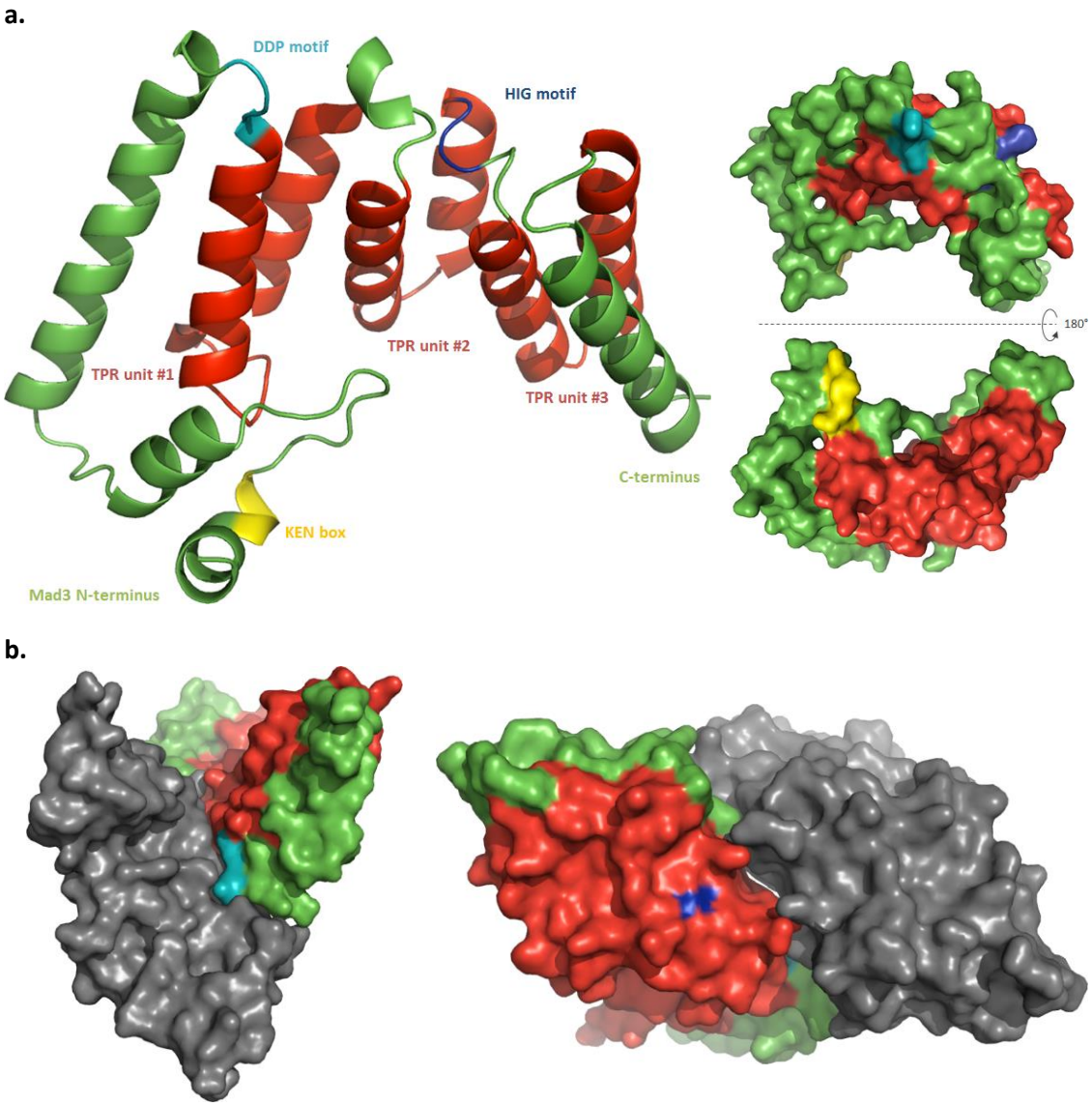

Figure 18: (a) Left: Structure of the *S.pombe* Mad3 amino terminus (residues 12-203) in ribbon representation as revealed by x-ray crystallography (Chao *et al.* 2012). The three individual TPR units are coloured red. The KEN box, HIG and DDP motifs are painted yellow, blue and cyan respectively. Right: Surface representations. **(b)** Two surface views of the *S.cerevisiae* Bub1 amino terminus (residues 31-198) homodimer as determimed by x-ray crystallography (Bolanos-Garcia *et al.* 2009). The two Bub1 molecules of the dimer are coloured in grey and green and the TPR domain of the latter is in red, the DDP motif in cyan and the buried GIG motif in dark blue. All 3D structure representations were prepared in PyMol (§2.5.3).

In vitro experiments indicate that recombinant *S.cerevisiae* Bub1 amino terminus is a dimer in solution (Bolanos-Garcia *et al.* 2009). In support of this, the unit cell in a crystal lattice consists of two Bub1$^{[1\text{-}230]}$ molecules interacting via their TPR domains (Figure 18b)(Bolanos-Garcia *et al.* 2009). Analysis of the interaction surface suggests that dimerisation is facilitated by region III, acidic in nature and situated in a turn between the first and second TPR unit, in addition to region I and V, which precede the first and last TPR unit,respectively (Bolanos-Garcia *et al.*

2009). These turns form a continuous binding interface that establishes a number of salt bridges stabilising the homodimer. Turn region I and V of *S.pombe* Bub1 and Mad3 encompass the highly conserved residue motifs DDP and H/GIG that have been the subject of studies in *S.cerevisiae* (Hardwick *et al.* 2000) and human (Harris *et al.* 2005, Bolanos-Garcia *et al.* 2009) cells and are essential for checkpoint functioning. These corresponding *S.pombe* sequence motifs could thus function in a similar manner by facilitating the dimerisation of Bub1 and Mad3. To investigate this, mutation analysis was carried out according to Table 19 with advice on the substitutions obtained from Dr. Victor Bolanos-Garcia (Oxford Brookes University, UK)(Bolanos-Garcia & Blundell 2011). The corresponding two-hybrid vectors were prepared by site-directed substitution mutagenesis (§2.4.10).

#	ORF	motif (residue #)	mutant motif	comments
1	Bub1	GIG (126-127-128)	AIA	predicted to disturb local conformation
2	Bub1	GIG (126-127-128)	GNG	introduction of subtle electrostatic charge by an uncharged polar residue
3	Mad3	DDP (69-70-71)	AAP	neutralise negative electrostatic charge; mutagenesis by Alicja Sochaj, Hardwick lab
4	Mad3	HIG (144-145-146)	HIV	predicted to disturb local conformation; mutagenesis by Alicja Sochaj, Hardwick lab
5	Mad3	HIG (144-145-146)	VIG	predicted to disturb local conformation; mutagenesis by Alicja Sochaj, Hardwick lab

Table 19: Mutagenesis studies of the highly conserved *S.pombe* Bub1 and Mad3 sequence motifs that form part of the presumed dimerisation interface.

Each amino acid in a peptide or protein has two degrees of backbone flexibility through rotation of the N – C_α and C – C_α bonds represented by the ϕ and ψ dihedral angles respectively. Tight turn V between the second and third TPR unit and characterised by the GIG motif in human BubR1 and *S.cerevisiae* Bub1 involves positive ϕ torsion angles of the glycine residues (D'Arcy *et al.* 2010). Thus replacing glycine 146 of *S.pombe* Mad3 with valine (denoted as Mad3$^{HIG>HIV}$), which is more likely to adopt a negative ϕ angle was predicted to disturb the local conformation of the 'HIG turn'. Indeed, in the two-hybrid assay this Mad3 mutation abolished the interaction with Bub1 (row 10 in Figure 16b). However, the Mad3$^{HIG>VIG}$ mutation was still able to still support the Bub1 interaction (row 11), which suggests that the histidine residue does not significantly contribute to the HIG turn conformation or Bub1 binding. Substitution of the isoleucine in the Bub1 GIG motif with an asparagine residue (denoted as Bub1$^{GIG>GNG}$) and a glycine to alanine Bub1$^{GIG>AIA}$ mutant resulted in abrogation of the Bub1 – Mad3 interaction in both cases (row 7 and 8 in Figure 16b). In contrast to the histidine residue of *S.pombe* Mad3 HIG, the first glycine residue of *S.cerevisiae* Bub1 GIG motif is still part of the preceding α-helix. Alanine substitution of both glycine residues in *S.pombe* Bub1$^{GIG>AIA}$ thus likely disrupts the local conformation which negatively affects the Bub1 – Mad3 association.

Even a subtle disruption of the electrostatic charge by the substitution of isoleucine for asparagine has repercussions for the interaction of Bub1$^{GIG>GNG}$ with Mad3. Even though the Bub1 GIG motif does not form part of the predicted dimerisation interface (see GIG motif locale in Figure 18b) its constitution is essential for the formation of the Bub1 – Mad3 dimer. The Bub1 GIG conformation is conceivably required in positioning the other residues of the tight-turn V that are at the Mad3 interface.

Unlike the H/GIG motif, the DDP motif is present at the dimerisation surface (see Figure 18b). Mutation of the Mad3 acidic DDP motif to produce Mad3$^{DDP>AAP}$ led to loss of interaction with Bub1 in the two-hybrid assay (row 9), which is very likely due to the loss of negative charges at the Mad3 surface required to support Bub1 association. To investigate the electrostatic surface of *S.pombe* Mad3 and its role in Bub1 dimerisation, the Mad3 and Bub1 amino terminus structure was analysed using the 'Adaptive Poisson-Boltzmann Solver' (APBS) module in PyMol (§2.5.3). As to date no structural information is available for *S.pombe* Bub1 the first 200 residues containing the TPR domain was therefore modelled upon the amino terminus of *S.cerevisiae* Bub1 for which the structure is determined by x-ray crystallography at a resolution of 1.74 Å (Bolanos-Garcia *et al.* 2009). The *in silico* model for the *S.pombe* Bub1 amino terminus as shown in Figure 19a was built using this structure as a template (PDB code 3ESL, chain B) by the I-TASSER protein structure prediction server (§2.5.3) (Roy *et al.* 2010). The evolutionary relationship of *S.pombe* Mad3 and Bub1 and structural similarity of their amino termini was emphasised by the remarkably low root mean square deviation (RMSD) of 1.162 obtained by superimposing the Bub1 homology model with the Mad3 crystal structure.

In an attempt to predict the interaction interface of the Bub1 – Mad3 complex, the possibility was explored where, given the structural similarity of Mad3 and Bub1, the Bub1 – Mad3 complex forms through a similar arrangement as the *S.cerevisiae* Bub1 – Bub1 dimer. For this, residues 21-184 of the homology model of *S.pombe* Bub1 and the *S.pombe* Mad3 structure (PDB code 4AEZ, chain C, residues 44-202) were superimposed to each of the two Bub1 monomers of the *S.cerevisiae* Bub1 crystal structure. Steric clashes of residue side chains at the interface were resolved using the Chiron webserver (§2.5.3) that minimises the Van der Waals repulsive energy without perturbing the polypeptide backbone (Ramachandran *et al.* 2011).

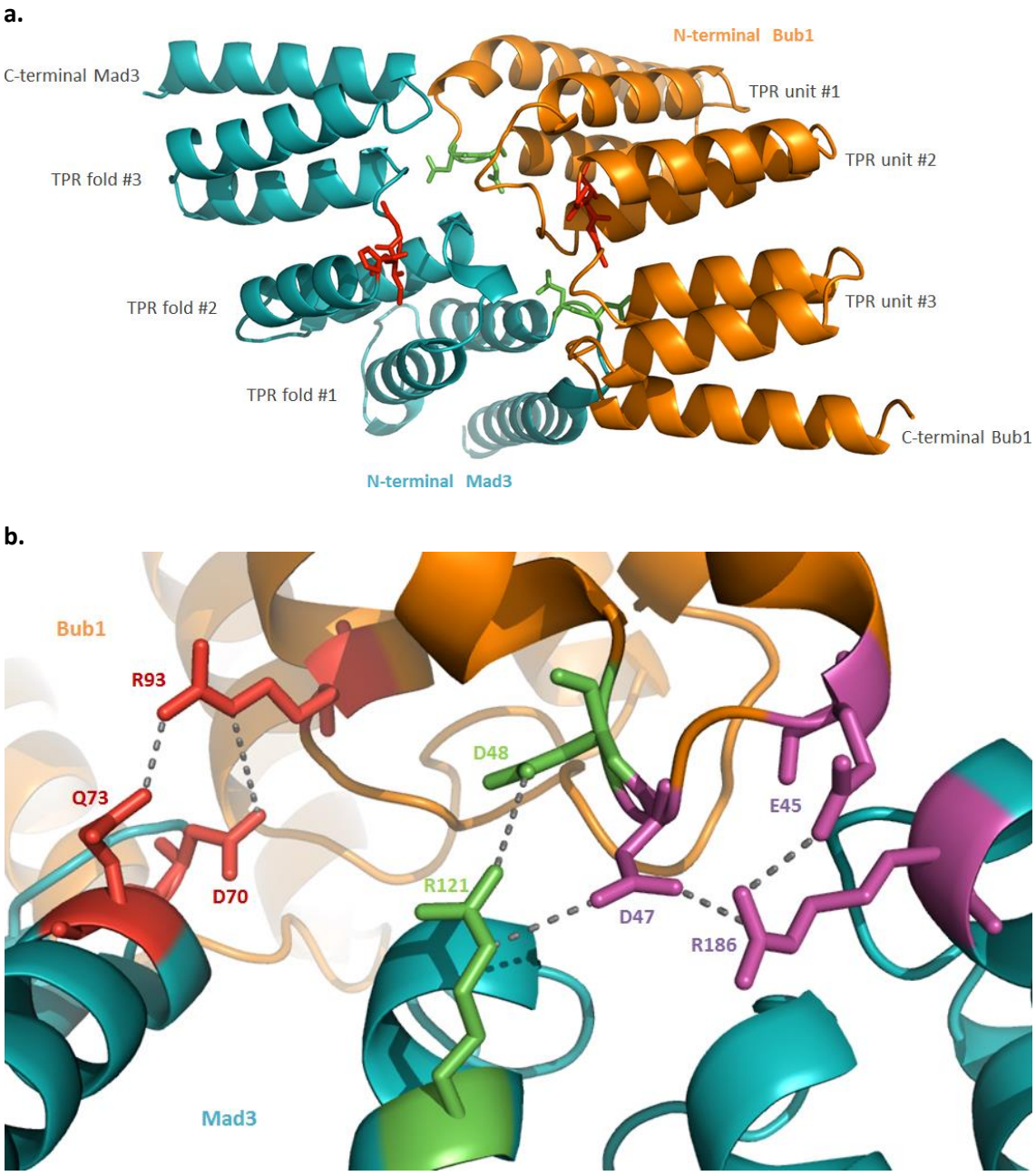

Figure 19: (a) Structure homology model of the *S.pombe* Mad3 TPR domain interacting with the Bub1 TPR domain. The amino termini of Mad3 (cyan colouring) and Bub1 (orange) were superimposed onto the crystal structure of the *S.cerevisiae* Bub1 dimer. H/GIG motifs are shown in red, DDP motifs in green. **(b)** Close-up of the TPR interface and amino acid residues that are predicted to stabilise the Bub1 (orange) and Mad3 (cyan) association. Bub1 Arg93, Mad3 Arg121 and Arg186 are key residues in their ability to form H-bonds or salt bridges across the interface (Table 20). The 3D structure representations were prepared in PyMol (§2.5.3).

Subsequent electrostatic surface analysis employing APBS software (§2.5.3) revealed complementarity in electrostatic surface potential charges of Mad3 and Bub1 (Figure 20a). Association can thus be largely driven through attraction of the negatively and positively charged patches with the corresponding patches across the interface in an antiparallel

position. Similar analysis of the Mad3$^{DDP>AAP}$ mutant protein surface suggests that the absence of the acidic patch no longer supports this scenario (Figure 20b) as suggested by the loss of interaction observed in the two-hybrid experiment.

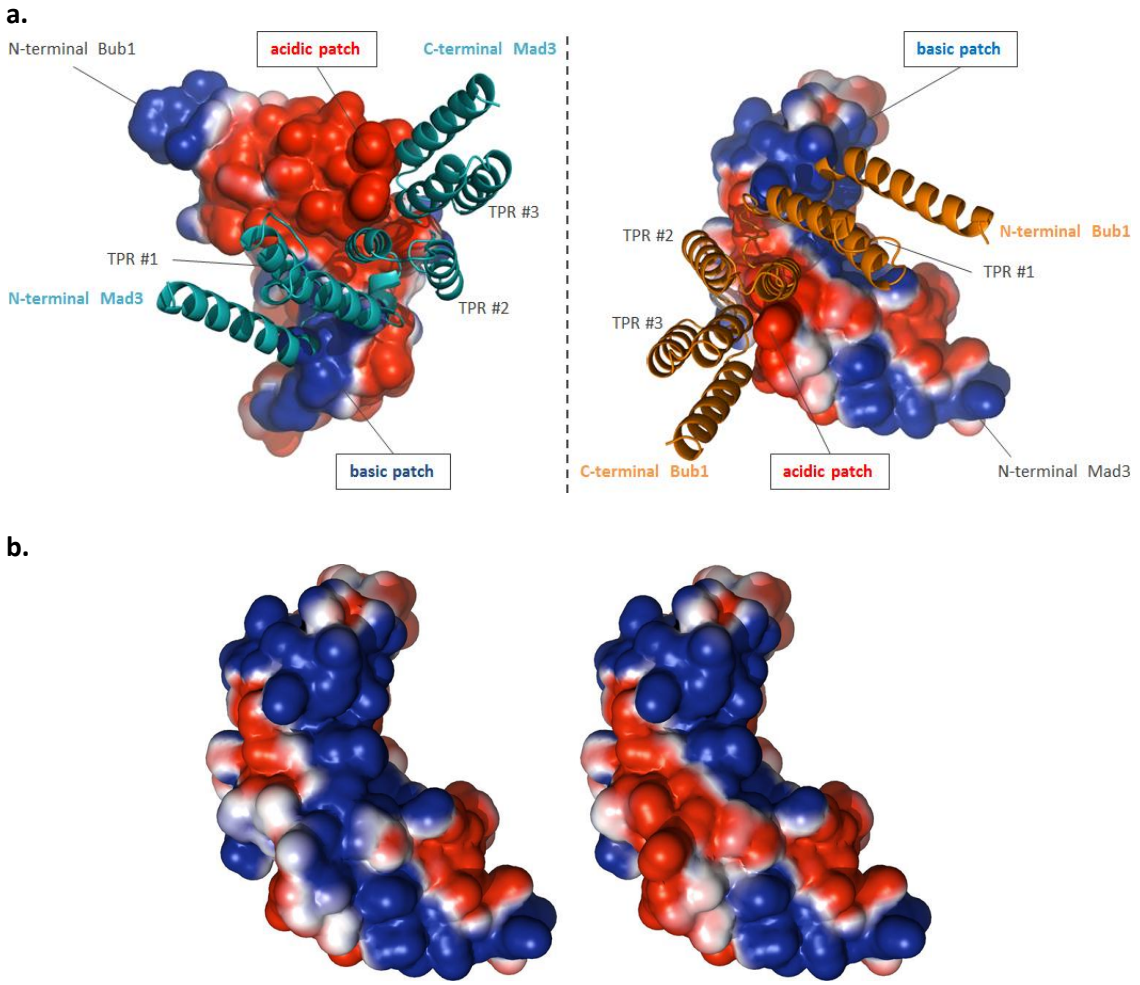

Figure 20: (a) Distribution of electrostatic surface potential of the Bub1 (left) and Mad3 (right) amino terminus with the respective dimer complement in ribbon representation. Compatibility of the basic and acidic patches at the dimerisation interface is predicted to drive association. **(b)** The Mad3$^{DDP>AAP}$ mutant (left; wild-type on the right) has a drastically altered dimerisation interface and its electrostatic potential is no longer compatible with Bub1. All 3D structure representations were prepared in PyMol (§2.5.3).

To analyse in detail the role of the Mad3 DDP residues in binding Bub1, the interface of the Bub1 – Mad3 complex was explored using PDBePISA software (§2.5.3) (Krissinel & Henrick 2007). The area covering the interface is 1,030 Å^2, which accounts for approximately one tenth of the total surface of a single TPR fold. Residues that are potentially involved in establishing hydrogen bonding or salt bridges across the interface are listed in Table 20. Interactions between arginine and aspartate residues are of particular importance (Mitchell *et al.* 1992) and illustrate the key role of the conserved Bub1 and Mad3 DDP motifs in engaging conserved

residues Mad3 R121, R186 and Bub1 R93, respectively. Thus mutation of this motif likely eliminated electrostatic surface complementarity as well as the ability to establish bonds.

#	Bub1 residue and atom	contact residue and atom	distance (Å)	nature
	***S.pombe* Bub1 – Mad3 complex**			
1	Glu 45 – $O_\varepsilon 2$	Mad3 – Arg 186 – N_ε	3.76	salt bridge
2	Glu 45 – $O_\varepsilon 2$	Mad3 – Arg 186 – $N_\eta 1$	2.77	H-bond or salt bridge [*]
3	Asp 47 – $O_\delta 2$	Mad3 – Arg 121 – N_ε	3.36	salt bridge [*]
4	Asp 47 – $O_\delta 2$	Mad3 – Arg 121 – H_ε	2.48	H-bond
5	Asp 47 – $O_\delta 2$	Mad3 – Arg 121 – $N_\eta 2$	3.22	H-bond or salt bridge
6	Asp 47 – $O_\delta 1$	Mad3 – Arg 186 – N_ε	3.99	salt bridge [*]
7	Asp 47 – $O_\delta 1$	Mad3 – Arg 186 – $N_\eta 1$	3.62	H-bond or salt bridge
8	Asp 48 – $O_\delta 1$	Mad3 – Arg 121 – $N_\eta 2$	3.81	H-bond or salt bridge [*]
9	Arg 93 – N	Mad3 – Asp 70 – $O_\delta 2$	3.85	H-bond [*]
10	Arg 93 – $N_\eta 2$	Mad3 – Gln 73 – $O_\varepsilon 2$	2.70	H-bond [*]
	***S.pombe* Bub1 homo-dimer**			
11	Glu 45 – O	Bub1 – Arg 168 – $N_\eta 1$	2.89	H-bond
12	Glu 45 – $O_\varepsilon 2$	Bub1 – Arg 168 – $N_\eta 1$	3.16	H-bond or salt bridge [*]
13	Asp 51 – $O_\delta 1$	Bub1 – Arg93 – $N_\eta 2$	3.96	salt bridge [*]
14	Cys 85 – S_γ	Bub1 – Arg 164 – $N_\eta 2$	2.76	H-bond [*]
15	Arg 93 – $N_\eta 2$	Bub1 – Asp 51 – $O_\delta 2$	3.11	H-bond or salt bridge [*]
16	Arg 168 – $N_\eta 1$	Bub1 – Glu 45 – O	2.69	H-bond [*]
17	Arg 168 – $N_\eta 1$	Bub1 – Glu 45 – $O_\varepsilon 2$	3.60	salt bridge
18	Arg 168 – $N_\eta 2$	Bub1 – Glu 45 – $O_\varepsilon 2$	3.02	H-bond or salt bridge [*]

Table 20: Residues potentially involved in establishing hydrogen bonds or salt bridges at the *S.pombe* Bub1 dimerisation interface with Mad3 or Bub1 as predicted by PDBePISA software (§2.5.3). The non-covalent bonds specified in Figure 19b and Figure 22a are as indicated [*].

The Gibbs solvation free energy gain upon formation of the TPR interface area and reduction of the solvent-accessible hydrophobic area were found to be approximately -1.8 kcal/mol, with Bub1 dropping 1.3 kcal/mol and Mad3 0.5 kcal/mol. These numbers do not include the energy released through non-covalent bonding established across the interface. The additional free energy gain is typically around 0.5 and 0.3 kcal/mol per H-bond or salt bridge, respectively, as per crude approximation although this number could be much higher (Desiraju 2011). Thus the Gibbs free energy of dissociation of the Mad3 – Bub1 binary complex was roughly estimated as -3 kcal/mol, which corresponds to a dissociation constant of 0.82 ($\ln K_d = RT / \Delta G°$ where R = 8.314 $J K^{-1} mol^{-1}$, T = 303 K and $\Delta G°$ = 12.6 kJ) suggesting a complex of medium affinity according to the classification by Kastritis *et al.* (Kastritis *et al.* 2011).

In brief, MS analysis revealed an interaction of Bub1 with Mad3 and the yeast two-hybrid assay demonstrated that a direct Bub1 association with Mad3 depends on the GIG motif of the former and the DDP and HIG motifs of the latter. The importance of these motifs in Bub1 binding was confirmed by Bub1 co-precipitations from *S.pombe* cells bearing HIG or DDP mutant *mad3* alleles. Compared to wild-type Mad3 (column 3 in Figure 21), the Bub1 interaction is reduced to 34% in the *mad3*$^{DDP>AAP}$ mutant and further to 6% in the *mad3*$^{HIG>HIV}$ mutant (column 4 and 5). Thus these evolutionary conserved and related sequence motifs of Bub1 and Mad3 significantly contribute to the stable association of these two proteins, with the DDP motifs establishing a receptive interface and the H/GIG motifs potentially fashioning a conformation amenable to a Bub1 – Mad3 interaction. The *mad3*$^{DDP>AAP}$ and *mad3*$^{HIG>HIV}$ mutant were found to be benomyl sensitive (row 8, 11 and 12 in Figure 21b), whilst the Mad3$^{HIG>VIG}$ mutant protein that was still able to bind Bub1 (row 11 in Figure 16) resisted the microtubule drug as well as cells expressing wild-type Mad3 (row 7, 9 and 10). Remarkably, the benomyl sensitivity of *mad3*$^{DDP>AAP}$ and *mad3*$^{HIG>HIV}$ mutant cells was equally penetrant to that of cells lacking Mad3 completely (row 4 and 8 in Figure 21b). The latter two phenotypes indicate that cells are not able to mediate a spindle checkpoint arrest when spindle microtubules are disrupted and that these mutations perhaps completely abrogate Mad3 function. Indeed, compared to 22% in *mad3* and 1% in *mad3Δ* cells, only 2.5% of *mad3*$^{DDP>AAP}$ mutant cells were able to arrest in metaphase with short spindles in the presence of dysfunctional kinetochores in *nuf2-3* mutant cells incubated at the restrictive temperature (communicated by Alicja Sochaj, Hardwick lab). Thus the checkpoint deficiency of *mad3*$^{DDP>AAP}$ and *mad3*$^{HIG>HIV}$ mutants suggest that the Bub1 – Mad3 interaction is important for a robust spindle checkpoint function. It remains to be investigated whether artificial tethering of Mad3 to Bub1 in these mutants is able to rescue this phenotype.

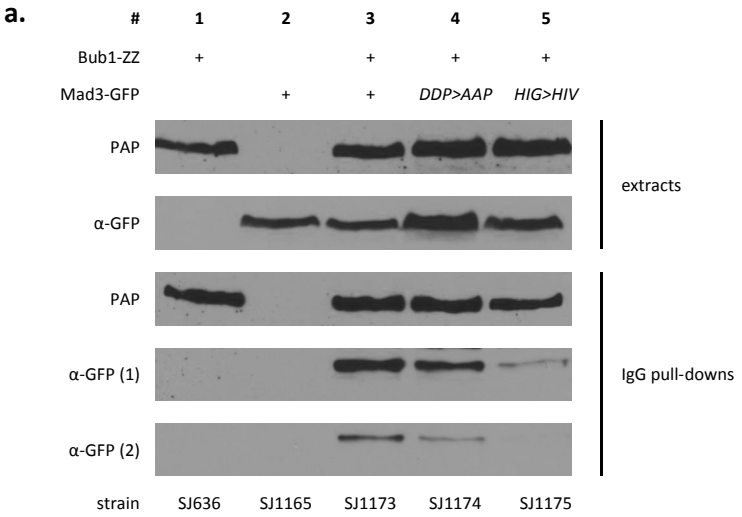

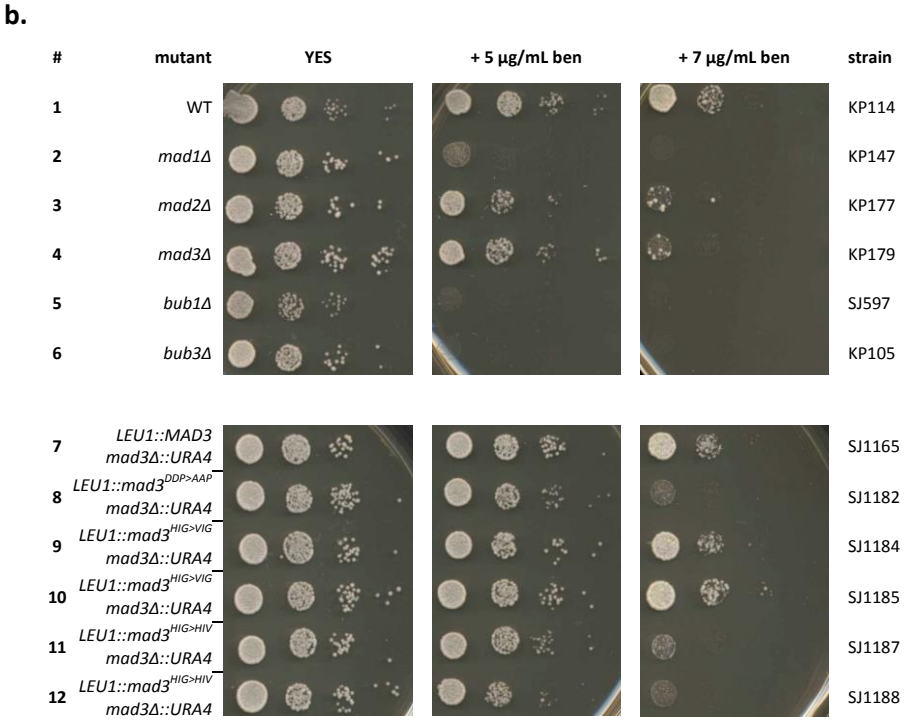

Figure 21: (a) Co-precipitation and immuno-blotting experiments of Bub1 complexes indicate that mutation of the Mad3 HIG or DDP motif destabilises the Bub1 – Mad3 interaction. Employing Image Studio Lite (LI-COR Biosciences, NE, USA) quantitation analysis (§2.5.3), it is estimated that 66% less Mad3$^{DDP>AAP}$ mutant protein associates with Bub1 and only 6% of Mad3$^{HIG>HIV}$ protein compared to wild-type Mad3. **(b)** Benomyl plate assays reveal that *mad3*$^{DDP>AAP}$ and *mad3*$^{HIG>HIV}$ mutant cells are unable to resist the microtubule depolymerising drug in concentrations that support growth in wild-type *mad3* and *mad3*$^{HIG>VIG}$ mutant cells.

Interestingly, yeast two-hybrid analysis indicated that, as in *S.cerevisiae*, *S.pombe* Bub1 homodimerisation could be another feature supported by the GIG and DDP motifs, as mutation of the former motif abolished the Bub1 – Bub1 interaction in the yeast two-hybrid

assay (row 13 and 14 in Figure 16b). *In vivo* Bub1 dimerisation and the dynamics of this process, its relevance and function are under current investigation. The Bub1 – Bub1 dimer structure prediction shown in Figure 22a was obtained through PyMol superimposition of two *S.pombe* Bub1 TPR molecules with the *S.cerevisiae* Bub1 homodimer structure followed by refinement using Chiron software (§2.5.3) to minimise steric clashes at the interface. Residues that are potentially involved in forming bonds at the homodimer interface according to PDBePISA software (§2.5.3) (Krissinel & Henrick 2007) are listed in Table 20. Of these, Arg93 and Arg168 are of particular importance in binding respectively Asp51 and Glu45 across the interface. As the Bub1$^{GIG>GNG}$ mutant protein is not able to homodimerise in the two-hybrid assay, the GIG motif could be important for the structural orientation of individual TPR units.

Taken together, in addition to binding Bub3 through its B3i motif, *S.pombe* Bub1 is able to directly interact with Mad3 through reciprocal engagement of TPR domains. The Bub3 independent association of Mad3 with Bub1 relies on related sequence motifs, preservation of which persisted throughout their molecular evolution. The ternary complex, here termed BUB+ (the BUB complex plus Mad3) and consisting of Mad3, Bub3 and Bub1, is not thought to form in *S.cerevisiae*. Indeed, MS analysis of *S.cerevisiae* Mad3, Bub1 and Bub3 did not substantiate its formation. As Bub1 TPR homodimerisation is achieved in a similar mode to binding Mad3, these interactions are highly likely of a mutually exclusive nature. Thus far, no evidence in favour of Mad3 homodimerisation has been demonstrated.

a.

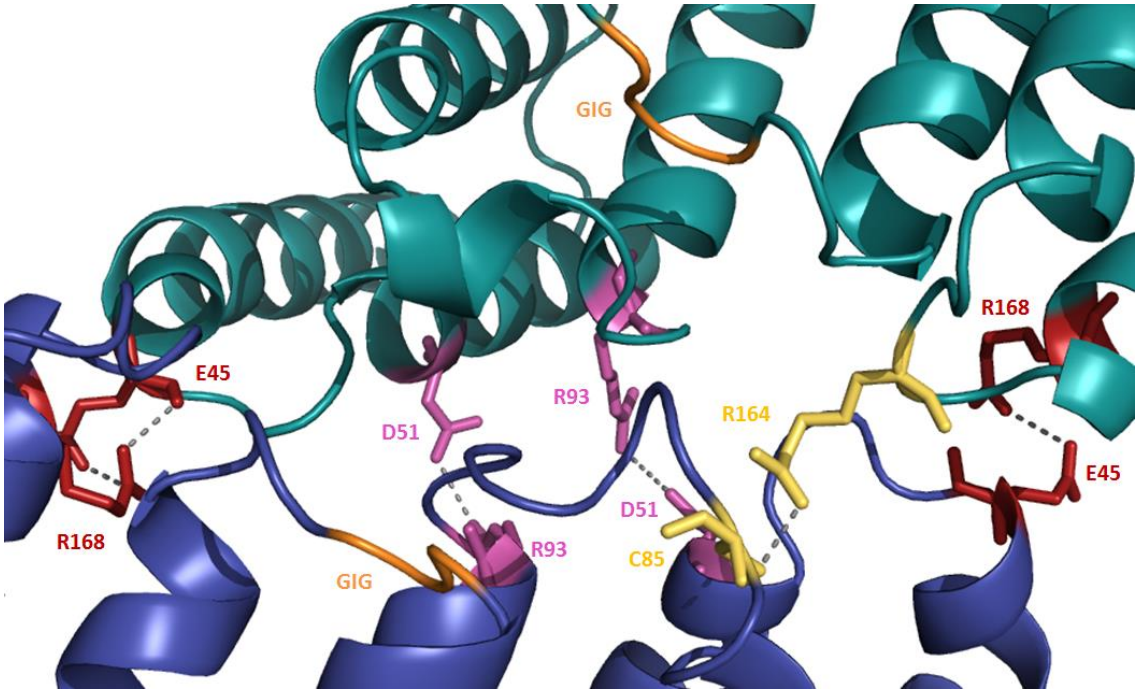

b.

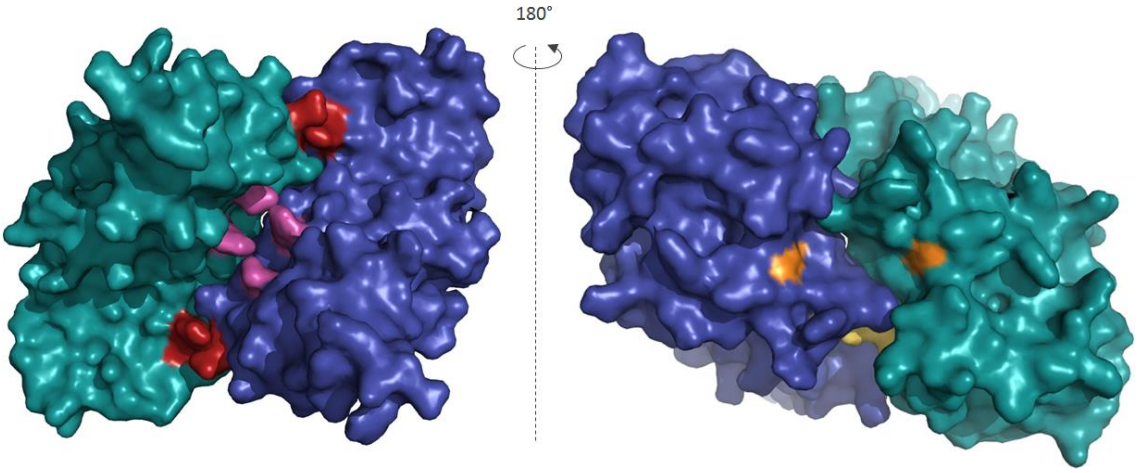

Figure 22: (a) Homology model of the *S.pombe* Bub1 TPR homodimer in ribbon representation modelled upon the *S.cerevisiae* Bub1 homodimer crystal structure. The GIG motif and residues that potentially form electrostatic interactions at the interface are named and coloured (see Table 20). **(b)** Two surface views of the *S.pombe* Bub1 TPR homodimer, coloured as in **(a)** above. Residues that are thought to establish interactions were coloured as above.

3.3.9 *S.cerevisiae* Bub3 interacts with Mad1 (and Bub1)

S.cerevisiae, but not *S.pombe*, Bub3 purifications did indicate the presence of Mad1. The *S.cerevisiae* Mad1 interaction with Bub1 and Bub3 (here termed the MBB complex) has been documented in early spindle checkpoint studies (Brady & Hardwick 2000). The *S.cerevisiae* Bub3 – Mad1 interaction identified by MS thus confirms this finding, although Bub3 and Bub1

did not seem to purify well through Mad1 isolations and full length Bub1 did not purify well from *S.cerevisiae* cells. An analogous MBB complex is thought to exist in *C.elegans* (Arshad Desai, personal communication). The complex can be reconstituted *in vitro* using human proteins (Seeley *et al.* 1999), but as yet conclusive evidence for its presence in species other than *S.cerevisiae* and *C.elegans* is lacking. Whether the MBB complex is unique to *S.cerevisiae* or elusive due to its instability in *S.pombe* remains to be determined. Mutations of the carboxy terminal RLK (arginine-leucine-lysine) motif in *S.cerevisiae* abolish the interaction with both Bub1 and Bub3 and renders cells checkpoint-deficient (Brady & Hardwick 2000). This motif is conserved in many eukaryotic species, including metazoa, and mutation thereof results in defective checkpoint function in both human cells (Kim *et al.* 2012) and *S.pombe* (Kevin Hardwick; not published).

3.3.10 Spindle checkpoint proteins are popular targets for kinases

By MS a total of 521 phosphorylated residues were identified for *S.pombe* spindle checkpoint proteins, of which 143 were found to be distinct (Table 21 and summary in Table 23). For *S.cerevisiae*, these numbers were 165 and 143 respectively (Table 22 and summary in Table 23). Phosphorylated residues were identified through additional mass of 80 Da or the neutral loss of phosphoric acid (98 Da) upon fragmentation and ionisation. Generally speaking, validation of each potential phosphorylation site requires visual examination of the peptide spectrum to ascertain its *in vivo* occurrence. Automated analysis providing so-called 'localisation' and 'debunker' scores for sites that gained 80 Da in mass can facilitate this process and assign confidence to residue modifications. Additional automated analysis was performed at the Yeast Resource Center for five *S.pombe* MS/MS runs (namely 3093, 3392, 3406, 3407 and 3437; see Table 16). In Table 21, high-confidence residues with localisation scores of 13 and over or debunker scores of 0.95 or over are underlined. Residues that fall below this threshold are given within brackets and sites that are obtained through neutral loss scanning remain to be manually validated upon request through the Yeast Resource Center. All residues identified as (potential) kinase substrates are highlighted in yellow in multiple sequence alignments in section 7.5 (supplementary information).

#	ORF	*S.pombe* phosphorylated residues
1	Mad1	S17[1] S45[1] S59[1] S114[3] T115[2] S170[2] S213[3] S227[2] Y287[1] T293[1] T303[1] S307[1] T313[1] T318[2] T332[1] S341[1] S342[2] S348[2] T367[1] S388[7] T391[2] S403[1] Y433[2] S439[2] T450[4] S451[8] S455[1] T489[1] T501[1] T517[1] S551[1] S569[1] S602[1] S611[3] T637[1] S645[2] S646[3] T647[4] S655[1] T672[1]
2	Mad2	S29[1] Y48[3] T88[1] S89[1] T140[1] S161[1] T165[2] S170[1]
3	Mad3	S19[1] S31[1] S33[2] T44[1] T64[2] S65[1] S67[2] Y78[2] T82[3] T91[2] S205[1] (S208[1]) (T210[1]) S212[3] T218[1] T219[1] S222[2] T223[2] S229[2] S231[2] (T233[1]) S243[2] 245Y[1] S246[2] S251[3] S259[2] S276[3] T278[1] S279[1] S289[10]
4	Bub1	S105[1] Y106[1] S188[1] Y194[1] S207[2] S211[2] S212[2] S213[1] T214[1] S217[2] S221[1] S226[1] S231[2] S234[6] S238[2] S245[6] S248[2] T252[4] S262[9] S263[9] S270[1] S296[1] S316[2] S321[14] S322[9] S323[15] S324[12] S327[42] Y330[6] S338[4] T340[13] T342[4] S344[1] S355[2] T356[1] S357[4] S372[6] S381[4] T383[2] S403[2] S405[8] S409[5] S410[7] S412[22] S415[18] S418[3] S419[6] Y420[4] T423[14] S431[2] S432[8] S434[2] T437[1] S438[1] T440[2] S443[6] S453[7] T455[13] S457[5] S462[4] Y465[2] S466[7] S474[1] S478[1] T482[1] Y483[4] S499[1] S529[3] S532[7] T534[5] T541[1] S545[19] Y548[2] S549[1] S555[1] S558[16] S600[3] Y626[1] S632[2] S634[1] T638[9] S697[1] S702[1] T741[1] S747[1] T873[1] Y889[2] S892[2] Y980[1] T997[1] S1001[2] T1008[4] S1012[3] S1026[1] T1027[1] S1030[1] S1038[1]
5	Bub3	S4[1] S11[1] S16[12] S17[4] S21[4] S23[4] S55[1] S56[1] T80[1] T85[1] S183[1] Y305[1]
6	Slp1	S11[4] S28[8] T31[5] S59[4] S76[4] S93[2] T97[2] S104[1] S107[2] (S116[1]) Y182[1] T218[1] S230[1] S237[1] S482[1]
7	Cut4	T122[1] S187[1] S198[1] S201[1] S211[2] S213[1] S223[2] S284[2] Y286[1] S290[1] S325[1] T349[1] T414[1] S417[1] T674[2] S675[1] T676[1] T681[1] S687[1] Y862[1] T864[1] S865[1] T870[1] S871[1] S936[1] S1368[1] S1457[2]
8	Apc5	Y286[1] T319[2] T322[2] S348[2] S351[6] S358[2] T404[1] T541[2] Y544[2] Y698[1]
9	Lid1	S198[1] Y199[1] Y490[1] Y491[1]
10	Apc2	T4[1] T8[1] S13[2] S20[1] S21[1] S602[1]
11	Nuc2	S243[2] S314[1] T315[1] Y509[1] T556[1]
12	Cut9	S49[1] T50[1] T52[2] T63[2] Y127[2] T130[1] Y133[1] T141[2] Y234[1] S242[2] S546[2] S615[1] S621[1] S625[1] S626[2] S629[6] S631[1] Y651[1] S654[1] S656[2] S668[1]
13	Cut23	T2[1] S4[3] T7[1] S64[1] S65[4] T66[7] T68[5] Y156[1] S291[6] T298[2] T388[1] S470[1] Y484[1] S495[7] Y497[4] S499[1]
14	Apc10	S14[4] T16[3] S19[1]
15	Apc15	S5[1]
16	Apc13	S3[2] Y5[1] Y7[2]
17	Apc14	S81[1]
18	Apc11	T15[1] T39[1] T87[1] S91[1]
19	Hcn1	T27[6] S30[5] S32[3] S44[2] T45[2] S48[9] S73[1]

Table 21: *In vivo* phospho-modifications detected by MS of *S.pombe* spindle checkpoint proteins (#1-5), Slp1 and APC subunits (#6-19). The number in superscript is the number of times this phosphorylated residue occured in the combined MS2 and MS3 data. These phosphorylation data are of all purifications performed in this study (interphase and mitotic cells and including repeat experiments). Underlined residues were confirmed by automated or manual verification (at least once when detected multiple times), whereas residues in brackets are of low confidence. All other residues are subject to validation, requiring re-analysis by the Yeast Resource Center. The multiple sequence alignment of checkpoint proteins in section 7.5 contains the residues indicated in this table in yellow high-light.

In addition to the checkpoint protein modifications, 15 distinct modifications for Slp1 and 108 for all APC subunits in *S.pombe* and 1 for Cdc20 plus 68 for the APC subunits in *S.cerevisiae* were catalogued (Table 21 and Table 22). APC subunits Hcn1/Cdc26, Apc13/Swm1 and Cut9/Cdc16 stand out by the large number of unique modifications relative to their size. Although no phospho-residues were detected for *S.cerevisiae* Apc11, 31% of STY residues of the *S.pombe* orthologue are potentially phosphorylated (Table 23).

#	ORF	*S.cerevisiae* phosphorylated residues
1	Mad1	S46[1] T73[2] T89[2] S199[1] S227[6] Y231[4] S232[1] T233[1] T240[1] Y252[3] S273[1] T278[1] S299[1] S313[2] T316[1] Y321[3] S324[7] Y425[2] S462[2] S479[1] Y494[1] T498[1] T502[12] S550[1] T560[1] T561[1] S662[1]
2	Mad2	Y20[1] S102[2] S105[5] S131[1] T133[1] T139[1] Y144[2] S165[1] S167[2]
3	Mad3	S14[7] S15[13] S17[3] S75[6] T79[2] Y81[1] Y84[1] Y151[1] S159[1] T250[1] S252[3] S268[10] Y366[1] S380[1] S434[1] S447[1] T457[5] S462[6] T463[1] T465[1] S466[1] S470[3] T478[1] S490[1] S495[2] S499[5]
4	Bub1	S14[2] S451[2] T550[2] T566[1] S596[1]
5	Bub3	S303[1]
6	Cdc20	T26[1]
7	Apc1	S267[1] S272[3] S285[1] S308[1] S310[1] S691[1] T995[1] S1103[1] S1192[1] S1193[1] S1208[3] S1209[2] S1443[1] S1447[2] S1451[2] T1459[1] S1462[5] S1468[10] S1469[4] S1472[1]
8	Apc5	S314[1] S414[1] S423[1]
9	Apc4	Y273[1] Y275[1] S553[1] Y603[1]
10	Apc2	S74[1] Y76[2] S77[1] S206[1] S208[1]
11	Cdc27	S215[1] S224[2] S264[1] S267[3] S270[1] S328[2]
12	Cdc16	S44[3] S46[3] S50[3] S54[1] T55[4] S95[2] S103[4] Y251[1] Y257[1] S742[1] S743[1] S788[2] S789[9] T791[1]
13	Mnd2	S293[3] S300[2] S324[2] T329[1] T335[2] S340[1]
14	Swm1	T52[2] S54[3] S59[8] Y374[1]
15	Cdc26	T7[3] T8[3] S12[16] T17[7] S18[14] S103[1]

Table 22: *In vivo* phospho-modifications detected by MS of *S.cerevisiae* spindle checkpoint proteins (#1-5), Cdc20 and APC subunits (#6-15). The number in superscript is the number of times this phosphorylated residue occurs in the combined MS2 and MS3 data. These phosphorylation data are of all purifications performed in this study (interphase and mitotic cells and including repeat experiments). All residues are subject to validation, requiring re-analysis by the Yeast Resource Center. The multiple sequence alignment of checkpoint proteins in section 7.5 contains the residues indicated in this table in yellow high-light.

In *S.pombe*, Bub1 accounted for the bulk of the observed phospho-modifications with potentially 97 serine, threonine or tyrosine (STY) residues phosphorylated (48% of total STY number). 54% of Mad3 STY residues were shown to be potentially phosphorylated. *S.cerevisiae* Bub1 was found to be unstable during purifications and its phosphorylation status was therefore difficult to assess, but Mad1, Mad2 and Mad3 were shown to be extensively modified by kinases (respectively 26, 22 and 30% of STY number). In general, all Mad and Bub proteins from both yeast species were detected as post-translational modifieds by the addition of phosphate groups. Phosphorylation of STY residues that are conserved in both *S.pombe* and *S.cerevisiae* are Mad1 S602/662 and T303/S313, Mad2 T140/133 and S170/165, Mad3 Y78/84, Bub1 S545/T566 and S532/T550. These residues are of particular interest for mutagenesis studies as these could indicate a conserved mechanism of functional regulation. The phosphorylated residues identified within Apc15/Mnd2 are of interest, too, as this APC subunit has a role in silencing spindle checkpoint signalling (Mansfeld *et al.* 2011, Uzunova *et al.* 2012) and is thought to position closely to APC-bound MCC complexes (Chao *et al.* 2012).

#	*S.pombe* ORF	kDa	P-res total	P-res unique	%P-STY	*S.cerevisiae* ORF	kDa	P-res total	P-res unique	%P-STY
1	Mad1	80	77	40	40	Mad1	88	61	27	26
2	Mad2	24	11	8	25	Mad2	22	16	9	22
3	Mad3	36	59	30	54	Mad3	58	79	26	30
4	Bub1	118	451	97	48	Bub1	118	8	5	3
5	Bub3	36	32	12	21	Bub3	38	1	1	2
6	Slp1	53	38	15	15	Cdc20	67	1	1	1
7	Cut4	165	32	27	10	Apc1	196	43	20	6
8	Apc5	85	21	10	8	Apc5	79	3	3	2
9	Lid1	83	4	4	3	Apc4	75	4	4	4
10	Apc2	79	7	6	5	Apc2	100	6	5	4
11	Nuc2	76	6	5	4	Cdc27	85	10	6	4
12	**Cut9**	**76**	**34**	**21**	**17**	**Cdc16**	**95**	**36**	**14**	**9**
13	Cut23	66	46	16	14	Cdc23	73	0	0	0
14	Apc10	21	8	3	8	Doc1	33	0	0	0
15	Apc15	16	1	1	6	**Mnd2**	**43**	**11**	**6**	**11**
16	**Apc13**	**16**	**5**	**3**	**20**	**Swm1**	**19**	**14**	**4**	**13**
17	**Apc11**	**11**	**4**	**4**	**31**	Apc11	19	0	0	0
18	**Hcn1**	**9**	**28**	**7**	**44**	**Cdc26**	**14**	**44**	**6**	**24**
19	Apc14*	12	1	1	6	Apc9*	31	0	0	0

Table 23: Summary of *in vivo* phospho-modified residues of spindle checkpoint proteins, Slp1/Cdc20 and APC subunits using MS2 and MS3 data (see §2.3.3). Proteins on the same row are orthologues, *except for *S.pombe* Apc14 and *S.cerevisiae* Apc9 that do not share homology and are simply grouped together for convenience. P-res total: total number of residues encountered that were phospho-modified. P-res unique: total number of unique or specific phospho-modifications. %P-STY: percentage of serine (S), threonine (T) and tyrosine (Y) residues that were uniquely modified. The top four %P-STY of *S.pombe* and *S.cerevisiae* APC subunits are indicated in bold typeface.

3.4 Conclusions and discussion

3.4.1 The rapid large-scale one-step purification method

Large-scale purification methods often take considerable time and effort. A typical timespan is 6 to 12 hours from harvesting cells to completion, which negatively impacts the stability of complexes, its phosphorylation status and eventually the yield. Here, a stream-lined rapid large-scale isolation method is described that should take no more than 1 hour from harvesting cells to preparing a liquid nitrogen cooled, broken up and powdered yeast lysate, with an additional 1 hour from reconstitution of the lysate to purified complexes on beads. The protocol described here combines the effective culture conditions of concentrated yeast media, the efficient and reliable breakage of yeast cells using an automated process, quick clearance of lysates employing glass fibre filters, the strong affinity of IgG to the ZZ tag, and the

fast and efficient handling of paramagnetic IgG Dynabeads. A typical purification process that used 25 grammes of yeast grindate and 25 mg of IgG coupled Dynabeads was shown to yield approximately 60 pmol of complexes. As part of a routine process, the final yield will depend on protein abundance and stability, and the quantity of beads. Following this procedure, large spectral coverage of protein complex components by tandem MS analysis can be obtained and evidence of weaker associations and *in vivo* modifications, such as phosphorylation, can be uncovered. Employing this protocol, parallel purification of spindle checkpoint complexes from *S.pombe* and *S.cerevisiae*, and analysis by tandem MS provided interesting insights into the similarities and disparities of checkpoint organisation of these two yeasts. In addition, a wealth of phospho-modification data was generated and novel binding partners identified. Verification of this data is currently on-going in the lab.

Perhaps the most challenging aspect was the presence of 'contaminating' or background proteins right across the board of a large number of (unrelated) preparations that were not witnessed in mock purifications. Thus likely to be 'passengers' or 'hitchhikers' of true interactors, their identification by additional purifications is of the essence. However, once a number of purifications is analysed, compilations of 'grey' or 'black' lists can simplifly further identification of potentially *bona fide* interactors. In those cases where the isolation of stable and clean complexes devoid of nonspecific protein interactors is desirable, preventative measures can be included. This can be achieved by the addition of non-denaturing nonionic detergents such as Triton X100, NP40 and Tween20 or by the controlled increase of salt concentration during wash steps. The protocol as devised here should be compatible with *in vivo* cross-linking strategies to stabilise weak protein – protein interactions (Miernyk & Thelen 2008). Lastly, financial constraints could dictate the cost-effective substitution of para-magnetic Dynabeads by column-packed Fractogel resin (EMD Millipore Corp, MA, USA) (Sawin *et al.* 2010).

In this study, mitotic spindle checkpoint complexes were purified from *nda3-km311/tub2-401* cells with cold-sensitive microtubules and interphase complexes from wild-type *nda3/tub2* cells with normal microtubules (§2.3.1). The latter complexes were isolated from cells grown at 30-32°C and mitotic checkpoint complexes from cells at 16-18°C. Although cells are able to robustly evoke mitotic arrests at low temperatures, it is conceivable that complexes purified from 'cold cells' are less stable than those from interphase cells. The main aim of this study was to describe and compare the different spindle checkpoint complexes that occur in the two yeast species. If comparison of Mad and Bub protein interactors from mitotic and interphase

cells is, however, desirable, additional control experiments will have to be performed, such as isolating interphase complexes from *nda3-km311*/*tub2-401* cells at the permissive temperature or from wild-type *nda3*/*tub2* cells at the restrictive temperature, and mitotic complexes from nocodazole arrested cells.

3.4.2 Divergent evolution can remodel well-conserved molecular pathways

The yeasts *S.pombe* and *S.cerevisiae* share a common ancestor that lived 330 – 1,100 million years ago (Sipiczki 2000, Heckman *et al.* 2001, Hedges 2002). In this study, analysis of physical interactions of spindle checkpoint proteins in the yeast *S.pombe* and *S.cerevisiae* indicated that molecular divergence during this vast timespan has given rise to notable dissimilarities in the way spindle checkpoint signalling is organised in these two species. Together with the Mph1/Mps1 kinase, the Mad and Bub proteins form the core of spindle checkpoint function, but despite their remarkable conservation throughout the Eukaryota domain of life (Vleugel *et al.* 2012), species specific variations did arise through molecular evolution and adaptation driven by physiological and environmental constraints.

The exact environmental or physiological constraints that confer evolutionary pressures and underlie these remodelling events are unknown. It could reflect the disparate nature in which chromosome biorientation is established in different species (number of chromosomes, number of microtubule attachments per kinetochore, presence of DASH complexes) and when during the cell cycle this occurs (S phase in *S.cerevisiae* versus mitotic entry in *S.pombe*), the extent of nuclear envelope breakdown during mitosis, the manner in which the checkpoint components monitor attachments or the fact that they have taken other duties upon them, such as mitotic timing (Meraldi *et al.* 2004) and possibly a response to DNA damage (Bihani & Hinds 2011). Remodelling of spindle checkpoint signalling in both *S.cerevisiae* and *S.pombe* has occurred without compromising on checkpoint functionality: the fidelity of their chromosome segregation machinery, even when mitotic microtubules are rebuilt after impairment, is well-documented. This work demonstrates that 'rewiring' of a well-conserved molecular mechanism can take place through the process of divergent molecular evolution.

3.4.3 *S.pombe* Bub3 and spindle checkpoint function

Unlike its *S.cerevisiae* and metazoan orthologues, *S.pombe* Bub3 was found not to associate with Slp1, Mad2 and Mad3 in forming a mitotic checkpoint complex (MCC) to inhibit the APC ligase. Several studies have noted the absence of the Bub3-interaction (B3i; formerly GLEBS) motif in Mad3 and its presence in other studied eukaryotes (Sczaniecka *et al.* 2008, Chao *et al.*

2012). Although in the absence of Bub3 the *S.cerevisiae* and human spindle checkpoint is compromised, MCC assembly and *in vitro* inhibition of the APC might not require its presence (Fang 2002, Kulukian *et al.* 2009, Foster & Morgan 2012). Artificial tethering of Mad2 to Mad3 is sufficient to delay metaphase in *S.cerevisiae* cells (Lau & Murray 2012), suggesting that Bub3 could facilitate, stimulate or stabilise the association of the checkpoint proteins with Cdc20 *in vivo*. Indeed, the ubiquitination of Cdc20 by *S.cerevisiae* APC, as occurs *in vivo* during a checkpoint arrest, requires the presence of both Bub3 and Mad3 (Foster & Morgan 2012). Why Bub3 is not required for *S.pombe* MCC formation and its subsequent disassembly by APC is as yet unknown. Remarkably, *S.pombe* Bub3 is not required for a checkpoint-mediated inhibition of APC^{Slp1}, as cells that lack Bub3 robustly delay anaphase (Tange & Niwa 2008, Vanoosthuyse *et al.* 2009, Windecker *et al.* 2009). In these cells, kinetochore localisation of Bub1 and the Mad proteins is greatly reduced and silencing of the checkpoint is ineffective. These findings advocate that the main role of Bub3 is to retain or target the checkpoint proteins at kinetochores (Taylor *et al.* 1998, Krenn *et al.* 2012), a crucial step in checkpoint silencing (Vanoosthuyse *et al.* 2009). Remarkably, although *S.pombe* Bub3 is per strict definition not a checkpoint protein, functional studies in this yeast species have been particularly revealing in regards to checkpoint silencing and kinetochore anchoring of checkpoint components.

3.4.4 *S.cerevisiae* Mad1 associates with Bub1 and Bub3

S.cerevisiae Mad1 interacts with both Bub1 and Bub3 (Brady & Hardwick 2000) to form the MBB complex. The formation of this complex is stimulated during a mitotic arrest and depends on the Mad1 RLK motif, mutation of which also abolishes spindle checkpoint function (Brady & Hardwick 2000). The Mad1 RLK motif is conserved in most studied organisms (see multiple sequence alignment in section 7.5.2, page 196), but evidence in favour of MBB formation in *S.pombe* and other eukaryotic cells other than *C.elegans* (Arshad Desai; personal communication) is lacking. Human Mad1 RLK mutations result in a reduction of kinetochore-bound Mad1 (Kim *et al.* 2012). A similar reduction is observed when Bub1 is removed by siRNA and levels are not further reduced in combination with the RLK motif mutant. This study advocates that the kinetochore anchoring of Mad1 is in part facilitated by Bub1 through a direct interaction (Kim *et al.* 2012), but MBB complexes have not been successfully isolated from human cells, although reconstitution can take place *in vitro* (Seeley *et al.* 1999). As yet, it cannot be ruled out that the reduced levels of Mad and Bub proteins seen at kinetochores are a consequence of checkpoint deficiency in human Mad1 mutant cells. In *S.pombe*, Mad1 kinetochore localisation depends on Bub1, but not *vice versa* (Heinrich *et al.* 2012).

3.4.5 A tight association of the MCC with the APC is not critical in achieving mitotic arrests

The spindle checkpoint-mediated anaphase delay in *S.cerevisiae*, unlike that in *S.pombe*, does not require a stable interaction of the MCC with the APC. As the MCC is a substrate of the APC E3 ubiquitin ligase it naturally requires temporary docking onto the APC. Human and *S.cerevisiae* cell studies reveal that during prometaphase the Apc15/Mnd2-mediated ubiquitination of Cdc20 promotes the disassembly of MCC complexes that primes cells for a rapid anaphase onset once chromosome biorientation has been established (Foster & Morgan 2012, Uzunova *et al.* 2012). The inability to detect *S.cerevisiae* APC^{MCC} complexes in mitotic MCC or APC preparations could be a result of the experimental setup used in this work. As yet, it cannot be ruled out that the mitotic cell lysates favour stabilisation of *S.pombe* APC^{MCC} but at the same time promote rapid disassembly of *S.cerevisiae* APC^{MCC} in mitotic lysates (peculiarly, the same conditions that could stabilise the Bub3 – Mad1 interaction in *S.cerevisiae* but not in *S.pombe* extracts). Although the ubiquitin ligase activity of purified *S.cerevisiae* APC^{Cdc20} can be readily inhibited by the addition of Mad3 *in vitro*, it is remarkable that few studies hint at isolating APC^{MCC} holo-enzyme complexes from this yeast (Passmore *et al.* 2005, Schuyler & Murray 2009, da Fonseca *et al.* 2011). On the other hand, the absence of APC^{MCC} complexes in mitotic MCC or APC preparations could indicate that *S.cerevisiae* MCC associates with few APC complexes, that this interaction is perhaps very fleeting, or that the MCC readily dissociates upon contacting the APC. In contrast, APC^{MCC} from *S.pombe* is remarkably stable compared to that of *S.cerevisiae*. Whether this finding is of relevance remains to be investigated. For instance, it could imply that APC inhibition in *S.cerevisiae* fundamentally relies on sequestration of Cdc20 and that in *S.pombe* inhibition of the APC occurs at multiple levels that requires stable binding of MCC complexes. Indeed, MCC facilitates the ubiquitination of Cdc20 during a checkpoint-mediated metaphase arrest, but this activity is not a requirement for the maintenance of this arrest (Foster & Morgan 2012). The association of checkpoint proteins with the APC can determine its substrate specificity and modulate catalysis: the *in vitro* APC activity towards securin can be inhibited by Mad3 alone, whereas Mad2 also prevents it from targeting Cdc20 (Foster & Morgan 2012).

However, purification of the *S.cerevisiae* APC E3 ubiquitin ligase complexes devoid of MCC inhibitors uniquely allows the study of its mode of action in *in vitro* assays. Such exploits revealed a wealth of information in regards to its activation by cofactors, the binding and targeting of substrates, its processivity and its inhibition or modulation by checkpoint components (Passmore *et al.* 2005, Schuyler & Murray 2009, Foster & Morgan 2012). Although

it appears that *S.cerevisiae* is a good model organism for *in vitro* mitotic APC ubiquitination studies, both *S.pombe* and metazoan MCC complexes stably associate with the APC. Thus *S.pombe* might ultimately be a better suited model organism for *in vivo* and *in vitro* studies. To this end, *in vitro S.pombe* APC ubiquitination assays have been developed (Yoon *et al.* 2002, Ors *et al.* 2009). To facilitate such studies in our lab, purified mitotic APC complexes devoid of MCC are isolated from *slp1-362* mutant cells that arrest in metaphase at the restrictive temperature with no APC-bound Slp1, Mad2 and Mad3 (Sczaniecka *et al.* 2008).

The way in which the MCC might dock onto the much larger APC is coming under closer scrutiny (Chao *et al.* 2012, Zhang *et al.* 2012). In a recent study, purified *S.pombe* MCC complexes produced by baculovirus vector-mediated expression in insect cells allowed its structural examination by x-ray crystallography (Chao *et al.* 2012). Subsequent *in silico* modelling of the APC^{MCC} holoenzyme already has provided much needed insight into the nature of APC^{Cdc20} inhibition by Mad2 and Mad3 (see page 22 and Figure 11) (Chao *et al.* 2012). Further structural, biophysical and thermodynamic studies could reveal the temporal and spatial nature in which both *S.pombe* and *S.cerevisiae* APC and MCC regulate their association (Zhang *et al.* 2012). Central to this regulation could be phosphorylation (discussed in §3.4.9), ubiquitination and allosteric modulation.

3.4.6 Relics of homodimerisation: ancient paralogues interact through related sequence motifs

Although *S.pombe* Mad3 was shown to have lost its ability to directly interact with Bub3, an indirect association was revealed that is facilitated by its 'ohnologue' Bub1. In this ternary complex, Bub1 engages both Mad3 and Bub3 in a direct manner. Bub1 associates with Bub3 through its B3i motif and yeast two-hybrid analysis showed that Bub1 physically interacts with Mad3 through reciprocal association of evolutionary related TPR domains for which the presence of the H/GIG and DDP motifs was shown to be essential. These residues are present in the tight turn regions that emanate from the antiparallel α-helices comprising the helix-turn-helix folds of a triptych of hairpin-like TPR units present in both Bub1 and Mad3. The Bub1 and Mad3 association is predicted to be similar to the homodimerisation of *S.cerevisiae* Bub1 observed *in vitro* and in its crystalline packing (Bolanos-Garcia *et al.* 2009).

The existence of this trimeric Mad3 – Bub1 – Bub3 complex (which is referred to as the 'BUB+ complex') is thought to be unique to *S.pombe* and possibly evolved as a result of the absence of the Mad3 B3i sequence. *S.pombe* Mad3 and orthologues from two other fission yeasts, namely *Schizosaccharomyces octosporus* and *cryophilus*, clearly lack the B3i motif required for

Bub3 binding. However, a putative B3i motif in truncated form could be present in Mad3 from the fission yeast *S.japonicus* (refer to Figure 27 on page 124). As taxonomic analysis based on rRNA sequence analysis indicate that *S.japonicus* is the most distantly related species within the *Schizosaccharomyces* genus (Sipiczki 2000, Helston *et al.* 2010) the loss of the B3i sequence motif most likely occurred after this yeast split from the lineage that gave rise to the other fission yeast species. It would be of interest to study *S.japonicus* checkpoint complex formation: if the presence of a Mad3 B3i motif can be confirmed it could be predicted that MCC complexes bear Bub3, that spindle checkpoint-mediated metaphase arrest depend on Bub3 and perhaps that Bub1 does not interact directly with Mad3. Perhaps in some of these aspects, *S.japonicus* appears to be an excellent model organism for spindle checkpoint studies as checkpoint complex behaviour seems to mirror metazoan mechanism.

S.pombe cells expressing Mad3$^{DDP>AAP}$ or Mad3$^{HIG>HIV}$ mutant protein exhibited increased sensitivity to microtubule disrupting drugs and were shown to be spindle checkpoint-deficient due to their inability to arrest in metaphase (personal communication with Alicja Sochaj, Hardwick lab). Thus, the interaction of Mad3 with Bub1 appears to be required for checkpoint function. *S.pombe* MCC complexes were shown not to contain Bub3, but Mad3 has evolved means of associating with Bub3 even though it is lacking a B3i motif. This could imply that the Bub1-mediated union of Bub3 with Mad3 is somehow a necessity and evolutionary constraint. Cells lacking Bub1 failed to translocate Mad3 and Bub3 to the mitotic nucleus (personal communication with Alicja Sochaj, Hardwick lab) (Kadura *et al.* 2005). As mitosis in yeast occurs without breakdown of the nuclear envelope, the ternary BUB+ complex could serve as a vehicle for nuclear import of checkpoint components. Bub3-dependent Mad3 localisation to kinetochores could assist in achieving checkpoint-mediated anaphase delays (Vanoosthuyse *et al.* 2009, Windecker *et al.* 2009, Krenn *et al.* 2012). Investigations are currently on-going to see whether artificial tethering of Mad3 to Bub1 can rescue the spindle checkpoint deficiency of *mad3*$^{DDP>AAP}$ and *mad3*$^{HIG>HIV}$ motif mutants. In addition, Bub1 GIG and DDP mutants are being generated.

Would it be possible for Bub1 to engage the MCC through association with Mad3? A structure mock-up of a Bub1 – Mad3 model superimposed onto the MCC structure by alignment of the Mad3 molecules in PyMol (data not shown) strongly suggests that this cannot be the case. Within a MCC complex (partial structure given in Figure 11a on page 24), Mad3 residue Lys92 (located in the tight turn between the first and second helix of the first TPR unit) contacts Slp1/Cdc20 near its D-box receptor (Chao *et al.* 2012). Further Mad3 contacts between Mad2

and Slp1/Cdc20 are provided by a helix-loop-helix structure preceding the α-helix prior to the TPR domain (refer to Figure 18a on page 81) (Chao *et al.* 2012). In the mock-up structure model, it is the latter α-helix preceding the TPR domain of Bub1 that noticeably overlaps with part of Mad2, and, short of major structural rearrangements, steric hindrance would clearly prevent Bub1 binding the MCC via Mad3. In support of this, MS analysis of Bub1 precipitations does not uncover Slp1 or Mad2 and *vice versa*.

In theory, the *S.pombe* Bub1 TPR domain can accommodate binding to both Mad3 and Spc7, the Blinkin orthologue. As illustrated by an *in silico* model of a prospective Bub1 TPR dimer interacting with small Blinkin fragments in Figure 23, TPR dimerisation and Blinkin binding involves different surfaces. This indeed suggests that Mad3 kinetochore localisation is directly facilitated by Bub1. Both Bub1 and Mad3 localisation in *S.pombe* is dependent on Bub3 (Heinrich *et al.* 2012) and in Bub1 mutants lacking the B3i motif kinetochore localisation of checkpoint proteins is greatly diminished (Vanoosthuyse *et al.* 2009). In human cells, mutation of the B3i motif in the human Mad3 orthologue BubR1 abrogates spindle checkpoint function (Elowe *et al.* 2010) as well as kinetochore localisation of checkpoint components (Krenn *et al.* 2012). This mutant is also affected in its ability to orchestrate chromosome biorientation (Elowe *et al.* 2010). Although *S.pombe* Mad3 is not implicated in this process, it stresses the Bub3 dependency of Mad3 and Bub1 for kinetochore association.

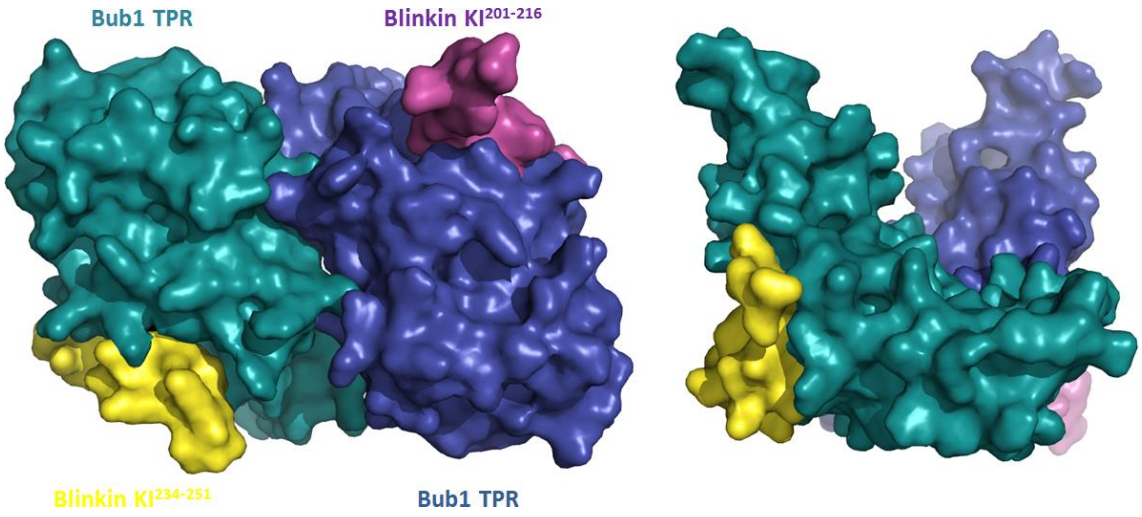

Figure 23: Two surface views of a homology structure model created to illustrate the distinct Bub1 TPR faces involved in homodimerisation (coloured in cyan and blue) and Blinkin binding (yellow and pink). Two different KI motif-bearing Blinkin fragments less than 20 residues in length interacting with human BubR1 or Bub1 TPR domains were determined by x-ray crystallography in two separate studies (yellow: (Bolanos-Garcia *et al.* 2011), green: (Krenn *et al.* 2012). The human BubR1 and Bub1 structures (not shown) were structurally aligned with the *S.pombe* Bub1 homodimer in Pymol. See §2.5.3 for additional information on modelling and structures used.

As has been observed for *S.cerevisiae* Bub1 *in vitro* (Bolanos-Garcia *et al.* 2009), *S.pombe* Bub1 also demonstrates a propensity for homodimerisation in the yeast two-hybrid assay presented here. This association is very likely achieved through the same Bub1 surface that facilitates its interaction with Mad3 as mutation analysis identifies residues that are critical for both the Bub1 – Mad3 binding and Bub1 homodimerisation. Thus well-conserved sequence motifs that enable homodimerisation also support the interaction of ancient paralogues: Mad3 – Bub1 association is achieved through evolutionary conserved and related interaction motifs.

At this moment in time, it is not known whether homodimerisation is essential for Bub1 or spindle checkpoint functioning. This could be somewhat difficult to investigate, as mutants that negatively affect homodimerisation could also abolish the interaction with Mad3. However, preliminary analysis of residue bonding at the dimerisation interface (listed in Table 20, page 86) has earmarked several residues that are potentially involved in the formation of the Bub1 homodimer and might not play a role in dimerisation of Mad3 with Bub1: Asp51, Cys85, Arg164 and Arg168. Care should be taken however to minimise disturbance of the electrostatic surface that could disrupt Mad3 – Bub1 dimerisation. Subtle substitutions of the charged polar arginines to lysines or even to polar uncharged residues such as serines or threonines are advisable. Replacing Cys85 by other small amino acids such as glycine can further destabilise Bub1 homodimers without affecting Mad3 binding.

Presumably, Bub1 homodimerisation and Bub1 – Mad3 complex formation are mutually exclusive as both processes involve the same Bub1 interface. It could thus be that the balance between these two dimerisation events is regulated. This could perhaps explain why the number of Mad3 peptides is much lower than that of Bub3 in the MS analysis of Bub1 interactors (table in §7.1, row 5 and 10), even though both proteins are of comparable size. The manner in which Bub1 homodimerisation is promoted over the Bub1 – Mad3 association could be regulated by kinase action. Several phosphorylated residues within the TPR domains of Mad3 (§7.5.3) and Bub1 (§7.5.6) were identified, although none of these mapped to the dimerisation interface. Figure 24 illustrates the complexes that could be formed through participation of Mad3, Bub1 and Bub3 in *S.pombe*. Evidence in favour of the existence of the large Bub1 – Bub3 dimer-dimer could be obtained by co-precipitations and determination of hydrodynamic properties of purified complexes (Schuyler & Pellman 2002, Erickson 2009). The approximate size and shape of complexes can be judged by combining calibrated size exclusion chromatography and sucrose density gradients. In the Hardwick lab, work is on-going in

producing baculovirus-expressed recombinant proteins to study further the assembly and architecture of checkpoint complexes.

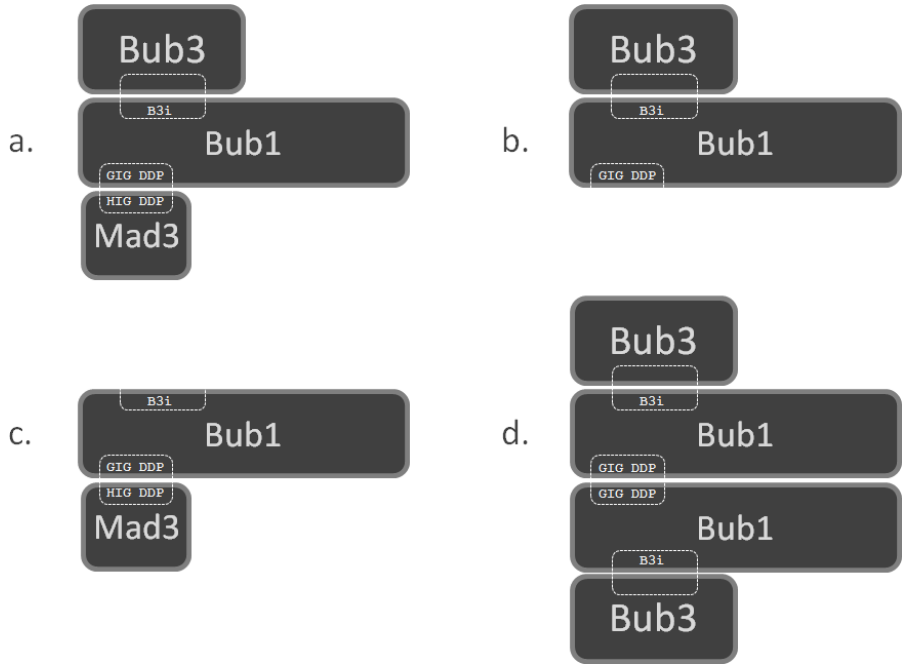

Figure 24: Complexes that can be formed through participation of Mad3, Bub1 and Bub3 in *S.pombe*. **(a)** Evidence in favour of this ternary BUB+ complex is presented in this work. MS analysis of Bub1 precipitations indicates however that not all Bub1 – Bub3 dimers accumulate Mad3 (see text). Thus the presence of **(b)** Bub1 – Bub3 dimers or perhaps **(d)** dimerisation of Bub1 – Bub3 dimers is a likely prospect. **(c)** Yeast lacking Bub3 are still able to form a binary Bub1 – Mad3 complex (see Table 18, page 35), but as yet it is not known whether such complexes exist side-by-side with BUB+ complexes in wild-type yeast.

The association of Mad3 with Bub1 in *S.pombe* and the lack thereof in *S.cerevisiae* raises intriguing questions. As introduced on page 14, Mad3 and Bub1 are related through ancestral '*Mad3Bub(R)1*' gene duplication events that, remarkably, arose independently in these two yeast species (Murray & Marks 2001, Kellis *et al.* 2004, Suijkerbuijk *et al.* 2012a). To date, nine such duplication events have been identified on the eukaryotic branch of the tree of Life (Suijkerbuijk *et al.* 2012a). Only a few species, such as the fungi *Kluyveromyces waltii* (Kellis *et al.* 2004), *Neurospora crassa*, *Cryptococcus neoformans*, *Ashbya gossypii* (Suijkerbuijk *et al.* 2012a), *Aspergillus nidulans* and *Aspergillus niger* (this study; data not shown) are known to get by with a single '*Mad3Bub(R)1*' gene copy. Parallel evolution has led to functionally divergent *BUB1*, *MAD3* and *BUBR1* gene copies that still retain significant sequence similarity betraying their shared ancestry. Remarkably, *S.pombe* Bub1 homodimerisation and heterodimerisation with Mad3 is achieved through evolutionary conserved interaction motifs. However, *S.cerevisiae* Mad3 and Bub1 are not known to associate, which supports the analysis

in this study by MS (§7.1) and yeast two-hybrid (results not shown). A molecular basis for this deficit is currently unexplored but closer analysis of dimerisation interfaces can reveal clues. For instance, the well-defined electrostatic surface potential of the TPR domain of *S.pombe* Bub1 and Mad3 encourages the formation of an interface as a result of charge complementarity (Figure 20, page 85). A similar arrangement is observed in *S.cerevisiae* Bub1, which has a tendency for homodimerisation *in vitro*, but is absent from human BubR1 that is able to form TPR-independent homodimers in a yeast two-hybrid assay (D'Arcy *et al.* 2010). Finally, no homodimerisation was observed for *S.pombe* or *S.cerevisiae* Mad3 in the two-hybrid assay (data not shown). In addition, no cross-species dimerisation of *S.pombe* and *S.cerevisiae* Bub1 or Mad3 was detected (data not shown).

3.4.7 TPR domains and spindle checkpoint studies

The '*Mad3Bub(R)1*' proto-gene duplication and subsequent parallel evolution that eventually gave rise to metazoan Bub1 and BubR1, *S.cerevisiae* Bub1 and Mad3, and *S.pombe* Bub1 and Mad3 occurred in separate events (Suijkerbuijk *et al.* 2012a). This implies that evolutionary forces that acted upon the dimerisation of these gene products either exploited an existing 'Mad3Bub(R)1' homodimerisation interface or evolved *de novo*. The latter scenario predicts ways of 'Mad3Bub(R)1' interactions that are not necessarily conserved between the metazoan and fungal lineage. Indeed, in some eukaryotic lineages the Bub1 interaction with Mad3 or BubR1 (i) was lost (*S.cerevisiae* Mad3 and Bub1), (ii) was retained (*S.pombe* Mad3 and Bub1) or (iii) was lost and evolved elsewhere within the molecules (possibly human BubR1 and Bub1) through molecular divergent evolution.

Clear evidence in favour of *in vivo* dimerisation of metazoan Bub1 and BubR1 is as yet lacking. The kinetochore recruitment of metazoan BubR1 is thought to be dependent on Bub1 and yeast two-hybrid analysis of human Bub1 and BubR1 alludes to a direct physical interaction (Kiyomitsu *et al.* 2007) facilitated by as yet unidentified interaction motifs downstream of the TPR domains (D'Arcy *et al.* 2010). Immuno-precipitation experiments show that Bub1 interacts with a phosphorylated species of BubR1, but it is uncertain whether this interaction is direct or facilitated by checkpoint or kinetochore proteins (Taylor *et al.* 2001). Neither Bub1 nor BubR1 are thought to undergo homodimerisation *in vitro* or *in vivo* (D'Arcy *et al.* 2010), although BubR1 can form homodimers in some yeast two-hybrid setups (Kiyomitsu *et al.* 2007).

The TPR domain of *S.cerevisiae* Mad3 (Hardwick *et al.* 2000) and human BubR1 (Lara-Gonzalez *et al.* 2011) is essential for the formation of the MCC complex. In addition, x-ray

crystallography and NMR studies revealed that the convex surface of the Bub1 and BubR1 TPR domain fold enables a physical and direct interaction with the kinetochore component Blinkin (Spc7/Spc105 in yeast; see Figure 23, page 101) (Bolanos-Garcia *et al.* 2009, Krenn *et al.* 2012). The TPR motifs are however neither sufficient nor essential for their kinetochore localisation (Lara-Gonzalez *et al.* 2011, Krenn *et al.* 2012), which suggests that additional binding sites that perhaps are regulated by Bub3 association remain to be uncovered (Taylor *et al.* 1998, Krenn *et al.* 2012).

Recently, careful analysis of the protein sequence and the structural organisation of the metazoan spindle checkpoint kinase Mps1 identified an amino terminal TPR domain consisting of three tandem repeats (Lee *et al.* 2012). Homodimerisation of human Mps1 has been observed *in vivo* and this association is thought to be essential for checkpoint-mediated metaphase arrests (Hewitt *et al.* 2010, Jelluma *et al.* 2010). Further studies showed that dimerisation is likely achieved through TPR-independent means (Thebault *et al.* 2012, Nijenhuis *et al.* 2013) and that this behaviour stimulates both its kinase activity and anchoring onto kinetochores (Hewitt *et al.* 2010, Jelluma *et al.* 2010, Lee *et al.* 2012). It is as yet unknown whether Mps1 binding of the kinetochore component Ndc80 is accomplished through its TPR domain (Kemmler *et al.* 2009), but x-ray crystallography studies reveal that this domain adopts a tertiary structure that is very similar to that of the Bub1 and BubR1 kinases (Lee *et al.* 2012, Thebault *et al.* 2012, Nijenhuis *et al.* 2013). The significant similarity of Mps1, Bub1 and BubR1 TPR domain primary sequences indicates a common ancestry perhaps through acquisition in early deuterostome or chordate[14] evolution (Lee *et al.* 2012). Finally, heterodimerisation of human Mps1 with Bub1 or BubR1 has been ruled out *in vitro* and TPR domains have not been identified in yeast Mph1/Mps1 (Lee *et al.* 2012).

3.4.8 Regulation of discrete spindle checkpoint complexes

Contemporary spindle checkpoint models pose that checkpoint components are organised into a hierarchy of complexes. Here, evidence is presented that reveals that some of these complexes could be unique to a single model organism. Even though most complexes are distinct entities, one checkpoint component can contribute to more than one single complex. Discrete checkpoint complexes than could be identified in the two yeast species are

[14] Deuterostomes and protostomes are bilateria, i.e. animals with a bilateral symmetry having a 'front and back end'. They are distinguished by their embryonic development: the blastopore or the first opening during protostome development becomes the mouth, which is formed by the second opening in deuterostomes. Chordates are deuterostome animals that possess a notochord and dorsal nerve cord.

summarised in Table 17 (page 75). For instance, Mad2 was found to interact with both Mad1 and Mad3, but the latter two are not known to be part of a single complex. Similarly, *S.pombe* Mad3 was shown to interact with both Mad2 and Bub1, but the latter two do not associate. Why some interactions are mutually exclusive is currently unexplained, but genetic and structural analysis can support biochemical findings. Bub3 associates with Mad3 and Bub1, but their manner of binding is very different in the two yeast species. The lack of a B3i sewince motif in *S.pombe* Mad3 is perhaps compensated by a TPR domain-dependent Bub1 – Mad3 interaction, which did not evolve in *S.cerevisiae*, and which allows formation of a stable ternary Mad3 – Bub1 – Bub3 complex. Since Bub3 can only accommodate a single B3i motif at a time (Larsen *et al.* 2007), Bub3 – Mad3 and Bub3 – Bub1 interactions are mutually exclusive in *S.cerevisiae*. Of course, 'back-to-back' recruitment of Mad and Bub proteins to their multiple docking sites on the Blinkin (Spc7/Spc105 in yeast) kinetochore component (Kiyomitsu *et al.* 2011) could dictate their association in an indirect manner (see also discussion on page 111).

The formation of checkpoint complexes is proposed to occur in a sequential manner in which the Mad2 – Mad1 complex primes Mad2 – Slp1/Cdc20 dimerisation and onwards maturation into the primary APC inhibitor MCC consisting of Mad2 – Slp1/Cdc20 – Mad3 and Bub3 in organisms other than *S.pombe*. Thus Mad2 commands a key role in checkpoint signalling that spans early events at the kinetochore and direct inhibition of the ultimate target, the APC. It is proposed that at least two distinct pools of Mad2 molecules co-exist: one that forms a tight interaction with Mad1 and one that is committed to MCC formation.

As yet it is not known whether a single molecule of Bub3 can cycle between interacting with Bub1 or Mad3 in *S.cerevisiae* cells, or whether *S.pombe* Mad3 can cycle between Bub1 and Mad2 or Slp1. It is likely that post-translational modifications that promote one interaction could kerb another and thus define a protein's destiny, unless recycling can take place. These questions could be addressed by *in situ* labelling experiments in which a protein is modified by a transitory interactor after which the modification is followed biochemically or perhaps by microscopy. Signalling by poly-ADP-ribosylation (PAR) of proteins is catalysed by PAR polymerases in metazoan cells, but this activity is absent in fungal cells. Thus a PAR polymerase targeted to a *S.pombe* kinetochore or fused to Bub1 could label Mad3 after which MCC or APC purifications could be probed for the presence of PAR modifications. A sharper picture of spindle checkpoint signalling could thus emerge.

The promiscuous, interwoven and hierarchical nature of spindle checkpoint protein interactions greatly complicates biochemical and genetic analysis. A single mutation in one gene can have primary as well as secondary repercussions in checkpoint signalling and determining causality can be challenging. For instance, a Mad2 mutation that precludes Mad1 interactions could lead to abrogation of spindle checkpoint function that indirectly prevents mutant Mad2 from associating with Mad3 and Slp1/Cdc20 to form MCC complexes. Biochemical as well as structural studies of checkpoint protein interactions and the way in which they are regulated are therefore of principal importance.

3.4.9 The yeast spindle checkpoint components are all phospho-proteins

This study identified 187 potential *in vivo* phosphorylation sites on *S.pombe* Mad and Bub proteins (Table 23) and 165 sites on *S.cerevisiae* Mad and Bub proteins. Thus far, 28 *S.pombe* sites have been validated with high confidence and 3 rejected (Table 21). The correct assignment of a phosphomodified residue is paramount for subsequent functional *in vivo* and *in vitro* studies of mutant protein. Phospho-residue assignment is thus an important aspect of phosphoproteomic studies and is largely an automated process in large-scale high-throughput MS data analysis (see also §2.3.3 and §3.3.10). At the YRC, localisation and validation scores of phosphosites from recent data sets are on request determined, first, by an in-house developed algorithm incorporated in the Debunker software package and, second, by expert manual validation (Lu *et al.* 2007). Identification, localisation and validation routines are regularly updated and improved upon, and re-analysis of legacy data sets is therefore important in identifying (new) phosphosites with high-confidence localisation and validation scores. Identification of post-translational modifications other than phosphorylation was beyond the scope of this project, but can be obtained by re-analysis of data sets upon request to the YRC.

The identification of post-translational modifications is likely to be key in resolving many of the outstanding questions in spindle checkpoint signalling (Zich & Hardwick 2010). Thus far, several studies have highlighted the role of kinases in establishing and maintaining checkpoint-mediated metaphase arrests (King *et al.* 2007a, Vanoosthuyse *et al.* 2009, Zich *et al.* 2012). The kinase action of Mph1/Mps1, Bub1, aurora B (Ark1/Ipl1), Cdk (Cdk1/Cdc28) and polo-like (Plo1/Cdc5) have all been implicated in checkpoint protein modifications (Table 24).

#	kinase	remarks / function	organism	reference(s)
	Slp1/Cdc20 as a substrate			
1	Bub1	checkpoint arrest	human	(Tang *et al.* 2004)
2	MAPK	checkpoint arrest	*X.laevis*	(Chung & Chen 2003)
3	PKA	DNA damage response	*S.cerevisiae*	(Searle *et al.* 2004)
4	Cdk	checkpoint arrest	*X.laevis*	(D'Angiolella *et al.* 2003)
5	Cdk1	potentiates checkpoint arrest	human	(Yudkovsky *et al.* 2000)
6	Cdc28	Cdk substrate screen	*S.cerevisiae*	(Ubersax *et al.* 2003)
7	Nek2	checkpoint arrest	human	(Liu *et al.* 2010b)
	Mad1 as a substrate			
8	Bub1	*in vitro*	human	(Seeley *et al.* 1999)
9	Plk1	kinetochore localisation	human	(Chi *et al.* 2008)
10	Mph1	checkpoint arrest?	*S.cerevisiae*	(Hardwick *et al.* 1996)
	Mad2 as a substrate			
11	Chk1	mitotic DNA damage arrest?	human	(Chila *et al.* 2013)
12	Mph1	spindle checkpoint arrest	*S.pombe*	(Zich *et al.* 2012)
13	Nek2	spindle checkpoint arrest	human	(Liu *et al.* 2010b)
	Mad3/BubR1 as a substrate			
14	aurora B	spindle checkpoint arrest	*S.cerevisiae*	(Rancati *et al.* 2005, King *et al.* 2007a)
15	Mps1	could be indirect	human	(Huang *et al.* 2008)
16	Plk1	chromosome biorientation	human	(Elowe *et al.* 2007, Matsumura *et al.* 2007)
17	Cdc5	polo-like kinase	*S.cerevisiae*	(Rancati *et al.* 2005)
18	Plx1	polo-like kinase, checkpoint arrest	*X.laevis*	(Wong & Fang 2007)
19	Cdk1	spindle checkpoint arrest	*X.laevis*	(Wong & Fang 2007)
20	Mph1	spindle checkpoint arrest	*S.pombe*	Hardwick lab, manuscript in preparation
21	Cdk1	Plk1 recruitment	human	(Elowe *et al.* 2007)
	Bub1 as a substrate			
22	Plk1	kinetochore localisation of Plk1	human	(Qi *et al.* 2006)
23	ATM	DNA damage response	human	(Yang *et al.* 2012)
24	Cdk1	kinetochore localisation of Plk1	human	(Yamaguchi *et al.* 2003, Qi *et al.* 2006)
25	MAPK	Bub1 activation	*X.laevis*	(Chen 2004)
26	p90RSK	Bub1 activation	*X.laevis*	(Schwab *et al.* 2001)
	Bub3 as a substrate			
27	Bub1	*in vitro*	*S.cerevisiae*	(Roberts *et al.* 1994)
	Mph1/Mps1 as a substrate			
28	aurora B	poor substrate *in vitro*	human	(Dou *et al.* 2011)
29	Cdk1	*in vitro*	human	(Dou *et al.* 2011)
30	Chk2	DNA damage	human	(Wei *et al.* 2005)
31	MAPK	kinetochore localisation	*X.laevis*	(Zhao & Chen 2006)
32	MAPK	*in vitro*	human	(Dou *et al.* 2011)

#	kinase	remarks / function	organism	reference(s)
33	Plk1	*in vitro*	human	(Dou *et al.* 2011)
	APC as a substrate			
34	Cdk1	APC acivity	human	(Hershko *et al.* 1994, Kraft *et al.* 2003)
35	Cdk	APC substrate recognition	*X.laevis*	(Patra & Dunphy 1998)
36	Plk1	APC acivity	human	(Kotani *et al.* 1999, Kraft *et al.* 2003)
37	PKA	APC acivity	human	(Kotani *et al.* 1998)

Table 24: Checkpoint proteins and APC subunits are substrates of kinases. This list is compiled by bringing together data from the published literature.

Phosphorylation of Mad2 by Mph1 is required for a mitotic arrest in *S.pombe* (Zich *et al.* 2012). *S.cerevisiae* Mad3 has been identified as an *in vitro* aurora B substrate and phosphorylation of serine 303 and 337 *in vivo* is a spindle checkpoint response to a lack of tension as a result of microtubule dysfunction or their incorrect attachments to kinetochores (King *et al.* 2007a). Some of the sites identified in this study as targeted by kinases are currently under investigation in the Hardwick lab. The role of *S.pombe* Slp1, Mad1, Mad2 and Mad3 phosphorylation is studied by site-directed mutagenesis and *in vivo* complementation. Five *in vivo* phosphorylation sites identified in this study within the amino terminus of Mad3 were mutated to alanine residues (creating a phospho 'null' site), namely S19, S31, S33, T44 and T64 in addition to S38, S40, T93 and S94. Cells containing '9 alanine' or '9 aspartic acid' *mad3* mutations are, however, still checkpoint-proficient. In time, analysis of other phospho-site mutants that would include aspartic acid substitutions ('phospho mimic') will hopefully shed a brighter light on the regulation of spindle checkpoint signalling by kinases as well as phosphatases.

This study uncovered a vast array of *in vivo* phospho-modifications of spindle checkpoint proteins and the $APC^{Slp1/Cdc20}$ in the two yeast species. Conclusions regarding the relevance and specificity of *in vivo* phospho-modifications for checkpoint functioning are difficult to draw from a single set of data for each arrested or cycling cell population, but it is to be expected that a number of these modifications will depend on spindle checkpoint status. Phosphorylation of Mad2, by for instance aurora B or Mph1, could restrict its interaction in regards to MCC formation or templating Mad2 – Slp1/Cdc20 complexes when tethered to Mad1. Or perhaps phosphorylation of Mad2 or Mad3 by Mph1/Mps1 could increase the affinity of the MCC binding the APC during a spindle checkpoint arrest (Zich *et al.* 2012). It is also tempting to speculate that differences in phosphorylation of APC subunit orthologues

could reflect the divergent modes of APC regulation, such as stable binding of MCC in *S.pombe* versus the rapid dissociation observed in *S.cerevisiae*.

In cultured human cells, MCC disassembly and checkpoint silencing requires prior phosphorylation of Cdc20 by a Cdk^{cyclin} complex (Miniowitz-Shemtov *et al.* 2012). Other studies have pinpointed sites whose phosphorylation is indispensable for spindle checkpoint functioning, even though the kinase responsible is in many cases unknown (Chen 2002, Wassmann *et al.* 2003, Huang *et al.* 2008). For instance, phosphorylation of specific Mad2 residues has been suggested to regulate the conformational transition from 'open' to 'closed' species (Kim *et al.* 2010).

APC subunits are known substrates of Cdk^{cyclin} complexes. The *S.cerevisiae* Cdc28 Cdk phosphorylates Cdc16, Cdc23 and Cdc27 *in vitro* and mutation of these sites *in vivo* delays anaphase as APC activity is compromised (Rudner & Murray 2000). Some of these Cdc28 phosphorylation sites identified were found to be phosphorylated *in vivo* in this study (Cdc16: S44, S95, S103 and Cdc27: S267, S328). Large-scale analysis of APC phosphorylation in cultured human cells reveals a total of 64 unique APC phosphorylation sites (Nuc2/Cdc27 orthologue Cdc27: 20, Cut4/Apc1 orthologue Apc1: 17, Cut23/Cdc23 orthologue Cdc23: 7, Apc2: 6, Apc5: 5, Apc7 (no apparent yeast orthologues): 4, Cut9/Cdc16 orthologue Apc6: 3, Lid1/Apc4 orthologue Apc4: 1, Apc10/Doc1 orthologue Apc10: 1), in addition to 5 BubR1 sites and 2 Cdc20 sites (Steen *et al.* 2008). This study compares phosphorylation patterns in nocodazole arrested cells to normal mitotic cells and observe increased levels of Apc1 modifications, whereas modifications on Cdc27, Apc4 and Cdc16 subunits remained fairly constant (Steen *et al.* 2008). Although the data presented here does not attempt to draw distinctions between interphase and mitotic modifications, it is interesting to note that Cut4/Apc1, Nuc2/Cdc27, Cut9/Cdc16 and *S.pombe* Cut23 (but not the *S.cerevisiae* orthologue Cdc23) APC subunits were shown to be readily phosphorylated in yeast too.

A study focussing on APC phospho-modification in HeLa cells (Kraft *et al.* 2003) identified a total of 51 sites (with the number of phospho-sites in descending order: Cdc27, Apc1, Apc7, Cdc16, Cdc23, Apc2, Apc4 and Apc5) of which 34 were exclusively found on mitotic APC purified from nocodazole arrested cells (compared to S phase APC). Some of these sites could be phosphorylated *in vitro* by the Cdk1 and Plk1 kinases that stimulate Cdc20 binding and increase the ubiquitination activity of the APC (Kraft *et al.* 2003).

3.4.10 Presence and absence of putative and known interactors of spindle checkpoint proteins

Just over two decades of spindle checkpoint research has uncovered over 50 potential checkpoint protein interactors (Table 25). Not all the associations have been verified *in vivo* or bear relevance to spindle checkpoint signalling at first sight.

Perhaps the most elusive and contentious spindle checkpoint protein interaction concerns their docking site on kinetochores. It has been shown that many of the spindle checkpoint proteins strongly localise to kinetochores during a spindle checkpoint arrest (Vigneron *et al.* 2004). In the MS data presented here kinetochore components with compelling coverage were conspicuous only in their absence. Two components, namely Ndc80 and Spc7, were identified with respectively 8% polypeptide coverage (from 2 unique peptides) and 6% coverage (from 4 unique peptides) in *S.pombe* Bub3 precipitations from mitotically arrested cells (see table row 732 and 773 in §7.1). A mere two peptides assigned to Spc7 and representing 2% coverage were uncovered from a mitotic Bub1 co-purification. This could indicate that the interaction of checkpoint proteins with the kinetochores is very dynamic or relatively unstable and can be easily disrupted during preparations due to kinase or phosphatase activities in cell extracts. In 2007, the human Spc7/Spc105 orthologue Blinkin was earmarked as a direct site of Bub1 and BubR1 recruitment (Kiyomitsu *et al.* 2007) but this discovery proved difficult to follow up in other model organisms. Subsequently, two x-ray diffraction crystallography studies revealed the TPR domain structure of BubR1 (Bolanos-Garcia *et al.* 2011) and Bub1 (Krenn *et al.* 2012) each in complex with a different Blinkin fragment that contains a single KI motif conform a KI(D/N)xxxF(L/I)xxLK consensus sequence (see also Figure 23, page 101). Recent findings confirm Spc7/Spc105 as the kinetochore anchor of Bub1 and Bub3 by *in vitro* reconstitution of the interaction and *in vivo* analysis of Spc7/Spc105 mutants (London *et al.* 2012, Shepperd *et al.* 2012, Yamagishi *et al.* 2012). Mph1/Mps1 phosphorylation of numerous conserved repeats, termed MELT motifs (conforming to a M(D/E)(I/L)(S/T) consensus sequence), at the amino terminus of Spc7/Spc105 is required for efficient recruitment of Bub1 and Bub3 and these sites are targeted by the antagonistic phosphatase activity of PP1 (London *et al.* 2012). The observation that multiple KI and MELT motifs are present suggests that a single Spc7/Spc105 molecule can bind several Bub1 or Bub3 containing complexes. This way, rapid kinetochore enrichment of Bub1 – Bub3, Bub1 – Mad3, Bub3 – Mad3 or Bub1 – Bub3 – Mad3 complexes is a likely prospect.

#	interactor	description of interactor	organism	method	reference(s)
	Mad1				
1	Dam1	DASH complex subunit	*S.cerevisiae*	iv	(Shang *et al.* 2003)
2	Hec1 (Ndc80)	kinetochore component	human	y2h	(Martin-Lluesma *et al.* 2002)
3	Hda2	histone deacetylase subunit	*S.cerevisiae*	y2h	(Newman *et al.* 2000)
4	Nek2	mitotic NUMA kinase	human	coP, y2h, iv	(Lou *et al.* 2004)
5	NUA	nucleoporin	*A.thaliana*	coP, y2h	(Ding *et al.* 2012)
6	NUP107	nucleoporin	*C.elegans*	y2h	(Rodenas *et al.* 2012)
7	Nup153	nucleoporin	human	coP, iv	(Lussi *et al.* 2010)
8	Nup53	nucleoporin subunit	*S.cerevisiae*	coP	(Scott *et al.* 2005)
9	Plk1	polo-like kinase	human	coP	(Chi *et al.* 2008)
10	Red	spindle pole associated	human	coP, iv	(Yeh *et al.* 2012)
11	Smc1	cohesion subunit	*S.cerevisiae*	Y2h	(Newman *et al.* 2000)
12	Spc25	kinetochore component	*S.cerevisiae*	y2h	(Newman *et al.* 2000)
13	TPR	nucleoporin associated	human	coP, iv	(Lee *et al.* 2008)
	Mad2				
14	CHFR	E3 ubiquitin ligase	human	coP, y2h	(Privette *et al.* 2008)
15	CHK1	DNA damage kinase	human	coP	(Chila *et al.* 2013)
16	EAP1	translation factor associated	*S.cerevisiae*	y2h*	(Wong *et al.* 2007)
17	ERCC1	DNA damage repair by nucleotide excision	human	coP	(Fung *et al.* 2008)
18	Kel1	cell morphology; mitotic exit	*S.cerevisiae*	y2h*	(Wong *et al.* 2007)
19	Nek2	mitotic NUMA kinase	human	coP	(Liu *et al.* 2010b)
20	Nup157	nucleoporin	*S.cerevisiae*	y2h*	(Uetz *et al.* 2000)
21	P31 (comet)	checkpoint silencing	human	coP, iv, y2h	(Habu *et al.* 2002)
22	Scm3	centromere protein	*S.cerevisiae*	y2h*	(Wong *et al.* 2007)
23	TPR	nucleoporin associated	human	coP, iv	(Lee *et al.* 2008)
24	Ufd2	ubiquitin chain assembly	*S.cerevisiae*	y2h*	(Wong *et al.* 2007)
25	YGR273C	*unknown*	*S.cerevisiae*	y2h*	(Wong *et al.* 2007)
26	YJL206C	transcriptional regulator?	*S.cerevisiae*	y2h*	(Wong *et al.* 2007)
27	XPD	DNA damage repair by nucleotide excision	*human*	coP	(Fung *et al.* 2008)
	Mad3 / BubR1				
28	Ajuba	microtubule associated	human	coP, iv	(Ferrand *et al.* 2009)
29	Apc1	APC subunit	*S.cerevisiae*	y2h*	(Wong *et al.* 2007)
30	Blinkin	kinetochore component	human	y2h	(Kiyomitsu *et al.* 2007)
31	Cdc28	cyclin dependent kinase	*S.cerevisiae*	y2h*	(Wong *et al.* 2007)
32	CENP-E	centromere kinesin	human	coP	(Chan *et al.* 1998)
33	Dam1	DASH complex subunit	*S.cerevisiae*	iv	(Shang *et al.* 2003)
34	PP2A	chromosome biorientation	*human*	iv, y2h	(Suijkerbuijk *et al.* 2012b)
35	Plx1	polo-like kinase	*X.laevis*	coP, iv	(Wong & Fang 2007)
36	Scm3	centromere protein	*S.cerevisiae*	y2h*	(Wong *et al.* 2007)

#	interactor	description of interactor	organism	method	reference(s)
37	Tap73	checkpoint function?	human	coP	(Tomasini *et al.* 2009)
	Bub1				
38	Bas1	transcription factor?	*S.cerevisiae*	y2h*	(Wong *et al.* 2007)
39	Blinkin	kinetochore component	human	y2h	(Kiyomitsu *et al.* 2007)
40	Dam1	DASH complex subunit	*S.cerevisiae*	iv	(Shang *et al.* 2003)
41	Dsn1	kinetochore component	*S.cerevisiae*	y2h*	(Wong *et al.* 2007)
42	Hap4	transcriptional activator	*S.cerevisiae*	y2h*	(Wong *et al.* 2007)
43	Plk1	polo-like kinase	human	coP, iv	(Qi *et al.* 2006)
44	Rgd2	GTPase-activating protein	*S.cerevisiae*	y2h*	(Wong *et al.* 2007)
45	Skp1	kinetochore component	*S.cerevisiae*	coP, iv	(Kitagawa *et al.* 2003)
46	Spc105	kinetochore component	*S.cerevisiae*	iv	(London *et al.* 2012)
47	Spc7	kinetochore component	*S.pombe*	coP, iv	(Shepperd *et al.* 2012)
48	Stu1	microtubule associated	*S.cerevisiae*	y2h*	(Wong *et al.* 2007)
49	Tap73	checkpoint function?	human	iv	(Tomasini *et al.* 2009)
50	Yra2	mRNA export	*S.cerevisiae*	y2h*	(Wong *et al.* 2007)
	Bub3				
51	DYLT3	dynein motor subunit	human	coP, iv	(Lo *et al.* 2007)
52	PARP-1	DNA damage response	mouse	coP	(Saxena *et al.* 2002)
53	p73	mitotic apoptosis	human	coP	(Niikura *et al.* 2010)
	Mph1/Mps1				
54	BLM	DNA damage response	human	coP	(Leng *et al.* 2006)
55	Chk2	DNA damage checkpoint	human	coP, iv, y2h	(Wei *et al.* 2005)
56	Dam1	DASH complex subunit	*S.cerevisiae*	iv	(Shang *et al.* 2003)
57	Ndc80	kinetochore component	*S.cerevisiae*	y2h, coP	(Kemmler *et al.* 2009)
58	Spo21	meiotic spindle pole	*S.cerevisiae*	y2h*	(Wong *et al.* 2007)
59	Spr6	sporulation?	*S.cerevisiae*	y2h*	(Wong *et al.* 2007)

Table 25: Summary of (mostly direct) interactions of the spindle checkpoint proteins discussed in literature, excluding other checkpoint proteins and Slp1/Cdc20. coP = co-precipitation, y2h = yeast two-hybrid, iv = *in vitro* binding studies, * = not confirmed by other means (e.g. colocalisation, co-precipitations, binding assays, etc.).

The *S.cerevisiae* myosin-like proteins Mlp1 and Mlp2 were shown to be strong hits in both Mad1 and Mad2 preparations. Similarly, the Mlp1 and Mlp2 *S.pombe* orthologues Nup211 and Alm1 co-purified with Mad1 and Mad2 too. Both Nup211/Mlp1 and Alm1/Mlp2[15] are large coiled-coil filamentous proteins that localise to the nucleoplasmic side of the nuclear pore complexes. The localisation of Mad1 and Mad2 with the nuclear pores has been scrutinised in

[15] The *S.cerevisiae* Mlp1 and Mlp2 and *S.pombe* Alm1 and Nup211 are homologues and both orthologues and paralogues alike share high sequence identity. It is not immediately clear which protein orthologues are homologues as functional data is lacking and different alignments result in different identity scores (data not shown).

both human and fungal cells in several studies (Campbell *et al.* 2001, Ikui *et al.* 2002, Iouk *et al.* 2002, Quimby *et al.* 2005, De Souza *et al.* 2009). Human Tpr and *D.melanogaster* Megator are Mlp orthologues that facilitate binding of Mad1 and Mad2 and are essential for robust checkpoint function (Lee *et al.* 2008, Lince-Faria *et al.* 2009). Mad1 targeting to nuclear pores is thought to be a bipartite process, in which an amino terminal region mediates the Mlp association and a carboxy terminal region binds Nup53 (Cairo *et al.* 2013). In *S.cerevisiae* cells, Mad1 and Mad2 associate with the nuclear pores during interphase, but only Mad2 is released upon a spindle checkpoint-mediated metaphase arrest (Iouk *et al.* 2002). The *S.cerevisiae* Mlp proteins have been identified as the docking site for several karyopherins or nuclear transport factors, namely Srp1 (also called Kap60) and Kap95 that facilitate the nuclear translocation of polypeptides (Denning *et al.* 2001, Ben-Efraim *et al.* 2009). Crucially, the Kap95 karyopherin is required for the nuclear import of Mad1 (Scott *et al.* 2005). A recent *S.cerevisiae* study surprisingly demonstrates a role for Mad1 in regulating karyopherin activity during mitotic arrests (Cairo *et al.* 2013). Remarkably, in nocodazole-arrested cells Mad1 and aurora B cooperate in a Mad2-independent process to inhibit Kap121 and prevent the nuclear import of the aurora B antagonist $PP1^{Glc7}$ (Cairo *et al.* 2013). In this study, MS protein identification and their peptide abundance in co-precipitations of *S.pombe* and *S.cerevisiae* Mad1 and Mad2 tentatively suggest a close interaction with the nuclear pore subunits C285.13c/Nup60 and Nup61/Nup2 via association with Nup211/Mlp1 and Alm1/Mlp2. Furthermore, several karyopherins were isolated, such as *S.cerevisiae* Kap95 and *S.pombe* Kap123, Cut15, Imp1 and Sal3. The latter, also known as Pse1, is an importin β-like nuclear transport factor orthologous to *S.cerevisiae* Kap121. Yeast experiments have indicated that Mad1 nuclear pore localisation is not a prerequisite for checkpoint-mediated metaphase arrests in *S.pombe* (communicated by Karen May, Hardwick lab; manuscript in preparation) and *S.cerevisiae* (Scott *et al.* 2005). However, it would be of interest to investigate the functional relationship of *S.pombe* karyopherins with checkpoint proteins at onset of anaphase.

S.pombe purifications of all checkpoint proteins did reveal a total of eight subunits of the chaperonin containing T-complex (CCT or TRiC: 'Tcp1 ring complex'). Using mammalian BHK-21 tissue cultured cells it is estimated that as many as 20% of novel polypeptide chains require the mediation of the CCT chaperonin complex for proper folding (Thulasiraman *et al.* 1999). This well-conserved complex exists as a cylindrical hetero-octameric duplex (Liou & Willison 1997). It is required for the production of functional APC activators in yeast and mammalian cells by aiding folding of the seven-bladed propeller-like WD40 domains of Cdc20 and Cdh1

(Camasses *et al.* 2003). Proper folding of this domain, also present in Bub3 and the APC subunit Lid1/Apc4, is a prerequisite for both the association of Cdc20 with the APC and for MCC formation. Although *S.cerevisiae* Bub3 is not thought to interact with the CCT complex (Camasses *et al.* 2003), the *S.pombe* MS data presented here show strong evidence of all eight CCT subunits in affinity precipitations of both Bub3 and the APC. Perhaps, binding of the *S.cerevisiae* CCT complex with the checkpoint proteins is of a lesser affinity as purifications do not contain subunits of the CCT complex or folding of the *S.pombe* WD40 domains requires greater CCT chaperonin assistance.

Several *S.pombe* protein hits of as yet uncharacterised function were uniquely identified in APC Lid1 purifications that would warrant further investigation (Table 34). Although two of these (*SPBC23G7.14* and *SPCC14G10.04* gene products) do not bear any structure domains that assisted sequence analysis and inference of their biological role, the other two carry domains that generally function in ubiquitination pathways. RING (for 'really interesting new gene') finger domains are zinc finger-type domains that bind two Zn^{2+} ions and are specific to many E3 ubiquitin ligases (Lipkowitz & Weissman 2011, Budhidarmo *et al.* 2012). They play a central role in catalysing the transfer of ubiquitin from an E2 enzyme to a substrate. CUE (for 'coupling of ubiquitin conjugation to endoplasmic reticulum degradation') domains have a high-affinity for mono and poly-ubiquitin chains on proteins (Kang *et al.* 2003, Prag *et al.* 2003). Although they mainly function in protein degradation (Dikic *et al.* 2009), CUEDC2 is a human CUE domain protein that was recently found to bind ubiquitinated Cdc20 and it is thought that this interaction could perhaps drive spindle checkpoint silencing by competing with Mad2 (Gao *et al.* 2011).

rank	interactor (kDa)	cycling	arrest	description
	Lid1-ZZ purification			
290	SPBC23G7.14 (16)	2 – 2 – 20%	*0*	Uncharacterised; similarity to *S.japonicus* XP_002172383
300	SPAP32A8.03c (55)	3 – 3 – 20%	*0*	RING finger protein; predicted ubiquitin-protein ligase E3
339	SPCC14G10.04 (53)	5 – 5 – 18%	2 – 2 – 8%	Well-conserved fungal protein; no apparent metazoan homologues
344	SPCC4G3.13c (24)	2 – 2 – 18%	2 – 2 – 16%	CUE domain protein; predicted to bind a ubiquitin-conjugating enzyme
	Mad2-ZZ purification			
759	Csi1 / SPBC2G2.14 (60)	2 – 2 – 8%	2 – 3 – 5%	Facilitates kinetochore clustering near spindle poles (Hou *et al.* 2012).

Table 26: Protein hits from *S.pombe* Lid1 and Mad2 purifications that warrant further investigation. Key: *a – b – c%* denotes the *total number of peptides – unique number of peptides – percentage of polypeptide coverage*.

A fifth *S.pombe* protein that uniquely purified with Mad2 from cycling as well as arrested cells is encoded by the *SPBC2G2.14* gene and was characterised in November 2012 (Hou *et al.*

2012). Named Csi1 (for 'chromosome segregation impaired protein 1'), it facilitates clustering of centromeres at the nuclear envelope near spindle pole bodies (Hou *et al.* 2012). Pole-proximate kinetochores are thought to enhance their capture by spindle microtubules (Grishchuk *et al.* 2007).

Finally, the association of *S.pombe* Bub1, Bub3 and Mad3 with the YEATS domain protein Tfg3, the uncharacterised gene product of *SPAC31G5.19* and the FACT complex subunits Pob3 and Spt16 are the topic of chapter 5.

4 Topological analysis of spindle checkpoint complexes by cross-linking and MS

4.1 Summary

Obtaining structure information of multi-protein complexes is a crucial step in fully appreciating the biology of multi-protein complexes and in gaining an understanding of their function and consequences of deleterious mutations in disease manifestations. X-ray crystallography, hydrodynamics, circular dichroism spectroscopy, electron microscopy and nuclear magnetic resonance have all yielded valuable insight into the architecture and structural arrangement of many protein complexes and their individual subunits. A relatively novel development is a technology that chemically links proximate lysine residues within protein complexes using short cross-linkers and the identification of cross-linked peptides after tryptic digests by tandem mass spectrometry. This approach in conjunction with the rapid one-step large-scale protein complex purification method developed in chapter 3 was employed to determine the spatial arrangement of *S.pombe* BUB (Bub1 – Bub3), MAD (Mad1 – Mad2) and *S.cerevisiae* MAD and NDC80 complex. The findings presented here provide a proof of principle for such a strategy and demonstrate that this procedure is a useful, additional tool in uncovering the architecture of native endogenous multi-protein complexes. The identification of several novel interfaces could, in time, provide clues to regulation of spindle checkpoint function.

4.2 Aims and background

As discussed at length in chapter 3, spindle checkpoint signalling is organised into a hierarchy of distinct multi-protein complexes that nonetheless share components. Biochemistry has been fundamental in revealing the nature of many of these complexes and the way in which their assembly is regulated. Without a shadow of doubt, structural determination of the Mad2 association with Cdc20 (Luo *et al.* 2000, Mapelli *et al.* 2007), the kinetochore anchoring of Bub1 and BubR1 (Bolanos-Garcia *et al.* 2011, Krenn *et al.* 2012) and the APC ubiquitin ligase complex with the MCC (Schreiber *et al.* 2011, Chao *et al.* 2012) has yielded desirable insight into the mechanistic mode of spindle checkpoint action. Knowledge of both subunit composition and macro-molecular architecture of a given protein complex greatly enhances functional studies in its ability to pinpoint interface residues for mutation analysis.

Not all protein complexes are amenable to x-ray diffraction crystallography, due to the presence of disordered regions or large flexible domains. One promising development is protein cross-linking in conjunction with MS to determine the spatial arrangement and to

glean mechanistic clues of protein complexes. Advances in cross-linking biochemistry and proteomics now enable the use of MS to model the topology of large endogenous multi-protein complexes under physiological conditions. This is achieved by chemical cross-linking of proximate lysine residues and by identifying proximities of subunits as a whole by MS analysis of cross-linked peptides (Rappsilber *et al.* 2000, Sinz 2006). The work presented in this chapter was set up as a collaboration with Dr. Juri Rappsilber's proteomics laboratory at the Wellcome Trust Centre for Cell Biology, Edinburgh. Employing this technique, recent work in the Rappsilber lab refined the three-dimensional structure of the *S.cerevisiae* transcription factor IIF in complex with RNA polymerase II, a combined complex of 15 subunits with a total mass of 670 kDa (Chen *et al.* 2010b). Here, the challenge set out is to combine the rapid one-step large-scale purification method developed in chapter 3 with the most recent cross-linking technology and MS analysis to probe the topology of spindle checkpoint complexes purified directly from native yeast extracts.

4.3 Results

4.3.1 Method development and validation

Six yeast protein complexes as detailed in Table 27 were isolated as described in section 2.3.1. *In vitro* proximity cross-linking of lysine residues using short amine-reactive BS2G (7.7 Å in length) or BS3 (11.4 Å) compounds was carried out whilst complexes were still bound to IgG Dynabeads, followed by tryptic digest and MS analysis as performed by Angel Zuo Chen in the Rappsilber lab (§2.3.4). During the course of this work, the advantages of retaining protein complexes on IgG Dynabeads became evident. First, employing this approach, buffer exchanges during preparation of the sample can be performed quickly and efficiently to maintain complex integrity. Second, loss of material during sample preparation is prevented. Third, artificial oligomerisation of complexes in non-physiological solutions is eliminated. And fourth, cross-linking between complexes that are immobilised and thus kept at a distance is prevented. The latter finding became apparent when a 1:1 mixture of L-[$^{13}C_6$]-lysine ("heavy") and L-[$^{12}C_6$]-lysine ("light") labeled MAD or NDC80 complexes was analysed and no cross-links between heavy and light lysine residues were detected. For this purpose, a lysine auxotrophic *S.cerevisiae* yeast strain (§2.2.2: SJ177) was engineered by PCR based gene deletion strategy (§2.2.4). "Heavy" and "light" complexes were isolated from *lys1Δ* yeast strains expressing Mad1-ZZ (§2.2.2: SJ180) and Spc25-ZZ (§2.2.2: SJ192) and grown in SILAC (for 'stable isotope labeling by amino acids in cell culture') optimised medium (§2.2.3). As the "heavy" and "light" cell masses were mixed prior to breakage of the cells, the absence of heavy and light cross-

links confirmed that interactions were stable during complex purification and that complexes did not aggregate in extracts or when bound to beads.

In addition to the MAD and MCC spindle checkpoint complexes from *S.cerevisiae*, the MAD and BUB+ from *S.pombe*, the APC E3 ubiquitin ligase and NDC80 kinetochore complex from *S.cerevisiae* was analysed (Table 27). The NDC80 complex is a structurally and functionally important component of outer-kinetochores (Ciferri *et al.* 2007, Wang *et al.* 2008). It regulates microtubule dynamics and is a target of aurora B and Mph1 kinase activity (Kemmler *et al.* 2009, Umbreit *et al.* 2012). Part of the human NDC80 complex was previously crystallised and investigated by x-ray crystallography (Figure 25b)(Ciferri *et al.* 2008). Other crystallography studies that facilitate validation of this cross-linker technology are that of a partial human Mad1 – Mad2 (Figure 26c)(Sironi *et al.* 2002) and a partial *S.cerevisiae* BUB complex (Figure 28)(Larsen *et al.* 2007). As anticipated, cross-linking of native MAD and BUB+ complexes both confirmed and complemented known tertiary and quaternary structure information. Unfortunately, no cross-links were detected for both the MCC and APC, presumably due to the presence of protein contaminants interfering with efficient cross-linking of the target components. In regards to the *S.pombe* BUB+ complex, as little Mad3 is known to associate with Bub1 and Bub3 (§3.3.6), no cross-links were identified that involved this protein and thus the focus was on the BUB binary complex Bub1 – Bub3.

#	complex	species	strain	x-linker	total x-links	intermolecular links	comments
1	MAD: Mad1*-Mad2	*S.cerevisiae*	SJ206 SJ180	BS2G	34	11	SILAC and normal culture
2	Ndc80-Nuf2-Spc24-Spc25*	*S.cerevisiae*	KH288 SJ192	BS2G	25	12	SILAC and normal culture
3	MCC with Mad3*	*S.cerevisiae*	SJ108	*n/a*	-	-	*too many contaminants*
4	APC with Apc4*	*S.cerevisiae*	SJ207	*n/a*	-	-	*too many contaminants*
5	MAD: Mad1*-Mad2	*S.pombe*	SJ1060	BS3	92	16	-
6	BUB: Bub1*-Bub3	*S.pombe*	SJ636	BS3	26	4	-

Table 27: Purified yeast complexes subjected to *in vitro* cross-linking and the number of lysine-lysine cross-links identified by MS analysis. The asterisk denotes the ZZ-tagged subunit used as a bait for purification purposes. Details of *S.cerevisiae* strains used are in section 2.2.2 and *S.pombe* strains in section 2.1.2. Some complexes were isotopically labelled in SILAC experiments to investigate undesirable but potential oligomerisation of complexes during purification and immobilisation on beads (see text). Guaranteed intermolecular links are those found between peptides derived from different proteins or between identical or overlapping peptides from the same protein species.

4.3.2 Topology of the *S.cerevisiae* NDC80 complex

The kinetochore NDC80 complex consists of four subunits, namely Nuf2, Spc25, Spc25 and the Ndc80. Part of its structure was previously determined by x-ray crystallography (Figure 25b) using truncated, fused and co-expressed human Ndc80-Spc25 and Nuf2-Spc24 polypeptides forming the so-called NDC80 "bonsai" complex (Ciferri *et al.* 2008). This confirmed findings of an earlier study employing the *in vitro* cross-linking technology on reconstituted complexes of truncated recombinant subunits showing that the extended coiled-coil regions of Nuf2 and Spc24 run parallel to those of Ndc80 and Spc25 (Maiolica *et al.* 2007). Both studies identify a brief discontinuity of the parallel fold in which a loop of about 50 amino acids emanates from the Ndc80 molecule. This loop sequence is well-conserved (Ciferri *et al.* 2008), is required for loading of the DASH complex and facilitating kinetochore attachments to microtubules (Maure *et al.* 2011). Here, proximity cross-linking of native *S.cerevisiae* NDC80 complexes did yield 25 cross-links that by their nature were divided over four groups (Table 28 and Figure 25a).

cross-link group	number identified	topological significance
A	9	short range intramolecular cross-links less than 35 residues apart
B	10	parallel coiled-coil fold of Nuf2 along Ndc80
C	4	long range intramolecular cross-links more than 36 residues apart
D	2	proximity of Spc25 amino terminal region to Spc24

Table 28: Proximity cross-links of the *S.cerevisiae* NDC80 complex identified by MS analysis were grouped according to their topological significance.

Group B are those that confirm the coiled-coil fold of Nuf2 and Spc24 running parallel to Ndc80 and Spc25. As in the human NDC80 complex, the parallel coiled-coil register allows for the looping of about 60 residues. Group C suggests that the globular carboxy terminal domain of Spc24 is in close proximity to predicted coiled-coil regions present in the amino terminal half of both Spc24 and Spc25 that are not included in the crystal structure data. These data thus pose that the complete structure fold of Spc24 is more compact than the crystallography data infers and possibly involves amino terminal regions folding over onto the carboxy terminus.

a.

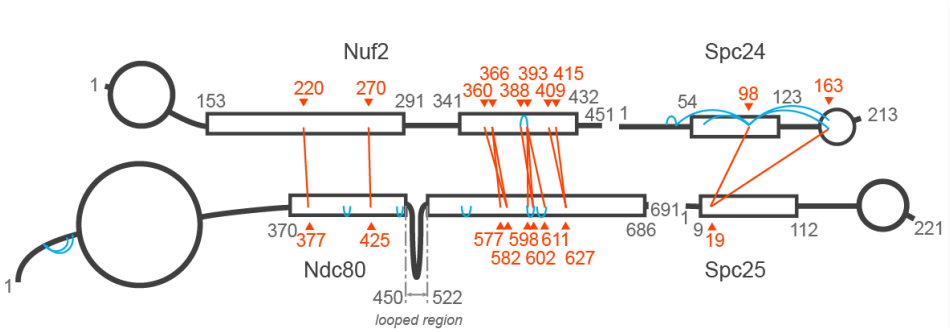

b.

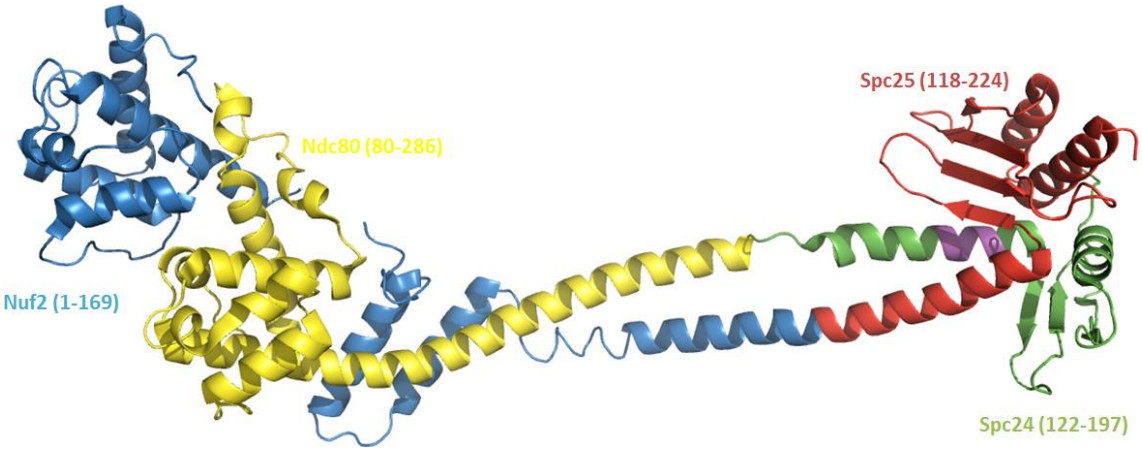

Figure 25: (a) Diagram visualising cross-links within the *S.cerevisiae* NDC80 complex. Structural globular domains are depicted as circles, predicted coiled-coil regions as rectangles. Blue coloured cross-links are intramolecular cross-links and those in red are between subunits of the complex. **(b)** Partial structure of human NDC80 complex (Ndc80 in yellow ribbon representation, Nuf2 in blue, Spc25 in red and Spc24 in green) in "bonsai" formation as revealed by x-ray diffraction crystallography (Ciferri *et al.* 2008). The data presented in this study suggest that the Spc24 region painted in magenta is proximate to amino terminal coiled-coil regions of both Spc24 and Spc25 that are not included in the crystal data. The 3D structure representation was prepared in PyMol (§2.5.3).

4.3.3 Topology of *S.pombe* and *S.cerevisiae* MAD complexes

Three individual purifications of *S.cerevisiae* Mad1 yielded a total of 34 unique cross-links of which 31 were formed between proximate lysine residues of the Mad1 dimer (eight of which were verifiable intermolecular links as they concern identical or partially overlapping peptides), 1 within the Mad2 dimer and 3 between the Mad1 and Mad2 polypeptides (Table 29). The MAD complex is a tetramer containing two copies of each Mad1 and Mad2 protein (Sironi *et al.* 2002). Cross-links of group A position Mad2 on its known binding site of Mad1 (Figure 26a). This finding is in agreement with an x-ray crystal study of human Mad2 in complex with a fragment of Mad1 (Figure 26c) (Sironi *et al.* 2002). An additional second proximate region (linker group B) was identified beyond the Mad1 sequence covered by the aforementioned crystal structure, but is included in a recently determined structure of the

Mad1 carboxy terminus (Kim *et al.* 2012). This region is adjacent to the well-conserved RLK motif that is essential for spindle checkpoint functioning and in *S.cerevisiae* required for binding Bub1 and Bub3 to form the MBB complex (Table 17)(Brady & Hardwick 2000). Indeed, this structural data tentatively suggest that binding of Mad2 could be mutually exclusive with that of Bub1 and Bub3. In support of this, *S.cerevisiae* Bub1 was never found to co-purify with Mad2 (§3.3.4). Hydrodynamic measurements and crystal studies of the Mad1 dimer has previously revealed that its extensive α-helical configuration folds into a long parallel coiled-coil structure also evidenced by linker group C. Finally, 'long distance' Mad1 linkers of group D provide evidence of a fold-back of several coiled-coil regions presumably creating a large helix-loop-helix formation in the process. Such a structural arrangement could perhaps be important for Mad2 association or Mad2 conformational conversion that is required for spindle checkpoint metaphase arrests (Mariani *et al.* 2012).

Analysis of the *S.pombe* MAD complex (Table 29 and Figure 26b) clearly indicates that its structural fold is similar to that of *S.cerevisiae*. This structure is thus well-conserved during molecular evolution.

cross-link group	number identified	significance
***S.cerevisiae* MAD (Mad1 – Mad2) complex**		
A	1	known Mad2 binding site on Mad1
B	3	novel proximate Mad1 – Mad2 regions that could be involved in dimerisation
C	20	parallel coiled-coil structures of Mad1
D	10	fold back of Mad1 coiled-coil regions creating a putative helix-loop-helix formation
***S.pombe* MAD (Mad1 – Mad2) complex**		
E	1	known Mad2 binding site on Mad1
F	2	novel proximate Mad1 – Mad2 regions that could be involved in dimerisation
G	63	parallel coiled-coil structures of Mad1
H	26	fold back of Mad1 coiled-coil regions creating helix-turn-helix formations (over 50 residues apart)

Table 29: Proximity cross-links of the *S.cerevisiae* and *S.pombe* MAD complexes identified by MS analysis were grouped according to their topological significance.

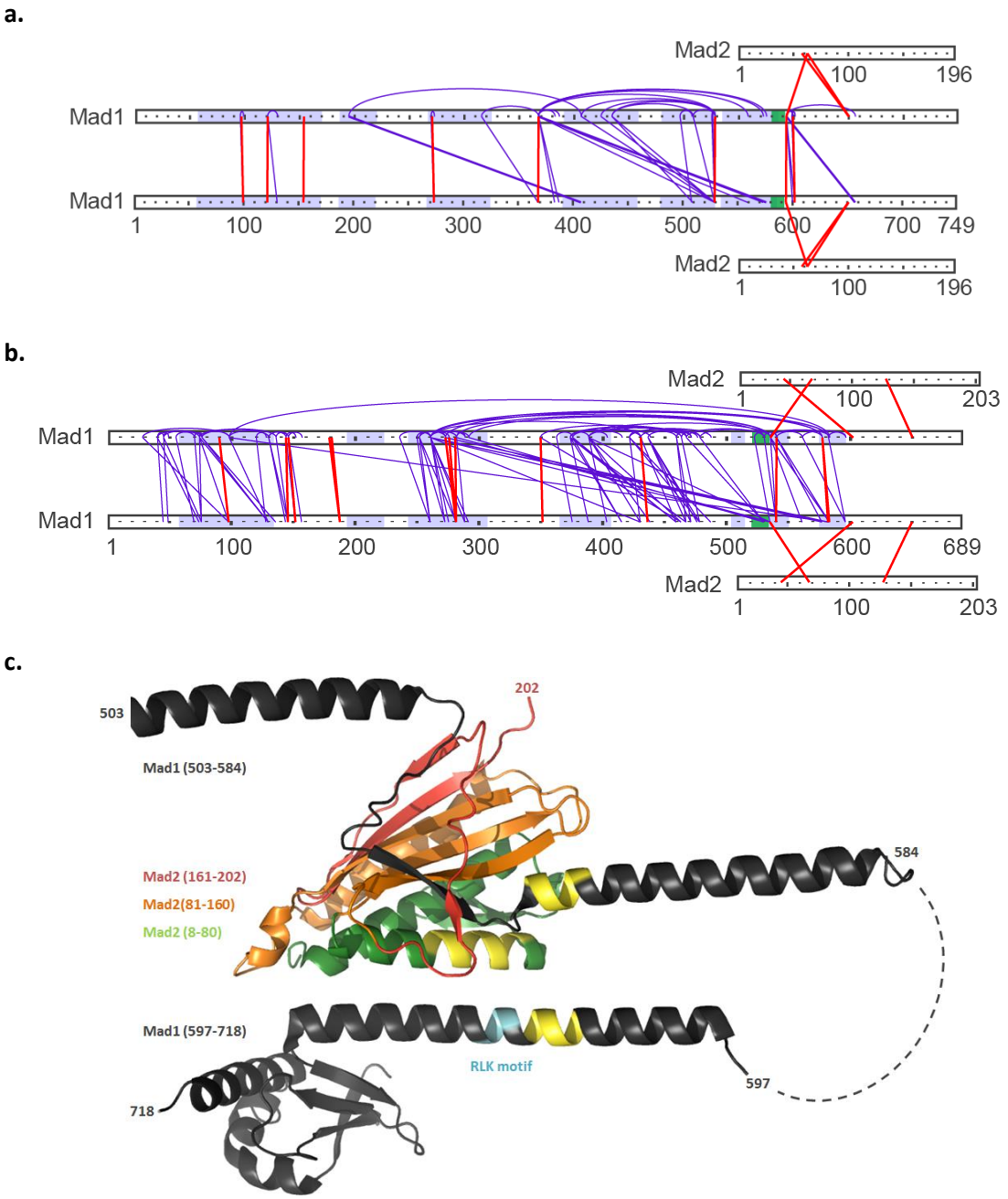

Figure 26: Diagrams visualising mapped cross-links within the **(a)** *S.cerevisiae* MAD complex and **(b)** the *S.pombe* MAD complex. Blue coloured cross-links are within or between Mad1 molecules and those in red are those between the two Mad1 molecules of the homodimer or between Mad1 and Mad2. Regions shaded in blue are predicted coiled-coil structures and the green region is the known Mad2 binding domain. **(c)** Top: partial structure of human Mad2 in complex with a short region of Mad1 (black ribbon representation) as revealed by x-ray crystallography (Sironi *et al.* 2002). The first approx. 160 residues of Mad2 are represented in green and orange ribbons, followed by the "safety belt" structure in red that is strapped onto the β-sheet fold of Mad1. The region in yellow are in close proximity, which is confirmed by the cross-linking data presented in this chapter. Bottom: Structure of the determined carboxy terminus of human Mad1 (Kim *et al.* 2012). The cross-linking data indicate that the region in yellow is in close proximity to the yellow regions in the top structure. The RLK motif is cyan coloured. Note in both representations only one half of the Mad1 parallel coiled-coil fold is presented. The 3D structure representations were prepared in PyMol (§2.5.3).

4.3.4 Topology of the *S.pombe* BUB complex

The *S.pombe* BUB complex consists of the Bub1 kinase and Bub3 (Table 17). In its entirety, the Bub3 polypeptide is organised in seven WD40 motifs that fold into a canonical seven-bladed β-propeller structure around a central axis (Larsen & Harrison 2004). Each blade comprises a four-stranded β-sheet. In 2007, *S.cerevisiae* Bub3 in association with the B3i motif sequence of Bub1 and, separately, Mad3 was crystallised and its structural fold determined by x-ray diffraction (Larsen *et al.* 2007). The B3i motif residues that facilitate Bub3 interactions is well-conserved in genes descended from the original '*Mad3Bub(R)1*' proto-gene with the *S.pombe* Mad3 protein being the only known exception. This motif consists of about 35 residues (Figure 27) and folds into a helix-loop-helix structure snaking along the Bub3 top face contacting all 7 propeller blades (Figure 28b) (Larsen & Harrison 2004).

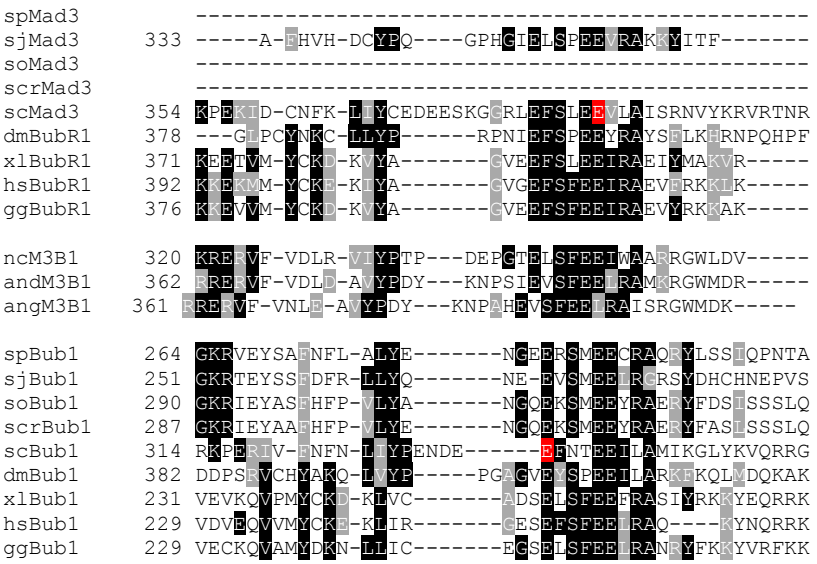

Figure 27: Multiple sequence alignment prepared in Clustal Ω (v1.1.0) of Mad3Bub(R)1 (M3B1 in figure above) sequences with the B3i motif. The alignment of the B3i motifs presented in the Larsen *et al.* manuscript that includes the human Nup98 sequence was used as a guide (Larsen *et al.* 2007). Residues in red are essential for Bub3 binding (*S.cerevisiae* Bub1 Glu333 and Mad3 Glu382) and mutation of these renders cells spindle checkpoint-deficient (Hoyt *et al.* 1991, Hardwick *et al.* 2000, Warren *et al.* 2002). Note that the Mad3 B3i motif is absent in three fission yeast species, namely *S.pombe* (sp), *S.cryophilus* (scr) and *S.octosporus* (so) but that the last 30 residues of the *S.japonicus* (sj) Mad3 sequence encode a somewhat degenerate but putative B3i motif (discussed on page 100). Other abbreviations used: *S.cerevisiae* (sc), *Neurospora crassa* (nc), *Aspergillus nidulans* (and), *Aspergillus niger* (ang) *D.melanogaster* (dm), *X.laevis* (xl), *Homo sapiens* (hs) and *Gallus gallus* (gg).

cross-link group	number identified	significance
A	3	interface of known Bub1 – Bub3 association
B	1	novel proximate Bub1 – Bub3 regions that could be involved in dimerisation
C	2	intra or intermolecular Bub1 cross-links that map to the TPR domain
D	16	short range intra or intermolecular Bub1 cross-links (less than 60 residues apart)
E	4	long range intra or intermolecular Bub1 cross-links (more than 61 residues apart)

Table 30: Proximity cross-links of the *S.pombe* BUB complex identified by MS analysis were grouped according to their topological significance.

a.

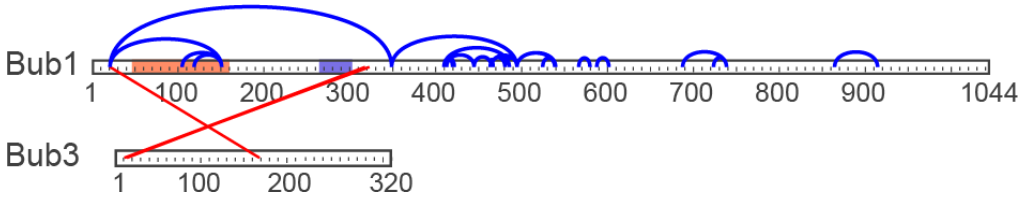

b.

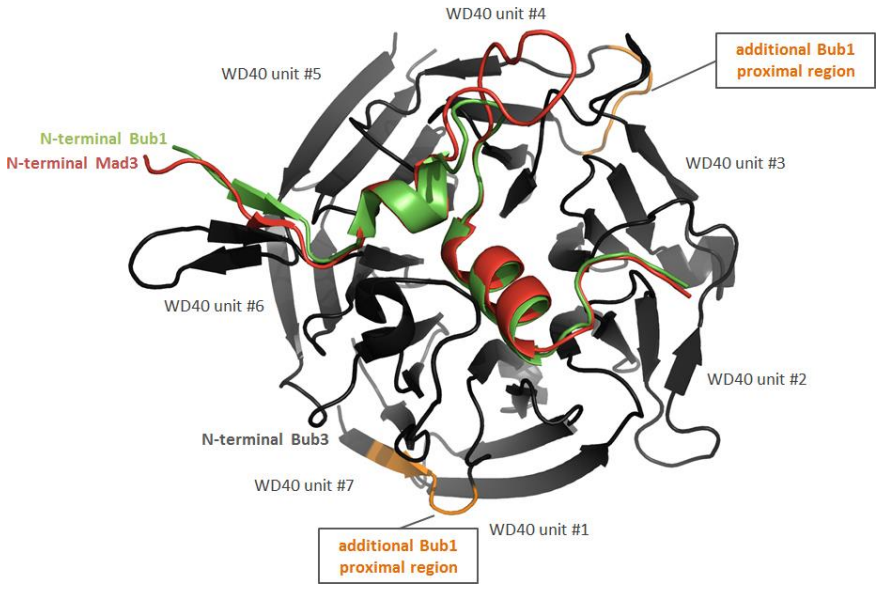

Figure 28: (a) Diagram visualising mapped cross-links within the *S.pombe* BUB complex. Blue coloured cross-links are within proteins and those in red are between subunits of the complex. The Bub1 B3i motif, which is known to facilitate association with Bub3 is shaded in blue. The shaded orange region is the TPR domain. **(b)** The characteristic seven-bladed WD40 propeller fold of *S.cerevisiae* Bub3 (dark shaded ribbon representation) in association with the B3i motif of Bub1 (green; residues 315-350) and Mad3 (red; 353-395) as determined by x-ray crystallography (Larsen *et al.* 2007). The B3i motifs are shown in contact with the same Bub3 molecule for illustration purpose only, as Bub3 can only accommodate a single B3i motif. The two regions coloured in orange are putative secondary proximate Bub1 regions suggested by the *S.pombe* cross-linking data of the Bub1 – Bub3 dimer. The 3D structure representation was prepared in PyMol (§2.5.3).

Cross-linking proximate residues of the *S.pombe* Bub1 – Bub3 complex (Table 30 and Figure 28a) revealed 2 links (group A) that map near the known Bub1 B3i motif and one link that

defines a second Bub1 proximate region situated at the very amino terminal ('group' B). 23 cross-links were identified for Bub1 that were either intra or intermolecular (groups C, D and E). Those of group C map to the three helix-turn-helix folds of the TPR domain, whilst the long range linkers of group E indicate that a tertiary or quaternary structure involves proximity of the Bub1 amino terminus to a region just carboxy terminal of the B3i motif. The density and presence of the linkers in a 200 residue region after residue 400 suggest a compact fold.

4.4 Conclusions and discussion

Recent developments in protein cross-linking chemistry, MS technology and MS spectra analysis provide an exciting new tool in determining the architecture of multi-protein complexes. Here, *in vitro* cross-linking was performed on endogenous and native complexes purified from yeast employing the large-scale single-step purification method refined in chapter 3. Perhaps the ultimate goal for structural protein complex studies is the APC^{MCC} holo-enzyme or spindle checkpoint protein complexes in association with their kinetochore binding partners. However, MS analysis of Bub1, Mph1 and Bub3 complexes from both yeast species indicate that their kinetochore association was extremely unstable (§3.4.10). In addition, the *S.cerevisiae* APC E3 ubiquitin ligase complex was purified short of bound MCC (§3.3.6). Endeavours focussing on *S.pombe* APC^{MCC} complexes found them little compliant to this cross-linking strategy as a larger than expected number of contaminants was present (MS data not shown). Although efforts in purifying stable and clean complexes are continuing, here MS analysis of cross-linked native MAD, BUB and NDC80 complexes provides a proof of concept in obtaining additional insights in the structural organisation of multi-protein complexes. These experiments uncovered both known and unknown domains of proximity and show that the primary sequences of these complexes mapping to those contained within crystal structures are of similar fold. Interestingly, a second proximate interface of the MAD and the BUB structure was found that could provide additional stabilisation of the complex. This region in Mad1 adjoins the RLK motif, which is highly conserved and essential for spindle checkpoint functioning in human (Kim *et al.* 2012), *S.cerevisiae* (Brady & Hardwick 2000) and *S.pombe* cells (Hardwick lab; not published). This motif is essential in forming the unique *S.cerevisiae* MBB complex during mitotic arrests (Brady & Hardwick 2000). Certainly, further investigation could come to a better understanding of its structural significance. It is anticipated that future developments in purification techniques, cross-linking chemistry and efficiency, and *in vitro* reconstitution of recombinant complexes produced by baculovirus-mediated insect cell expression systems will significantly boost knowledge of spindle checkpoint complexes and

their mode of action. Elucidating sites of proximity by employing this method can thus greatly facilitate efforts to engineer complexes that either abolish or enhance associations such as those of the checkpoint proteins with a kinetochore or the APC E3 ubiquitin ligase complex. Of particular interest would be the interaction of Bub1 and Bub3 with Spc7/Spc105. The association of these two checkpoint proteins with their kinetochore anchor is interdependent and thus far only the Bub1 TPR binding to a KI motif of Blinkin (Spc7/Spc105) has been revealed although several binding sites are anticipated (Bolanos-Garcia *et al.* 2012, Krenn *et al.* 2012), among which is the unknown receptor domain of phosphorylated MELT motifs (Shepperd *et al.* 2012, Yamagishi *et al.* 2012).

5 *S.pombe* Bub1 interacts with novel chromatin factors that resist DNA damage

5.1 Summary

Analysis of *S.pombe* BUB+ (Bub1 – Bub3 – Mad3) spindle checkpoint complex interactors by tandem MS uncovered four novel interactors that are generally considered to be chromatin associated factors. This includes an uncharacterised gene product of *SPAC31G5.19*, which is thought to encode a bromodomain ATPase protein. Abo1, for 'ATPase with bromodomain orthologue 1', is essential in binding the quaternary complex, termed TAPAS (for 'Tfg3, Abo1, Pob3 and Spt16') to the BUB+ complex. A stable association further relies on Bub1 associating with Bub3. This chapter attempts to investigate the functional relevance of the BUB+ complex interacting with the TAPAS chromatin remodeller.

A *bub1Δ* and kinase dead mutant was shown to lose viability in the presence of genotoxic drugs, a phenotype shared with *abo1Δ*, *tfg3Δ* and *pob3Δ* cells. Genotoxic sensitivity of cells deficient in TAPAS or Bub1 did not appear to be due to the loss of DNA damage checkpoint or DNA replication checkpoint functions. Evidence in favour of a Bub1-dependent response to DNA double strand breaks is presented, although no evidence has been forthcoming that this function relies on its association with TAPAS.

Taken together, the findings presented here suggest that at least some of the chromatin remodelling activities of TAPAS and Bub1 are implicated in parallel pathways that respond to DNA damage. They argue in favour of a greater role for Bub1 kinase beyond its duty in mitotic checkpoint signalling, in safeguarding a cell's genetic heritage.

5.2 Aims and background

The MS analysis of *S.pombe* Bub1, Bub3 and Mad3 interactors in chapter 3 identified several proteins that are generally associated with chromatin modifying activities. The following four proteins were uncovered with relatively high peptide counts and polypeptide coverage (summarised in Table 31):

i. An uncharacterised gene product encoded by the *SPAC31G5.19* gene, whose sequence is predicted to contain a bromodomain-like motif in addition to one or two AAA family ATPase domains. Orthologous to human ATAD2 (or ANCCA), *C.elegans* Lex-1 and *S.cerevisiae* Yta7, it is here named Abo1[16], an acronym for 'ATPase with bromodomain

[16] *S.pombe SPAC31G5.19* (chromosome 1) and *SPBP22H7.05c* (chromosome 2) are paralogous genes, whose products are named here respectively Abo1 and Abo2.

orthologue'. This name was submitted to PomBase.org, a resource by and for the *S.pombe* research community, in March 2013.

ii. The YEATS domain protein Tfg3 (also known as Anc1, Taf14, Swp29 or Taf30) that is commonly found associating with chromatin remodelling complexes and some transcription factor complexes.

iii. Spt16 (previously known as Cdc68).

iv. Pob3, which together with Spt16 forms the binary FACT complex that is involved in nucleosome remodelling activities.

Although not often described as such, the Bub1 kinase is by virtue of its ability to phosphorylate nucleosomal histone H2A a *bona fide* chromatin modifier, albeit one with a very specific activity (Kawashima *et al.* 2010). On the other hand, the novel BUB+ interactors described here are involved in many chromatin remodelling processes (see discussion below) and their absence lead to a broad phenotypic spectrum. Pleiotropy is often a limitation in the experimental exploration of unknown protein function in regards to association with other protein factors. In this case, much is known about their spindle checkpoint interactors Bub1 and Bub3. In this chapter, the function of these chromatin remodellers is explored in the context of their physical interaction with the BUB+ complex and the emphasis is on BUB functions shared or complementing those of its most direct interactor.

Sequence analysis of *S.pombe* Abo1 (see §5.3.1) suggests it contains a distinct amino terminal AAA domain ATPase (approximately 230 amino acids in length) and a carboxy terminal bromodomain (approximately 50 amino acids) that are separated by a second putative ATPase domain that is found just about halfway through the polypeptide (Figure 29). A similar domain arrangement is observed in the *S.cerevisiae* orthologue Yta7, the second ATPase domain being described as degenerate and potentially non-functional (Jambunathan *et al.* 2005, Gradolatto *et al.* 2009).

#	protein hit	number of unique peptides	total number of peptides	% polypeptide coverage
	Bub1-ZZ, interphase cells			
1	Bub1	118	2278	70
2	Bub3	28	512	73
3	Mad3	7	12	31
4	Tfg3	16	67	70
5	Abo1	55	331	37
6	Pob3	6	6	18
7	Spt16	6	7	9
	Bub1-ZZ, mitotic arrest			
8	Bub1	351	2517	82
9	Bub3	72	458	75
10	Mad3	3	3	15
11	Tfg3	26	66	55
12	Abo1	156	506	55
13	Pob3	4	6	14
14	Spt16	6	17	14
	Bub3-ZZ, interphase cells			
15	Bub1	262	2121	82
16	Bub3	55	905	80
17	Mad3	5	6	19
18	Tfg3	23	80	66
19	Abo1	108	511	55
20	Pob3	4	4	12
21	Spt16	7	9	9
	Mad3-ZZ, interphase cells			
22	Bub1	98	354	67
23	Bub3	23	99	59
24	Mad3	106	818	87
25	Tfg3	5	6	35
26	Abo1	19	35	20
27	Pob3	0	0	0
28	Spt16	0	0	0

Table 31: The presence of Tfg3, Abo1 (the gene product of *SPAC31G5.19*), Pob3 and Spt16 proteins in precipitations of Bub1, Bub3 and Mad3 as identified by tandem MS analysis (see chapter 3).

Figure 29: Schematic representation of predicted functional and structural domain arrangement of the bromodomain ATPase Abo1, a gene product of *SPAC31G5.19*. A bromodomain is preceded by two AAA family ATPase domains, the second of which could be of degenerate nature (see §5.3.1). The Abo2 paralogue and *S.cerevisiae* Yta7 orthologue have a similar domain organisation.

AAA (for 'ATPases associated with diverse cellular activities') domain ATPases belong to the AAA+ superfamily of ring-shaped P-loop NTPases, which are represented in all three kingdoms of life (Erzberger & Berger 2006, Snider & Houry 2008, Snider *et al.* 2008). They catalyse the remodelling or translocation of substrates by releasing energy through the hydrolysis of ATP and function in, for example, transcription regulation, DNA replication and repair, protein degradation, chaperone activities and membrane fusion events (Zhang & Wigley 2008). It is thought that ATP hydrolysis by the so-called Walker A and B motifs is stimulated by ligand binding. This so-called 'glutamate' switch induces a conformational change that engages the glutamate residue situated within the DEAxx box of the active site (Hanson & Whiteheart 2005, Zhang & Wigley 2008, Mogni *et al.* 2009). Another typical feature of AAA domain ATPases is the arginine-finger[17] that reaches into the catalytic site and is most often provided in *trans* by a second AAA domain within the same polypeptide or through oligomerisation of AAA ATPases (Erzberger & Berger 2006). Whereas Abo1 remains uncharacterised, a small number of studies describe its orthologues from *S.cerevisiae* (named Yta7[18]), *C.elegans* (Lex-1), human and mouse (ATAD2, also called ANCCA). The Yta7 bromodomain has been described as a pseudo or non-canonical bromodomain since it is thought to lack some of the residues required for engaging acetyl-lysine residues (Jambunathan *et al.* 2005, Gradolatto *et al.* 2009). For instance, the tyrosine residue in the binding pocket that crucially establishes a hydrogen bond with acetylated lysine is not present in *S.cerevisiae* Yta7 (Jambunathan *et al.* 2005) and the two *S.pombe* bromodomain ATPases (see also multiple sequence alignment of a few

[17] 'Glutamate switches' and 'arginine fingers' set the AAA family of ATPases apart from the SWI2/SNF2 family that typically contain seven sequence motifs also found in DExx box helicases and are mostly chromatin remodellers (i.e. the bromodomain ATPase Swi2), which are stimulated by DNA (single stranded, double stranded or nucleosomal) (Durr *et al.* 2006, Durr & Hopfner 2006). Both SWI2/SNF2 and AAA family ATPases are P-loop ATPases with the characteristic Walker A (ATP binding) and Walker B (that includes the DExx box required for ATP hydrolysis) motifs. Whereas AAA DNA helicases have been identified, SWI2/SNF2 ATPases stop short of actual DNA helicase activities.

[18] Yta7 is an acronym for 'yeast tat-binding protein analogue 7', as it shares homology in its ATPase domain with human tat-binding proteins TBP1 and TBP7, which are ATPase subunits of the metazoan 26S proteosome (Schnall *et al.* 1994).

bromodomain ATPases in supplementary section 7.7). The Yta7 bromodomain is able to bind histone H3, but modifications such as methylation and acetylation are thought to reduce the affinity (Gradolatto *et al.* 2008). Nonetheless, the bromodomain of human ATAD2 is said to bind the acetylated lys14 residue of histone H3 (Revenko *et al.* 2010).

Yta7 interacts with a range of chromatin modifying complexes, such as the histone acetyltransferases NuA3 and SAGA (also called SLIK) and the chromatin remodellers RSC, INO80, ISW2 (CHRAC) and ISW1b (Tackett *et al.* 2005, Lambert *et al.* 2009). Lex-1 and Yta7 are implicated in establishing and maintaining chromatin boundaries that serve to isolate 'silent' or transcriptionally repressed chromatin from surrounding regions with active transcription (Jambunathan *et al.* 2005, Tackett *et al.* 2005, Tseng *et al.* 2007, Gradolatto *et al.* 2009). Deletion of *YTA7* leads to silencing of genes up and downstream of *HMR*, the silent mating type locus on the right flank of the *MAT* locus (Jambunathan *et al.* 2005, Tackett *et al.* 2005). In addition, Yta7 functions as a transcriptional regulator of histone genes, whose expression is tightly controlled and restricted to S phase (Gradolatto *et al.* 2008, Fillingham *et al.* 2009, Kurat *et al.* 2011). It is proposed that gene activation by the Rtt109-dependent histone acetylation is facilitated by Yta7, which prevents the Rtt106 repressor from spreading onto regulatory elements by establishing a boundary (Gradolatto *et al.* 2008, Fillingham *et al.* 2009, Kurat *et al.* 2011, Zunder & Rine 2012). Conversely, a recent study observed an increase in histone H3 levels in the absence of Yta7 and a consequent reduction in nucleosome spacing (Lombardi *et al.* 2011). This suggests an additional role in histone H3 eviction or degradation. In addition, cells that lack Yta7 exhibit growth defects when environmental stresses are exerted, such as elevation of temperature, DNA synthesis inhibition and exposure to genotoxic drugs (Gradolatto *et al.* 2008). The metazoan orthologue ATAD2 binds to E2F transcription factors at promoter regions and regulates the cell cycle-dependent transcription of genes coding for cyclins and cdk's (Revenko *et al.* 2010). Together with the MLL histone methyltransferase, it is also implicated in tumour formation when hormone-responsive genes are aberrantly expressed, such as the androgen signalling receptor in prostate cancer (Zou *et al.* 2007, Ciro *et al.* 2009, Zou *et al.* 2009, Revenko *et al.* 2010, Duan *et al.* 2012).

S.pombe Tfg3 and its *S.cerevisiae* orthologue Taf14 are auxiliary factors to chromatin remodelling complexes (INO80, RSC, SWI/SNF, NuA3 and mediator) and general transcription factors (TFIIB, TFIID and TFIIF) (Kabani *et al.* 2005, Schulze *et al.* 2009, Schulze *et al.* 2010). Tfg3/Taf14 and the human leukemogenic proteins ENL, AF9 and GAS41 are thought to recruit TFII and remodelling complexes to chromatin by directly engaging histone H1 and H3 through

their YEATS (for 'Yaf9, ENL, AF9, Taf14 and Sas5') domain (Zeisig *et al.* 2005). A YEATS domain is a well-conserved feature of some chromatin remodellers, around 83 amino acids in length, and is able to engage post-translationally modified histone residues (Schulze *et al.* 2009). In a genome wide *S.cerevisiae* study, overexpression of Taf14 resulted in genomic instability for reasons unknown (Ouspenski *et al.* 1999). Tfg3 and Taf14 are not essential under normal growth conditions, but several studies suggest that they are required for viability under stress conditions, such as elevated temperatures, exposure to UV light and γ radiation, heavy metals, DNA alkylating agents, hydroxyurea, microtubule poisons in addition to osmotic and oxidative stresses (Henry *et al.* 1994, Kimura & Ishihama 2004, Erlich *et al.* 2008).

Since nucleosomes hinder gene transcription by RNA polymerases they will need to be taken apart or moved away. Whereas gene transcription by RNA polymerase III is assisted by 'sliding' or transfer of the nucleosomes, genes transcribed by RNA polymerase II undergo partial nucleosome disassembly (Studitsky *et al.* 1997, Kireeva *et al.* 2002). The latter activity is undertaken by the heterodimeric FACT (for 'facilitates chromatin transcription') complex consisting of Spt16 (formerly known as yeast Cdc68, p140 in metazoa) and Pob3 (SSRP1 in metazoa). Specifically, transcription through chromatin is assisted by the eviction of a single H2A – H2B dimer from each nucleosome revealing a histone hexamer (Belotserkovskaya *et al.* 2003). In addition to nucleosome disassembly, FACT function in conjunction with the chromodomain helicase Cdh1 and histone chaperone Spt6 has also been implicated in the reassembly of nucleosomes after transcription elongation by the RNA polymerase II has taken place in (Reinberg & Sims 2006). Lastly, the FACT complex was found to have a direct role in the formation of heterochromatin at the mating type locus and at centromeres in *S.pombe* (Lejeune *et al.* 2007). Cells that lack Pob3 fail to load Swi6 onto methylated Lys9 of histone H3 and as a consequence exhibit chromosome segregation defects (Lejeune *et al.* 2007).

5.3 Results

5.3.1 *S.pombe abo1* (*SPAC31G5.19*) gene and protein sequence analysis

The *S.pombe* community's repository PomBase (§2.5.3) indicates that the *S.pombe SPAC31G5.19* gene and its protein product are currently uncharacterised. Analysis of the protein sequence using NCBI's Conserved Domain Database (§2.5.3) and EMBL's InterProScan (§2.5.3) did indicate that the gene encodes a protein with a theoretical mass of 135.3 kDa comprising potentially two AAA family ATPase domains followed by a single bromodomain (Table 32 and Figure 29). The structure and function of these domains is discussed in section 5.2 above.

#	proposed feature	characteristics	residues	tools
1	AAA ATPase domain	P-loop, Walker A and B domain, arginine finger	263 - 526 core: 303 - 438	CDD, InterProScan
2	AAA ATPase domain	P-loop, Walker A and B domain, arginine finger	576 - 754 core: 601 - 705	InterProScan
3	bromodomain	acetyl-lysine binding site	814 - 919	CDD

Table 32: CDD and InterProscan searches utilising PFAM, TIGRFAM, GENE3D, SMART and other databases containing protein domain signatures predict that the ABO1 (formerly *SPAC31G5.19*) gene of *S.pombe* encodes a protein, here named Abo1 (see text), with two putative AAA ATPase domains followed by a bromodomain. A multiple sequence alignment of *S.pombe* Abo1, Abo2, *S.cerevisiae* Yta7, human ATAD2 and other orthologues is given in supplementary chapter §7.7.

S.pombe SPAC31G5.19 orthology analysis using a variety of databases, such as OrthoDB, PomBase, UniProt, the *Schizosaccharomyces* Comparative Genome Project, PhylomeDB and TreeFam (§2.5.3) revealed one paralogous gene product, *SPBP22H7.05c*, as yet uncharacterised, on chromosome 2 (*SPAC31G5.19* is situated on chromosome 1) and the presence of orthologous gene products in most of the lineages of the eukaryotic domain of Life (see Table 33). All known *Schizosaccharomyces* species have two paralogous genes, whereas other fungal species seem to function with a single copy. At least two paralogues are present in most metazoan cells, with the ATAD2 paralogous gene product generally having the highest sequence identity with the *S.pombe SPAC31G5.19* gene product.

Notably, the order of the two prospective ATPase domains followed by a single putative bromodomain is extremely well conserved through evolution and thus typifies the extensively conserved set of proteins listed in Table 33. Hence in this work, the name of the *SPAC31G5.19* gene product is proposed as 'ATPase with bromodomain orthologue 1', abbreviated to Abo1, and *SPBP22H7.05c* thus as Abo2.

A multiple protein sequence alignment was prepared for the bromodomain ATPases listed in Table 33 with ClustalΩ software (§2.5.3) using default settings. Part of this alignment that includes *S.pombe* Abo1, Abo2, *S.cerevisiae* Yta7, human ATAD2 and *C.elegans* Lex-1 is given in supplementary chapter §7.7. This alignment was used to create a phylogenetic profile with a neighbour-joining clustering method to construct a tree, illustrated in Figure 30, using the ClustalW2 phylogeny server (§2.5.3). Here, branch lengths are proportional to the number of mutations that occurred along each branch during molecular evolution and nodes represent a common ancestor. The *Schizosaccharomyces* Abo1 sequences group separately from the Abo2 sequences, the most distantly related *S.japonicus* species making up the most distant node in each of the two clusters. This strongly suggest that duplication of the *abo* protogene occurred prior to *Schizosaccharomyces* speciation, as all other fungal genomes analysed carry a single

abo gene (data not shown). Similarly, all metazoan ATAD2 sequences are clustered away from ATAD2B sequences, indicating that *abo* protogene duplications might have arisen on several occasions. In-depth genomic synteny analysis could provide further evidence for these events.

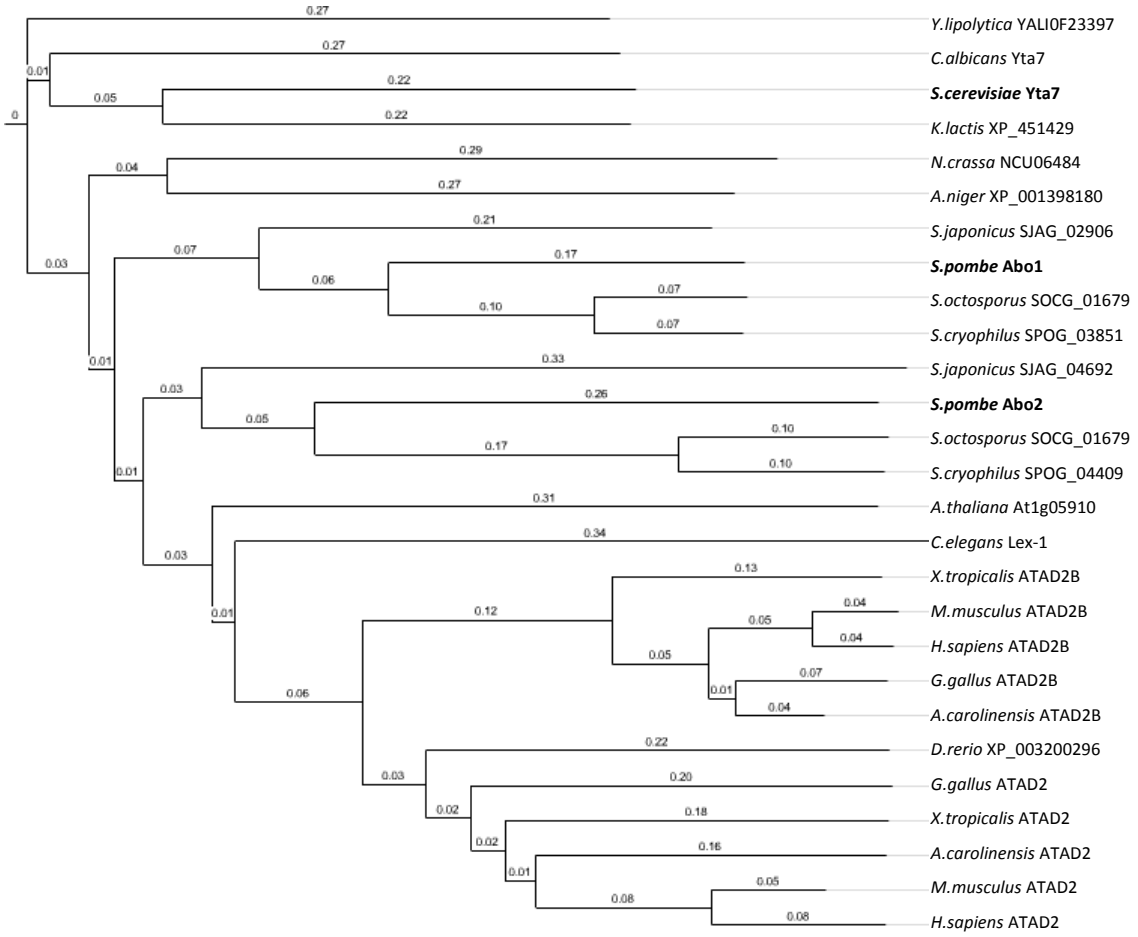

Figure 30: Phylogenetic tree of bromodomain ATPase protein sequences visualised with branch lengths using iTOL software (§2.5.3). Each node represents a common ancestral *ABO* gene product.

#	protein name / id	species	residues (aa)	% similarity/identity	global similarity
1	Abo1 / SPAC31G5.19	*S.pombe*	1190	100 / 100	1.00
2	SPOG_03851 (Abo1)	*S.cryophilus*	1184	85 / 80	0.62
3	SOCG_01679 (Abo1)	*S.octosporus*	1176	85 / 80	0.60
4	SJAG_04692 (Abo1)	*S.japonicus*	1127	55 / 60	0.10
5	SJAG_02906 (Abo2)	*S.japonicus*	1152	79 / 55	0.48
6	ATAD2	*M.musculus*	1040	59 / 53	0.12
7	YALI0F23397	*Y.lipolytica*	1309	59 / 52	0.20
8	SOCG_00067 (Abo2)	*S.octosporus*	1232	59 / 52	0.16
9	SPOG_04409 (Abo2)	*S.cryophilus*	1228	58 / 52	0.15
10	Yta7	*S.cerevisiae*	1379	58 / 51	0.19
11	NCU06484 / XP_957124	*N.crassa*	1955	38 / 51	0.20

#	protein name / id	species	residues (aa)	% similarity/identity	global similarity
12	ATAD2	*H.sapiens*	1390	51 / 50	0.09
13	Yta7 / XP_722018	*C.albicans*	1314	59 / 49	0.20
14	XP_451429	*K.lactis*	1319	59 / 49	0.19
15	ATAD2B / XP_003215429	*Anolis carolinensis*	1138	52 / 48	0.11
16	XP_003200296	*D.rerio*	1335	52 / 46	0.10
17	ATAD2	*G.gallus*	1319	51 / 46	0.09
18	ATAD2 / XP_002941445	*X.tropicalis*	1366	51 / 45	0.10
19	Lex-1	*C.elegans*	1291	50 / 45	0.05
20	ATAD2B	*G.gallus*	1415	50 / 45	0.08
21	ATAD2B / XP_002936030	*X.tropicalis*	1507	50 / 45	0.09
22	ATAD2B	*H.sapiens*	1458	48 / 43	0.08
23	ATAD2B	*M.musculus*	1460	48 / 43	0.09
24	Abo2 / SPBP22H7.05c	*S.pombe*	1201	60 / 43	0.16
25	ATAD2 / XP_003219463	*Anolis carolinensis*	1423	48 / 42	0.09
26	XP_001398180	*A.niger*	1667	53 / 40	0.26
27	At1g05910	*A.thaliana*	1210	52 / 28	0.09

Table 33: Bromodomain ATPase orthologues ranked according to their sequence identity with Abo1. Percentage protein sequence similarities and identities were calculated from a ClustalΩ multiple sequence alignment using the SIAS tool (§2.5.3). This tool uses the BLOSUM62 matrix to calculate global similarities with *S.pombe* Abo1 as reference sequence.

5.3.2 *S.pombe abo1* (*SPAC31G5.19*) gene deletion

As the *S.pombe SPAC31G5.19* gene, denoted as *abo1*, and its protein product Abo1 are as yet uncharacterised[19], a heterozygous diploid deletion mutant strain was created. The *h+ ade6-210* strain KP114 (§2.1.2) was mated overnight with *h- ade6*-216 strain KP116 on a SPA plate (§2.1.3) at 25°C and checked for the presence of conjugating cells the next day. Cells were then streaked onto synthetic PMG medium lacking adenine (§2.1.3) to form isolated colonies existing of diploid cells that are adenine prototroph through heteroallelic complementation of the two *ade6* mutant alleles. Complete replacement of one *abo1* open reading frame for a nourseothricin acetyltransferase (*NAT1*) selectable marker gene by DNA recombination was carried out by standard transformation procedures (Forsburg & Rhind 2006). This involves PCR amplification (§2.4.4) of the *NAT1* gene flanked by *TEF* promoter and terminator sequences from plasmid pFA6a-NatMX6 (§2.4.2) using DNA oligos SJo76 and SJo77 (§2.4.1) carrying about 70 nucleotides of homology to the 5′ and 3′ UTR regions of *abo1*. Transformation (§2.1.4) and positive selection of transformants was carried out on YES plates supplemented with clonNAT

[19] *S.cerevisiae* cells deleted for the *abo1* orthologue *YTA7* are viable (Tackett *et al.* 2005).

(§2.1.3) and checked for diploid maintenance on PMG medium lacking adenine. Confirmation of successful targeting and deletion of the *abo1* gene DNA was obtained by PCR (§2.4.4) using genomic DNA extracted (§2.4.3) from clonNAT resistant strains.

Sporulation of heterozygous *abo1Δ::natmx6* / *abo1* cells was induced on SPA medium (§2.1.3). Then tetrads were dissected (§2.1.7) and spores were allowed to germinate on rich plates. Germination at both 25 and 32°C reproducibly resulted in two large and two small colonies in the majority of cases (Figure 31a). As the former colonies die on medium containing clonNAT they thus correspond to the haploid wild-type offspring. In the minute colonies, cell growth is clearly negatively affected and a mixture of both elongated and undersized morphologies is represented.

Next, 120 µL of YES medium in several wells on a microtiter plate was each inoculated with cells from a single small colony. After overnight growth at 32°C in a shaking plate incubator, cells were collected from each well and observed by light microscopy. The vast majority of cells appeared with normal cell morphology, but a small number of cells, no more than 2%, were of elongated appearance (Figure 31b). Indicative of a prolonged S phase or G2 arrest, these cells could perhaps be responding to the persistence of unreplicated or unrepaired DNA. Within 7 days all propagating cells appeared to resume growth with normal cell morphology, albeit with a lower growth rate than that of wild-type cells (Figure 31c). As the plating efficiency of the *abo1Δ* mutant was slightly lower, this seems to suggest that cell viability is to some extent compromised (data not shown). Taken together, *S.pombe* cells were thus consistently able to complement the lack of Abo1 by gaining as yet unknown suppressors and thus *abo1* is in essence a non-essential gene.

The nature of such suppresors is intriguing. they are unlikely to be gene mutations (which are predominantly stochastic, rare and non-targeted events) as the vast majority of *abo1Δ* cells were viable post-germination and reproducibly resumed ‘normal’ growth after an initial ‘stalling’ event. As the Abo1 bromodomain ATPase is predicted to have chromatin modifying properties, perhaps an epigenetic remodelling event is able to suppress the lack of Abo1 function. For instance, the spreading of heterochromatin beyond unmaintained chromatin barriers could silence essential genes and would need to be counteracted by upregulation of unknown activators.

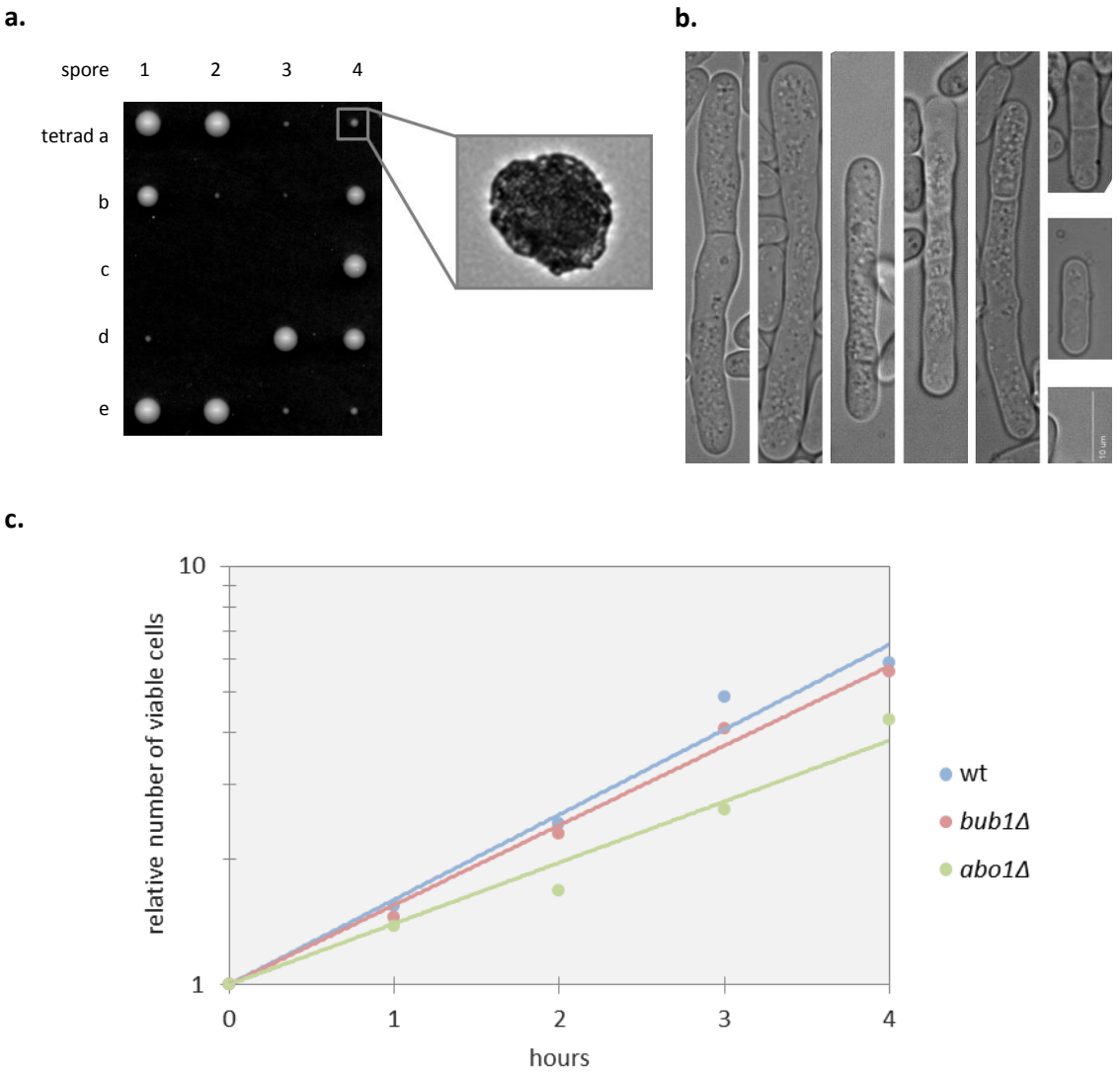

Figure 31: (a) Tetrad analysis of sporulated heterozygous diploid *abo1Δ* / *abo1* yeast SJ987.11. Each horizontal row contains the four dissected spores from a single ascus sac on rich YES medium, typically giving rise to two large and two small colonies. Cells from large colonies die on medium containing clonNAT, indicating that they have grown from wild-type spores. The smaller colonies are thus *abo1*Δ. **(b)** Elongated cell phenotype in a small proportion (around 1%) of the *abo1Δ* cell population. The morphologically normal cells on the right are approximately 12 - 20 µm in length, compared to around 50 µm of some of the longer cells. 10 µm scale bar at bottom right. **(c)** The growth rate of indicated strains from mid-log cultures at 32°C was determined in a plate assay by counting the number of viable cells able to form colonies (§2.1.9). The growth rate of *abo1Δ* cells is lower than that of *bub1Δ* and wild-type cells.

5.3.3 The novel TAPAS complex of 'Tfg3, Abo1, Pob3 and Spt16' is a BUB+ interactor

To facilitate co-precipitations and immuno-blotting experiments three strains were constructed with a carboxy terminal tagged Abo1 or Bub1: *abo1-zz::kanmx6* (SJ977), *abo1-gfp::kanmx6* (SJ986) and *bub1-zz::kanmx6* (SJ636; complete genotypes are listed in §2.1.2). To tag Abo1, diploid strains were engineered by PCR-based endogenous gene targeting purposes

(§2.1.4) as described above using pFA6a-GFP-KanMX6 and pKW804 (§2.4.2) as template DNA. After sporulation was induced, spores were dissected from tetrads using a micro-manipulator (§2.1.7) and allowed to germinate on rich medium. Unlike *abo1*Δ spores, all four spores developed into colonies of equal size, indicating that a ZZ or GFP carboxy terminal tag on Abo1 does not seriously hamper cell growth.

To corroborate the Bub1 association with Abo1, Abo1-ZZ complexes were purified as described in section 2.3.1 and analysed by tandem MS at the Scripps Research Institute, CA, USA (§2.3.3). In addition to Abo1 and Bub1, peptides for Bub3, Tfg3, Pob3 and Spt16 were present in precipitates (Table 34).

#	protein hit	number of unique peptides	total number of peptides	% polypeptide coverage
1	Bub1	2 / 8	3 / 10	3 / 12
2	Bub3	2 / 7	2 / 12	8 / 23
3	Abo1	55 / 56	777 / 128	25 / 39
4	Spt16	10 / 9	19 / 11	8 / 11
5	Pob3	4 / 6	6 / 8	10 / 14
6	Tfg3	14 / 17	244 / 54	40 / 58

Table 34: MS data of two *S.pombe* ZZ-epitope tagged Abo1 precipitations (strain SJ977). Five unique phosphorylation sites were identified for the Abo1 bromodomain ATPase (data not shown).

Next, to probe the interaction of the BUB+ complex with Abo1, four strains were created by genetic crosses and selecting single-spore offspring for the desired genotype: *abo1-zz bub1-ha* (SJ989), *abo1-gfp bub1-zz* (SJ599) and *abo1-gfp bub3-zz* (SJ658; complete genotypes are listed in §2.1.2). In addition, *mad3*Δ, *bub1Δ* and *bub3Δ* mutant strains were utilised to ascertain the Mad3, Bub1 and Bub3 dependence of the Abo1 interaction with the BUB+ complex. Immuno-blotting of ZZ tagged and precipitated Abo1 complexes indicated that its interaction with Bub1 depends on Bub3, but not on Mad3 (column 3 - 5 in Figure 32a). Indeed, Bub3-ZZ was shown to associate with Abo1 (column 13). Surprisingly, this binding was abolished in the absence of Bub1 (column 15). Thus the interaction of Abo1 with the BUB+ complex appears to depend on both Bub1 and Bub3. To confirm this, Bub1-ZZ precipitations were probed for the presence of Abo1. As expected, Bub1 did bind Abo1, but in the absence of Bub3 this interaction was significantly diminished (estimated to be less than 1%; column 9 and 10 in Figure 32b). Together, these findings argue that the stable association of Bub1 with Abo1 requires the presence of Bub3.

To test whether the Abo1 interaction with Bub1 or Bub3 requires Bub1 – Bub3 dimer formation or merely the presence of Bub1 and Bub3 monomers, a *bub1*$^{b3i\Delta}$ mutant allele was used that encodes Bub1 protein deleted for the Bub3-interaction motif (residues 264 - 299) (Vanoosthuyse *et al.* 2009). Bub1$^{b3i\Delta}$ was ZZ tagged using the method described before to create *bub1*$^{b3i\Delta}$*-zz::kanmx6* strain SJ687, which was used to make *bub1*$^{b3i\Delta}$*-zz abo1-gfp* strain SJ772. As shown, when either Bub1$^{b3i\Delta}$ or Bub3 complexes were analysed, no discernible Abo1 could be detected in a *bub1*$^{b3i\Delta}$ mutant background (column 11 and 14 in Figure 32). These experiments show that a interaction of Abo1 with Bub1 can be established but that it requires complex formation between Bub1 and Bub3 for this association to be stable. This could indicate that Bub3 binding to Bub1 induces conformational changes that promote Bub1 association with Abo1, that secondary Abo1 binding sites exist on Bub1 – Bub3 (e.g. with Bub3 directly) that require a prior interaction with Bub1 or that Abo1 binding requires chromatin association of Bub1 and Bub3. Also, the binding process could be negatively regulated by phosphorylation: as can be seen in column 5 of Figure 32a Bub1 is hyperphosphorylated in the absence of Bub3. Bub1 targeting to kinetochores during a mitotic arrest requires Bub3 and is essential for the efficient PP1 phosphatase-dependent silencing of the spindle checkpoint upon anaphase onset (Vanoosthuyse & Hardwick 2009b, Vanoosthuyse *et al.* 2009). In a similar manner, the Bub3-dependent localisation of Bub1 near sites of chromatin could for instance be a factor in driving dephosphorylation and subsequent Abo1 binding.

The Abo1 interaction with the Bub1 kinase was shown not to depend on the carboxy terminal 720 amino acids of the latter that include its kinase domain: a ZZ tagged amino terminal Bub1$^{[1\text{-}324]}$ fragment, which comprises both the TPR and B3i motif and created by PCR-mediated targeting of the endogenous *bub1* gene (strain SJ634), was found sufficient to bind Abo1 (column 12 in Figure 32b). Remarkably, MS analysis of precipitated *S.cerevisiae* Mad3, that unlike its *S.pombe* orthologue contains both a TPR and B3i motif and does not bind Bub1, identified Yta7 with a total of 4 peptides (3 unique peptides that cover 3.6% of the polypeptide sequence; data not shown).

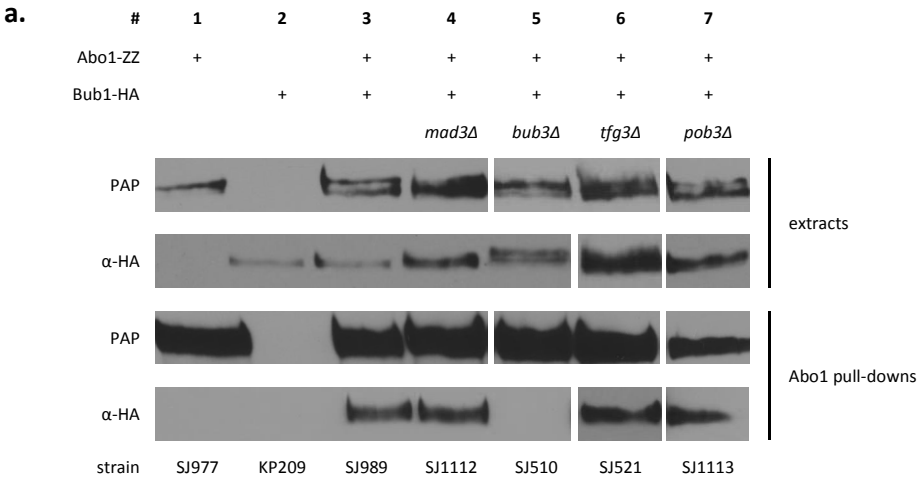

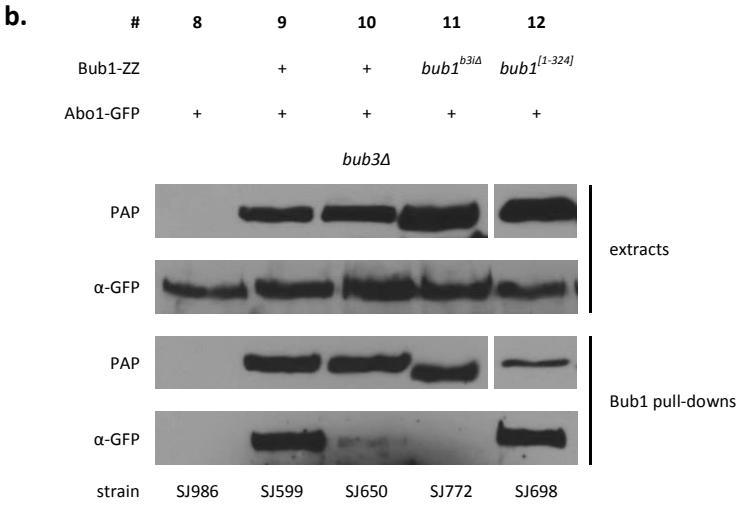

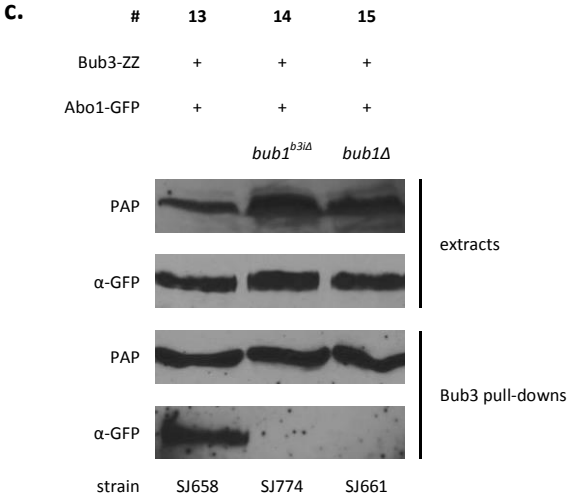

(figure continues on next page)

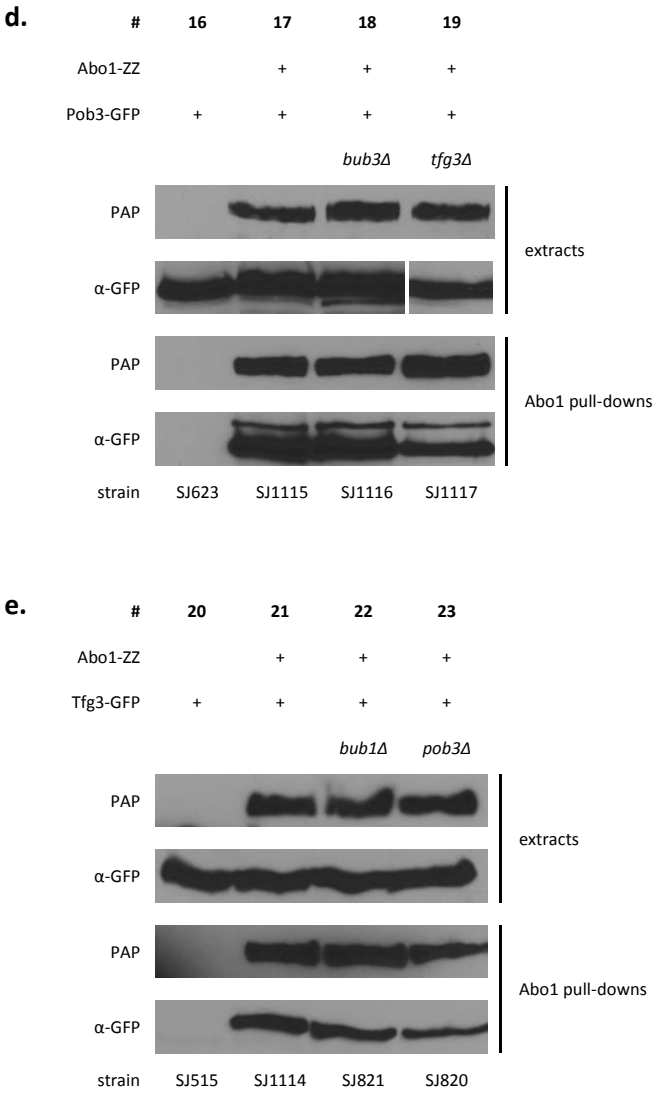

Figure 32: Western blot analysis of Bub1 and Abo1 co-precipitations. **(a)** The interaction of Abo1 with Bub1 depends on Bub3 but not on Mad3, Tfg3 or Pob3. **(b)** The Abo1 interaction with the 324 amino terminal residues of Bub1 is stabilised in the presence of Bub3, which requires a Bub1 – Bub3 interaction. A *bub1*$^{b3i\Delta}$ mutant cannot bind Abo1 or Bub3. **(c)** The interaction of Bub3 with Abo1 depends on their association with Bub1. **(d)** The interaction of Abo1 with Pob3 does not rely on Bub3 or Tfg3. **(e)** The interaction of Abo1 with Tfg3 is neither dependent on Bub1 or Pob3.

To further unravel the architecture of the TAPAS – BUB+ complex a series of strains was built to examine the interaction dependency on individual components. Successive co-precipitations and immuno-blotting revealed that the Bub1 – Abo1 interaction does not depend on the presence of Tfg3 or Pob3 (columns 6 and 7 in Figure 32a), that the Abo1 – Pob3 interaction does not depend on Bub3 or Tfg3 (column 18 and 19 in Figure 32d) and that the Abo1 – Tfg3 interaction does not depend on Bub1 or Pob3 (column 22 and 23 in Figure 32e).

These experiments show that 'Tfg3, Abo1, Pob3 and Spt16' (here termed TAPAS) can exist as a quaternary complex, whose formation does not depend on its interaction with the BUB+

complex. Although the physical interaction of the BUB+ and TAPAS components could not be confirmed by means of yeast two-hybrid or *in vitro* binding experiments (data not shown), the coprecipitation experiments described above lead to a prospective model of the TAPAS – BUB+ macro-molecular complex as depicted in Figure 33. In part support of this model, it should be noted that both Abo1 and Tfg3 (but not BUB+ components) were identified by tandem MS through precipitations of FACT complex subunits Pob3 and Spt16 (communicated by Alexander Kagansky, Robin Allshire lab; unpublished). The MS data presented here suggests that not all Abo1 – Tfg3 dimers interact with the FACT complex or that this interaction is not particularly stable: the total numbers of peptides and the percentage of polypeptide coverage for Pob3 and Spt16 were significantly lower than those for Bub1, Bub3, Abo1 or Tfg3 (see Table 31 and Table 34).

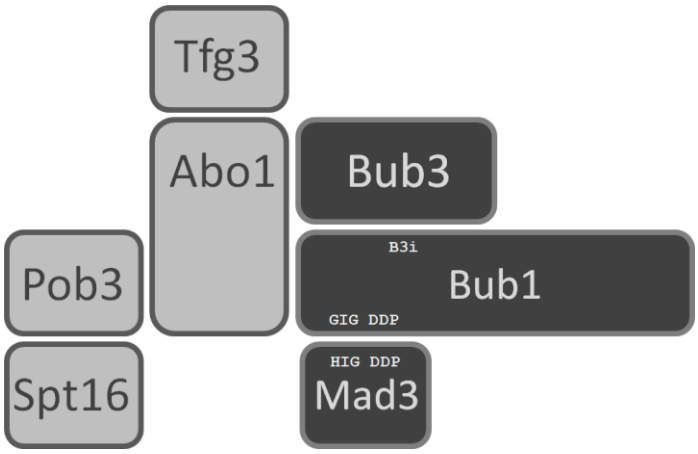

Figure 33: Prospective architecture of the BUB+ complex in association with the TAPAS (for 'Tfg3, Abo1, Pob3 and Spt16') complex. Stable association of TAPAS (lighter shade) with BUB+ (darker shade) depends on both Bub1 and Bub3.

5.3.4 The TAPAS components Abo1, Tfg3 and Pob3 are found in the cell nucleus

To determine the cellular localisation of Abo1, Tfg3 and Pob3, strains expressing endogenous protein carrying a carboxy terminal GFP fusion were analysed by fluorescence microscopy. Although high exposure times were required (1,000 ms) for Abo1, it was found to be a nuclear protein, absent from the nucleolus and appears to localise to chromatin during interphase and S phase (hydroxyurea arrest) in a speckled pattern and more robustly so during a *nda3-km311* induced metaphase arrest (see panels in Figure 34).

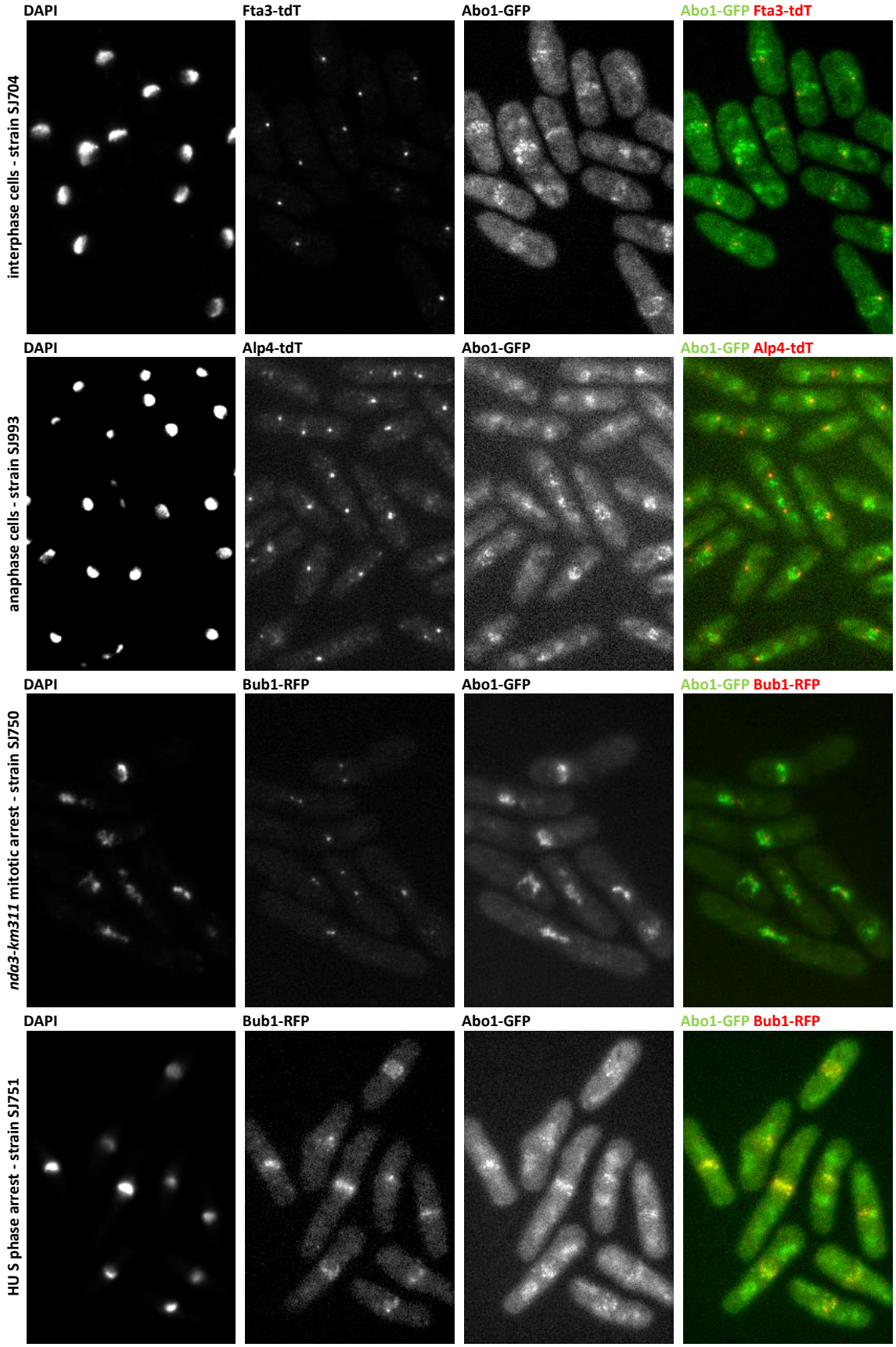

Figure 34: Abo1 and Bub1 localisation by fluorescence microscopy during interphase, *nda-km311* metaphase arrest and hydroxyurea S phase arrest. Fta3 and Alp4 are a kinetochore and a spindle pole marker, respectively.

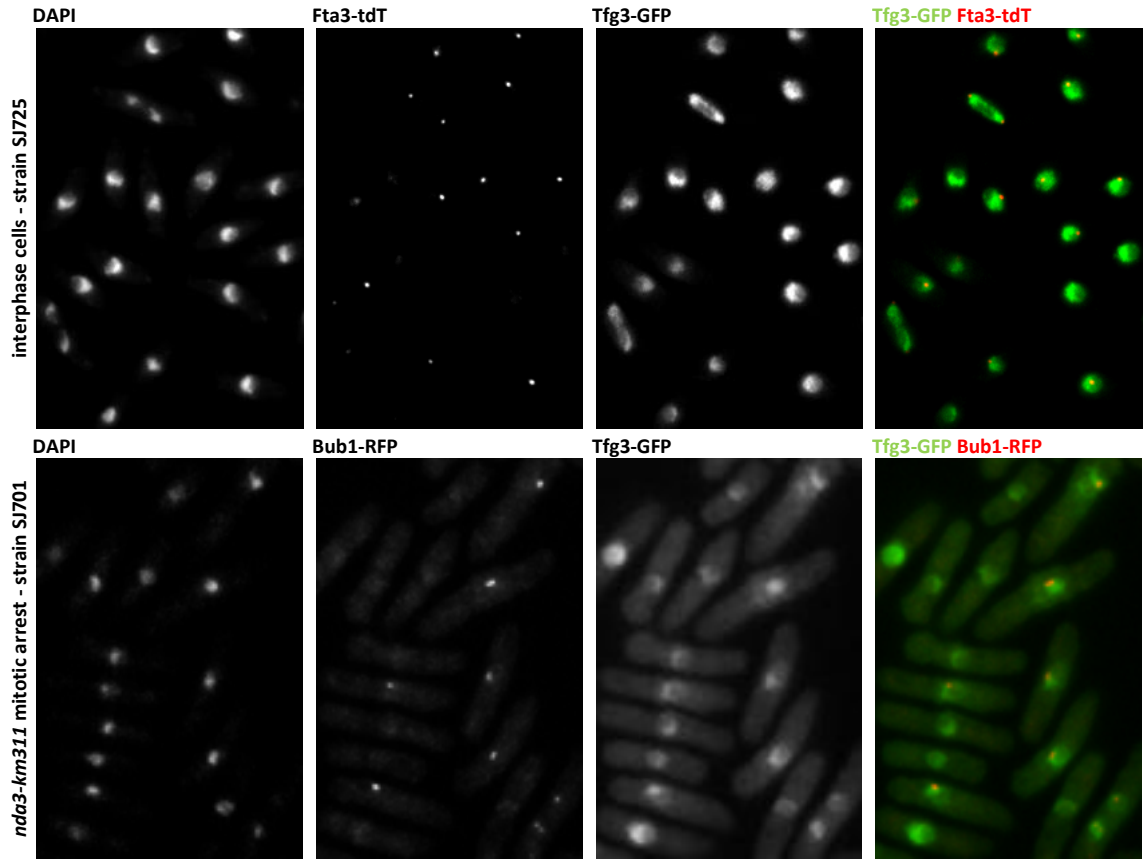

Figure 35: Tfg3-GFP localisation studied by fluorescence microscopy in interphase and *nda3-km311* arrested mitotic cells. Fta3 is a kinetochore protein fused to the tandem tomato red chromophore (tdT).

Apparent localisation of Abo1 at kinetochores and spindle pole bodies (as noted by means of its colocalisation with the kinetochore marker Fta3 and the spindle pole marker Alp4) was observed in few cases. Intriguingly, colocalisation of Abo1 with its interactor Bub1 was not clearly observed during metaphase, but the chromatin-wide presence of Bub1 during a hydroxyurea S phase arrest is perhaps more prominent than during a mitotic arrest.

Both Tfg3 (panels in Figure 35) and Pob3 (Figure 36) are nuclear proteins. Unlike the chromatin-like localisation of Abo1 and Bub1, distribution of Tfg3 and Pob3 was shown to be diffuse, but even, throughout the nucleus with an apparent nucleolar exclusion. The nuclear localisation of Tfg3, Abo1 and Pob3 during interphase and metaphase arrests was found not to depend on the presence of Bub1 or Bub3 and *vice versa* (data not shown).

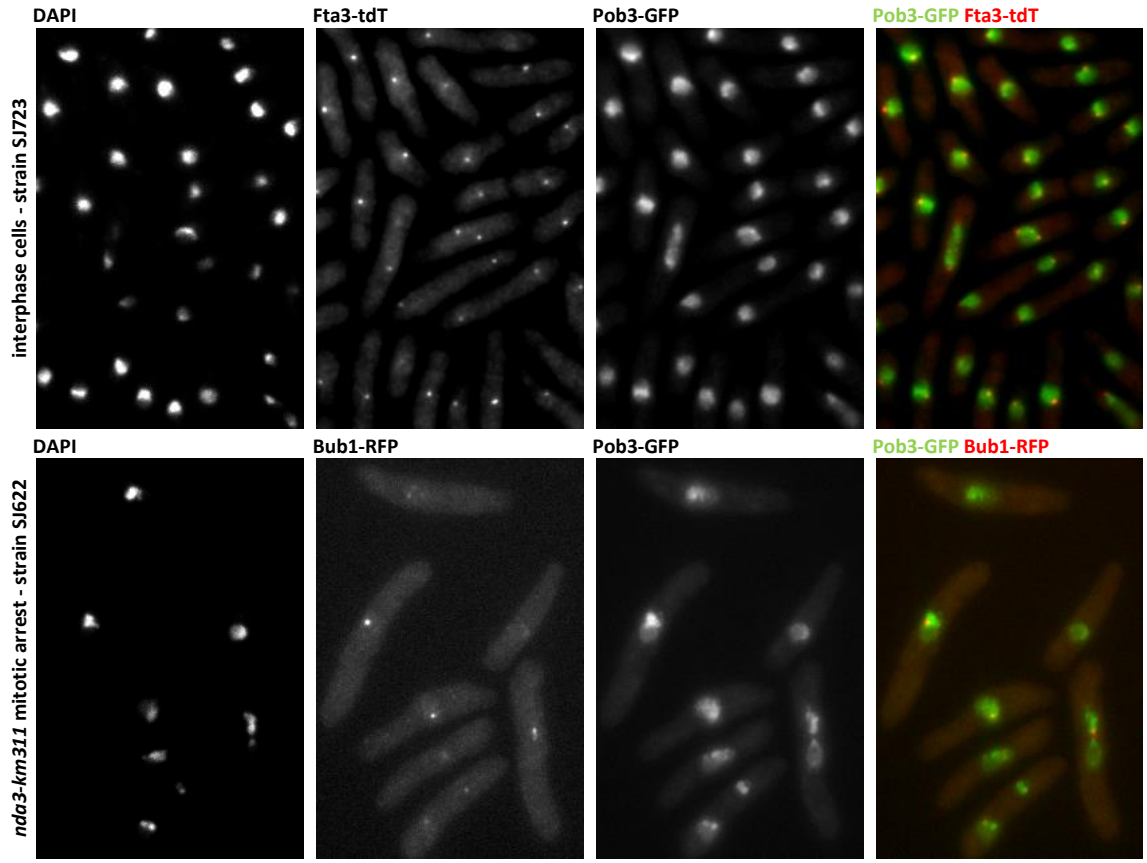

Figure 36: Pob3-GFP localisation studied by fluorescence microscopy in interphase cells and *nda3-KM311* arrested mitotic

5.3.5 Cells lacking Abo1 are spindle checkpoint-proficient and effectively load Sgo2 at centromeres

The molecular interaction of Abo1 with Bub1 could indicate that both proteins are engaged in similar biological pathways. The mitotic function of Bub1 is two-fold: first, when chromosomes fail to biorient on the mitotic spindle it mediates a spindle checkpoint arrest and, second, it targets shugoshin and the chromosomal passenger complex to centromeres by phosphorylating histone H2A. Many AAA family domain ATPases are involved in the remodelling of protein complexes and perhaps the Abo1 ATPase could regulate the formation of the multitude of checkpoint complexes during a mitotic arrest. Or, as Abo1 orthologues and the FACT complex function in chromatin remodelling processes, they could perhaps facilitate histone modifications by creating access to centromeric nucleosomes or presenting histone H2A to the Bub1 kinase.

Cells that undergo microtubule perturbation delay metaphase in a checkpoint-dependent manner and recover by silencing the spindle checkpoint when correct chromosome biorientation has taken place. First, to investigate whether the loss of Abo1, Tfg3 or Pob3 affects viability when microtubules are destabilised, cells were exposed to the microtubule

poison benomyl in a plate assay (§2.1.8). This experiment indicates that *abo1Δ*, *pob3Δ* or *tfg3Δ* cells are not overly sensitive to microtubule disruption, which kills spindle checkpoint-deficient cells such as those lacking Mph1, Bub1 or Bub3 (Figure 37). Second, microtubules were disrupted by seeding and incubating cells bearing the cold-sensitive *nda3-km311* β-tubulin allele on cold plates for 10 hours at 18°C after which microtubule formation and cell recovery was stimulated at 32°C (§2.1.10). Taking into account the slight cold-sensitivity of the *pob3Δ* and *abo1Δ* mutant, TAPAS mutants were able to recover from microtubule injury and silence the spindle checkpoint effectively once the spindle had reformed (Figure 38). Third, the spindle checkpoint response in a population of *nda3-KM311* cells at 18°C was scored by determining the percentage of cells with Cdc13-GFP foci representing cyclin B accumulation at the spindle pole bodies during a mitotic arrest. TAPAS mutants were able to properly arrest in metaphase as Cdc13 enriches at the spindle pole body during prometaphase in a proportion of cells similar to that of a wild-type population (Figure 39).

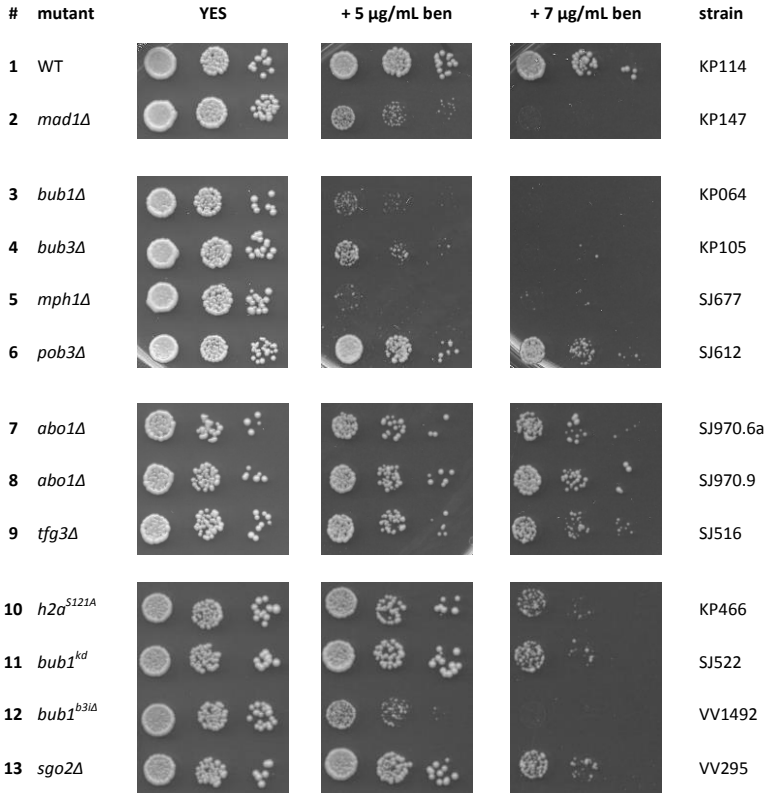

Figure 37: The microtubule poison benomyl depolymerises microtubules and prevents formation of the mitotic spindle. Cells lacking Abo1, Tfg3 or Pob3 resist exposure to benomyl in concentrations that kill *mad1Δ*, *bub1Δ*, *bub3Δ* and *mph1Δ* spindle checkpoint mutant cells. Cells with un-phosphorylatable Bub1 kinase substrate histone $H2A^{S121A}$ share a similar sensitivity to the drug as a Bub1 kinase dead ($bub1^{kd}$) mutant or a *sgo2Δ* mutant. Note that the benomyl sensitivity of *bub3Δ* cells is similar to that of a Bub1 mutant lacking the B3i motif ($bub1^{b3iΔ}$).

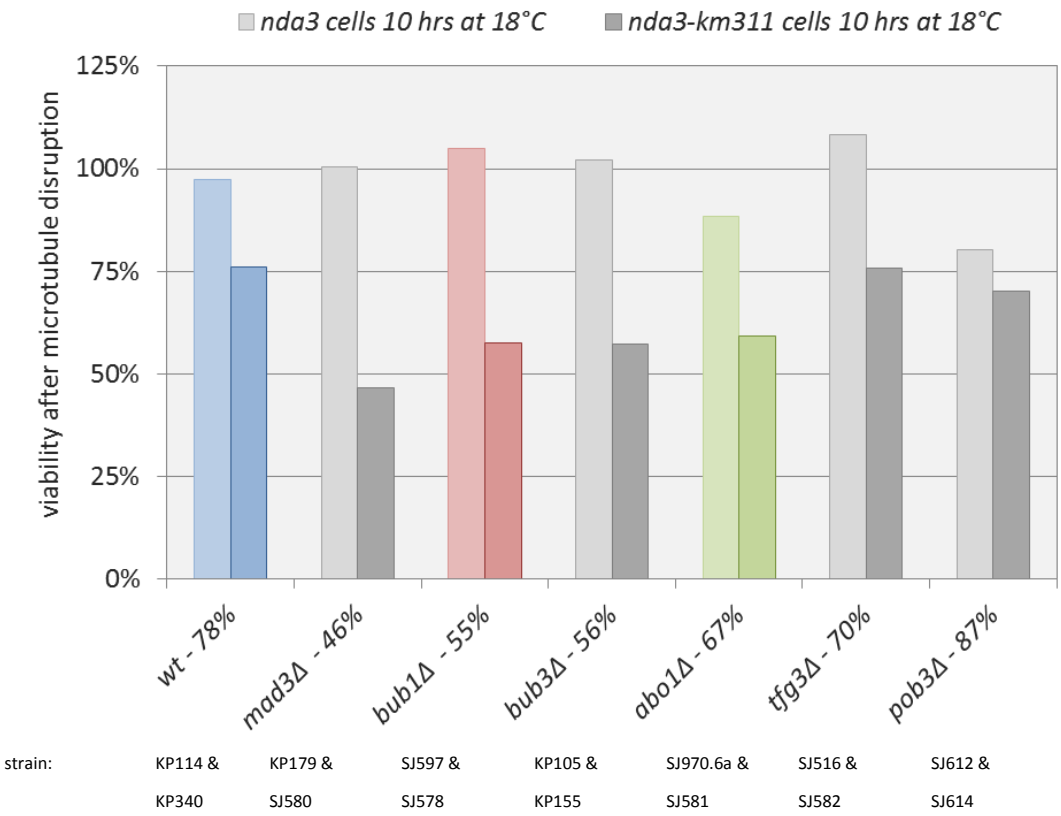

Figure 38: Viability of wild-type and mutant cells after microtubule disruption. BUB+ and TAPAS mutants in a wild-type *nda3* and a *nda3-km311* mutant background were plated and incubated at either the permissive or restrictive temperature (32°C and 18°C respectively). Plates kept at 18°C were moved to 32°C after 10 hours and cell viability was determined by comparing the number of colonies formed on 'cold' plates to those on 'warm' plates after 4 days. *abo1Δ* and *pob3Δ* cells were found to be slightly cold-sensitive as respectively 88% and 80% of cells recovered compared to 97% for wild-type cells. The percentage viability corrected for the perceived cold-sensitivity in a wild-type *nda3* background is given in the label. For each strain, a minimum of 1000 cells were plated over 3 plates (§2.1.10).

Together, these experiments indicate that unlike cells lacking Bub1 or Bub3, cells deficient in Abo1, Pob3 and Tfg3 are not sensitive to microtubule disruption and properly delay anaphase in a spindle checkpoint-dependent manner. Thus the TAPAS complex does not function in the spindle checkpoint mechanism.

a.

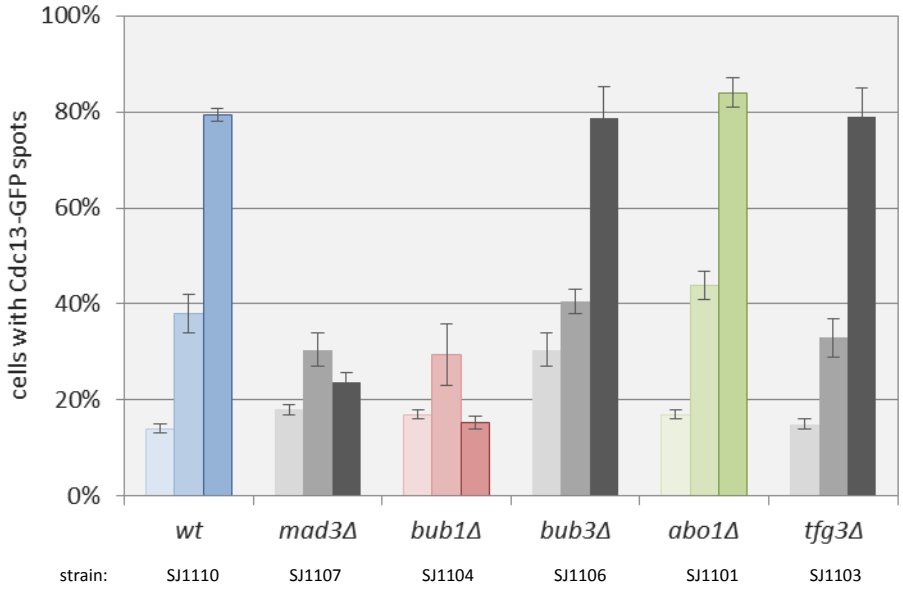

b.

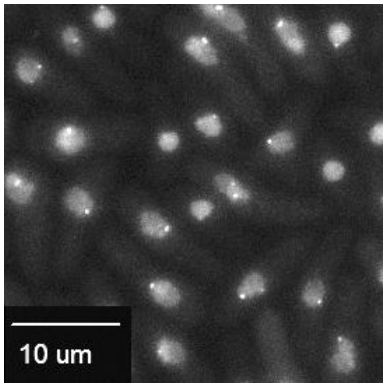

strain SJ1110

Figure 39: (a) Wild-type or mutant cells with Cdc13-GFP spots as a proportion of the total population in a *nda3-km311* cold-labile microtubule background at 0, 4 and 8 hours after incubation at 18°C. Error bars indicate the relative standard error of two independent experiments. **(b)** Picture of wild-type *S.pombe* cells with diffuse nuclear Cdc13-GFP and spindle pole body accumulation of Cdc13-GFP during metaphase observed as a bright spot by fluorescent microscopy.

Next, to see whether Abo1 is required for the Bub1 kinase to phosphorylate centromeric histone H2A and contribute to establishing biorientation in a Bub1-dependent manner, mitotic Sgo2 enrichment was scored in Bub1 kinase dead (*bub1*^{kd}), *abo1Δ and tfg3Δ* cells. To achieve a spindle checkpoint-mediated metaphase arrest, a mid-log phase culture of *nda3-km311 sgo2-cherry* cells was shifted to 18°C for 8 hours, after which the cell population was scored for their ability to form Sgo2 foci. In wild-type cells, mitotic Sgo2-cherry foci was observed by fluorescence microscopy (Figure 40a). In contrast to *bub1*^{kd} cells, which are unable to load Sgo2 at centromeres, Sgo2 targeting was not affected in *tfg3Δ* and *abo1Δ* cells as the

proportion of cells with Sgo2 foci was similar to that of wild-type cells (Figure 40b). These observations suggest that Sgo2 loading onto phosphorylated nucleosomal histone H2A does not depend on the TAPAS chromatin remodeller.

a.

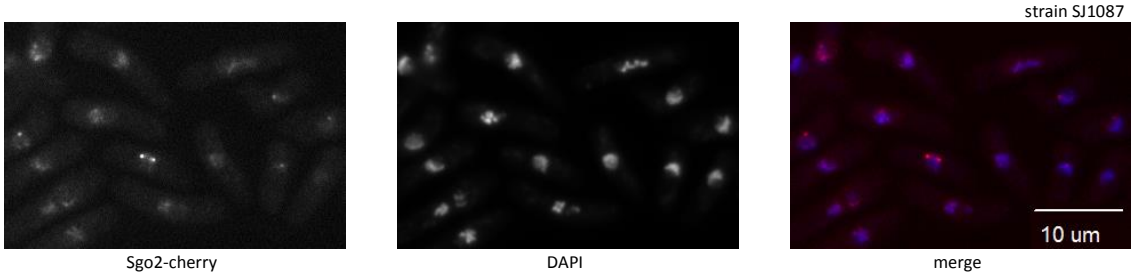

b.

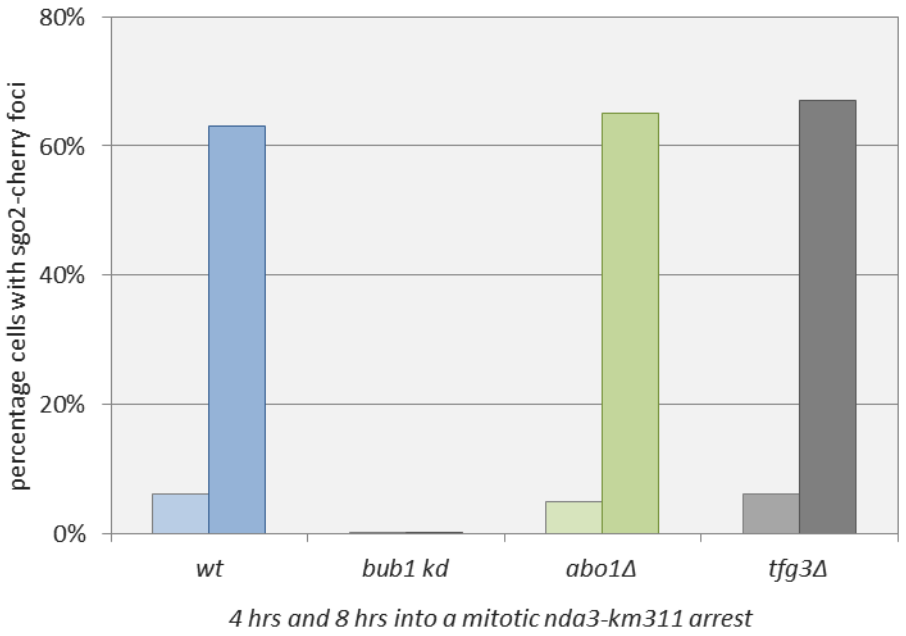

Figure 40: (a) Sgo2-cherry accumulates at centromeres during mitosis and can be observed with fluorescence microscopy as bright foci. **(b)** Bub1 kinase-dependent Sgo2 loading during a mitotic *nda3-km311* arrest did not depend on Abo1 or Tfg3 function. Cells were scored for the presence of Sgo2 foci 4 and 8 hours into a mitotic arrest at 18°C induced by depolymerising cold-sensitive spindle microtubules using the *nda3-km311* allele. A minimum of 250 cells were analysed. Strains used: SJ1087, SJ576, SJ851, SJ574.

To assess the ability of mutant cells to segregate their chromosomes in correct fashion, yeast strains were created by the addition of a linear short chromosome (termed 'ch16') containing the *ade6-216* mutant allele that complements the *ade6-210* allele on chromosome 3 (§2.1.12). This allowed cells to grow on medium lacking adenine, forming completely white colonies, and facilitates assessing ch16 loss during one cell division on adenine supplemented medium by

counting the number of half-sectored colonies (see example of a half-sector colony in Figure 41a). The percentage of chromosome loss for wild-type cells is zero, whereas that for *pob3Δ* and *abo1Δ* cells was shown to be respectively 0.26 and 0.72%, compared to around 7.5% for the *tfg3Δ* and *mph1Δ* mutants (Figure 41c).

a.

b.

#	strain	half-sectored	white	% loss
1	wild-type	0	1624	0
2	*bub1Δ*	51	1374	3.7
3	*mph1Δ*	78	991	7.9
4	*abo1Δ*	11	1433	0.8
5	*tfg3Δ*	87	1085	8.0
6	*pob3Δ*	2	1272	0.2

c.

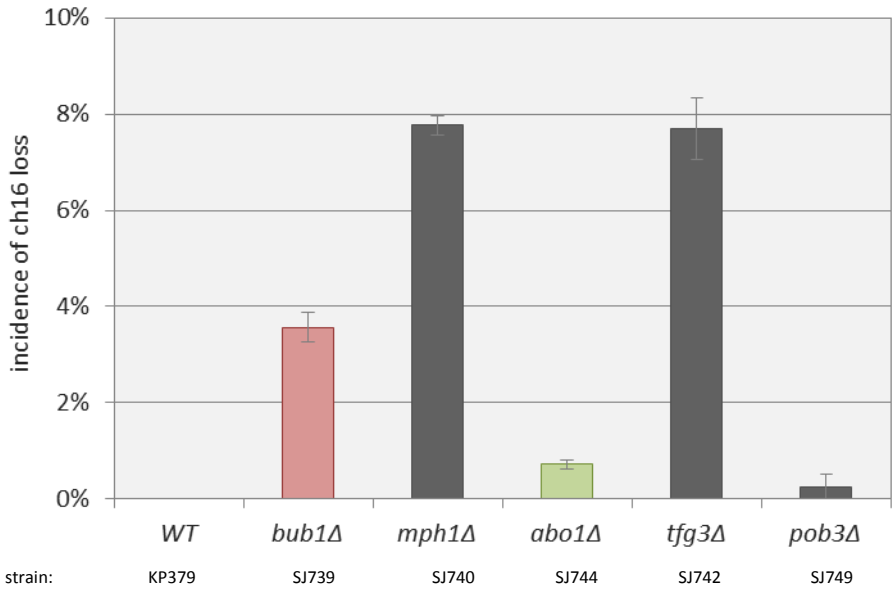

Figure 41: (a) Top: example of a half-sectored colony (i.e. half white, half red) as a result of mini-chromosome ch16 loss in the first cell division after plating of single cells. Bottom: a completely white colony indicating successful transmission of ch16. **(b)** Results from a single chromosome missegregation assay. Mini-chromosome loss was scored in the half-sectoring assay by counting the number of half-sectored and completely white colonies. The percentage of ch16 loss for wild-type cells and each mutant was calculated. Note that no half-sectored colonies were encountered from wild-type cell populations. **(c)** Results from two independent chromosome missegregation assays represented by bar graph. Error bars indicate the relative standard error of these two experiments.

The loss rates for *pob3Δ* and *mph1Δ* cells have been noted in other studies and are thought to be a result of a partial loss of centromeric heterochromatin in the former and the inability to promote chromosome biorientation and delay anaphase in the latter mutant (Lejeune *et al.*

2007, Zich *et al.* 2012, Meyer *et al.* 2013). The rate of chromosome loss for *abo1Δ* was shown to be much lower than that of *bub1Δ* cells but similar to that of *pob3Δ* cells. This could perhaps indicate that the Abo1 ATPase facilitates the nucleosome remodelling activities of the FACT complex at the centromeres and the loading of heterochromatin protein Swi6. Surprisingly, the loss rate for cells lacking Tfg3 was much higher than those lacking Bub1, Abo1 or Pob3 and the error rate for the mitotic transmission of the mini-chromosome was similar to that of *mph1Δ* cells that are checkpoint-deficient and were unable to correct erroneous microtubule attachments to kinetochores. Mutations in *tfg3* and orthologous genes lead to complex pleiotropic phenotypes, one of which is genomic instability in *S.cerevisiae* and their gene products interact with a multitude of chromatin remodelling and transcription factor complexes (see §5.2). The high rate of chromosome loss in this assay could thus be the result of the loss of multiple Tfg3 functions, but does not relate to its loss of interaction with the BUB+ complex as Bub1 no longer did interact with Tfg3 in cells that lack Abo1 (refer to Figure 32), which experienced a much lower chromosome loss rate.

5.3.6 Bub1 and TAPAS mutants are sensitive to genotoxic stress

As discussed in section 5.2, *S.cerevisiae* cells deleted for the *abo1* orthologue *YTA7* or the *tfg3* orthologue *TAF14* were sensitive to a variety of environmental stresses. More often than not, the exact causes remain unexplained. Anecdotal and published data (see §5.4) prompted a more thorough exploration of shared BUB and TAPAS mutant phenotypes by assaying exposure to several stress factors, including toxic and osmotic stress. Plates with YES medium containing high salt (0.9 M KCl), a heavy metal (0.05 and 0.1 mM cadmium sulphate) or genotoxic agents (8.0 mM hydroxyurea, 10 µg/mL camptothecin, 0.01% and 0.02% methyl methanesulfonate, 2 and 5 µg/mL bleomycin or zeocin) were prepared and serial dilutions of wild-type and mutant cells were transferred onto the plates' surface using a pin replicator tool (§2.1.8). To monitor the efficacy of genotoxic compounds in the next experiments a set of mutant strains was used that are listed in the following table.

#	mutant	description	strain	reference
1	*arp8Δ*	subunit of the INO80 chromatin-remodelling complex involved in DNA damage repair	SJ673	(Hogan *et al.* 2010)
2	*cds1Δ*	DNA replication checkpoint kinase	SJ790	(Rhind & Russell 2000)
3	*chk1Δ*	DNA damage checkpoint kinase	SJ730	(Rhind & Russell 2000)
4	*rad3Δ*	DNA damage checkpoint ATR kinase	SJ678	(Langerak & Russell 2011)
5	*rad22Δ*	*S.cerevisiae* and metazoan Rad52 homologue, involved in repair of DNA damage	SJ881	(Kim *et al.* 2000)
6	*rhp54Δ*	*S.cerevisiae* and metazoan Rad54 homologue, double-strand break repair via homologous recombination	SJ882	(Catlett & Forsburg 2003)

Table 35: *S.pombe* control mutant strains, which inadequately respond to DNA damage, used in viability assays.

Unlike the TAPAS null mutants (*tfg3Δ*, *abo1Δ* and *pob3Δ*), *bub1*Δ and *bub3*Δ cells were not sensitive to osmotic stress (Figure 42). Cells lacking Abo1, Tfg3 and Pob3 were found to be sensitive to the presence of heavy metal Cd^{2+} and a slight sensitivity was observed for *bub1Δ*, but not the *bub3Δ* mutant (Figure 43). Compared to wild-type, *mad2Δ*, *mad3Δ* and perhaps *mad1Δ* and *bub3Δ* cells, *bub1Δ* and TAPAS null mutants were unable to resist the 'radiomimetic' compounds bleomycin and zeocin that induce DNA double strand breaks and viability was clearly reduced (Figure 44).

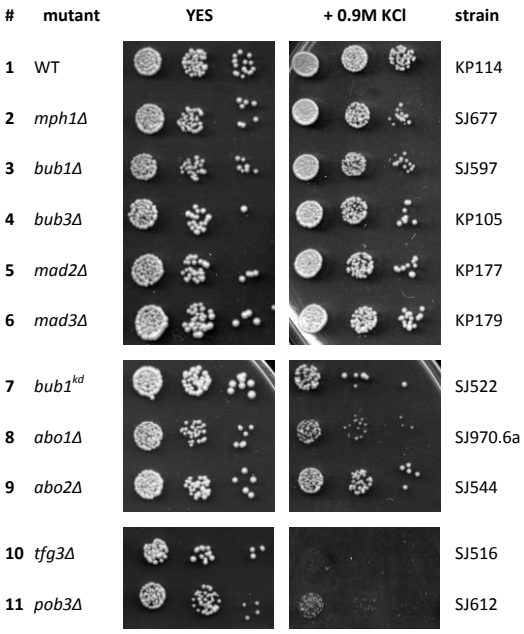

Figure 42: Sensitivity of spindle checkpoint and TAPAS mutants to osmotic stress. Yeast were compared for growth on YES media supplemented with 0.9M KCl after 3 days at 30°C. Whereas *tfg3Δ* and *pob3Δ* cells were unable to tolerate a high salt concentration, the *abo1Δ* mutant was moderately sensitive and the *mad*, *bub* and *mph1Δ* mutants were able to resist osmotic stress as well as wild-type cells.

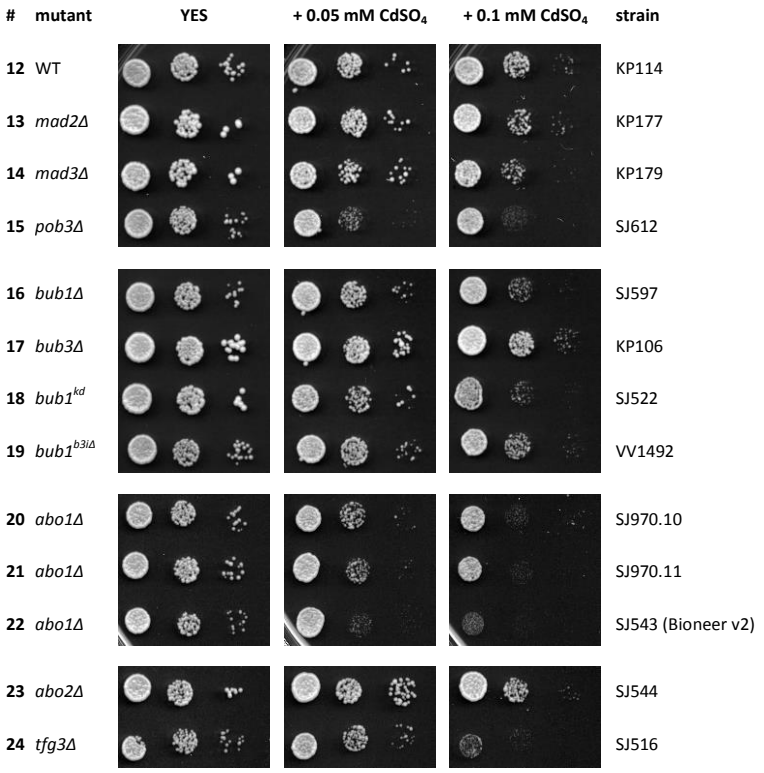

Figure 43: Sensitivity of spindle checkpoint and TAPAS mutants to the heavy metal Cd^{2+}, which is toxic to many living organisms. Yeast were compared for growth on YES media supplemented with 0.05 or 0.1 mM $CdSO_4$ after 5 days at 25°C. *bub1Δ* (but not *bub3Δ*, *mad2Δ* or *mad3Δ*) cells were slightly sensitive to Cd^{2+} and growth of *abo1Δ* and *pob3Δ* cells was clearly weak. *tfg3Δ* cells were least able to resist the presence of the heavy metal ion.

Genotoxic sensitivity was also apparent when TAPAS null mutants, *bub1Δ* and also *bub3Δ* were exposed to the DNA alkylating agent methyl methanesulfonate (MMS; Figure 45). Compared to *chk1Δ* and *rad3Δ* cells, viability of *bub1Δ* and *mph1Δ* was lower in the presence of DNA double strand breaks, but higher when genomic DNA undergoes alkylation. The Rad3 ATR kinase was required for cell cycle arrest in the response to blocked DNA replication or DNA damage and has also been shown to facilitate double strand break repair by homologous recombination (Jimenez *et al.* 1992, Prudden *et al.* 2003).

Not all of the *bub1Δ* and TAPAS mutant phenotypes in regard to genotoxicity overlap. Unlike *abo1Δ* and *tfg3Δ* cells, the *bub1Δ* and *bub3Δ* mutants were slightly sensitive to the DNA replication inhibitor hydroxyurea, and the topoisomerase inhibitor camptothecin rapidly kills *abo1Δ* cells, but not *bub1Δ* and *bub3Δ* cells. Compared to *chk1Δ* and *rad3Δ* cells, viability of *bub1Δ* and *mph1Δ* was lower in the presence of DNA double strand breaks, but higher when genomic DNA undergoes alkylation. *abo1Δ* cells also died faster on bleomycin and zeocin than *chk1Δ* or *rad3Δ.*

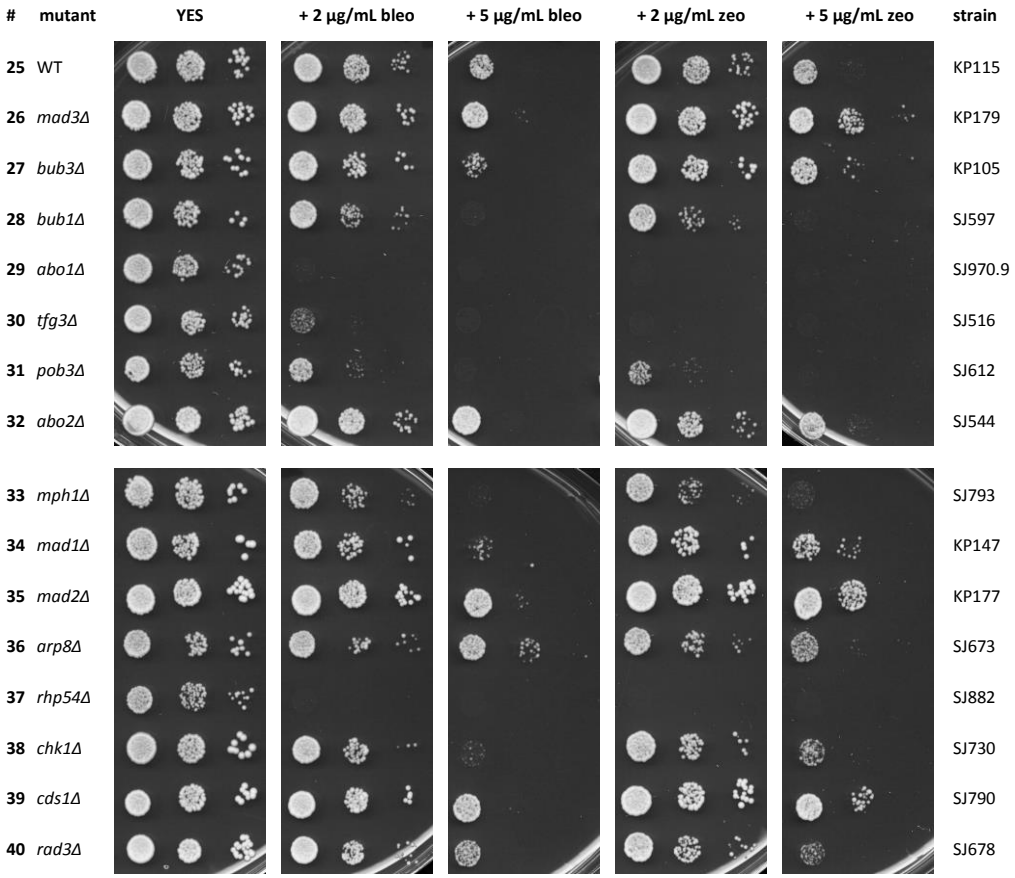

Figure 44: Sensitivity of spindle checkpoint and TAPAS mutants to the so-called 'radiation mimetics' bleomycin (bleo) and zeocin (zeo), chemical compounds that induce DNA double strand breaks. Cells were compared for growth on YES media supplemented with 2 or 5 µg/mL bleomycin or zeocin after 3 days at 30°C. *abo1Δ*, *tfg3Δ*, *pob3Δ*, *bub1Δ* and also *mph1Δ* cells were all sensitive to the presence of bleomycin and zeocin. Cells that lack Abo1 or Tfg3 were most sensitive and growth of *bub1Δ* and *mph1Δ* cells was clearly affected at concentrations of 5 µg/mL compared to wild-type, *chk1Δ* and *rad3Δ* cells. Note that for this assay zeocin is a good substitute for the more costly bleomycin compound.

Thus the sensitivity of the *bub1Δ* mutant to genotoxic agents is not of a broad spectrum, but mainly so to MMS and the radiation mimetic drugs, whereas Abo1 might function in a wider response to DNA damage and environmental stress. Therefore, the focus was on assaying the response to DNA damage, and the way in which the TAPAS – BUB+ complex might resist or respond to DNA lesions arising from exposure to MMS and 'radiomimetic' compounds. In the following assays, zeocin rather than bleomycin was used as it has a very similar activity as bleomycin (refer to Figure 44) and is more cost-effective in scaled-up experiments.

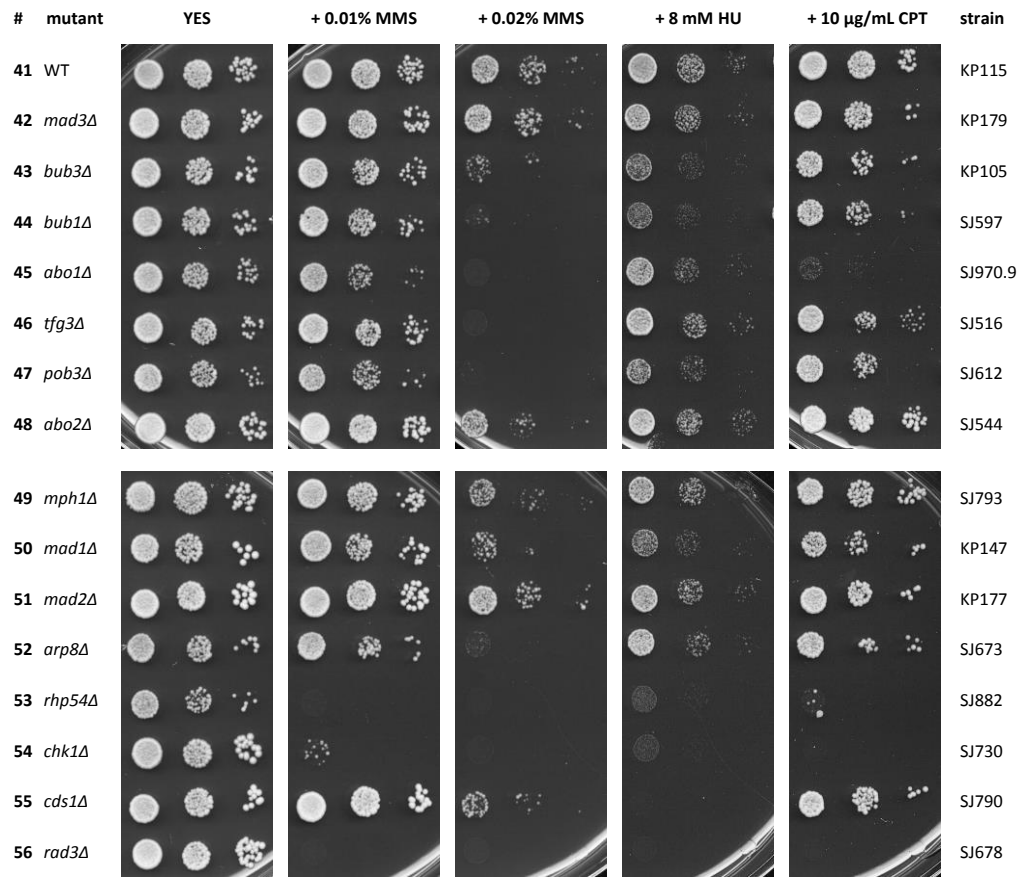

Figure 45: Mutant yeast screened by plate assay at 30°C for 3 days against a variety of genotoxic compounds. *bub3Δ*, *bub1Δ*, *abo1Δ*, *tfg3Δ* and *pob3Δ* cells were sensitive to the DNA alkylating agent methyl methanesulfonate (MMS). Cells lacking Tfg3 or Pob3 were also sensitive to the topoisomerase inhibitor camptothecin (CPT), but not to such an extreme extent as cells that lack Abo1. Note that *bub1Δ* and *bub3Δ* mutant cells were moderately sensitive to high concentrations of the DNA replication inhibitor hydroxyurea (HU).

To investigate the DNA damage response to the transient presence of genotoxic agents, rather than chronic exposure in the plate assays above, mutant cell viability was measured by employing plate recovery assays (§2.1.9). Cells were treated with hydroxyurea, MMS or zeocin for up to 5 hours in small cultures after which the compounds were washed out and cells allowed to recover on solid rich medium. The viability was scored as the number of single cells able to form colonies within 4 days at 32°C. In addition, cells were exposed to ionising radiation in the form of γ-rays sourced by the radioisotope caesium-137 (§2.1.11), which induces both single and double strand breaks in DNA, and UV-C light of 254 nm, which results in a wide variety of DNA lesions, such as inter and intra-strand crosslinks and interferes with DNA replication and transcription processes.

Treating cells with hydroxyurea leads to blocking of DNA replication by inhibition of the ribonucleotide reductase complex and subsequent triggering of the DNA replication

checkpoint when the nucleotide availability has declined. BUB+ and TAPAS mutant cells were found to tolerate a relatively high concentration of 20 mM hydroxyurea for 3 hrs (Figure 46) suggesting that these cells were able to sense DNA replication stress, invoke the replication checkpoint and successfully stall and restart replication forks. Thus the BUB+ and TAPAS components are unlikely to have a role in monitoring DNA replication progression and the replication checkpoint.

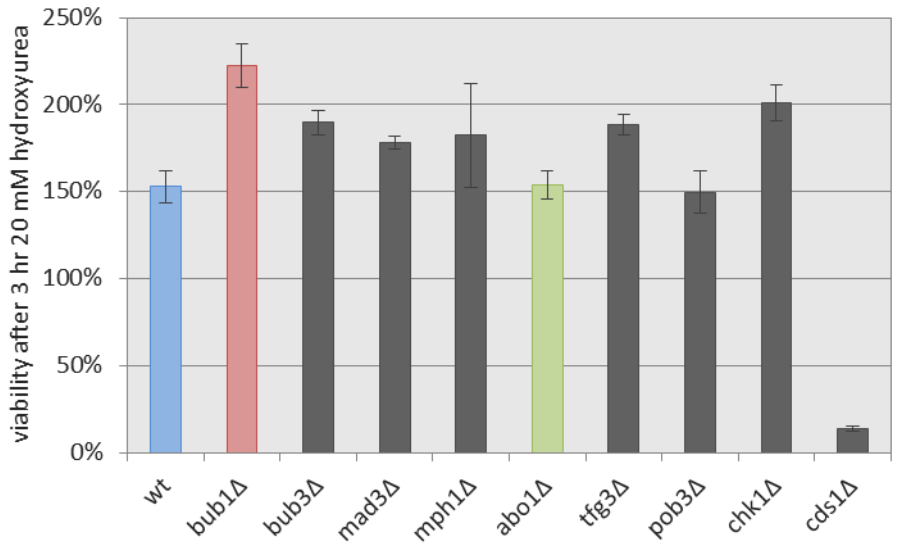

Figure 46: Viability of wild-type and mutant strains exposed to 20 mM hydroxyurea for 3 hours compared to unexposed cells at t=0. Unlike cells that lack the DNA replication checkpoint effector Cds1, the transient presence of hydroxyurea is not toxic to cells deficient in BUB+ or TAPAS components. Error bars indicate the relative standard error of two independent experiments in which a minimum of 1000 cells were plated over three plates per experiment.

As can be seen in Figure 47, *abo1Δ* mutant cells were hypersensitive to zeocin and thus struggle to cope with the formation of DNA double-strand breaks that in *S.pombe* are usually repaired by homologous recombination (refer to §1.5.3). In addition, DNA alkylation by MMS, which disrupts DNA replication and is mostly repaired by the base excision repair mechanism (§1.5.3) leads to a drop in viability compared to wild-type cells (Figure 48). In addition, *abo1Δ* mutant cells were shown to lose viability when exposed to UV light (Figure 49) or γ-rays (Figure 50), indicating that Abo1 is involved in DNA damage response to at least two different types of DNA lesions and perhaps functions in a mechanism of DNA damage repair or tolerance that covers a more general or upstream event in damage signalling. Its interactors Pob3 and Tfg3 were found to be mostly sensitive to UV and to a lesser extent zeocin, but not to MMS. However, *pob3Δ* cells did lose viability when exposed to γ-rays, whereas *tfg3Δ* cells were able to resist.

Cells that lack Bub1 were somewhat sensitive to UV, but the transient treatment with MMS and zeocin did not have the adverse effect which could have been expected from the phenotype observed in the plate assays above: *bub1Δ* was not hypersensitive to zeocin, MMS or γ-ray exposure. In these transient exposure assays, *bub3Δ* cells were shown to tolerate zeocin, UV and γ-rays, but just as in the plate assay they were mildly sensitive to the genotoxic effects of MMS. The viability of *mph1Δ* mutant cells was not negatively affected by temporary exposure to genotoxic conditions.

Taken together, the response of Bub1 and TAPAS mutants to genotoxic insults is varied and difficult to reconcile. This suggests that Bub1 and TAPAS function in a complex network of redundant or partially redundant pathways to resist genotoxic insults. In regards to the presence of DNA double strand breaks, viability of *bub1Δ* cells is lower than *rad3Δ* or *chk1Δ* cells during transient, but not chronic exposure to zeocin. Generally speaking, the *bub1Δ* phenotypes described are more penetrant in zeocin and MMS plate assays. This perhaps indicates that the continual presence of DNA damaging agents has an adverse effect on viability. Or, as a mid-log phase *S.pombe* culture comprises approximately 70% cells in G2, genotoxic drugs are most harmful to *bub1Δ* cells that are in S or M phase.

a.

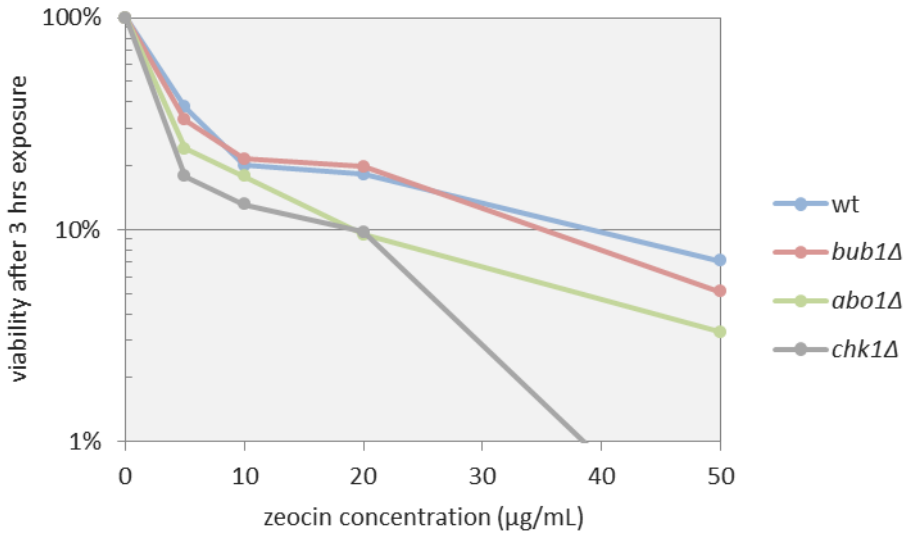

b.

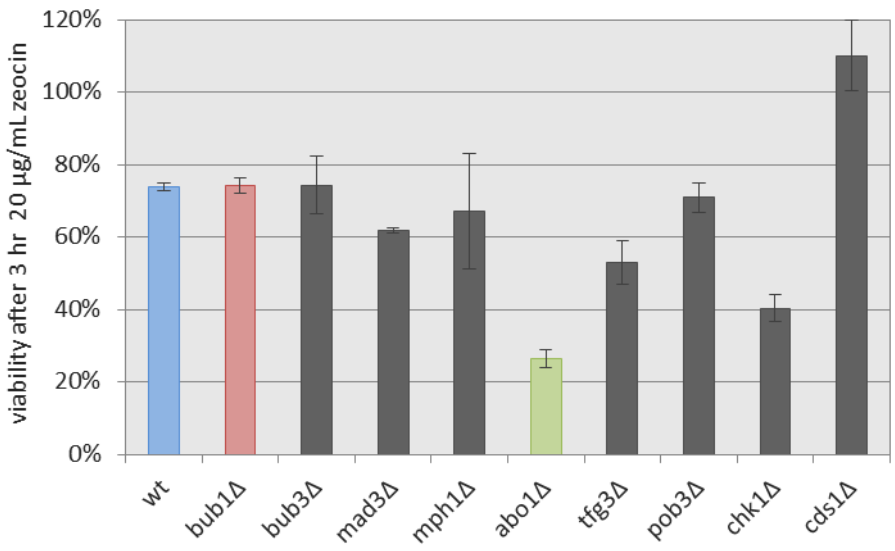

Figure 47: (a) Viability of wild-type and mutant strains exposed for 3 hours to increasing concentrations of zeocin, relative to unexposed cells at t = 3 hours. **(b)** Survival rate of indicated wild-type and mutant strains exposed to 20 µg/mL zeocin compared to unexposed cells at t = 0. Error bars indicate the relative standard error of two independent experiments in which a minimum of 1000 cells were plated over three plates per experiment.

a.

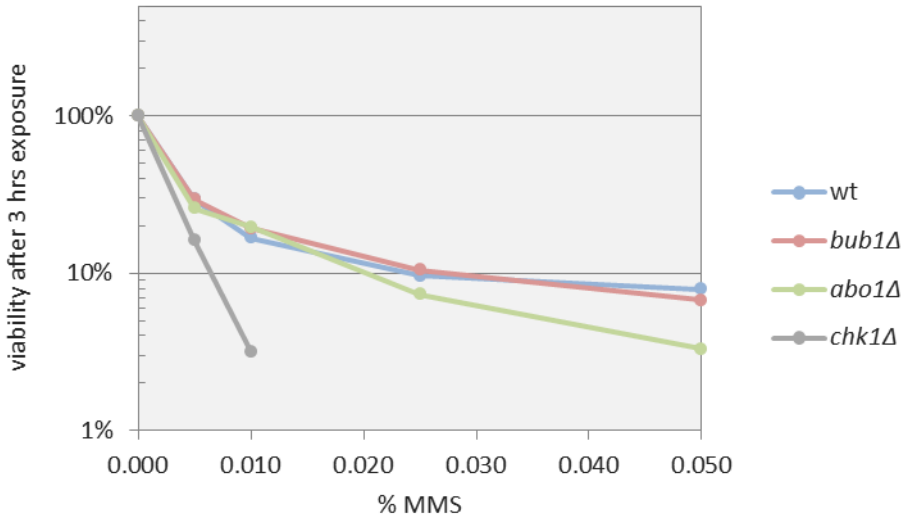

b.

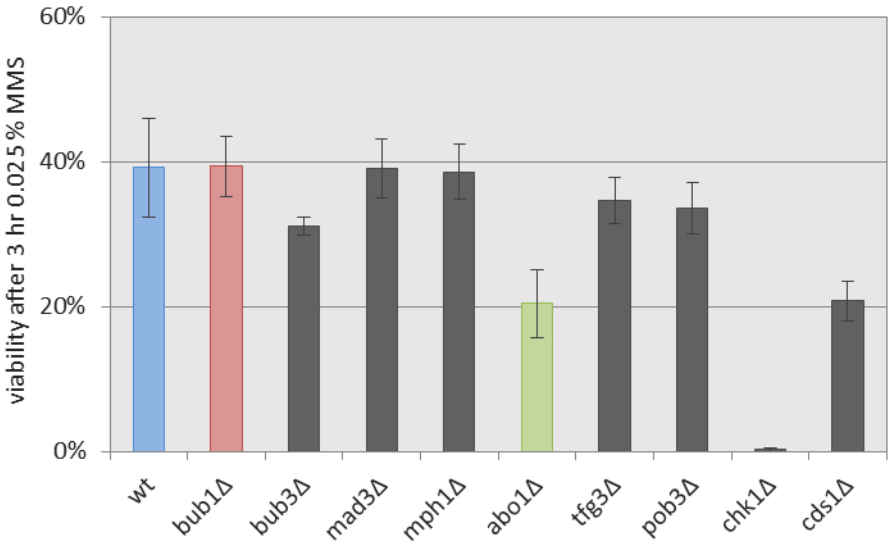

Figure 48: (a) Viability of wild-type and mutants strain exposed for 3 hours to increasing concentrations of MMS, relative to unexposed cells at t = 3 hours. **(b)** Survival rate of indicated wild-type and mutant strains exposed to 0.025% MMS compared to unexposed cells at t = 0. Error bars indicate the relative standard error of two independent experiments in which a minimum of 1000 cells were plated over three plates per experiment.

a.

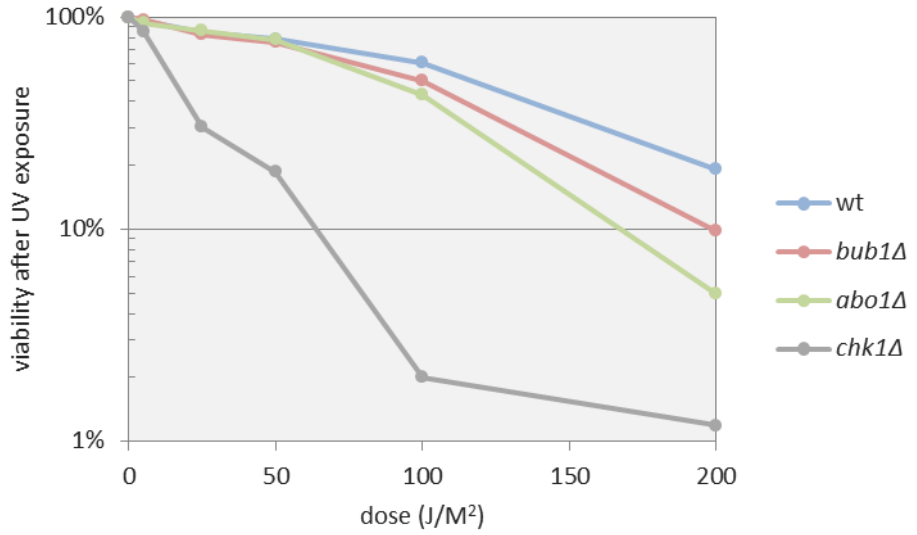

b.

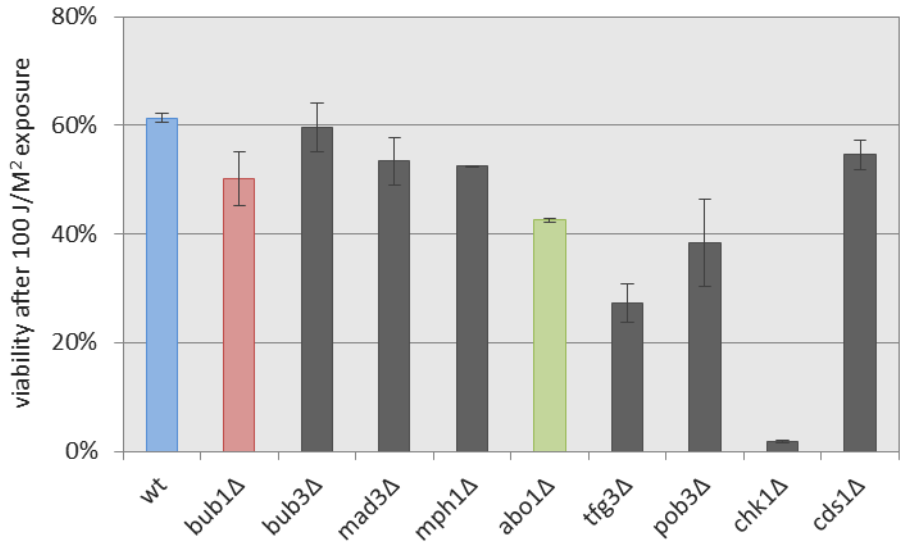

Figure 49: (a) Viability of mutant strains exposed to 254 nm UV light at the indicated dose. **(b)** Survival rate of wild-type and mutant strains exposed to UV light at 100 J/M^2 compared to unexposed cells. Error bars indicate the relative standard error of two independent experiments in which a minimum of 1000 cells were plated over three plates per experiment.

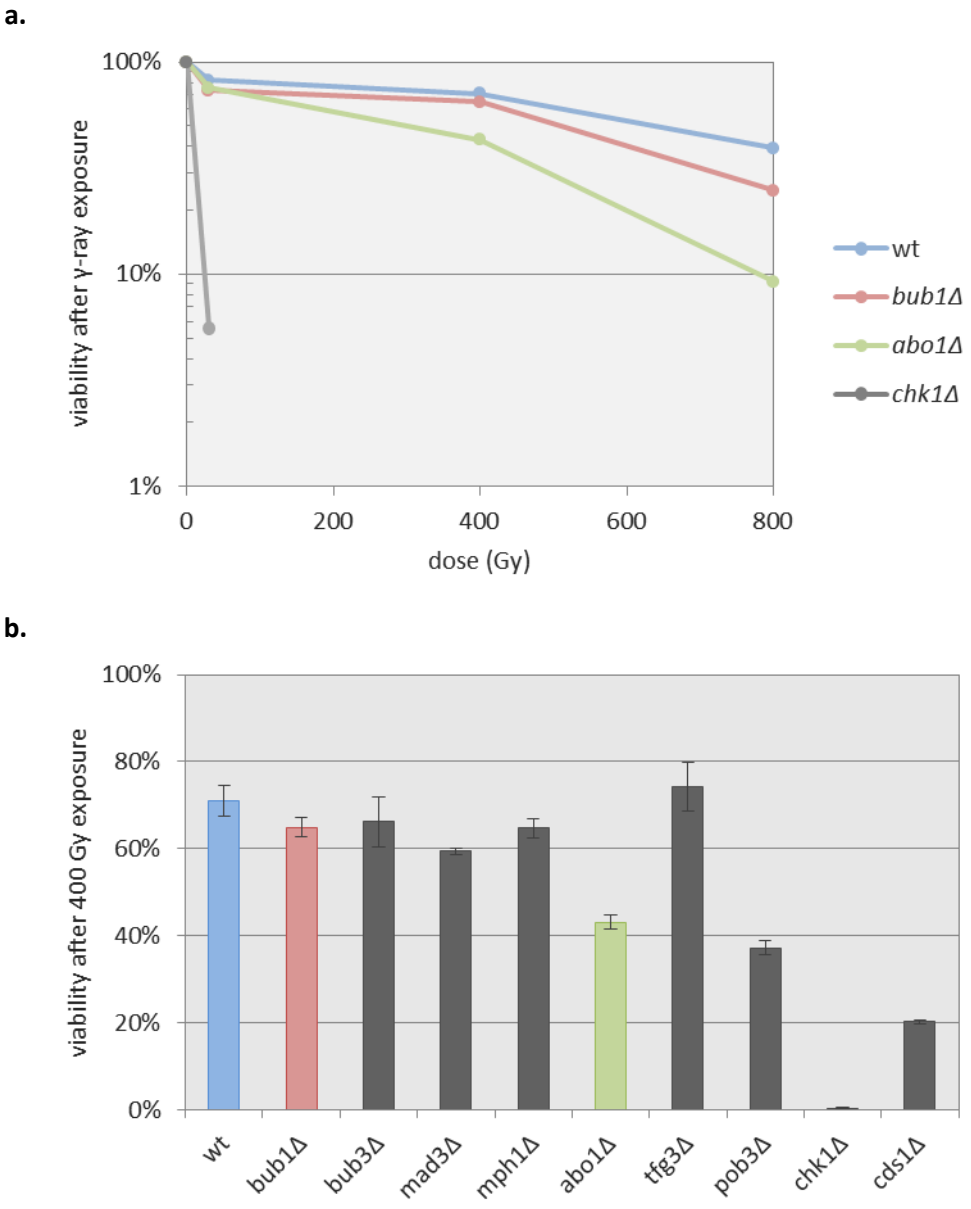

Figure 50: (a) Viability of mutant strains after exposure to γ-rays at the indicated dose. **(b)** Survival rate of wild-type and mutant strains exposed to a radiation dose of 400 Gy compared to unexposed cells. Error bars indicate the relative standard error of two independent experiments in which a minimum of 1000 cells were plated over three plates per experiment.

5.3.7 Assaying the DNA damage response of BUB and TAPAS mutants

Next, in an attempt to understand the mechanisms that underlie the sensitivity to DNA damaging agents, wild-type, *bub1Δ*, *abo1Δ* and *tfg3Δ* cells were incubated with 0.01% MMS or 5 µg/mL zeocin and the formation of so-called repair foci was followed by counting cells with bright Rad22-GFP dots (Figure 51b and c). Rad22 is the *S.pombe* orthologue of *S.cerevisiae* and metazoan Rad52, and is for instance essential for the repair of double strand breaks by homologous recombination. Repair foci are discrete assemblies of proteins that accumulate at the site of DNA lesions and facilitate DNA damage signalling and repair. In the absence of genotoxic compounds, a single Rad22-GFP nuclear dot was observed in about 10% of cells from a mid-log phase culture that has been suggested to correspond to sites of post-replicative repair (Meister *et al.* 2005). In wild-type and all mutant strains analysed, the percentage of cells with Rad22-GFP foci was around 25% within 3 hours and 70% after 7 hours of incubation with the genotoxic compounds. After the drugs were washed out, multiple Rad22 foci were still observed in at least 20-25% of proliferating wild-type and mutant cells some 16 hours after exposure, indicating that daughter cells can inherit Rad22 containing repair assemblies or that traces of genotoxic compounds are still present in the growth medium. These findings suggest that Abo1 and Bub1 are not required for the detection of DNA lesions and the molecular processes leading to the gathering of Rad22 at sites of damage.

Although the dynamics of Rad22-GFP foci proved difficult to follow and quantitate, these experiments did show that *bub1Δ*, *abo1Δ* and *tfg3Δ* mutant cells were able to detect DNA lesions and respond by accumulating repair and signalling proteins at the site of damage. Examining *bub1Δ* and *abo1Δ* cell morphology by light microscope after 10 hour exposures with 0.01% MMS or 5 µg/mL zeocin did suggest that cells were able to robustly arrest in response to DNA damage, as they exhibited typical elongated cells with single nuclei, indicative of prolonged G2 arrests (Figure 51a). This indicates that Abo1 and Bub1 are not essential in monitoring DNA damage or eliciting a DNA damage checkpoint arrest.

Next, to investigate whether Bub1 assembles together with Rad22 at sites of damaged DNA, a *bub1-rfp rad22-gfp* strain was treated with either 0.005% MMS or 5 µg/mL zeocin. During incubation with MMS, Bub1-RFP appeared in small speckles throughout the nucleus (Figure 51c) and was rarely found to localise together with Rad22-GFP spots, whereas during zeocin treatment its appearance was diffuse, with a few cells (less than 2%) containing a single bright dot (Figure 51b) that, in a large number of cells analysed, was never observed to coincide with Rad22-GFP foci. Presumably, the Bub1-RFP foci seen in a small number of cells are a result of

improper kinetochore microtubule attachment in mitotic cells, whereas Rad22-GFP localises to the site of a DNA double-strand break.

Taken together, the absence of Bub1 from Rad22-positive repair foci during DNA damage suggest that a Bub1 function in response to DNA damage takes place away from sites of damage, that Bub1 attends these sites very briefly, that Bub1 needs to be displaced from these sites, or at least that Bub1 cannot be observed by current means at Rad22 repair assemblies as perhaps few molecules are required. The presence of Abo1 at DNA lesions remains to be investigated.

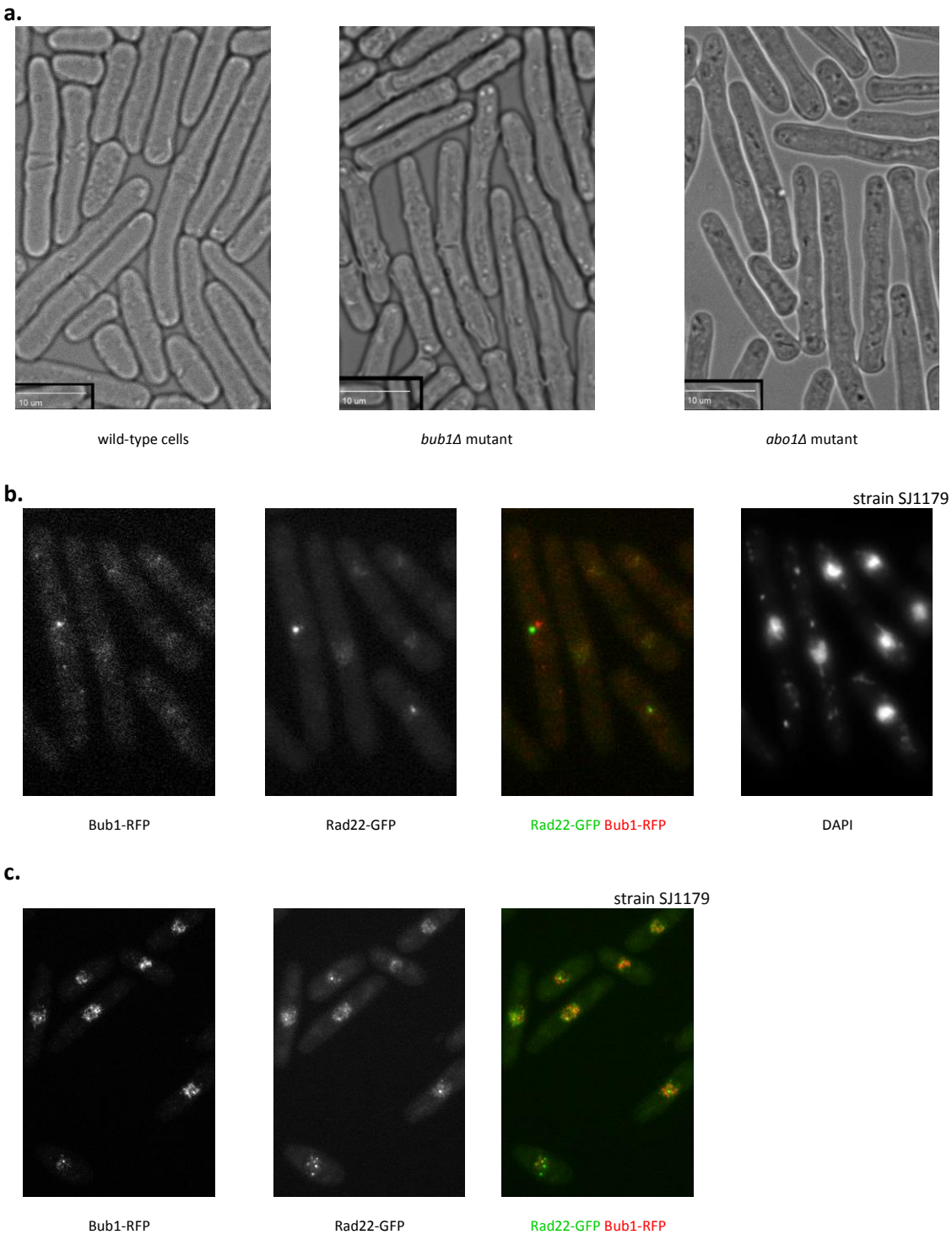

Figure 51: (a) *S.pombe* cell growth during a S - G2 DNA damage checkpoint arrest results in an elongated cell morphology. Cells were exposed to 0.005% MMS for 10 hours and visualised by phase-contrast microscopy. Cells treated with 5 µg/mL zeocin for the same time are of similar appearance. **(b)** Bub1-RFP and Rad22-GFP foci observed in wild-type cell nuclei after exposure to zeocin for 7 hours do not localise together. **(c)** Granulated Bub1-RFP appearance in wild-type cells treated with 0.01% MMS for 4 hours. Very few Rad22-foci were observed to localise with a Bub1 'speckle'.

5.3.8 BUB+ and TAPAS genetic interactions

To learn more about the molecular mechanisms in which Bub1 and the TAPAS components resist DNA damage and to explore whether they function in the same or similar pathways, double mutants were created and viability was monitored by spotting serial diluted yeast onto plates containing varying amounts of zeocin or MMS (§2.1.8). Again, mutant strains deficient in certain aspects of the DNA damage response were used as controls (see Table 35).

Among the Mad and Bub spindle checkpoint components, and as seen in §5.3.6, *bub1Δ* cells stood out as being unable to resist concentrations of genotoxic compounds that did not kill the others (row 7 - 9 and 15 - 17 in Figure 52). Remarkably, the Bub1 'kinase dead' mutant *bub1*^{kd} had a similar sensitivity to both zeocin and MMS as a *bub1Δ* mutant (row 8, 9 and 12 in Figure 52). However, the viability of the *h2a*^{S121A} mutant was not affected (row 13) even though the Bub1 kinase is unable to phosphorylate histone H2A^{S121A} (H2A residue Ser121 being its canonical substrate). This suggests that the Bub1 kinase recognises an as yet unidentified different or additional substrate in the presence of damaged DNA. Note that *bub1*^{b3iΔ} (and *sgo2Δ*) mutant cells were somewhat sensitive to zeocin and MMS (row 11 and 14), but not to the same extent as *bub1Δ* and *bub1*^{kd}. This strongly suggests that the Bub1 and Abo1 response to DNA damage does not depend on their physical interaction, which was abolished in the *bub1*^{b3iΔ} mutant (see Figure 32).

The *bub1Δ* allele was tested in combination with other *mad* and *bub* null alleles on medium containing zeocin and MMS (row 19 - 26 in Figure 53). The sensitivity of all double mutants on MMS was similar to that of *bub1Δ*, which was in marked contrast to their response to zeocin: all three *mad* null mutants were shown to alleviate the sensitivity of the *bub1Δ* mutant. However, a *bub1Δ bub3Δ* double null mutant was found to have a similar sensitivity as the *bub1Δ* single mutant on both MMS and zeocin. Suppression of *bub1Δ* phenotypes by *mad* null mutants could for instance indicate that a Bub1-dependent pathway is now bypassed or no longer inhibited in the absence of the *mad* gene products.

To investigate whether the *bub1Δ* mutant dies on zeocin as a direct result of impaired response to DNA double strand breaks, a *spd1Δ* mutant allele was used. Spd1 is an inhibitor of ribonucleotide reductase (RNR; see also the final paragraphs of §1.5.5), which catalyses the synthesis of dNTPs required for DNA replication and repair (Moss *et al.* 2010, Nestoras *et al.* 2010). During repair of double strand breaks, introduced by for instance zeocin, DNA synthesis is required for single strand DNA gap filling and by deleting *spd1*, the pool of readily available

nucleotides greatly facilitates repair. In the case of *bub1Δ* and *bub1^{kd}*, the *spd1Δ* mutant significantly increased the cellular resistance to zeocin and somewhat improved growth of the *bub1^{b3iΔ}* mutant (row 28 - 33 in Figure 53). In contrast, MMS sensitivity of the *spd1Δ bub1Δ* double mutant was similar to that of the *bub1Δ* mutant, indicating that cell death of the *bub1Δ* mutant in the presence of MMS could not be rescued by increasing RNR activity to repair DNA lesions.

Next, a similar analysis was carried out for the TAPAS mutant strains *abo1Δ, tfg3Δ* and *pob3Δ*. First, these mutant alleles were combined with a *bub1*Δ mutant allele to see whether Bub1 and Abo1 function in the same pathway to resist DNA damage. As can be seen in rows 50 – 54 in Figure 54, the phenotype of these double mutants were more severe than for each single mutant on both MMS and zeocin. This suggests that Bub1 or the TAPAS components function in at least two separate, perhaps alternative pathways to resist DNA damage or that other unknown synthetic interactions underlie this phenotype. Maybe surprisingly and in contrast to the *bub1*Δ mutant, *spd1Δ* did not alleviate the reduced viability of the *abo1Δ* mutant in the presence of zeocin. Thus RNR-dependent production of nucleotides to promote synthesis-dependent DNA repair did alleviate the Bub1 deficiency, but not the Abo1 deficiency. This could indicate that in the *abo1Δ* mutant repair of DNA double strand breaks induced by zeocin is unable to progress to the stage requiring DNA synthesis. The Abo1 bromodomain ATPase could thus function in the initial stages of damage detection and repair.

Finally, viability of cells lacking the Abo1 ATPase bromodomain paralogue Abo2 was not compromised in the presence of genotoxic compounds such as bleomycin, zeocin (row 32 in Figure 44 on page 156), MMS, hydroxyurea and camptothecin (row 48 in Figure 45 on page 157). However, combining the *abo2Δ* allele with *bub1Δ* rendered cells more sensitive to both zeocin and MMS than *bub1Δ* alone (row 45, 49 and 55 in Figure 54). Unless other unknown synthetic interactions give rise to this phenotype, the unexpected worsened fitness strongly suggests that at least some of the functions of Bub1 and Abo2 could overlap.

Taken together, the results in this section indicate once more that Bub1 and TAPAS function in a complex network of interactions that possibly serve several molecular pathways to resist DNA damage. Determining genetic interactions, as for instance by a synthetic lethal screen, would be a powerful and important tool in further unravelling the nature and organisation of the molecular mechanisms involved.

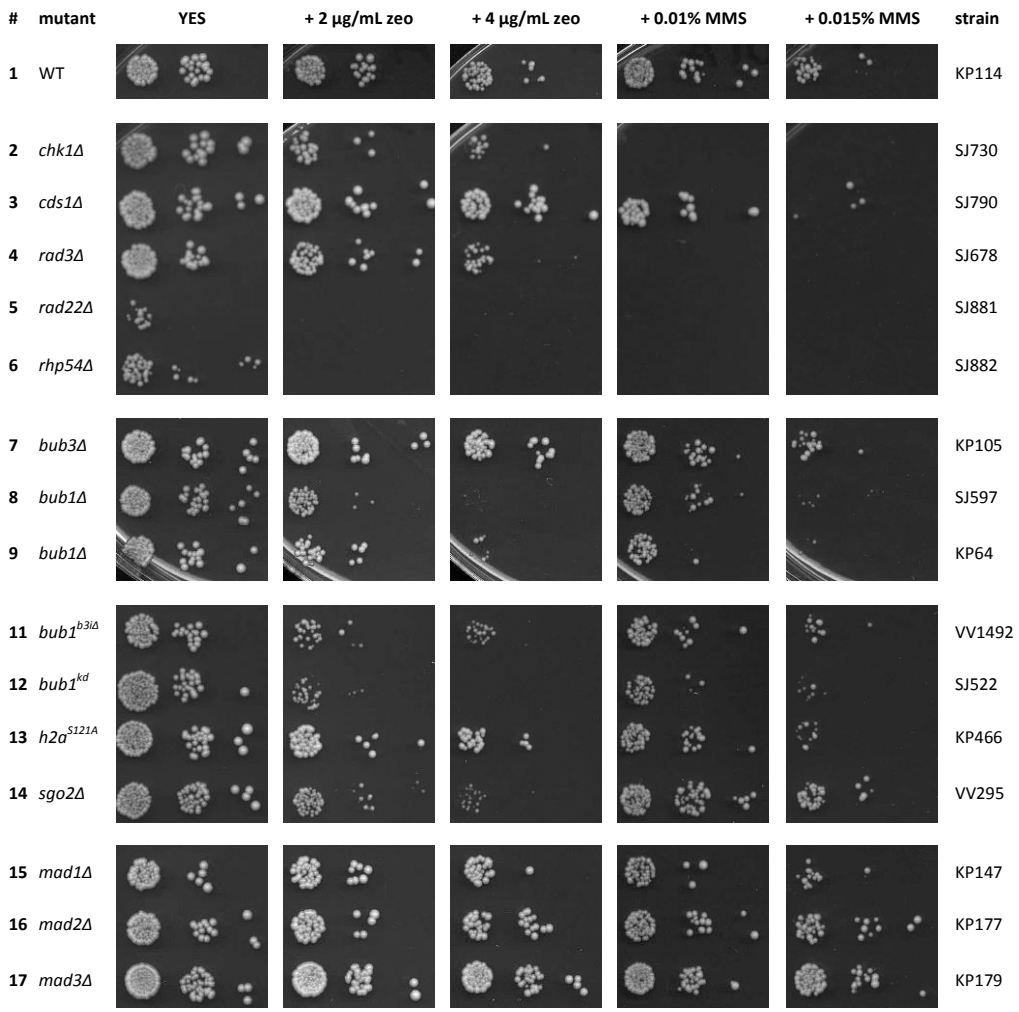

Figure 52: Sensitivity of Mad and Bub-deficient cells treated with zeocin (zeo) or MMS in a plate assay. Suspensions of serial-diluted yeast were spotted on YES plates supplemented with 2 or 4 µg/mL zeocin and 0.01% or 0.015% MMS. Sensitivity of cells with the Bub1 kinase dead allele *bub1*^{kd} was similar to that of *bub1Δ* cells lacking Bub1 function altogether. However, *sgo2Δ* cells and cells with the Bub3-and-Abo1 loss-of-interaction allele *bub1*^{b3iΔ} were not as sensitive to zeocin as *bub1Δ* and *bub1*^{kd}. Cells with mutated Bub1 substrate histone H2A mutation S121A appeared to have a functional DNA damage response to zeocin and MMS.

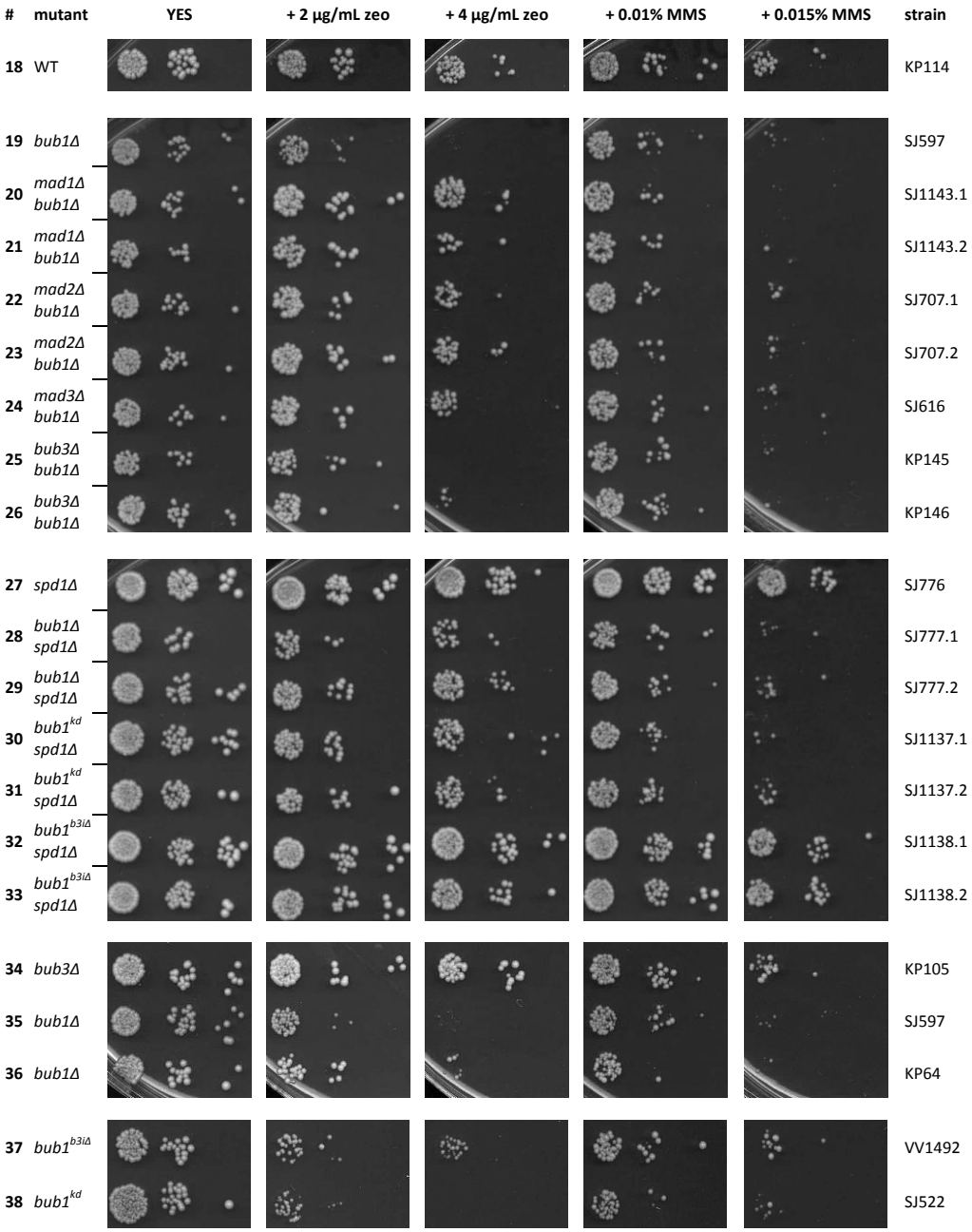

Figure 53: Sensitivity of Bub1-deficient cells to zeocin (but not MMS) is suppressed by deleting *mad1*, *mad2* or *mad3*, but not *bub3*. Deletion of the *spd1* gene, encoding a ribonucleotide reductase inhibitor, was found to alleviate the sensitivity of both *bub1Δ* and *bub1^{kd}* to zeocin. Suspensions of serial-diluted yeast were spotted on YES plates supplemented with 2 or 4 µg/mL zeocin and 0.01% or 0.015% MMS.

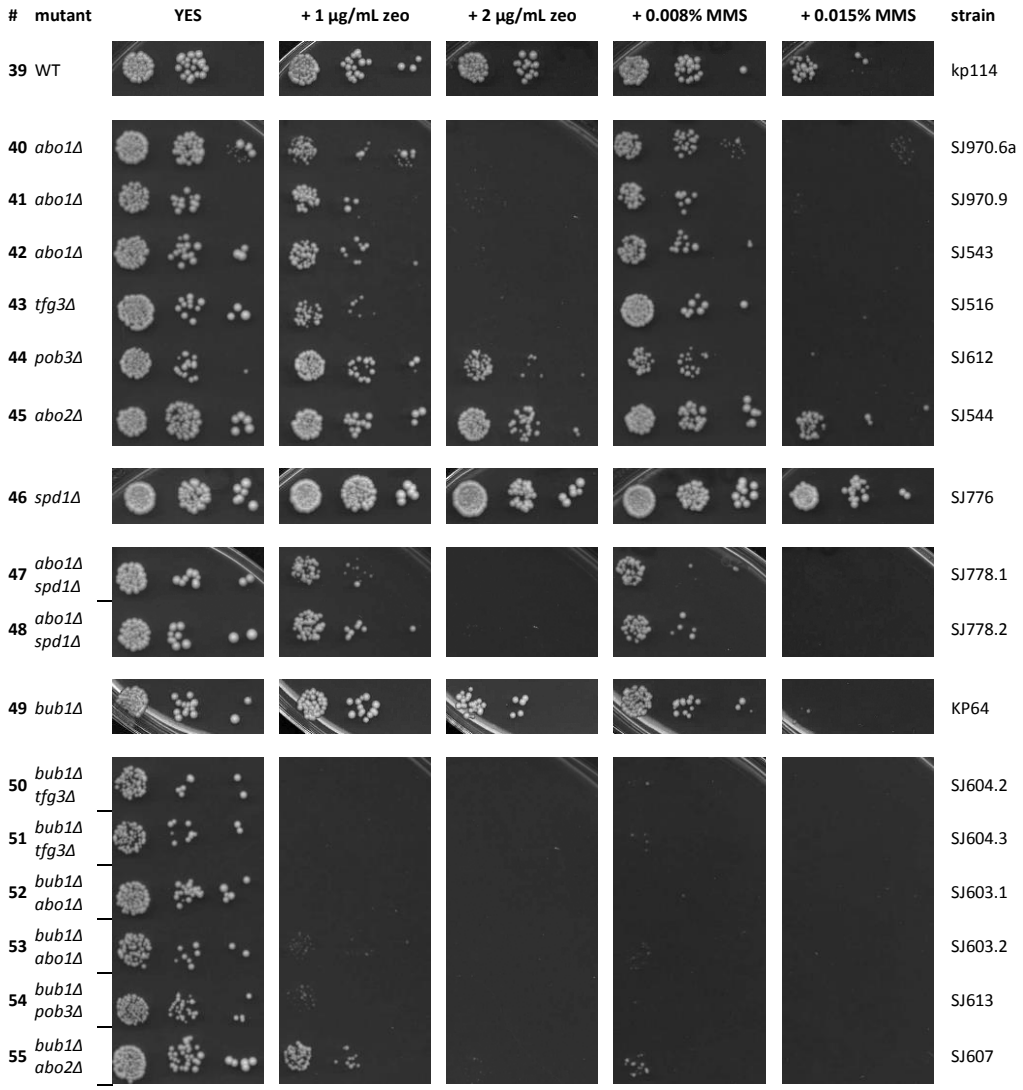

Figure 54: The sensitivity of *abo1Δ* mutant cells to zeocin is not rescued by deleting *spd1*. Combining a *bub1Δ* mutation with *abo1Δ*, *tfg3Δ* or *pob3Δ* was found to exacerbate sensitivity in all cases. Suspensions of serial-diluted yeast were spotted on YES plates supplemented with 1 or 2 µg/mL zeocin and 0.008% or 0.015% MMS (note that in these plate assays less drug was used than in the other two assays in this section).

5.4 Conclusions and discussion

Identification by mass-spectrometry of interactors of the *S.pombe* BUB+ spindle checkpoint complex revealed a novel quaternary TAPAS complex consisting of Tfg3, Abo1, Pob3 and Spt16. The stable association of BUB+ with TAPAS depends on the presence of Bub1, Bub3 and the ATPase bromodomain protein Abo1. A Bub1 mutant protein that lacks the B3i motif is not only deficient in binding Bub3 but also disrupts TAPAS binding.

The interaction of the *S.cerevisiae* Abo1 orthologue Yta7 with FACT subunits Pob3 and Spt16 has been described in several studies (Tackett *et al.* 2005, Gradolatto *et al.* 2009). A separate study identifies both the *S.cerevisiae* Tfg3 orthologue Taf14 and the FACT complex as

constituents of the NuA3 histone acetyltransferase complex (John *et al.* 2000). This report extends these observations and suggests that in *S.pombe* Abo1, Tfg3 and the FACT proteins form a quaternary complex. Remarkably, no Abo1 interactors were identified that could suggest the presence of chromatin remodellers or histone acetyltransferase complexes that are binding partners of Yta7, Tfg3/Taf14 and the FACT complex. This could perhaps imply that the functional Yta7 homologue in regards to facilitating transcription is actually the Abo1 paralogue Abo2.

The ATPase bromodomain Abo1 and the other TAPAS components are commonly described in published literature as chromatin remodelling factors and the experiments presented in this chapter provide evidence in favour of a function in the response to DNA damage. In addition, cells lacking Bub1 were also senstitive to DNA damage. These findings were followed up in this chapter to clarify whether the association of BUB+ and TAPAS confers the robust cellular resistance to genotoxic insults. Several findings, however, have led me to believe that the interaction is not imperative for a Bub1 or TAPAS-dependent DNA damage response. First, both *bub1Δ* and *abo1Δ* cells were sensitive to chronic zeocin and MMS exposure, but $bub1^{b3iΔ}$ cells that no longer support the Bub1 interaction with Abo1 were only minimally affected in their ability to resist these agents. Second, viability of a *bub1Δ abo1Δ* double mutant was much lower than that of a *bub1Δ* or *abo1Δ* mutant alone. This synthetic genetic interaction strongly suggests that Abo1 and Bub1 have overlapping but independent functions.

Nonetheless, much was gained about each protein's functioning in regards to the cellular response to the presence of DNA damage:

1) Neither Bub1 nor Abo1 is essential for the DNA damage checkpoint, as cells exposed to genotoxins were able to arrest the cell cycle and exhibited a long cell morphology. Both Bub1 and Abo1 function to resist the chronic presence of DNA double strand breaks (induced by zeocin or bleomycin) and alkylated DNA (induced by MMS) supporting viability of cells. In *S.pombe*, double strand breaks are mainly repaired through homologous recombination during G2, whereas alkylated nucleobases that disrupt DNA replication are mostly repaired by the base excision repair mechanism.

2) Cells lacking Abo1 were found to be sensitive to both chronic and transient exposure with zeocin, MMS, ionising radiation and UV light, whereas Bub1 only to chronic exposure. The sensitivity of *bub1Δ* and *abo1Δ* was more pronounced than that of a *rad3Δ* or *chk1Δ* mutant during chronic, but not transient, exposure to MMS or zeocin.

3) Cells lacking Abo1, but not Bub1, were highly sensitive to the drug camptothecin that prevents the DNA topoisomerase II from re-joining the DNA backbone after relaxation of supercoiling during transcription and replication (Pommier *et al.* 2003).

4) A *bub1Δ* or *abo1Δ* mutant was not sensitive to DNA replication stress in the temporary presence of hydroxyurea. Bub1 and Abo1 are thus unlikely to function in the DNA replication checkpoint.

5) Increasing the available pool of dNTPs (by deleting the *spd1* gene encoding a ribonucleotide reductase inhibitor) to facilitate repair of DNA double strand breaks by homologous recombination relieved sensitivity of the *bub1Δ* but not the *abo1Δ* mutant to zeocin. To investigate the contribution of Bub1 to the repair of strand breaks, the controlled introduction of a double strand break could be used to further dissect the molecular pathway responsible (Prudden *et al.* 2003).

6) The phenotype of TAPAS mutants in the presence of genotoxic compounds was more severe and broader than a *bub1Δ* or *bub1*^{kd} mutant. This could perhaps indicate that TAPAS components have functions in multiple pathways that respond to DNA damage.

7) Surprisingly, sensitivity of the *bub1Δ* mutant to zeocin, but not to MMS, was suppressed in the absence of Mad1, Mad2 or Mad3, but not Bub3. This indicates that pathway choice in *bub1Δ* cells is restricted by *mad* gene products and can only be bypassed in their absence. It would be interesting to investigate whether a *mad3Δ bub1*^{kd} mutant, in which the Mad3 and TAPAS interaction with Bub1 is retained, is able to resist zeocin (Figure 55). Also, would a *mad3*$^{HIG>VIG}$ mutant (see §3.3.8) be able to repress the *bub1Δ* or *bub1*^{kd} phenotype?

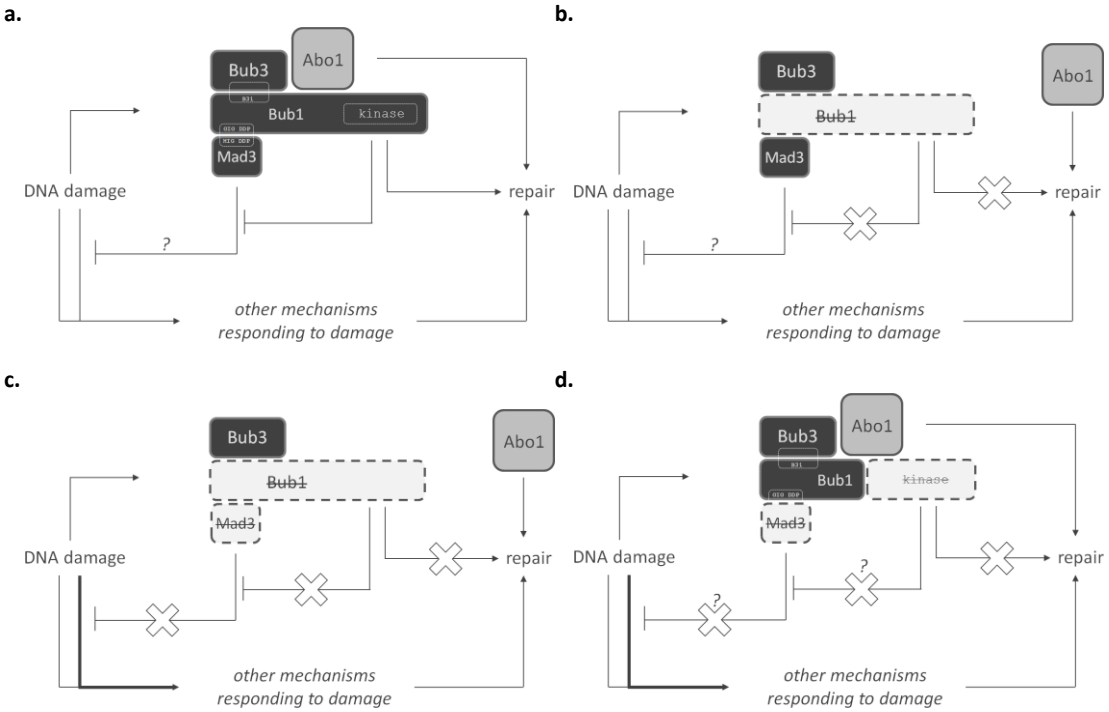

Figure 55: (a) Schematic of potential BUB+ and TAPAS molecular mechanisms responding to DNA damage together with other BUB+ or TAPAS-independent pathways. **(b)** Repair of damaged DNA is only partially achieved in the absence of Bub1 kinase action. **(c)** Only in the absence of Mad3 complementary DNA damage repair mechanisms can make up for Bub1 deficiency. **(d)** An as yet untested model in which *mad3Δ* represses the *bub1*^{kd} phenotype. Note that unlike in (c) the Abo1 ATPase bromodomain protein and Bub3 still interact with Bub1^{kd}.

8) Although the absence of the Abo1 paralogue Abo2 did not confer sensitivity to zeocin or MMS, a *bub1Δ abo2Δ* double mutant was sicker than a *bub1Δ* mutant alone. Cells that lack both Abo1 and Abo2 were very sick even without genotoxic treatment and attempts are under way to create a conditional 'shut-down' Abo1 allele under control of an inducible *nmt41* promoter to make *nmt41::abo1, abo2Δ* and *nmt41::abo1, abo2Δ, bub1Δ* mutant cells. Abo2 could substitute for some of the functions of Abo1, but it remains to be investigated whether Bub1 can interact with Abo2 in the absence of Abo1.

9) Bub1 and Rad22 were not shown to clearly colocalise in cells exposed to genotoxic agents. This could suggest that Bub1 function is not exerted at the site of DNA damage but elsewhere in the cell, or that Bub1 only very briefly associates at these sites. Rather than by fluorescence microscopy, the presence of Abo1 and Bub1 at an engineered site of a DNA double strand break (see point 5) could be investigated by chromatin immuno-precipitation (ChIP) and quantitative real-time PCR.

10) Rad22 foci was still able to form in *abo1Δ* or *bub1Δ* cells. Thus DNA repair proteins are able to assemble at sites of DNA damage in a Bub1 or Abo1-independent process. However, it is as yet not clear if their dynamics (e.g. quantity, timing and rate of appearance and disappearance) are similar to those of wild-type cells. In addition, it is not known whether the *abo1Δ bub1Δ, abo2Δ bub1Δ* or *abo1Δ abo2Δ* double mutant are able to detect DNA lesions and assemble repair foci.

11) Bub1 kinase action seems essential in the response to DNA double strand breaks, and an as yet unknown substrate (not histone H2A Ser121) may be part of this mechanism. Although viability of *sgo2Δ* cells was slightly compromised in the presence of double strand breaks, it is not known whether a Bub1-dependent Sgo2-loading process (akin to promoting chromosome biorientation in mitosis) exist as a response to DNA damage. In human cells, Sgo2 has been identified as a target of the ATM or ATR kinase (Matsuoka *et al.* 2007).

Unequivocally, both Bub1 and TAPAS complexes function to resist DNA damage. Analysis of cells that lack Bub1 in combination with *abo1Δ*, *tfg3Δ* or *pob3Δ* alleles suggests that Bub1 and TAPAS function in at least two different molecular pathways to resist DNA damage. Perhaps these pathways intersect by means of the TAPAS - BUB+ association and further genetic analysis would be required to dissect these respective pathways and how TAPAS might regulate BUB+ or *vice versa*. Biochemical analysis of the Bub1 – Abo1 association has as yet not revealed clear evidence in favour of cell cycle regulation and it remains to be tested whether the association is regulated in response to DNA damage. In this regard, it is not known whether formation of the TAPAS – BUB+ solely occurs on chromatin and whether purified complexes are stable when treated with DNase.

The *S.cerevisiae* Abo1 orthologue Yta7 has been associated with unknown functions in the DNA damage response due to synthetic lethalities with for instance the chromatin regulators Asf1 and Spt16 during genotoxic exposure (Gradolatto *et al.* 2009). Yta7 regulates the nucleosome density of chromatin boundaries and histone gene expression (Lombardi *et al.* 2011). It has been noted that the DNA damage sensitivity of cells deleted for Yta7 could be due to an unbalanced free histone pool available for DNA replication processes (Zunder & Rine 2012). This could lead to unstable chromatin that increases exposure of DNA to genotoxic agents. A more direct function in the DNA damage response for Yta7 is suggested by its interaction with the DNA damage checkpoint kinase Rad53 as a substrate (Smolka *et al.* 2005,

Breitkreutz *et al.* 2010) and Yta7 undergoes phosphorylation when cells are treated with MMS (Chen *et al.* 2010a). In regards to the interaction of Abo1 with Bub1, cell cycle regulation of the TAPAS - BUB+ interaction is a prospect and could be revealed by monitoring the Bub1 binding to Abo1 in the absence and presence of genotoxic agents.

Both Bub1 and the TAPAS complex are documented chromatin remodellers. Bub1 phosphorylates histone H2A when chromosomes fail to biorient during mitosis (Kawashima *et al.* 2010), whereas the *S.cerevisiae* Abo1 orthologue Yta7 and the FACT complex function in regulating nucleosome densities of chromatin (Belotserkovskaya *et al.* 2004, Zunder & Rine 2012). Chromatin remodelling at sites of DNA damage is important for signalling and repair (Dinant *et al.* 2008, Luijsterburg & van Attikum 2011). Nucleosomes need to be displaced to allow access for repair processes and histone modifications are a requirement for recruiting repair factors and initiating a checkpoint arrest. Bub1 kinase-dependent histone phosphorylation and TAPAS-dependent nucleosome remodelling actions could thus facilitate DNA damage signalling and repair.

Even though the functional relevance of the TAPAS – BUB+ association remains to be unravelled, this work strongly suggests that the function of some of the spindle checkpoint components is not restricted to spindle checkpoint mediated anaphase delays. Sometimes referred to as molecular 'cross-talk', there is a growing body of evidence in favour of molecular and genetic links between the two pathways encompassing the response to spindle dysfunction and DNA damage (see Table 36). Several mechanisms have been uncovered that suggest that protein factors of the DNA damage response function in the spindle checkpoint responding to a failure in establishing biorientation. Sometimes, the evidence is indirect, such as the localisation of 53BP1 (Crb2/Rad9 in yeast) at kinetochores during mitosis in metazoan cells (Jullien *et al.* 2002). However, human cell studies suggest that the phosphorylation of Bub1 by ATM (Tel1 in yeast) is essential for checkpoint-mediated anaphase delays (Yang *et al.* 2011) and that the kinetochore localisation of aurora B depends on Chk1 kinase action (Zachos *et al.* 2007, Peddibhotla *et al.* 2009). *Vice versa*, some spindle checkpoint components function in the response to DNA damage: Bub1-dependent phosphorylation of histone H2A at T121 seems to facilitate DNA repair in metazoan cells (Yang *et al.* 2012) and Mps1 kinase regulates Chk2 (Cds1/Rad53 in yeast) kinase function in response to DNA damage (Yeh *et al.* 2009).

#	species / cells	reported key findings	reference
1	human cell line	Aurora B is activated and recruits Mps1 and Mad2 to kinetochores in response to UV irradiation of mitotic cells. Anaphase is delayed in an Mps1-dependent manner, independent of the DNA damage response.	(Zhang *et al.* 2013)
2	human cell line	Mad2 is stabilised upon Chk1-dependent phosphorylation. Apparent colocalisation of Mad2 and Chk1 observed by fluorescence microscopy.	(Chila *et al.* 2013)
3	human cell line *X.laevis* eggs	MRN complex and CtIP are required for fidelity of chromosome segregation. Lack of MRN and CtIP disrupts RCC1 association with chromosomes, results in spindle deformations and chromosome misalignment, and triggers mitotic checkpoint.	(Rozier *et al.* 2013)
4	*S.pombe*	Cells deficient for Mad1 are found to be sensitive to hydroxyurea, bleomycin and UV light.	(Pan *et al.* 2012)
5	human cell line	Bub1 depleted cells are hypersensitive to ionising radiation. In response to DNA damage ATM phosphorylates Bub1 S314 and in turn Bub1 phosphorylates histone H2A at T121. Phosphorylated Bub1 S314 colocalises with damage induced H2AX foci.	(Yang *et al.* 2012)
6	human cell line	Mitotic spindle checkpoint signalling requires the aurora B-mediated phosphorylation of ATM and the ATM-dependent phosphorylation of Bub1.	(Yang *et al.* 2011)
7	*S.cerevisiae*	Tel1 and Mec1 have a spindle checkpoint-independent role in chromosome segregation, but may function in a similar pathway as the Bub1 kinase.	(McCulley & Petes 2010)
8	*S.cerevisiae*	DNA double strand breaks induce γ-H2AX and other epigenetic changes at the centromere that lead to a Mec1-dependent spindle checkpoint-mediated mitotic arrests. *mad2Δ* mutants are epistatic with *rad53Δ* and Mad1, Mad2 and Mad3 (but not Bub1 and Bub3) prolong mitotic arrests in the response to DNA breaks.	(Dotiwala *et al.* 2010)
9	human cell line	Chk2 phosphorylates and reinforces Mps1 activation by positive feedback in response to DNA damage.	(Yeh *et al.* 2009)
10	human cell line	In the absence of DNA damage, Chk1 kinase can regulate Aurora B localisation during mitosis and is essential for chromosome segregation and cytokinesis.	(Peddibhotla *et al.* 2009)
11	human cell line	Activation of the DNA damage response to SV40 large T antigen depends on its association with Bub1.	(Cotsiki *et al.* 2004, Hein *et al.* 2009)
12	*S.cerevisiae*	Cells with a deficient DNA damage checkpoint arrest in metaphase in a spindle checkpoint-dependent manner. This arrest depends on all Mad and Bub spindle checkpoint proteins, Mec1 and Tel1, but not on Chk1, Rad53 or functional kinetochores.	(Kim & Burke 2008)
13	human cell line	Mad2 may negatively regulate DNA repair and interacts with two DNA damage proteins involved in nucleotide excision repair (ERCC1 and XPD).	(Fung *et al.* 2008)
14	human cell line	DNA double-strand breaks during mitosis lead to BubR1 activation and arrests in prometaphase.	(Choi & Lee 2008)
15	human and avian cell lines	Cells lacking Chk1 are unable to arrest in mitosis in the presence of the microtubule poison taxol, but not nocodazole. Chk1-dependent phosphorylation and activation of aurora B is required to target BubR1 to kinetochores.	(Zachos *et al.* 2007)
16	*S.cerevisiae*	The *Xenopus* ATR orthologue XATR (Rad3/Mec1 in yeast) induces a mitotic delay in *mec1Δ* cells in a Mad1 and Mad2-dependent but Rad9 and Rad53 independent manner, indicating a conserved mechanism.	(McSherry *et al.* 2007)
17	human cell line	Chk1 is a negative regulator of polo kinase. In the absence of Chk1 cells arrest in metaphase in a spindle checkpoint-dependent manner.	(Tang *et al.* 2006)
18	murine cell line	Cells lacking BubR1 are defective in their response to genotoxic agents.	(Fang *et al.* 2006)
19	human cell line	DNA replication stress can lead to cyclin B accumulation and mitotic delays followed by p53-independent apoptosis	(Duensing *et al.* 2006)
20	human cell line	Mps1 phosphorylates BLM, a DNA helicase required for the repair of stalled-	(Leng *et al.* 2006)

#	species / cells	reported key findings	reference
		replication forks and the DNA damage response.	
21	*S.cerevisiae*	Although Rad53 and Rad9 do not function in spindle checkpoint function, a spindle checkpoint-mediated arrest triggers phosphorylation of both proteins in the absence, and presence, mitotic DNA damage.	(Clemenson & Marsolier-Kergoat 2006)
22	*S.pombe*	DNA damage checkpoint-deficient *crb2Δ* cells arrest in mitosis in a Mad2-dependent fashion in response to the genotoxin camptothecin.	(Collura *et al.* 2005)
23	human cell line	Mps1 activates Chk2 by phosphorylation in response to DNA damage.	(Wei *et al.* 2005)
24	*Drosophila* cells	Cells lacking Chk1 arrest in metaphase in a response to DNA damage induced by ionising radiation.	(Royou *et al.* 2005)
25	human cell line	A mitotic exit DNA damage checkpoint, regulated by Chk1, mediates mitotic catastrophe when mitotic DNA damage occurs.	(Huang *et al.* 2005)
26	human cell line	A pathway that facilitates resistance to cisplatin is antagonised by Mad2. Mad2 overexpression in the presence of this drugs leads to a mitotic arrest followed by apoptosis.	(Cheung *et al.* 2005)
27	human cell line	Mitotic cells undergoing DNA damage do not delay mitotic exit. An unidentified, spindle checkpoint-independent mitotic checkpoint responding to DNA-decatenation might however exist.	(Skoufias *et al.* 2004)
28	human cell line	Mitotic cells with damaged DNA arrest in metaphase in a spindle checkpoint-dependent manner and undergo a regulated mitotic catastrophe. Cells lacking BubR1 or Mad2 escape mitosis in the presence of DNA lesions and missegregate chromosomes.	(Nitta *et al.* 2004)
29	human cell line	The spindle checkpoint mechanism is required for the post-mitotic p53-dependent G1 checkpoint.	(Vogel *et al.* 2004, Leng *et al.* 2006)
30	*S.cerevisiae*	DNA damage checkpoint-deficient *mec1Δ* cells delay mitosis in a spindle checkpoint-dependent manner.	(Clerici *et al.* 2004)
31	*S.pombe*	Mad2, but not Mad1, Mad3 or Bub1 might act to delay mitosis in the presence of the DNA replication inhibitor hydroxyurea.	(Sugimoto *et al.* 2004)
32	*S.pombe*	*taz1Δ* mutant cells defective in telomere maintenance require the spindle checkpoint and Rad3 for viability.	(Miller & Cooper 2003)
33	human cell line	Mitotic DNA damage leads to ATM-dependent decondensation of chromosomes, inhibition of $CDK^{cyclinB}$ complexes, degradation of Cdc25 and subsequent cell cycle reversal back into a G2-like state.	(Chow *et al.* 2003)
34	*S.cerevisiae*	DNA damage checkpoint-deficient *mec1Δ* or *rad9Δ* cells requires decreased histone deacetylase activity to arrest in mitosis in a spindle checkpoint-dependent manner.	(Scott & Plon 2003)
35	human cell line	DNA damage occurring in prophase lead to Mad2-dependent delay in progress through metaphase. This delay is P53 independent.	(Mikhailov *et al.* 2002)
36	*S.cerevisiae*	Spindle checkpoint activation in the presence of single-stranded DNA at unprotected telomeres.	(Maringele & Lydall 2002)
37	*S.cerevisiae*	DNA damage checkpoint-deficient *rad9Δ rad24Δ* cells delay mitosis in a Mad2-dependent manner in response to DNA damage and DNA replication stress.	(Garber & Rine 2002)
38	human cell line	DNA damage-independent loading of 53BP1 (Crb2/Rad9 in yeast) at kinetochores during mitosis. 53BP1 is hyperphosphorylated during in response to spindle disruption.	(Jullien *et al.* 2002)
39	human cell line	Plk1 is inhibited by DNA damage in mitosis, blocking mitotic exit.	(Smits *et al.* 2000)

Table 36: Evidence in favour of molecular 'cross-talk' between the spindle checkpoint and DNA damage response from the published literature.

Could the TAPAS – BUB+ association perhaps govern a DNA damage response during mitosis? A careful experimental design would be required to investigate this challenging question. As yet, only a relatively small number of studies have covered the controversial topic of a specific DNA damage response during mitosis. Unlike yeast, metazoan cells can spend prolonged times in mitosis during which the occurrence of genotoxic damage clearly is a risk that needs to be controlled. Aneuploidy is a major hazard if DNA breakages remain unrepaired before the onset of anaphase, although hyper-condensation of chromosomes could interfere with both DNA damage detection and repair.

The yeast *S.cerevisiae* lacks a defined G2 phase as S phase and M phase partially overlap. Thus cells that undergo significant DNA damage do not delay entry into mitosis, but uniquely arrest in metaphase, in a mechanism that stabilises securin (Yamamoto *et al.* 1996) and depends on Mad1, Mad2 and Mad3 (Dotiwala *et al.* 2010) and perhaps Bub1 and Bub3 (Kim & Burke 2008). Few potential mechanisms have thus far been uncovered in other species and evidence remains scarce. Initial reports on the existence of a 'mitotic DNA damage checkpoint' that was suggested to delay mitotic exit were conflicting and seem to depend on the cell types and drugs used in these experiments (Smits *et al.* 2000, Mikhailov *et al.* 2002). An ATM-independent but spindle checkpoint-dependent mechanism was observed in a variety of cultured human cells that had DNA damage introduced by exposure to the DNA topoisomerase inhibitor adriamycin or by pulses of laser light (Mikhailov *et al.* 2002). In contrast to the introduction of minor DNA damage, it was found that mitosis was prolonged by extensive damage to chromosomes (Mikhailov *et al.* 2002). In these experiments, although the bipolar spindle array was not affected in the presence of DNA damage, the observed anaphase delay did depend on a functional spindle checkpoint. In addition and surprisingly, ATM inhibition by either caffeine (a pesticide produced by many plant species) or wortmannin (produced by the fungi *Penicillium funiculosum*) does not abolish this delay. The authors therefore suggest that extensive mitotic DNA damage does not lead to a DNA damage response but rather that disruption of microtubule attachments to kinetochores results in a spindle checkpoint-mediated anaphase arrest (Mikhailov *et al.* 2002). In a separate study, the ATM-dependent modification and consequent inhibition of mitotic polo-like kinase Plk1 (Plo1/Cdc5 in yeast) that prevented mitotic exit in the presence of DNA damage was observed (Smits *et al.* 2000, van Vugt *et al.* 2001). Another research group identified an ATM-dependent mechanism in cultured cells that relies on the dephosphorylation and inhibition of Plk1 by PP2A phosphatase (Jang *et al.* 2007, Lee *et al.* 2010). As a result cells accumulate in interphase (or a G1-like state,

but with high levels of cyclin B and inactive Cdk and Plk1) with duplicated genomic content and have thus exited mitosis without segregating chromosomes (Hyun *et al.* 2012).

Accumulating evidence suggests that Bub1 functions at the interface of the cellular response to DNA damage and spindle dysfunction in metazoan cells and, as dscribed in this report, in *S.pombe*. Thus the BUB complex confers chromosomal stability through at least three molecular mechanisms: mediating spindle checkpoint arrests, promoting chromosome biorientation and the DNA damage response. Bub1 and in particular its B3i and kinase domain are thus excellent targets for chemical compounds disrupting Bub1 function to enhance the therapeutic response to anti-tumour agents.

If the DNA damage response does not depend on the interaction of TAPAS with BUB+, what could be the functional relevance of their association? The collective function of the four TAPAS subunits is the facilitation of chromatin remodelling and some of the TAPAS components are known to support RNA polymerase II-dependent transcription initiation and elongation, in addition to epigenetic regulation of chromatin features, such as the maintenance of barriers that insulate transcriptionally active genes from repressive heterochromatic influence. In particular, there seems to be a link between stress survival and TAPAS function that indicates that either TAPAS facilitates the expression of 'stress genes' or simply functions in stabilising chromatin and RNA polymerase II complexes during stress conditions. At the same time some studies allude to further uncharacterised functions in the regulation of microtubule dynamics and cell cycle progression. In particular, it has been observed that post-metaphase cell cycle progression is affected in cells that lack Yta7 after release from a nocodazole block (Gradolatto *et al.* 2008). This defect has not been studied in detail and the mechanism responsible hence remains obscure. Although the data presented here focus on the *S.pombe* Abo1 protein, a brief detour into *S.cerevisiae* cell studies revealed that the absence of Yta7 renders cells more sensitive to microtubule disruption, but not as a result of deficiencies in the spindle checkpoint or chromosome biorientation (data not shown). In addition, tantalising evidence was uncovered by mass-spectrometry analysis of Mad3 interactors for a physical interaction with Yta7.

Several chromatin remodellers are present at centromeric heterochromatin during the latter stages of mitosis to facilitate chromosome biorientation. There, the RSC and ISWI chromatin remodelling complexes facilitate tension-dependent nucleosome remodelling (Verdaasdonk *et al.* 2012). Nucleosome eviction and reloading is important for centromere integrity,

kinetochore structure and spindle microtubule dynamics. As the spindle checkpoint is able to sense tension there could be a direct mechanism to provide feedback to nucleosome remodelling processes, potentially provided by the BUB+ association with TAPAS. Both Bub1 and shugoshin are suggested to act in conformational changes of kinetochore and cohesin complexes during biorientation (Haase *et al.* 2012). The observed chromosome missegregation in the *abo1Δ* mutant could thus be a result of aberrant nucleosome remodelling processes at the centromere during tension. This could make centromeric DNA liable to breakages when too few nucleosomes are present to assemble a heterochromatic structure able to resist the pulling forces of microtubules. It would be very interesting to assay the chromosome loss rates of *abo1Δ bub1Δ* and *abo1Δ abo2Δ* double mutants to see whether these genes also synthetically interact as they do in the DNA damage response. Moreover, a genetic screen for additional Abo1 and Bub1 synthetic interactors could yield clues about such a mechanism and possibly resolve the curious enigma of the Bub1 – Abo1 physical interaction.

6 Final discussion

Deficiencies in spindle checkpoint function and the DNA damage response can result in genomic and chromosomal instabilities that contribute to carcinogenesis and disease in humans (Baker *et al.* 2005, Jackson & Bartek 2009). The molecular components governing the aforementioned mechanisms are broadly conserved from yeast to man. However, molecular evolution has led to changes in the way these pathways are regulated. In some aspects this has greatly assisted scientific efforts to unravel their fundamental function using tractable model organisms such as the yeasts *S.pombe* and *S.cerevisiae*, although parallels from one organism to another are sometimes difficult to draw. As revealed in this work, understanding protein interactions is of crucial importance. Some of these interactions concern two of the most well-studied spindle checkpoint proteins, Mad3 and Bub1, which are thought to have evolved from a single '*Mad3Bub(R)1'* proto-gene.

Through a scaled-up mass-spectrometry analysis of checkpoint protein interactors it is shown here that physical interactions among spindle checkpoint proteins are largely conserved, although variations have been identified in *S.pombe* and *S.cerevisiae.* The direct interaction of *S.pombe* Mad3 with Bub1 was shown to be enabled by reciprocal engagement of conserved and related TPR domains, in which mutation of highly conserved sequence motifs greatly destabilise the interaction and significantly diminish spindle checkpoint function. These motifs are present in both human and *S.cerevisiae* orthologous proteins, although in the latter species Mad3 and Bub1 are not thought to interact even though mutation of one of these motifs renders cells spindle checkpoint deficient (Hardwick *et al.* 2000). Thus even though these *S.pombe* and *S.cerevisiae* Mad3 mutants have a similar phenotype, the underlying mechanism could indeed be of a different nature.

Another example highlighted through this work is that of the Mad3 and Bub1 B3i sequence motifs required for their interaction with Bub3 (Larsen *et al.* 2007, Vanoosthuyse *et al.* 2009). This motif is present in both Bub1 and Mad3 in *S.cerevisiae*, and in Bub1 but not in Mad3 in *S.pombe*. Here it is shown that *S.pombe* Bub1 B3i is also important in binding a chromatin remodelling complex called TAPAS. As a consequence, phenotypic analysis of a $bub1^{b3i\Delta}$ mutant should take into account not only the Bub3 loss of interaction, but also that with the TAPAS complex.

Biochemical analysis of the TAPAS complex, consisting of the bromodomain ATPase Abo1, Tfg3 and the FACT subunits Pob3 and Spt16, reveals that its association with the BUB+ complex depends on Abo1 and both Bub1 and Bub3. Functional analysis of TAPAS components show that they are not involved in spindle checkpoint function. TAPAS mutants are however hypersensitive to genotoxic insults, a phenotype that to some extent is shared with *bub1Δ* mutants, which are shown to be unable to robustly resist the presence of DNA double strand breaks (induced by zeocin) or alkylated DNA bases (produced by MMS). However, genotoxic sensitivity of a $bub1^{b3i\Delta}$ mutant is less pronounced than that of a *bub1Δ* mutant, indicating that resistance to genotoxic exposure is not conferred by the Bub1 association with TAPAS. Sensitivity of cells deficient in TAPAS or Bub1 does not appear to be due to the loss of DNA damage checkpoint or DNA replication checkpoint functions.

Nonetheless, this work identifies new *S.pombe* genes that are involved in the DNA damage response and in particular the response to DNA double strand breaks. In human cell studies, both Bub1 (Baker *et al.* 2009, Bolanos-Garcia & Blundell 2011) and the Abo1 orthologue ATAD2 have been linked to oncogenesis (Caron *et al.* 2010, Hsia *et al.* 2010, Kalashnikova *et al.* 2010). It is anticipated that the yeast *S.pombe* will take an important role in future studies elucidating their molecular mechanism, underlining its role as a key model organism in unravelling eukaryotic pathways that act to prevent chromosomal instability.

Although this study was unable to directly link the apparent DNA damage sensitivity to a loss of interaction of BUB+ with TAPAS, it has revealed a complex network of genetic requirements and interactions. This shows that components of the mitotic spindle checkpoint evolved to gain function within the DNA damage response. Prime examples are the three *MAD* gene products of the yeast *S.cerevisiae* that mediate a metaphase arrest not only when chromosome biorientation is disturbed, but also in the presence of DNA strand breaks (Dotiwala *et al.* 2010). Molecular evolution can thus lead to ever more 'selfish genes' (Dawkins 1976) by becoming involved in other vital molecular processes. From an evolutionary point of view, imparting mitotic proteins with non-mitotic functions also allows cells to make the most of valuable resources and provides critical redundancy of molecular pathways. In regards to the former argument, this makes especially sense for *S.pombe* cells that spend most of their time, perhaps up to 90%, out with M phase. It is thus conceivable that cells respond to environmental factors through interplay of components from two of the most conserved and widely studied molecular mechanisms ensuring genetic integrity and chromosomal stability.

Finally, this work presents tools to investigate protein interaction networks and unravel the architecture of multi-protein complexes. It is hoped that by combining the large-scale rapid purification technology and mass-spectrometry analysis of cross-linked complexes fundamental insights into the functioning of large protein complexes, such as the APC^{MCC} and kinetochores, will be gained.

7 Supplemental information

7.1 *S.pombe* MS data

Key for each hit, both from cycling and mitotically arrested cells: ***unique peptides / total peptides / % polypeptide coverage***

			cycling		arrest		cycling		arrest		cycling		arrest		cycling		arrest		cycling		arrest	
#	protein hit	kDa	Mad1						Mad2				Mad3				Bub1				Bub3		Lid1	
9	Mad1	80	322	2509	90	229	2521	85	135	963	73	58	222	46	-	-	-	-	-	-	-	-	-	-	-	-
1	Mad2	24	54	607	88	34	425	84	36	1032	73	21	67	38	3	3	7	17	477	60	-	-	-	-	-	-	-	-	4	4	16
10	Mad3	36	-	-	-	-	-	-	2	4	10	18	45	42	106	818	87	67	794	78	7	12	31	3	3	15	5	6	19	-	-	-	13	17	41
4	Bub1	118	-	-	-	-	-	-	-	-	-	-	-	-	98	354	67	8	12	11	118	2278	70	351	2517	82	262	2121	82	285	1995	80	-	-	-	-
5	Bub3	36	-	-	-	-	-	-	-	-	-	-	-	-	23	99	59	-	-	-	28	512	73	72	458	75	55	905	80	73	938	78	-	-	-	-
7	Slp1	53	-	-	-	-	-	-	4	4	15	13	32	17	11	18	25	54	942	72	-	-	-	-	-	-	-	-	-	-	-	-	-	24	57	66
17	Cut4	165	-	-	2	2	3	3	3	3	3	-	-	2	2	2	2	64	401	35	-	-	-	-	-	-	-	-	-	239	945	57	173	1627	62
13	Apc5	85	-	-	-	-	-	-	-	-	-	-	-	2	2	5	46	372	60	-	-	-	-	-	-	-	-	-	-	115	611	63	92	937	75
15	Lid1	83	-	-	-	-	-	-	-	-	-	-	-	3	3	10	54	275	56	-	-	-	-	-	-	-	-	-	-	116	697	64	109	998	75
12	Apc2	79	-	-	-	-	-	-	-	-	-	-	-	-	-	-	40	292	58	-	-	-	-	-	-	-	-	-	-	102	488	69	96	1014	74
11	Nuc2	76	-	-	-	-	-	-	-	-	-	2	2	4	-	-	50	333	61	-	-	-	-	-	-	-	-	-	-	142	742	75	123	1302	80
16	Cut9	76	-	-	-	-	-	-	-	-	-	-	-	-	5	5	11	54	238	59	-	-	-	-	-	-	-	-	-	157	588	72	135	1045	86
8	Cut23	66	-	-	-	-	-	-	-	-	-	-	-	-	4	5	10	35	423	53	-	-	-	-	-	-	-	-	-	121	991	75	98	1593	74
6	Apc10	21	-	-	-	-	-	-	-	-	-	-	-	-	-	-	-	15	191	78	-	-	-	-	-	-	-	-	-	32	233	83	21	336	81
43	Apc15	16	-	-	-	-	-	-	-	-	-	-	-	-	-	-	-	8	18	27	-	-	-	-	-	-	-	-	-	6	18	22	18	44	38
3	Apc13	16	-	-	-	-	-	-	-	-	-	2	10	8	-	-	-	9	173	73	-	-	-	-	-	-	-	-	-	38	252	91	28	310	90
18	Apc14	12	-	-	-	-	-	-	-	-	-	7	28	35	-	-	-	2	3	22	-	-	-	-	-	-	-	-	-	28	64	76	9	65	56
19	Apc11	11	-	-	-	-	-	-	-	-	-	4	8	18	-	-	-	4	21	39	-	-	-	-	-	-	-	-	-	12	40	84	13	78	64
2	Hcn1	9	-	-	-	-	-	-	-	-	-	2	7	29	-	-	-	16	119	89	-	-	-	-	-	-	-	-	-	23	299	81	23	419	88
14	Tfg3	28	-	-	-	-	-	-	-	-	-	-	-	-	5	6	35	-	-	-	16	76	70	26	66	55	23	80	66	7	10	41	-	-	-	-
20	Abo1	135	-	-	-	-	-	-	-	-	-	-	-	-	19	35	20	-	-	-	55	331	37	156	506	55	108	511	55	33	58	35	3	3	-	-
263	Pob3	57	-	-	-	-	-	-	-	-	-	-	-	-	-	-	-	-	-	-	6	6	18	4	6	14	4	4	12	-	-	-	-	-	-
125	Spt16	116	-	-	-	-	-	-	-	-	-	-	-	-	-	-	-	-	-	-	6	7	9	6	17	14	7	9	9	-	-	-	2	4	5	-	-	-
29	H2A.1	14	3	7	18	4	21	23	-	-	-	-	-	-	-	-	-	-	-	-	13	34	63	5	21	37	7	16	41	3	7	18	-	-	2	2	27
28	H2A.2	14	3	7	18	4	21	23	-	-	-	-	-	-	3	4	15	-	-	-	13	34	63	5	21	38	-	-	3	7	18	-	-	2	2	27
54	H3	15	-	-	-	5	5	24	-	-	-	2	3	13	3	3	15	-	-	-	-	-	-	5	5	28	7	10	48	2	2	13	-	-	2	3	29
93	Pht1	19	-	-	-	-	-	-	-	-	-	-	-	-	-	-	-	-	-	-	2	4	23	-	-	-	-	-	-	-	-	-	-	-	-	-
21	Cct1	60	3	3	6	-	-	-	7	10	14	-	-	-	4	4	11	-	-	-	-	-	-	5	5	16	41	103	65	67	280	82	4	4	12	4	5	7
23	Cct2	57	3	3	10	2	2	7	2	2	4	-	-	-	7	8	23	-	-	-	-	-	-	4	4	14	29	70	56	47	139	80	7	8	21	3	4	10
32	Cct3	58	6	7	22	-	-	-	7	7	16	-	-	-	7	8	15	-	-	-	-	-	-	4	4	15	39	93	59	59	101	79	7	8	21	7	7	17
27	Cct4	57	10	10	35	5	6	17	13	19	39	-	-	-	8	8	23	7	8	16	2	2	10	11	12	27	32	67	57	49	127	77	12	12	36	10	15	34
26	Cct5	59	5	6	13	2	2	3	5	6	20	-	-	-	-	-	-	3	5	16	-	-	-	2	2	6	37	94	60	48	125	79	3	3	9	5	7	20
24	Cct6	59	7	7	17	3	3	10	5	5	19	-	-	-	8	16	21	-	-	-	-	-	-	8	11	28	30	69	55	43	137	74	8	8	25	9	12	28
22	Cct7	61	2	3	9	2	2	4	-	-	-	-	-	-	2	2	6	-	-	-	-	-	-	4	4	8	46	86	62	58	176	82	2	3	7	3	3	7
34	Cct8	60	5	5	16	3	3	7	7	7	16	-	-	-	10	10	18	-	-	-	2	4	2	11	12	19	38	89	50	53	87	78	4	5	11	3	3	12
70	Nup211	211	70	94	42	20	22	16	9	10	8	-	-	-	-	-	-	-	-	-	3	3	4	-	-	-	-	-	-	-	-	-	-	-	-	-	-
1102	Alm1	198	3	3	3	3	3	2	-	-	-	-	-	-	-	-	-	-	-	-	-	-	-	2	2	1	-	-	-	-	-	-	2	2	1	-	-
610	Nup40	40	-	-	-	-	-	-	-	-	-	-	-	-	2	2	10	-	-	-	-	-	-	-	-	-	-	-	-	-	-	-	-	-	-	-	-
506	Nup60	80	5	5	13	-	-	-	-	-	-	-	-	-	-	-	-	-	-	-	-	-	-	-	-	-	-	-	-	-	-	-	-	-	-	-	-
254	Nup61	61	5	6	19	-	-	-	2	2	6	-	-	-	3	3	9	-	-	-	-	-	-	-	-	-	5	7	15	-	-	-	-	-	-	-	-

			cycling			arrest			cycling			arrest			cycling			arrest			cycling			arrest			cycling			arrest			cycling			arrest		
#	protein hit	kDa	Mad1						Mad2						Mad3						Bub1						Bub3						Lid1					
443	Imp1	60	-	-	-	-	-	-	4	4	14	-	-	-	-	-	-	-	-	-	-	-	-	2	2	6	2	2	5	-	-	-	3	3	12	3	3	11
139	Sal3	122	4	5	6	-	-	-	16	23	24	-	-	-	2	5	4	-	-	-	-	-	-	4	4	7	7	8	12	-	-	-	14	20	25	4	4	8
674	Kap95	95	2	2	3	2	2	4	-	-	-	-	-	-	-	-	-	-	-	-	-	-	-	2	2	4	3	4	7	-	-	-	3	3	5	2	3	5
175	Kap123	118	-	-	-	-	-	-	8	14	17	-	-	-	-	-	-	-	-	-	-	-	-	4	4	6	4	4	9	-	-	-	2	2	4	3	3	6
33	Cdc2	34	-	-	-	-	-	-	-	-	-	-	-	-	-	-	-	11	35	43	-	-	-	-	-	-	-	-	-	-	-	-	6	10	36	16	30	55
48	Cdc13	56	-	-	-	-	-	-	-	-	-	-	-	-	-	-	-	10	30	28	-	-	-	-	-	-	-	-	-	-	-	-	-	-	-	7	9	19
49	Sty1	40	2	2	18	-	-	-	9	18	41	-	-	-	5	6	15	-	-	-	-	-	-	-	-	-	2	2	9	-	-	-	11	15	44	2	2	7
79	Mes1	11	-	-	-	-	-	-	-	-	-	2	3	26	-	-	-	-	-	-	-	-	-	-	-	-	-	-	-	-	-	-	-	-	3	5	31
53	Cdc4	16	-	-	-	-	-	-	-	-	-	-	-	-	-	-	-	-	-	-	-	-	-	-	-	-	-	-	-	-	-	-	3	4	53	-	-	-
135	Cka1	40	2	3	7	-	-	-	2	3	10	-	-	-	2	2	10	-	-	-	2	7	10	8	10	21	6	7	28	2	2	12	-	-	-	-	-	-
163	Alp7	53	2	2	7	-	-	-	2	2	8	-	-	-	-	-	-	-	-	-	-	-	-	-	-	-	-	-	-	2	2	4	8	11	23	-	-	-
209	Alp14	89	-	-	-	-	-	-	9	10	19	-	-	-	-	-	-	-	-	-	-	-	-	-	-	-	2	2	4	-	-	-	12	14	22	-	-	-
732	Ndc80	72	-	-	-	-	-	-	-	-	-	-	-	-	-	-	-	-	-	-	-	-	-	-	-	-	-	-	-	2	2	8	-	-	-	-	-	-
773	Spc7	154	-	-	-	-	-	-	-	-	-	-	-	-	-	-	-	-	-	-	-	-	-	2	2	2	4	6	5	4	4	6	-	-	-	-	-	-
290	SPBC23G7.14	16	-	-	-	-	-	-	-	-	-	-	-	-	-	-	-	-	-	-	-	-	-	-	-	-	-	-	-	-	-	-	2	2	20	-	-	-
300	SPAP32A8.03c	55	-	-	-	-	-	-	-	-	-	-	-	-	-	-	-	-	-	-	-	-	-	-	-	-	-	-	-	-	-	-	3	3	20	-	-	-
339	SPCC14G10.04	53	-	-	-	-	-	-	-	-	-	-	-	-	-	-	-	-	-	-	-	-	-	-	-	-	-	-	-	-	-	-	5	5	18	2	2	8
344	SPCC4G3.13c	24	-	-	-	-	-	-	-	-	-	-	-	-	-	-	-	-	-	-	-	-	-	-	-	-	-	-	-	-	-	-	2	2	18	2	2	16
759	Csi1	60	-	-	-	-	-	-	2	2	8	2	3	5	-	-	-	-	-	-	-	-	-	-	-	-	-	-	-	-	-	-	-	-	-	-	-	-
40	SPAC222.08c	26	-	-	-	-	-	-	4	7	33	-	-	-	-	-	-	-	-	-	-	-	-	-	-	-	3	3	16	-	-	-	11	22	50	2	2	7
30	Tuf1	48	11	14	37	2	2	8	19	56	51	-	-	-	7	10	28	-	-	-	-	-	-	5	5	18	8	10	35	15	29	48	2	2	7	-	-	-
31	SPCC622.14	34	-	-	-	-	-	-	4	4	22	-	-	-	6	7	29	-	-	-	-	-	-	-	-	-	5	9	25	-	-	-	7	24	43	2	2	9
36	Rpp101	11	-	-	-	-	-	-	-	-	-	-	-	-	3	9	34	-	-	-	-	-	-	-	-	-	3	10	34	-	-	-	-	-	-	2	2	15
37	Rpp102	11	-	-	-	-	-	-	3	4	67	-	-	-	3	9	34	-	-	-	-	-	-	-	-	-	3	10	34	-	-	-	-	-	-	2	2	15
38	Mug64	33	-	-	-	-	-	-	2	2	13	-	-	-	12	24	52	-	-	-	-	-	-	2	2	16	8	13	39	-	-	-	2	2	13	6	8	28
39	SPBC29A10.16c	14	-	-	-	-	-	-	-	-	-	-	-	-	4	9	41	-	-	-	-	-	-	3	4	47	4	7	58	-	-	-	-	-	-	7	8	65
41	Grx4	27	4	5	21	-	-	-	5	8	30	-	-	-	-	-	-	-	-	-	-	-	-	3	4	22	3	3	15	-	-	-	6	17	34	-	-	-
42	Atp16	17	-	-	-	-	-	-	-	-	-	-	-	-	3	6	27	-	-	-	-	-	-	-	-	-	6	8	73	-	-	-	-	-	-	4	6	61
44	Ypt1	23	-	-	-	-	-	-	-	-	-	-	-	-	11	20	49	-	-	-	-	-	-	-	-	-	6	7	28	-	-	-	-	-	-	11	14	36
45	SPCPB16A4.05c	31	4	4	28	2	2	9	7	16	39	-	-	-	-	-	-	-	-	-	-	-	-	2	2	10	2	7	13	-	-	-	8	12	46	-	-	-
46	Rpl902	21	3	4	19	2	5	15	7	13	48	-	-	-	3	5	16	2	4	21	3	4	21	5	9	25	3	5	15	2	2	15	2	3	16	-	-	-
47	Rpp103	11	-	-	-	-	-	-	-	-	-	-	-	-	2	5	34	-	-	-	-	-	-	-	-	-	2	4	34	-	-	-	-	-	-	-	-	-
50	SPBP8B7.17c	56	2	3	8	-	-	-	2	18	9	-	-	-	-	-	-	-	-	-	2	4	8	2	18	7	-	-	-	-	-	-	-	-	-	3	7	14
51	Trp1	83	2	2	7	-	-	-	12	30	29	-	-	-	-	-	-	-	-	-	-	-	-	-	-	-	4	5	12	-	-	-	16	23	28	-	-	-
52	Trx1	11	2	2	25	-	-	-	-	-	-	-	-	-	3	4	54	-	-	-	-	-	-	3	3	39	2	2	26	-	-	-	-	-	-	4	4	35
55	Rpt4	21	-	-	-	-	-	-	2	3	17	-	-	-	3	8	26	-	-	-	-	-	-	2	4	17	3	6	24	2	3	17	2	3	17	4	5	28
56	SPAP8A3.07c	41	6	8	22	5	7	14	7	10	26	-	-	-	4	4	16	-	-	-	2	18	8	2	2	7	3	4	9	4	5	18	4	5	18	4	5	16
57	Ypt3	24	-	-	-	-	-	-	-	-	-	-	-	-	8	9	31	-	-	-	-	-	-	-	-	-	4	5	23	-	-	-	-	-	-	9	12	49
58	Gst3	28	-	-	-	-	-	-	-	-	-	-	-	-	3	5	10	-	-	-	-	-	-	2	3	16	5	5	27	-	-	-	-	-	-	5	8	40
59	Vam6	104	-	-	-	-	-	-	-	-	-	-	-	-	-	-	-	-	-	-	-	-	-	3	3	6	-	-	-	2	36	4	-	-	-	-	-	-

7.2 *S.pombe* MS protein hit ontology

#	protein	ontology
1	Mad2	mitotic spindle checkpoint protein
2	Hcn1	anaphase-promoting complex subunit
3	Apc13	anaphase-promoting complex subunit
4	Bub1	mitotic spindle checkpoint protein kinase
5	Bub3	mitotic spindle checkpoint protein
6	Apc10	anaphase-promoting complex subunit
7	Slp1	cell-cycle regulated activator of anaphase-promoting complex (APC)
8	Cut23	anaphase-promoting complex subunit
9	Mad1	mitotic spindle checkpoint protein
10	Mad3	mitotic spindle checkpoint protein
11	Nuc2	anaphase-promoting complex subunit
12	Apc2	anaphase-promoting complex subunit
13	Apc5	anaphase-promoting complex subunit
14	Tfg3	YEATS domain transcription factor TFIIF complex subunit
15	Lid1	anaphase-promoting complex subunit
16	Cut9	anaphase-promoting complex subunit
17	Cut4	anaphase-promoting complex subunit
18	Apc14	anaphase-promoting complex subunit
19	Apc11	anaphase-promoting complex subunit
20	Abo1	ATPase with bromodomain protein
21	Cct1	chaperonin-containing T-complex alpha subunit
22	Cct7	chaperonin-containing T-complex eta subunit
23	Cct2	chaperonin-containing T-complex beta subunit
24	Cct6	chaperonin-containing T-complex zeta subunit
25	H2B	histone H2B
26	Cct5	chaperonin-containing T-complex epsilon subunit
27	Cct4	chaperonin-containing T-complex delta subunit
28	H2A.2	histone H2A.1
29	H2A.1	histone H2A.1
30	Tuf1	mitochondrial translation elongation factor EF-Tu
31	SPCC622.14	GTPase activating protein
32	Cct3	chaperonin-containing T-complex gamma subunit
33	Cdc2	Cdk cyclin-dependent protein kinase
34	Cct8	chaperonin-containing T-complex theta subunit
35	H4	histone H4 h4.2, histone H4 h4.1, histone H4 h4.3
36	Rpp101	60S acidic ribosomal protein
37	Rpp102	60S acidic ribosomal protein
38	Mug64	BAR domain protein; conserved fungal protein
39	SPBC29A10.16c	cytochrome b5
40	SPAC222.08c	glutamine aminotransferase subunit? negative genetic with Cut3 and DASH complex?
41	Grx4	glutaredoxin
42	Atp16	F1-ATPase delta subunit; oxidative phosphorylation
43	Apc15	anaphase-promoting complex subunit
44	Ypt1	GTPase Ypt1
45	SPCPB16A4.05c	predicted urease accessory protein UREG

#	protein	ontology
46	Rpl902	60S ribosomal protein L9
47	Rpp103	60S acidic ribosomal protein Rpp1-3
48	Cdc13	cyclin Cdc13
49	Sty1	MAP kinase
50	SPBP8B7.17c	predicted phosphomethylpyrimidine kinase; TENA/THI family protein;
51	Trp1	anthranilate synthase component II
52	Trx1	cytosolic thioredoxin
53	Cdc4	myosin II light chain; actomyosin contractile ring; cytokinesis
54	H3	histone H3.1/H3.2/H3.3
55	Rpt4	predicted 19S proteasome regulatory subunit
56	SPAP8A3.07c	predicted phospho-2-dehydro-3-deoxyheptonate aldolase
57	Ypt3	GTPase Ypt3
70	Nup211	nuclear pore complex associated protein
79	Mes1	meiotic anaphase II; APC inhibitor
93	Pht1	histone H2A variant
125	Spt16	FACT complex subunit
135	Cka1	kinase; TOR signaling cascade; cell polarity regulator
139	Sal3	karyopherin
163	Alp7	TACC/TOG protein; mcirotubule associated
175	Kap123	karyopherin
209	Alp14	TACC/TOG protein; mcirotubule associated
254	Nup61	nucleoporin
263	Pob3	FACT complex subunit
290	SPBC23G7.14	associates with APC: sequence orphan? fungal specific? mitochondrial?
300	SPAP32A8.03c	associates with APC: predicted: ubiquitin-protein ligase E3; RING finger domain protein
339	SPCC14G10.04	associates with APC: well-conserved fungal protein
344	SPCC4G3.13c	associates with APC: CUE domain protein; binds ubiquitin-conjugating enzymes?
443	Imp1	karyopherin
506	Nup60	nucleoporin
610	Nup40	nucleoporin
674	Kap95	karyopherin
732	Ndc80	kinetochore component; NDC80 complex subunit
759	Csi1	associates with Mad2: a Sad1 and Spc7 interactor
773	Spc7	kinetochore component; Blinkin and Spc105 orhologue
1102	Alm1	nuclear pore complex associated protein

Table 37: Ontology of 80 proteins (including the top 57) of *S.pombe* Mad, Bub and APC protein purifications, ranked as described in section 3.3.3.

7.3 *S.cerevisiae* MS data

Key for each hit, both from cycling and mitotically arrested cells: ***unique peptides / total peptides / % polypeptide coverage***

#	protein hit	kDa	Mad1			Mad2			Mad3			Bub1			Bub3			Apc4		
			cycling		arrest	cycling		arrest	cycling		arrest	cycling		arrest	cycling		arrest	cycling		arrest
2	Mad1	88	172	6331	79	210	3190	79	168	5210	76	215	1496	78	-	-	-	-	-	-	-	-	-	-	-	-	-	-	-	-
1	Mad2	22	42	991	77	45	488	90	71	2544	93	49	705	90	-	-	-	2	2	12	-	-	-	-	-	-	-	-	-	-
3	Mad3	60	-	-	-	-	-	-	-	-	-	-	9	8	42	1870	55	98	1587	75	-	-	-	-	-	-	-	-	-	-
18	Bub1	118	-	-	-	-	-	-	-	-	-	-	-	-	12	22	11	36	99	35	61	91	87	317	52	7	9	11	-	-	-
5	Bub3	38	-	-	-	-	-	-	-	-	-	2	4	11	20	368	51	44	340	81	8	21	19	26	75	61	1800	85	42	1153	66	-	-	-	-	-	-
26	Cdc20	67	-	-	-	-	-	-	3	3	7	16	26	33	-	-	-	5	9	11	-	-	-	-	-	-	6	7	13	3	7	8	-	-	-	-	-	-
20	Cdh1	63	-	-	-	-	-	-	-	-	-	-	-	-	-	-	-	-	-	-	-	-	-	-	-	-	-	-	-	-	-	22	42	45	16	21	37
11	Apc1	196	-	-	-	-	-	-	-	-	-	-	-	-	-	-	-	-	-	-	-	-	-	-	-	-	-	-	-	-	-	262	2414	73	273	1429	69
12	Apc5	79	-	-	-	-	-	-	-	-	-	-	-	-	-	-	-	-	-	-	-	-	-	-	-	-	-	-	-	-	-	93	841	74	92	781	65
8	Apc4	75	-	-	-	-	-	-	-	-	-	-	-	-	-	-	-	-	-	-	-	-	-	-	-	-	-	-	-	-	-	144	1647	85	113	727	81
10	Apc2	100	-	-	-	-	-	-	-	-	-	-	-	-	-	-	-	-	-	-	-	-	-	-	-	-	-	-	-	-	-	139	1289	77	125	648	76
13	Cdc27	85	-	-	-	-	-	-	-	-	-	-	-	-	-	-	-	-	-	-	-	-	-	-	-	-	-	-	-	-	-	114	882	71	100	543	68
9	Cdc16	95	-	-	-	-	-	-	-	-	-	-	-	-	-	-	-	-	-	-	-	-	-	-	-	-	-	-	-	-	-	182	2026	80	154	1159	77
6	Cdc23	73	-	-	-	-	-	-	-	-	-	-	-	-	-	-	-	-	-	-	-	-	-	-	-	-	-	-	-	-	-	124	1580	83	114	989	76
7	Doc1	29	-	-	-	-	-	-	-	-	-	-	-	-	-	-	-	-	-	-	-	-	-	-	-	-	-	-	-	-	-	30	380	80	22	119	74
16	Mnd2	43	-	-	-	-	-	-	-	-	-	-	-	-	-	-	-	-	-	-	-	-	-	-	-	-	-	-	-	-	-	41	218	58	32	104	49
17	Swm1	19	-	-	-	-	-	-	-	-	-	-	-	-	-	-	-	-	-	-	-	-	-	-	-	-	-	-	-	-	-	22	96	48	14	40	71
15	Apc9	31	-	-	-	-	-	-	-	-	-	-	-	-	-	-	-	-	-	-	-	-	-	-	-	-	-	-	-	-	-	34	238	58	27	90	57
14	Apc11	19	-	-	-	-	-	-	-	-	-	-	-	-	-	-	-	-	-	-	-	-	-	-	-	-	-	-	-	-	-	18	134	67	12	37	72
4	Cdc26	14	-	-	-	-	-	-	-	-	-	-	-	-	-	-	-	-	-	-	-	-	-	-	-	-	-	-	-	-	-	24	634	92	19	175	78
37	Mlp1	218	24	33	17	2	5	2	7	8	6	5	5	5	-	-	-	-	-	-	-	-	-	-	-	-	-	-	-	-	-	-	-	-	-	-	-
22	Mlp2	195	71	133	40	34	42	24	55	123	33	24	31	18	-	-	-	-	-	-	-	-	-	-	-	2	2	1	-	-	-	-	-	-	-	-	-
52	Nup2	78	2	5	6	-	-	-	-	-	-	-	-	-	-	-	-	-	-	-	-	-	-	-	-	-	-	-	-	-	-	-	-	-	-	-	-
19	Nop10	7	-	-	-	-	-	-	-	2	5	38	-	-	-	-	-	3	8	50	-	-	-	-	-	5	15	50	-	-	-	-	-	-	-	-	-	-
44	Kap95	95	2	3	3	-	-	-	4	8	9	-	-	-	-	-	-	-	-	-	-	-	-	-	-	-	-	-	-	-	-	-	-	-	-	-	-
21	Ded1	66	-	-	-	-	-	-	-	-	-	-	-	-	2	3	7	-	-	-	-	-	-	-	-	-	-	-	-	-	-	16	37	34	-	-	-
23	Sec53	29	-	-	-	-	-	-	-	-	-	-	-	-	2	4	9	-	-	-	-	-	-	-	-	-	-	-	-	-	-	6	15	23	-	-	-
24	Yhb1	45	-	-	-	-	-	-	-	-	-	2	2	8	-	-	-	-	-	-	-	-	-	-	-	-	-	-	-	-	-	8	13	34	4	6	18
25	Sam1	42	-	-	-	-	-	-	-	-	-	-	-	-	-	-	-	-	-	-	-	-	-	-	-	2	4	6	-	-	-	8	19	23	2	3	8
27	Bmh1	30	-	-	-	-	-	-	-	-	-	-	-	-	-	-	-	-	-	-	-	-	-	-	-	-	-	-	-	-	-	3	6	14	3	8	18
28	Bmh2	31	-	-	-	-	-	-	-	-	-	-	-	-	-	-	-	-	-	-	-	-	-	-	-	3	5	17	-	-	-	3	6	14	3	8	17
29	Nap1	48	-	-	-	-	-	-	-	-	-	-	-	-	-	-	-	-	-	-	-	-	-	-	-	-	-	-	-	-	-	5	10	21	-	-	-
30	Lys21	49	-	-	-	3	6	10	3	10	11	-	-	-	-	-	-	-	-	-	-	-	-	-	-	-	-	-	-	-	-	-	-	-	-	-	-
31	Tub1	50	-	-	-	-	-	-	-	-	-	-	-	-	-	-	-	-	-	-	-	-	-	-	-	-	-	-	-	-	-	4	8	17	3	4	10
32	Gcd7	43	-	-	-	-	-	-	-	-	-	-	-	-	-	-	-	-	-	-	-	-	-	-	-	-	-	-	-	-	-	5	8	21	6	7	26
33	Hel2	73	-	-	-	-	-	-	-	-	-	-	-	-	-	-	-	-	-	-	-	-	-	-	-	-	-	-	-	-	-	3	23	4	-	-	-
34	Sod1	16	2	3	18	-	-	-	-	-	-	-	-	-	-	-	-	-	-	-	-	-	-	-	-	-	-	-	-	-	-	-	-	-	-	-	-
35	Rex4	33	-	-	-	-	-	-	-	-	-	-	-	-	-	-	-	-	-	-	-	-	-	-	-	-	-	-	-	-	-	-	-	-	3	-	25
36	Trx1	11	-	-	-	-	-	-	-	-	-	-	-	-	-	-	-	2	2	24	-	-	-	-	-	-	-	-	-	-	-	-	-	-	3	-	-
38	YIL002W-A	8	-	-	-	2	3	15	-	-	-	-	-	-	-	-	-	-	-	-	-	-	-	-	-	-	-	-	-	-	-	-	-	-	-	-	-

			cycling			arrest			cycling			arrest			cycling			arrest			cycling			arrest			cycling			arrest		
#	protein hit	kDa	Mad1						Mad2						Mad3						Bub1						Bub3						Apc4		
39	Wtm1	48	4	8	11	-	-	-	3	3	8	-	-	-	-	-	-	-	-	-	-	-	-	-	-	-	-	-	-	-	-	-	-
40	Phb1	31	-	-	-	-	-	-	-	-	-	-	-	-	-	-	-	-	-	-	-	-	-	-	-	-	-	-	-	-	-	2	2	21
41	Hxt4	62	-	-	-	-	-	-	-	-	-	-	-	-	-	-	-	-	-	-	-	-	-	-	-	-	-	-	-	-	-	3	6	10
42	Fpr3	47	-	-	-	-	-	-	3	5	12	-	-	-	-	-	-	4	6	12	-	-	-	-	-	-	4	5	12	-	-	-	2	3	9
43	Rpc40	38	-	-	-	-	-	-	-	-	-	-	-	-	2	2	7	-	-	-	-	-	-	-	-	-	-	-	-	-	-	4	4	19	-	-	-
45	Lyp1	68	-	-	-	-	-	-	-	-	-	-	-	-	-	-	-	-	-	-	-	-	-	-	-	-	-	-	-	-	-	-	2	5	7
46	Pre5	26	-	-	-	-	-	-	-	-	-	-	-	-	-	-	-	-	-	-	-	-	-	-	-	-	-	-	-	-	-	2	2	17	-	-	-
47	Yhm2	34	-	-	-	-	-	-	-	-	-	-	-	-	-	-	-	-	-	-	-	-	-	-	-	-	-	-	-	-	-	-	-	-	2	3	11
48	Gln1	42	-	-	-	-	-	-	-	-	-	-	-	-	-	-	-	-	-	-	-	-	-	-	-	-	-	-	-	-	-	2	2	7	2	2	16
49	Tma16	21	-	-	-	-	-	-	-	-	-	-	-	-	2	2	15	-	-	-	-	-	-	-	-	-	-	-	-	-	-	-	-	-	-	-	-
50	Pho84	64	-	-	-	-	-	-	-	-	-	-	-	-	-	-	-	-	-	-	-	-	-	-	-	-	-	-	-	-	-	-	-	-	3	5	9
51	Rrs1	23	-	-	-	-	-	-	-	-	-	-	-	-	-	-	-	-	-	-	-	-	-	-	-	-	2	2	14	-	-	-	-	-	-	-	-
53	Cbp6	19	-	-	-	2	2	14	-	-	-	-	-	-	-	-	-	-	-	-	-	-	-	-	-	-	-	-	-	-	-	-	-	-	-	-	-
54	Ifa38	39	-	-	-	-	-	-	-	-	-	-	-	-	-	-	-	-	-	-	-	-	-	-	-	-	-	-	-	-	-	-	-	-	2	2	14
55	Rxt2	49	-	-	-	-	-	-	-	-	-	-	-	-	-	-	-	-	-	-	-	-	-	-	-	-	2	4	7	-	-	-	-	-	-	-	-
56	Rpa49	47	-	-	-	-	-	-	-	-	-	-	-	-	-	-	-	-	-	-	-	-	-	-	-	-	3	3	13	-	-	-	-	-	-	-	-
57	Gnd2	54	-	-	-	-	-	-	-	-	-	-	-	-	-	-	-	-	-	-	-	-	-	-	-	-	-	-	-	-	-	-	4	7	7	-	-	-
58	Sam2	42	-	-	-	-	-	-	-	-	-	-	-	-	-	-	-	-	-	-	-	-	-	-	-	-	2	4	6	-	-	-	-	-	-	-	-
59	Rnr2	46	2	2	12	-	-	-	-	-	-	-	-	-	-	-	-	-	-	-	-	-	-	-	-	-	-	-	-	-	-	-	-	-	-	-	-
60	Snz1	32	-	-	-	-	-	-	-	-	-	-	-	-	-	-	-	-	-	-	-	-	-	-	-	-	2	3	8	-	-	-	-	-	-	-	-
61	Ipp1	32	-	-	-	-	-	-	-	-	-	-	-	-	-	-	-	-	-	-	-	-	-	-	-	-	-	-	-	-	-	-	-	-	2	2	12
62	Kgd2	50	-	-	-	-	-	-	3	4	9	-	-	-	-	-	-	-	-	-	-	-	-	-	-	-	-	-	-	-	-	-	-	-	-	-	-
63	Snu66	66	-	-	-	-	-	-	-	-	-	-	-	-	-	-	-	-	-	-	-	-	-	-	-	-	-	-	-	-	-	3	4	8	-	-	-
64	Ubp12	143	-	-	-	-	-	-	-	-	-	-	-	-	-	-	-	3	8	4	-	-	-	-	-	-	-	-	-	-	-	-	-	-	-	-	-	-
65	Etp1	68	-	-	-	-	-	-	2	3	7	-	-	-	-	-	-	-	-	-	-	-	-	-	-	-	2	2	6	-	-	-	-	-	-	-	-	-
66	Fol2	28	-	-	-	-	-	-	-	-	-	-	-	-	-	-	-	2	2	10	-	-	-	-	-	-	-	-	-	-	-	-	-	-	-	-	-	-
67	Lat1	52	-	-	-	-	-	-	-	-	-	-	-	-	-	-	-	2	2	6	-	-	-	-	-	-	2	3	6	-	-	-	-	-	-	-	-	-
68	Brx1	34	-	-	-	-	-	-	-	-	-	-	-	-	-	-	-	-	-	-	-	-	-	-	-	-	-	-	-	-	-	-	2	2	9	-	-	-
69	Aac3	33	-	-	-	-	-	-	-	-	-	-	-	-	-	-	-	-	-	-	-	-	-	-	-	-	-	-	-	-	-	-	-	-	2	3	6
70	Dbp3	59	-	-	-	-	-	-	-	-	-	2	3	6	-	-	-	-	-	-	-	-	-	-	-	-	-	-	-	-	-	-	-	-	-	-	-	-
71	Cic1	43	-	-	-	-	-	-	-	-	-	-	-	-	-	-	-	2	2	9	-	-	-	-	-	-	-	-	-	-	-	-	-	-	-	-	-	-
72	Etr1	42	2	2	9	-	-	-	-	-	-	-	-	-	-	-	-	-	-	-	-	-	-	-	-	-	-	-	-	-	-	-	-	-	-	-	-
73	Ilv5	44	-	-	-	-	-	-	-	-	-	-	-	-	-	-	-	2	2	5	-	-	-	-	-	-	-	-	-	-	-	-	3	3	9	2	2	7
74	Ado1	36	-	-	-	-	-	-	-	-	-	-	-	-	-	-	-	-	-	-	-	-	-	-	-	-	-	-	-	-	-	-	-	-	2	2	9
75	Rvb1	50	-	-	-	-	-	-	-	-	-	-	-	-	-	-	-	-	-	-	-	-	-	-	-	-	-	-	-	-	-	3	3	8	-	-	-
76	Srp54	60	-	-	-	-	-	-	-	-	-	-	-	-	2	3	6	3	3	8	-	-	-	-	-	-	2	2	6	-	-	-	-	-	-	-	-
77	Tod6	59	-	-	-	-	-	-	-	-	-	2	2	8	-	-	-	-	-	-	-	-	-	-	-	-	-	-	-	-	-	-	-	-	-	-	-	-
78	Pct1	49	-	-	-	-	-	-	-	-	-	-	-	-	-	-	-	-	-	-	-	-	-	-	-	-	-	-	-	-	-	2	3	5	-	-	-
79	Pyc1	130	-	-	-	-	-	-	-	-	-	-	-	-	-	-	-	-	-	-	-	-	-	-	-	-	-	-	-	-	-	3	5	5	-	-	-
80	Gup1	65	-	-	-	-	-	-	-	-	-	-	-	-	-	-	-	-	-	-	-	-	-	-	-	-	2	4	4	-	-	-	-	-	-	-	-

7.4 *S.cerevisiae* MS protein hit ontology

#	protein	ontology
1	Mad2	mitotic spindle checkpoint protein
2	Mad1	mitotic spindle checkpoint protein
3	Mad3	mitotic spindle checkpoint protein
4	Cdc26	subunit of the E3 ubiquitin ligase anaphase-promoting complex (APC)
5	Bub3	mitotic spindle checkpoint protein
6	Cdc23	subunit of the E3 ubiquitin ligase anaphase-promoting complex (APC)
7	Doc1	subunit of the E3 ubiquitin ligase anaphase-promoting complex (APC)
8	Apc4	subunit of the E3 ubiquitin ligase anaphase-promoting complex (APC)
9	Cdc16	subunit of the E3 ubiquitin ligase anaphase-promoting complex (APC)
10	Apc2	subunit of the E3 ubiquitin ligase anaphase-promoting complex (APC)
11	Apc1	subunit of the E3 ubiquitin ligase anaphase-promoting complex (APC)
12	Apc5	subunit of the E3 ubiquitin ligase anaphase-promoting complex (APC)
13	Cdc27	subunit of the E3 ubiquitin ligase anaphase-promoting complex (APC)
14	Apc11	subunit of the E3 ubiquitin ligase anaphase-promoting complex (APC)
15	Apc9	subunit of the E3 ubiquitin ligase anaphase-promoting complex (APC)
16	Mnd2	subunit of the E3 ubiquitin ligase anaphase-promoting complex (APC)
17	Swm1	subunit of the E3 ubiquitin ligase anaphase-promoting complex (APC)
18	Bub1	mitotic spindle checkpoint protein
19	Nop10	constituent of small nucleolar ribonucleoprotein particles
20	Cdh1	cell-cycle regulated activator of anaphase-promoting complex (APC)
21	Ded1	ATP-dependent DEAD-box RNA helicase, required for translation initiation
22	Mlp2	myosin-like protein (MLP) associated with the nuclear envelope
23	Sec53	phosphomannomutase, involved in synthesis of GDP-mannose
24	Yhb1	nitric oxide oxidoreductase
25	Sam1	S-adenosylmethionine synthetase
26	Cdc20	cell-cycle regulated activator of anaphase-promoting complex (APC)
27	Bmh1	14-3-3 protein; controls proteome at post-transcriptional level
28	Bmh2	14-3-3 protein; controls proteome at post-transcriptional level
29	Nap1	regulation of microtubule dynamics and bud morphology
30	Lys21	homocitrate synthase isozyme
31	Tub1	α-tubulin
32	Gcd7	subunit of the translation initiation factor eIF2B
33	Hel2	RING finger E3 ubiquitin ligase
34	Sod1	cytosolic copper-zinc superoxide dismutase
35	Rex4	putative RNA exonuclease
36	Trx1	cytoplasmic thioredoxin
37	Mlp1	myosin-like protein (MLP) associated with the nuclear envelope
38	YIL002W-A	protein of unknown function
39	Wtm1	transcriptional modulator
40	Phb1	subunit of the prohibitin complex
41	Hxt4	glucose transporter
42	Fpr3	nucleolar peptidyl-prolyl cis-trans isomerase
43	Rpc40	RNA polymerase I and III subunit
44	Kap95	karyopherin beta, mediates nuclear import
45	Lyp1	lysine permease

#	protein	ontology
46	Pre5	subunit of the 20S proteasome
47	Yhm2	mitochondrial DNA-binding protein
48	Gln1	glutamine synthetase
49	Tma16	protein of unknown function
50	Pho84	inorganic phosphate transporter
51	Rrs1	nuclear export of pre-ribosomal subunits
52	Nup2	nucleoporin involved in nucleocytoplasmic transport
53	Cbp6	mitochondrial translational activator
54	Ifa38	β-keto-reductase
55	Rxt2	subunit of the histone deacetylase Rpd3L complex
56	Rpa49	RNA polymerase I subunit
57	Gnd2	6-phosphogluconate dehydrogenase
58	Sam2	S-adenosylmethionine synthetase
59	Rnr2	ribonucleotide-diphosphate reductase
60	Snz1	protein involved in vitamin B6 biosynthesis
61	Ipp1	cytoplasmic inorganic pyrophosphatase
62	Kgd2	component of the mitochondrial alpha-ketoglutarate dehydrogenasecomplex
63	Snu66	component of the snRNP complex involved in pre-mRNA splicing via spliceosome
64	Ubp12	ubiquitin carboxyl-terminal hydrolase
65	Etp1	protein of unknown function
66	Fol2	GTP-cyclohydrolase I
67	Lat1	dihydrolipoamide acetyltransferase component
68	Brx1	constituent of 66S pre-ribosomal particles
69	Aac3	mitochondrial inner membrane ADP/ATP translocator
70	Dbp3	RNA-dependent ATPase
71	Cic1	proteasome regulator
72	Etr1	2-enoyl thioester reductase
73	Ilv5	acetohydroxyacid reductoisomerase
74	Ado1	adenosine kinase
75	Rvb1	transcriptional regulation
76	Srp54	subunit of signal recognition particle
77	Tod6	protein involved in rRNA and ribosome biogenesis
78	Pct1	cholinephosphate cytidylyltransferase
79	Pyc1	pyruvate carboxylase
80	Gup1	GPI anchor remodeller

Table 38: Ontology of the top 80 proteins of *S.cerevisiae* Mad, Bub and APC protein purifications, ranked as described in section 3.3.3.

7.5 Multiple sequence alignments

Multiple sequence alignments of *S.pombe*, *S.cerevisiae*, *S.japonicus*, *X.laevis* and human spindle checkpoint proteins and Slp1/Cdc20 (details in Table 39) were created in Clustal Ω (v1.1.0; http://www.ebi.ac.uk/tools/msa/clustalo) using default parameters. Shading of residues by similarity according to amino acid physico-chemical properties (for at least 4 out of 5 aligned residues) was applied using BoxShade software (v3.21; http://sourceforge.net/

projects/boxshade). In addition, *S.pombe* and *S.cerevisiae* residues that are identified by mass spectrometry as phospho-modified (see Table 21 and Table 22) are highlighted in yellow.

#	species	Slp1/Cdc20	Mad1	Mad2	Mad3	Bub1	Bub3
1	*S.pombe*	NP_593161.1	NP_595516.1	NP_596370.1	NP_588043.2	NP_588140.1	NP_593798.1
2	*S.cerevisiae*	NP_011399.1	NP_011429.3	NP_012504.3	NP_012521.3	NP_011704.3	NP_014669.1
3	*S.japonicus*	XP_002171937.1	XP_002175955.1	XP_002172580.1	XP_002175784.1	XP_002172349.1	XP_002173655.1
4	*X.laevis*	NP_001079443.1	AAD25081	NP_001081096.1	NP_001079357.1	AAK12628.1	NP_001083768.1
5	*H.sapiens*	NP_001246.2	NP_003541.2	NP_002349.1	NP_001202.4	NP_004327.1	NP_004716.1

Table 39: NCBI reference or GenBank numbers of spindle checkpoint proteins and Slp1/Cdc20 orthologues used for preparation of multiple sequence alignments.

7.5.1 Mad2 orthologues

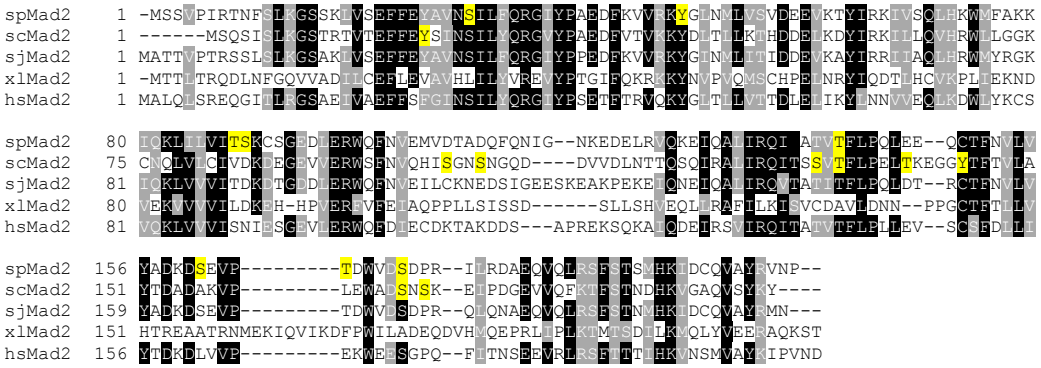

7.5.2 Mad1 orthologues

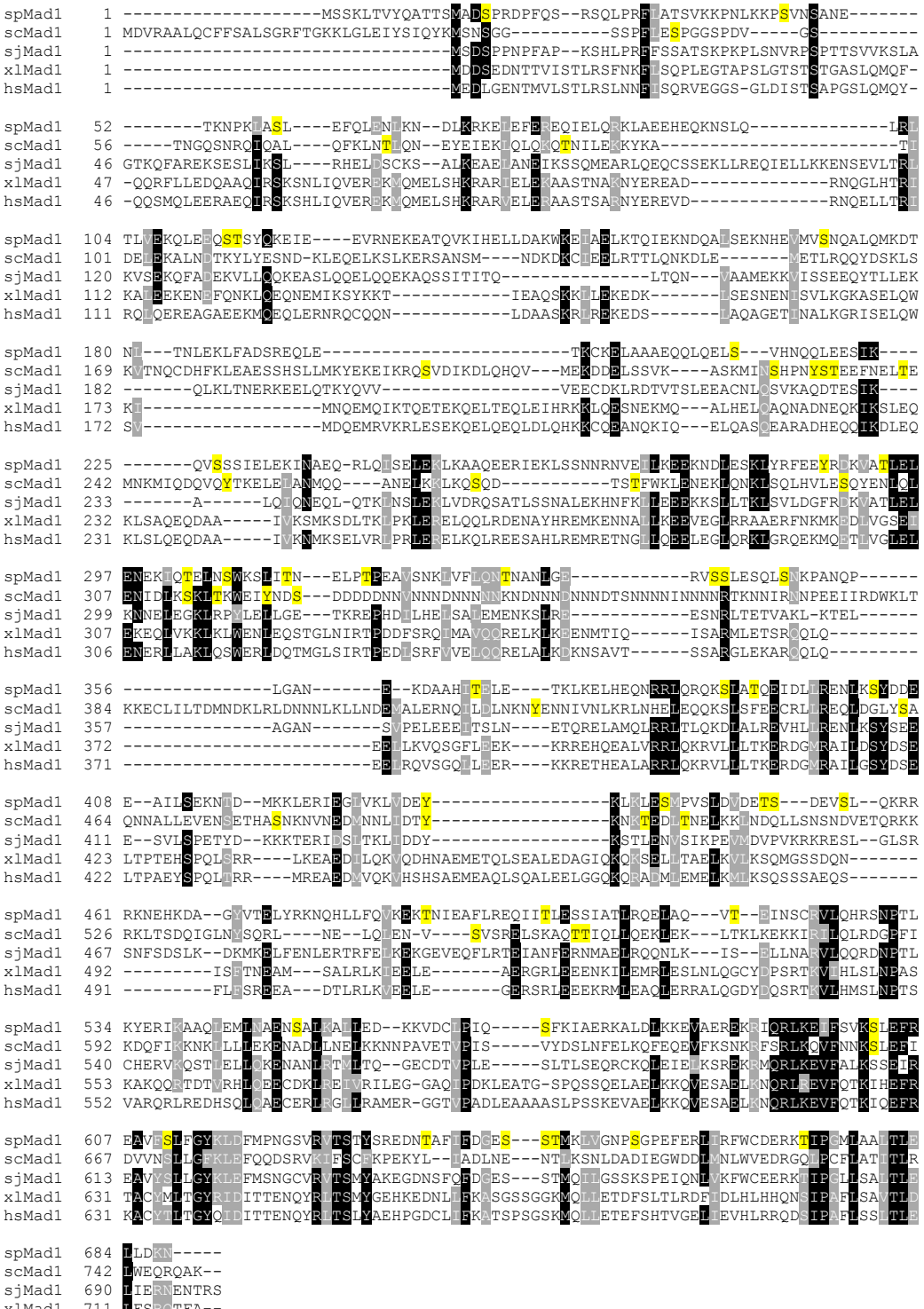

7.5.3 Mad3 orthologues

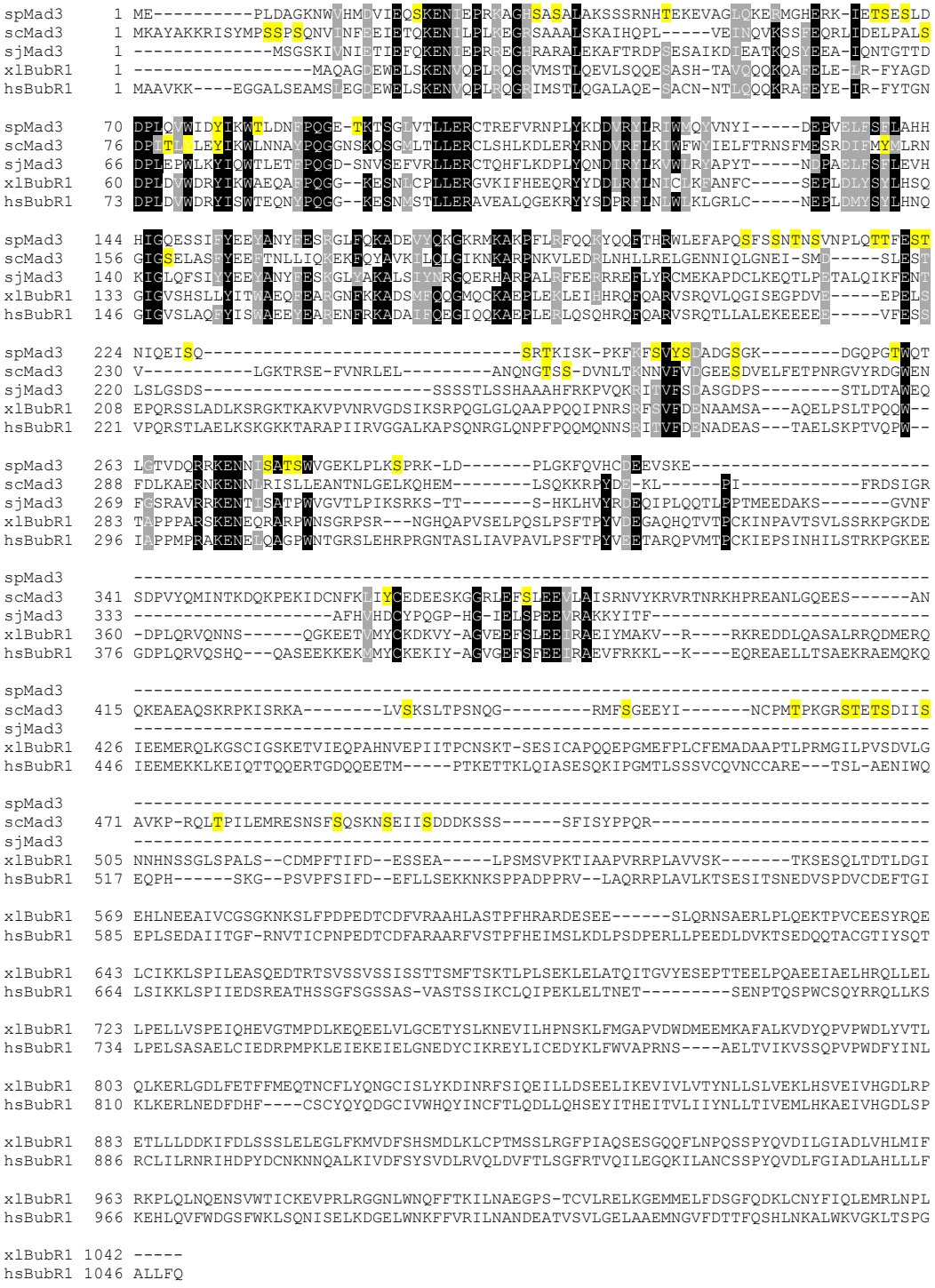

7.5.4 Bub3 orthologues

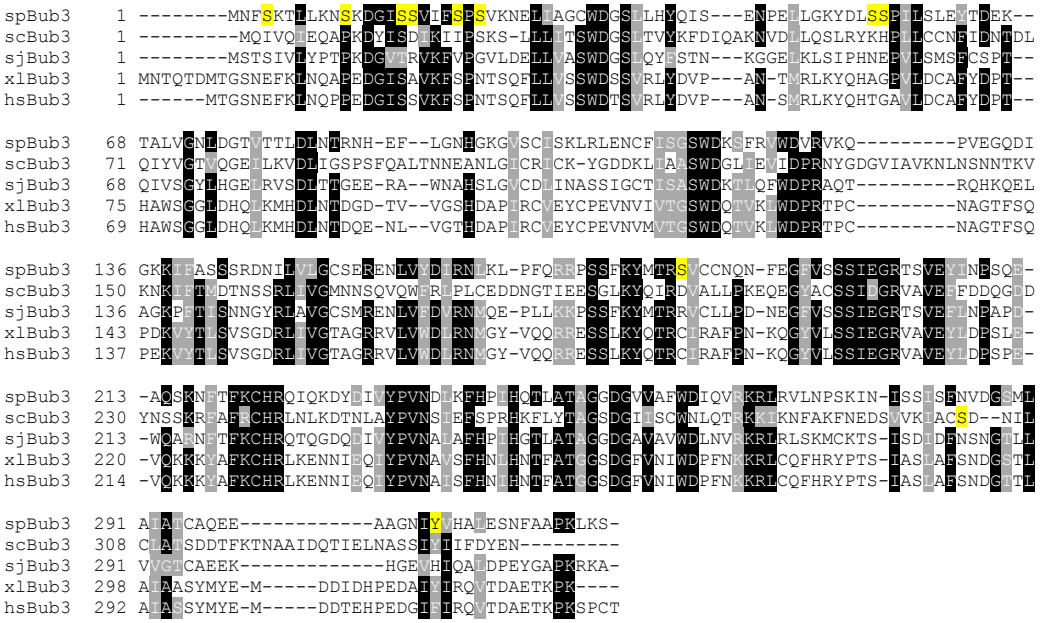

7.5.5 Slp1/Cdc20 orthologues

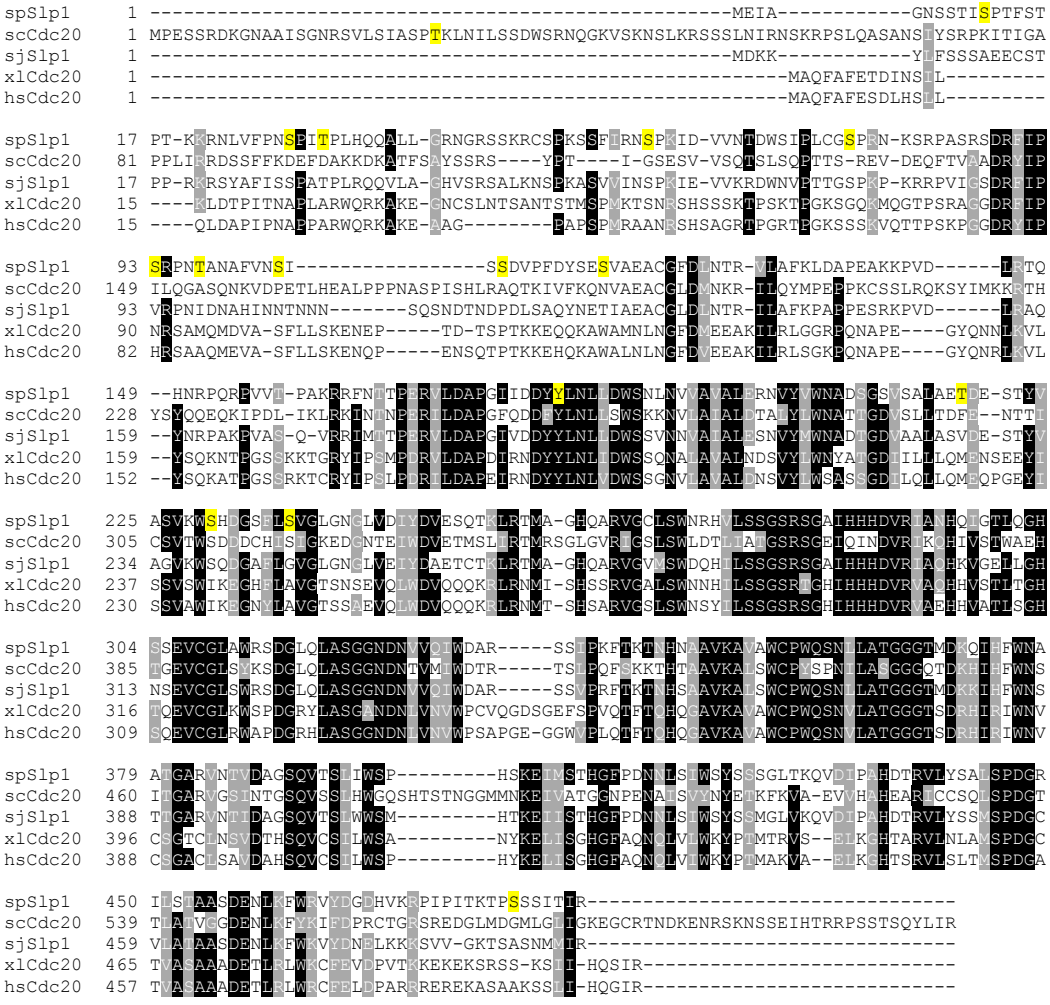

7.5.6 Bub1 orthologues

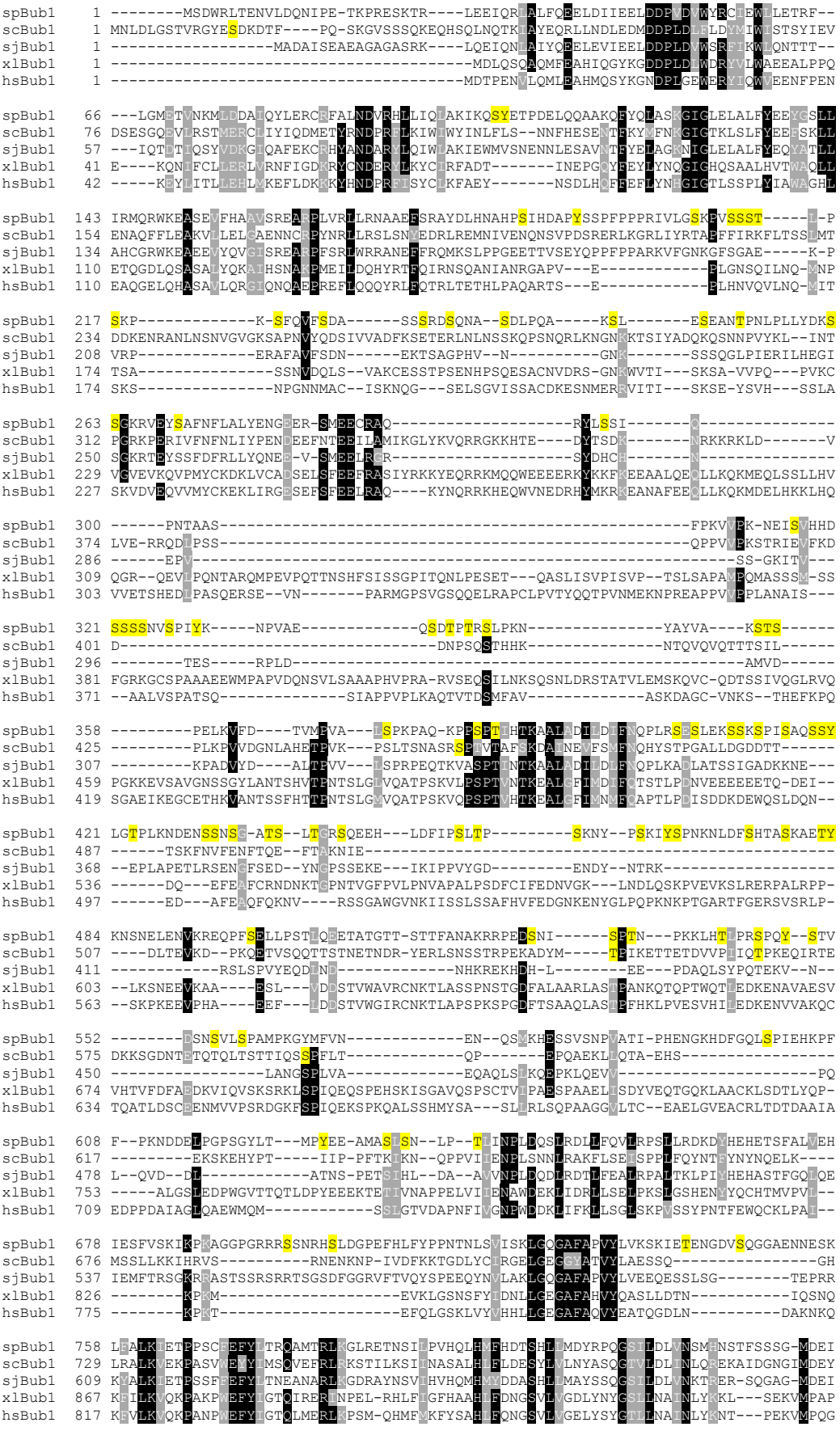

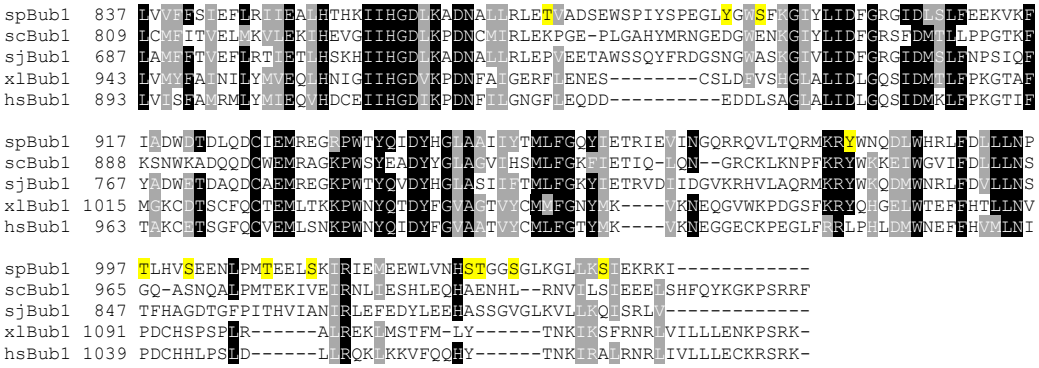

7.6 *In vitro* cross-linked residues of protein complexes identified by tandem MS

Table 40: Proximate lysine – lysine residues that are identified by MS analysis of *in vitro* cross-linked protein complexes (chapter 4.3): *S.cerevisiae* NDC80 complex (#1-25) and Mad1 – Mad2 (26-59), *S.pombe* Bub1 – Bub3 (60-85) and Mad1 – Mad2 (86-179). Cross-links were grouped by virtue of their structural implications.

#	subunit I	residue number	subunit II	residue number	spectra	group	Comments
	***S.cerevisiae* Ndc80 complex**						
1	Ndc80	48	Ndc80	67	1	A	within protein
2	Ndc80	48	Ndc80	69	3	A	within protein
3	Ndc80	404	Ndc80	409	1	A	within protein
4	Ndc80	445	Ndc80	448	5	A	within protein
5	Ndc80	548	Ndc80	554	1	A	within protein
6	Ndc80	598	Ndc80	602	15	A	within protein
7	Ndc80	602	Ndc80	613	1	A	within protein
8	Nuf2	388	Nuf2	393	2	A	within protein
9	Spc24	32	Spc24	42	2	A	within protein
10	Spc24	42	Spc24	98	1	C	within protein
11	Spc24	62	Spc24	98	1	C	within protein
12	Spc24	98	Spc24	163	3	C	within protein
13	Spc24	98	Spc24	205	1	C	within protein
14	Ndc80	377	Nuf2	220	1	B	between proteins
15	Ndc80	425	Nuf2	270	1	B	between proteins
16	Ndc80	577	Nuf2	366	2	B	between proteins
17	Ndc80	582	Nuf2	360	2	B	between proteins
18	Ndc80	582	Nuf2	366	1	B	between proteins
19	Ndc80	602	Nuf2	388	2	B	between proteins
20	Ndc80	602	Nuf2	393	1	B	between proteins
21	Ndc80	611	Nuf2	393	3	B	between proteins
22	Ndc80	627	Nuf2	409	1	B	between proteins
23	Ndc80	627	Nuf2	415	5	B	between proteins
24	Spc24	98	Spc25	19	1	D	between proteins
25	Spc24	163	Spc25	19	1	D	between proteins
	***S.cerevisiae* Mad1 – Mad2 complex**						
26	Mad1	94	Mad1	97	1	C	within or between proteins
27	Mad1	95	Mad1	97	1	C	between proteins
28	Mad1	119	Mad1	119	1	C	between proteins
29	Mad1	119	Mad1	128	8	C	within or between proteins
30	Mad1	152	Mad1	152	3	C	between proteins
31	Mad1	193	Mad1	405	1	D	within or between proteins
32	Mad1	268	Mad1	271	9	C	within or between proteins
33	Mad1	269	Mad1	271	3	C	between proteins
34	Mad1	314	Mad1	366	5	D	within or between proteins
35	Mad1	366	Mad1	366	1	C	between proteins
36	Mad1	366	Mad1	381	21	C	within or between proteins

#	subunit I	residue number	subunit II	residue number	spectra	group	Comments
37	Mad1	366	Mad1	385	1	C	within or between proteins
38	Mad1	366	Mad1	527	2	D	within or between proteins
39	Mad1	366	Mad1	557	17	D	within or between proteins
40	Mad1	366	Mad1	571	9	D	within or between proteins
41	Mad1	366	Mad1	574	2	D	within or between proteins
42	Mad1	405	Mad1	527	2	D	within or between proteins
43	Mad1	423	Mad1	527	4	D	within or between proteins
44	Mad1	433	Mad1	507	1	D	within or between proteins
45	Mad1	433	Mad1	527	3	D	within or between proteins
46	Mad1	495	Mad1	506	2	C	within or between proteins
47	Mad1	507	Mad1	527	3	C	within or between proteins
48	Mad1	524	Mad1	527	9	C	within or between proteins
49	Mad1	525	Mad1	527	8	C	within or between proteins
50	Mad1	527	Mad1	527	14	C	between proteins
51	Mad1	592	Mad1	592	1	C	between proteins
52	Mad1	592	Mad1	598	34	C	within or between proteins
53	Mad1	592	Mad1	600	20	C	within or between proteins
54	Mad1	592	Mad1	655	1	B	within or between proteins
55	Mad1	597	Mad1	600	8	C	within or between proteins
56	Mad1	598	Mad1	600	20	C	between proteins
57	Mad1	592	Mad2	61	15	A	between proteins
58	Mad1	649	Mad2	56	7	B	between proteins
59	Mad1	649	Mad2	61	1	B	between proteins
	***S.pombe* Bub1 – Bub3 complex**						
60	Bub1	19	Bub3	167	1	B	between proteins
61	Bub1	316	Bub3	9	1	A	between proteins
62	Bub1	321	Bub3	9	1	A	between proteins
63	Bub1	321	Bub3	12	1	A	between proteins
64	Bub1	19	Bub1	149	2	E	within protein
65	Bub1	19	Bub1	347	1	E	within protein
66	Bub1	103	Bub1	149	1	C	within protein
67	Bub1	117	Bub1	149	1	C	within protein
68	Bub1	347	Bub1	493	2	E	within protein
69	Bub1	408	Bub1	418	1	D	within protein
70	Bub1	408	Bub1	484	1	E	within protein
71	Bub1	409	Bub1	420	1	D	within protein
72	Bub1	411	Bub1	443	1	D	within protein
73	Bub1	443	Bub1	463	1	D	within protein
74	Bub1	462	Bub1	465	1	D	within protein
75	Bub1	463	Bub1	479	1	D	within protein
76	Bub1	463	Bub1	493	2	D	within protein
77	Bub1	479	Bub1	493	5	D	within protein
78	Bub1	493	Bub1	537	1	D	within protein
79	Bub1	493	Bub1	538	1	D	within protein
80	Bub1	523	Bub1	537	1	D	within protein
81	Bub1	565	Bub1	578	1	D	within protein
82	Bub1	586	Bub1	600	2	D	within protein
83	Bub1	686	Bub1	737	1	D	within protein
84	Bub1	722	Bub1	737	2	D	within protein
85	Bub1	863	Bub1	913	1	D	within protein
	***S.pombe* Mad1 – Mad2 complex**						
86	Mad1	534	Mad2	66	2	E	between proteins
87	Mad1	601	Mad2	43	1	F	between proteins
88	Mad1	649	Mad2	126	1	F	between proteins
89	Mad1	26	Mad1	96	4	H	within or between proteins
90	Mad1	38	Mad1	43	1	G	within or between proteins
91	Mad1	38	Mad1	72	1	G	within or between proteins
92	Mad1	43	Mad1	47	1	G	within or between proteins
93	Mad1	43	Mad1	74	1	G	within or between proteins

#	subunit I	residue number	subunit II	residue number	spectra	group	Comments
94	Mad1	53	Mad1	68	1	G	within or between proteins
95	Mad1	68	Mad1	74	3	G	within or between proteins
96	Mad1	72	Mad1	128	1	H	within or between proteins
97	Mad1	72	Mad1	74	1	G	within or between proteins
98	Mad1	72	Mad1	96	1	G	within or between proteins
99	Mad1	74	Mad1	128	1	H	within or between proteins
100	Mad1	74	Mad1	134	1	H	within or between proteins
101	Mad1	88	Mad1	96	20	G	between proteins
102	Mad1	96	Mad1	128	2	G	within or between proteins
103	Mad1	96	Mad1	582	1	H	within or between proteins
104	Mad1	118	Mad1	126	1	G	within or between proteins
105	Mad1	128	Mad1	142	1	G	within or between proteins
106	Mad1	128	Mad1	144	1	G	within or between proteins
107	Mad1	134	Mad1	144	3	G	within or between proteins
108	Mad1	134	Mad1	155	1	G	within or between proteins
109	Mad1	142	Mad1	144	1	G	between proteins
110	Mad1	142	Mad1	150	1	G	within or between proteins
111	Mad1	144	Mad1	150	1	G	between proteins
112	Mad1	144	Mad1	155	1	G	within or between proteins
113	Mad1	177	Mad1	186	1	G	between proteins
114	Mad1	179	Mad1	186	1	G	between proteins
115	Mad1	234	Mad1	259	1	G	within or between proteins
116	Mad1	248	Mad1	259	1	G	within or between proteins
117	Mad1	250	Mad1	259	1	G	within or between proteins
118	Mad1	250	Mad1	271	1	G	within or between proteins
119	Mad1	250	Mad1	280	1	G	within or between proteins
120	Mad1	259	Mad1	271	15	G	within or between proteins
121	Mad1	259	Mad1	274	2	G	within or between proteins
122	Mad1	259	Mad1	280	4	G	within or between proteins
123	Mad1	259	Mad1	287	1	G	within or between proteins
124	Mad1	259	Mad1	290	3	G	within or between proteins
125	Mad1	259	Mad1	429	1	H	within or between proteins
126	Mad1	259	Mad1	534	2	H	within or between proteins
127	Mad1	259	Mad1	576	2	H	within or between proteins
128	Mad1	259	Mad1	581	1	H	within or between proteins
129	Mad1	271	Mad1	280	2	G	between proteins
130	Mad1	271	Mad1	576	1	H	within or between proteins
131	Mad1	271	Mad1	581	1	H	within or between proteins
132	Mad1	274	Mad1	280	4	G	between proteins
133	Mad1	279	Mad1	280	1	G	between proteins
134	Mad1	280	Mad1	287	3	G	within or between proteins
135	Mad1	280	Mad1	534	1	H	within or between proteins
136	Mad1	290	Mad1	529	1	H	within or between proteins
137	Mad1	361	Mad1	374	4	G	within or between proteins
138	Mad1	371	Mad1	374	1	G	within or between proteins
139	Mad1	372	Mad1	387	1	G	within or between proteins
140	Mad1	372	Mad1	414	1	G	within or between proteins
141	Mad1	372	Mad1	458	1	H	within or between proteins
142	Mad1	372	Mad1	466	1	H	within or between proteins
143	Mad1	374	Mad1	414	1	H	within or between proteins
144	Mad1	374	Mad1	458	2	H	within or between proteins
145	Mad1	348	Mad1	350	1	G	between proteins
146	Mad1	348	Mad1	462	1	H	within or between proteins
147	Mad1	387	Mad1	402	1	G	within or between proteins
148	Mad1	387	Mad1	429	2	G	within or between proteins
149	Mad1	387	Mad1	437	1	H	within or between proteins
150	Mad1	387	Mad1	462	1	H	within or between proteins
151	Mad1	387	Mad1	534	1	H	within or between proteins
152	Mad1	420	Mad1	429	1	G	within or between proteins

#	subunit I	residue number	subunit II	residue number	spectra	group	Comments
153	Mad1	420	Mad1	477	1	H	within or between proteins
154	Mad1	420	Mad1	486	1	H	within or between proteins
155	Mad1	429	Mad1	435	1	G	between proteins
156	Mad1	429	Mad1	458	1	G	within or between proteins
157	Mad1	435	Mad1	466	1	G	within or between proteins
158	Mad1	435	Mad1	470	2	G	within or between proteins
159	Mad1	435	Mad1	475	1	G	within or between proteins
160	Mad1	435	Mad1	477	1	G	within or between proteins
161	Mad1	458	Mad1	466	2	G	within or between proteins
162	Mad1	458	Mad1	470	1	G	within or between proteins
163	Mad1	462	Mad1	477	2	G	within or between proteins
164	Mad1	466	Mad1	529	1	H	within or between proteins
165	Mad1	477	Mad1	529	3	H	within or between proteins
166	Mad1	521	Mad1	534	1	G	within or between proteins
167	Mad1	529	Mad1	539	1	G	within or between proteins
168	Mad1	534	Mad1	539	1	G	within or between proteins
169	Mad1	534	Mad1	560	1	G	within or between proteins
170	Mad1	534	Mad1	582	4	G	within or between proteins
171	Mad1	539	Mad1	539	2	G	between proteins
172	Mad1	539	Mad1	576	2	G	within or between proteins
173	Mad1	539	Mad1	582	3	H	within or between proteins
174	Mad1	560	Mad1	595	2	G	within or between proteins
175	Mad1	576	Mad1	581	13	G	between proteins
176	Mad1	576	Mad1	582	1	G	between proteins
177	Mad1	581	Mad1	595	1	G	within or between proteins

7.7 ClustalΩ sequence alignment of Abo1/Yta7 paralogues and orthologues

The approximate position of the first AAA family ATPase domain of *S.pombe* Abo1, *S.cerevisiae* Yta7, *C.elegans* Lex-1 and human ATAD2 is shaded in red, the second domain in orange and the bromodomain in blue.

```
spAbo1   ------------------------------------------------MK---------------------------- 2
spAbo2   ------------------------------------------MRRRARSIRFSSDDNEDNE-EDDDYYS--NAHSE 31
scYta7   ------------------------------------------MARNLRNRRG-SDVEDASN-AKVGYET--QIKDE 30
sjAbo1   ------------------------------------------MESSS---SSNDENVTE-VDDDE--------- 19
sjAbo2   ------------------------------------------MPMEPSDEES-ENV------ADEGEQS------- 20
ceLEX1   ------------------------MPRSDG----FSP-RKNLRRSARDHSR-SYAGQCNEDFDDMYAPSSRRRSS 45
hsATAD2  MVVL-RSSLELHNHS-----------AASATGSLDLSSDFLSLEHIGRRRL--RSA-GAAQKK---------PAATT 53
hsATAD2B MVNTRKSSLRLLGSKSPGPGPGPG--AGAEPGATGGSSHFISSRTRS-------SK-TRAASC----------PAAKA 58
mmATAD2  ------------------------------------------------------------------------------ 0
mmATAD2B MVNTRKSSLRLLGSKSPGPGPGPGAGAGAEPGATGGSSHFISSRTRS-------SK-TRAASC----------PAAKA 60

spAbo1   ----------------------E----------------------E---------------------------------- 4
spAbo2   KSEDHSN-HIKVSHFDPSSYKQKLV-------------SVRETQR-------------------NRKFS-SLQKH--LN- 74
scYta7   NGII----HTTTRSLRKINYAE-------------------I-------------------EKVFD-FLEDDQVMDK 64
sjAbo1   -----NN-PTRIRMKHHNDYTEDEDD------------ELLEITR-------------------PKKFN-KLSTT----- 56
sjAbo2   ------------AQIEDNNFTE----------------------Q---------------------PSA-YLE-------- 37
ceLEX1   GGVDGNGYTRSGRKINHNRYYEEEYH--EAISSEEDERRYRTRRS-----------------SNSMTYR-----QQVMQA 101
hsATAD2  -AKAGDGSSV-----KEVETYHRTR----------ALRSLRKDAQNSSDSSFEKNVEITEQLANGRHFTRQLARQQADKK 117
hsATAD2B GGSGGAGVTL-----DEARKVEVDGSLSDSHVSPPAKRTLKQPDSVCKDKSKSR--------STGQREEWNLSTGQAR-- 123
mmATAD2  ------------------------------------------------------------------------------ 0
mmATAD2B GGSGG---AL-----DEARKAEVDGSLSDSHVSPPAKRTLKQPDSVCKDKSKSR--------STGQREEWNIPSGQTR-- 122

spAbo1   --------ASEHG---GSA----DETQELSPVSDSS----------------DEMP-NNAKRRRRSQ-SMIA-NKRIHQ- 49
spAbo2   TETPSF-----------------SVSIENPSKPSA----------------A----FNDASLGKKSTEHQIDGIRNGSS 116
scYta7   DETPVDVTSDEHHNNNQKGDDEDDDVDLVSPHENAR----------------TNEELTNERNIRKRK-AHDP--EEDDE- 124
sjAbo1   -------------------------TTSSPTSHSS----------------NESA-FPKKHRSSSTFSVAITPNRYHS- 92
sjAbo2   --------SMPSG---EKESELEDDVEVKDDNSDDP---------------DFEP-VNHRRRRQS-NSRP-SKRARR- 86
ceLEX1   ID--------ES-----------KRNQKVPPAKRKRIYLSDEE-EEDFAEAAHVENTVPERAIRRST---RRRSSM---- 154
hsATAD2  KE--------EH-----------RE-DKVIPV------TRSLRARNIVQSTEHLHEDNGDVEVRRSC---RIR-SRYSGV 167
hsATAD2B -L--------TS-----------QP-GATLPNGHSGLSLRSHPLRGEKKGDGDLSCINGDMEVRKSC---RSRKNRFESV 179
mmATAD2  ------------------------------------------------------------------------------ 0
mmATAD2B -L--------TS-----------QP-GATLPNGHSSLSLRSHPLRGEKKGDGDLSCINGDIEVRKSC---RSRKNRFESV 178

spAbo1   AF----QEDEGDED-------------------------------WEEEEHKPKAKRRY---------------------- 73
spAbo2   NLQMEGNDKELDTDNNEDESTTFKD-----------------EEDDL----ISPKSY---------------------- 152
scYta7   SF----HEEDVDDDEEEEEADEFED-----------------EYLDEDSKDNNRRRR---------------------- 160
sjAbo1   -------------SSEHSHTPKYHQLYDPAVVLSQKHSSPLYELFDRNHKRTPQKYYPSNTSRS---------------- 143
sjAbo2   SV----VKDEDDED----------E-----------------EYYETQT------RR---------------------- 106
ceLEX1   ----------------------HEELGVS--------E--------QEESPVRRTRK--AAKRLGS--EQPEENLAADDPLP 194
hsATAD2  NQ-----------------SMLFDKLITN-------TAEAVLQKMDDMKKMRRQRMRELEDLGVFNETEESNL------N 217
hsATAD2B NQ-----------------SLLFDQLVNS-------TAEAVLQEMDNINIRQNRRSGEVERLRMWTDTEFENM------D 229
mmATAD2  ------------------------------------------------------------------------------ 0
mmATAD2B NQ-----------------SLLFDQLVNS-------TAEAVLQEMDNINIRRNRRSGEVERLRMWTDTEFENM------D 228

spAbo1   ----NTRS-NE-----SFSEGDD---------------------------EPFEVS-----ESSALEDELSD-SE--DSF 108
spAbo2   ----LTSSKTFSYPK-APTESTNGD----------------------YLDEDYVDGQSDPESSNASDSDFAD-SPDDLTK 204
scYta7   ----AADRKFV-----VPDPDDD-------------------------EEYDED-----DEEGDRISHSA-SSKRLKR 198
sjAbo1   ----LKTKDSSSPPR-SPSDNSSRTAEEEQDD--------DNVSLYTLSDDDYSLSN-DIEDDEGEDSEYVYKSERKSQR 209
sjAbo2   ----SHRS--------SVSYGDN-------------------------DNYEED-----SSNASFVD-TE-SE--LTS 138
ceLEX1   MEGGGE---IV-LPIAE----IDGMAEQENEDLIEKIGREEEE--EGAE-EDEQSGEKDPEEEEDDSS------------ 251
hsATAD2  MYTRGKQKDIQ-RTDEETTDNQEGSVESSE----EGEDQEHEDDGEDEDDEDDDDDDDDDDEDD------------ 280
hsATAD2B MYSRVKRRRKS-LRRN-----SY------------GIQNHHEVSTEGEEEE---------SQEEDGDI------------ 270
mmATAD2  ------------------------------------------------------------------------------ 0
mmATAD2B MYSRVKRRRKS-LRRN-----SY------------GIQNHHEVSTEGEEEE---------SQEEDGDI------------ 269

spAbo1   IR-S----VRSKPKYKPGTRRSTRLRNRRSQ-DEEE-------------------------SEEEHRPILRRRTSRINY 156
spAbo2   VR------------SPIPSRRGRRKRKMRGPILPVK----------KNLRVKKAMSPLRAERNSPDFRRKLRSRDNRPNY 262
scYta7   AN-SRRTRSSRHPETPPPVRRALRSRTRHSRTSNEENDDENDNSRNEALTLADEIREL-QEDSPIREKRFLRRRTKPVNY 276
sjAbo1   KRTRRSTRRKRRKPSPAPVRRSSRIKNNMAD-------------------------------------------------- 240
sjAbo2   LE-S----EEFSSEEQTGTRRSARLRNRQHANGEEE-------------------------EEEEHRPTLRRRKSRPDY 187
ceLEX1   ------------------------------------------------NAESSEESTAPRQYSLRRRQPVVQF 276
hsATAD2  ---------------------------------------------EDEEDGEEENQKRYYLRQRKATVYY 305
hsATAD2B ---------------------------------------------EVEEAEGEENDRPYNLRQRKTVDRY 295
mmATAD2  ------------------------------------------------------------------------------ 0
mmATAD2B ---------------------------------------------EVEEAEGEENDRPYNLRQRKTVDRY 294

spAbo1   SVPLAFPPVDEMDGD--PSSQVNQ---SRSRKTH----------------------SELAITKLLRQQVS--SFMPYID- 206
spAbo2   HLFDYYNEI-----------ASSPNPSTTKITY---N-----------PPKLPMK-----------DFATLPIGY- 301
scYta7   KLPPPLTASNAEEFIDKNNNALSFHNDSPARRGRGGWNASQNSGPTRRLFPTGGPFGGNDVTTIFGKNTNFYNQVPSAF- 355
sjAbo1   ----------------KPAGSAQNAAASSLRRSRSAT------FSSIRSFPPAV--------------LDAFSKLPLGIG 284
sjAbo2   RLPAPDYGPDELDQL--NNTTTSN---SNRKKTA----------------------AEHVVIRLLQKQVN--NPVDLDF- 237
ceLEX1   NASEARENRRA-----RL-----EHHRVANQN----------------------RHH-----------RNRNGSRRR 310
hsATAD2  QAPLEKPRHQR-----KPN-IFYSGPASPARPRYRLSS-----------AGPRSPYCKR-----------MNRRRHAIH 356
hsATAD2B QAPPIVPAHQK-----KRENTLPDIHRSPAR-------------------------RSH-----------IRRKKHAIH 333
mmATAD2  ---------------------------------------------MSL-----------LKMRRHAIH 12
mmATAD2B QAPPIVPAHQK-----KRENTLPDIHRSPAR-------------------------RSH-----------IRRKKHAIH 332
```

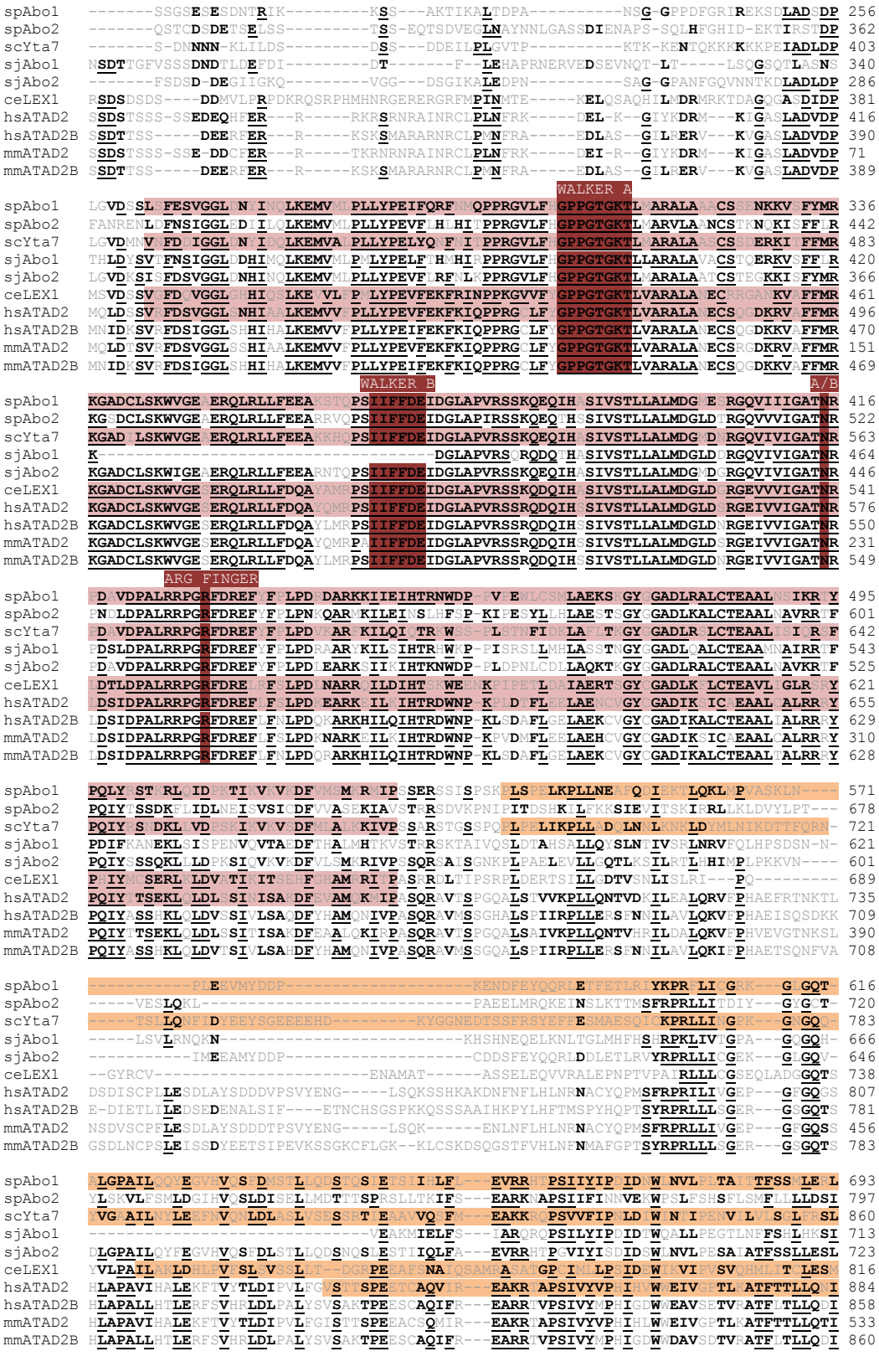
WALKER A
WALKER B
A/B
ARG FINGER

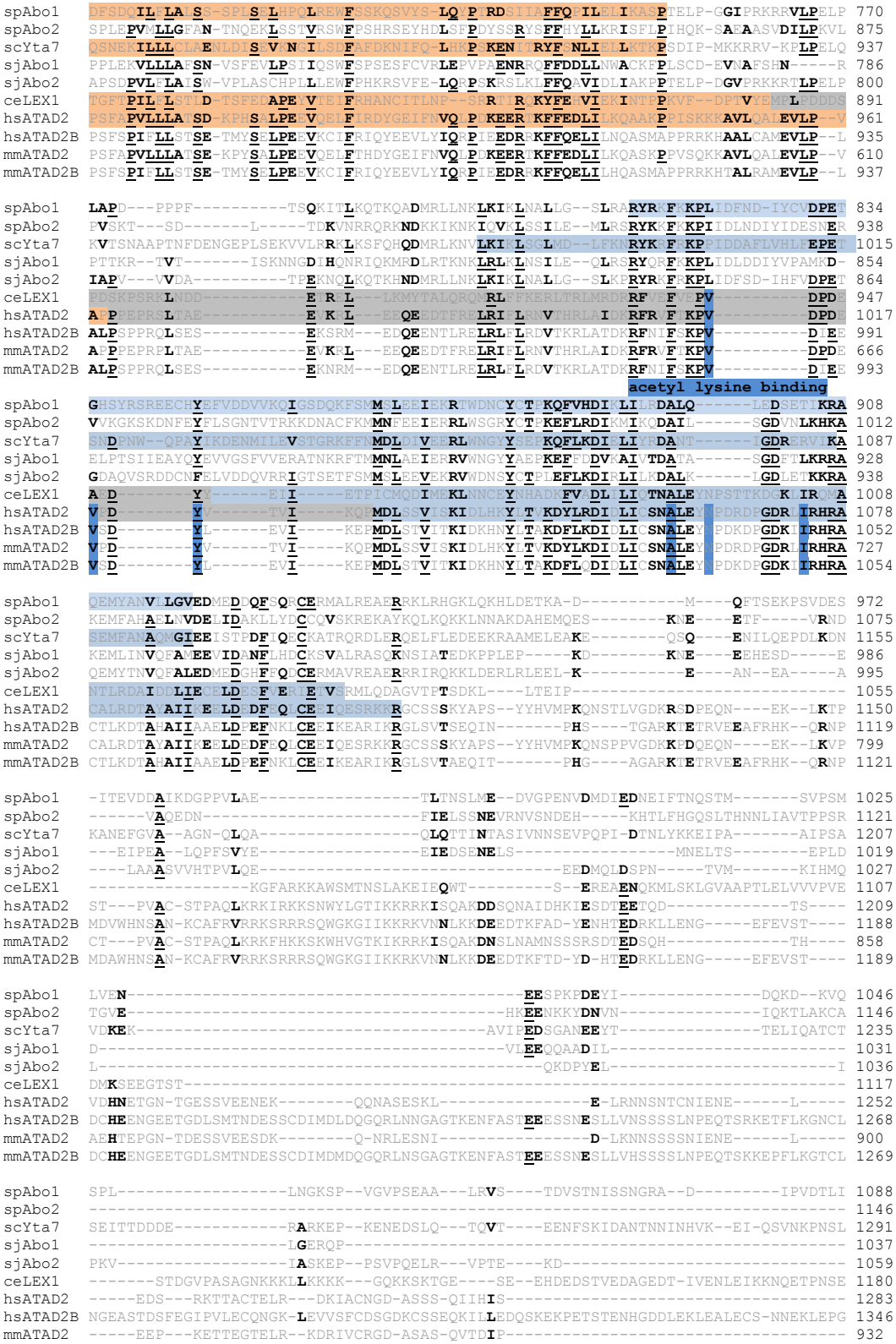
acetyl lysine binding

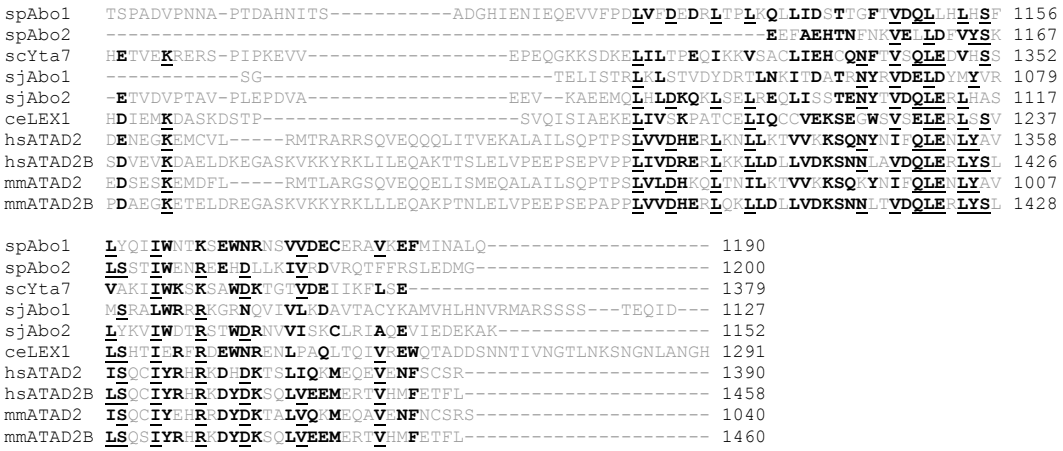
spAbo1 TSPADVPNNA-PTDAHNITS----------ADGHIENIEQEVVFPDLVFDEDRLTPLKQLLIDSTTGFTVDQLLHLHSF 1156
spAbo2 ----------EEFAEHTNFNKVELLDFVYSK 1167
scYta7 HETVEKRERS-PIPKEVV----------EPEQGKKSDKELILTPEQIKKVSACLIEHCQNFTVSQLEDVHSS 1352
sjAbo1 ----------SG----------TELISTRLKLSTVDYDRTLNKITDATPNYRVDELDYMYVR 1079
sjAbo2 -ETVDVPTAV-PLEPDVA----------EEV--KAEEMQLHLDKQKLSELREQLISSTENYTVDQLERLHAS 1117
ceLEX1 HDIEMKDASKDSTP----------SVQISIAEKELIVSKPATCELIQCCVEKSECWSVSELERLSSV 1237
hsATAD2 DENEGKEMCVL-----RMTRARRSQVEQQQLITVEKALAILSQPTPSLVVDHERLKNLLKTVVKKSQNYIFQLENLYAV 1358
hsATAD2B SDVEVKDAELDKEGASKVKKYRKLILEQAKTTSLELVPEEPSEPVPPLIVDRERLKKLLDLLVDKSNNLAVDQLERLYSL 1426
mmATAD2 EDSESKEMDFL-----RMTLARGSQVEQQELISMEQALAILSQPTPSLVLDHKQLTNILKTVVKKSQKYNIFQLENLYAV 1007
mmATAD2B PDAEGKETELDREGASKVKKYRKLLLEQAKPTNLELVPEEPSEPAPPLVVDHERLQKLLDLLVDKSNNLTVDQLERLYSL 1428
spAbo1 LYQIIWNTKSEWNRNSVVDECERAVKEFMINALQ---------- 1190
spAbo2 LSSTIWENREEHDLLKIVRDVRQTFFRSLEDMG---------- 1200
scYta7 VAKIIWKSKSAWDKTGTVDEIIKFLSE---------- 1379
sjAbo1 MSRALWRRKGRNQVIVLKDAVTACYKAMVHLHNVRMARSSSS---TEQID--- 1127
sjAbo2 LYKVIWDTRSTWDRNVVISKCLRIAQEVIEDEKAK---------- 1152
ceLEX1 LSHTIERRDEWNRENLPAQLTQIVREWQTADDSNNTIVNGTLNKSNGNLANGH 1291
hsATAD2 ISQCIYRHRKDHDKTSLIQKMEQEVENFSCSR---------- 1390
hsATAD2B LSQCIYRHRKDYDKSQLVEEMERTVHMFETFL---------- 1458
mmATAD2 ISQCIYEHRRDYDKTALVQKMEQAVENFNCSRS---------- 1040
mmATAD2B LSQSIYRHRKDYDKSQLVEEMERTVHMFETFL---------- 1460

8 Literature cited

Acquaviva C, Herzog F, Kraft C & Pines J **2004** The anaphase promoting complex/cyclosome is recruited to centromeres by the spindle assembly checkpoint *Nat Cell Biol* 6: 892-8

Adams IR & Kilmartin JV **2000** Spindle pole body duplication: a model for centrosome duplication? *Trends Cell Biol* 10: 329-35

Alfa C **1993** *Experiments with fission yeast : a laboratory course manual* Cold Spring Harbor Laboratory Press, Plainview, N.Y.

Allen JB, Zhou Z, Siede W, Friedberg EC & Elledge SJ **1994** The SAD1/RAD53 protein kinase controls multiple checkpoints and DNA damage-induced transcription in yeast *Genes & development* 8: 2401-15

Allshire RC, Nimmo ER, Ekwall K, Javerzat JP & Cranston G **1995** Mutations derepressing silent centromeric domains in fission yeast disrupt chromosome segregation *Genes Dev* 9: 218-33

Altmann KH & Gertsch J **2007** Anticancer drugs from nature--natural products as a unique source of new microtubule-stabilizing agents *Nat Prod Rep* 24: 327-57

Arbel A, Zenvirth D & Simchen G **1999** Sister chromatid-based DNA repair is mediated by RAD54, not by DMC1 or TID1 *The EMBO journal* 18: 2648-58

Asakawa K & Toda T **2006** Cooperation of EB1-Mal3 and the Bub1 spindle checkpoint *Cell Cycle* 5: 27-30

Bader JR & Vaughan KT **2010** Dynein at the kinetochore: Timing, Interactions and Functions *Semin Cell Dev Biol* 21: 269-75

Bahler J, Wu JQ, Longtine MS, Shah NG, McKenzie A, 3rd, Steever AB, Wach A, Philippsen P & Pringle JR **1998** Heterologous modules for efficient and versatile PCR-based gene targeting in Schizosaccharomyces pombe *Yeast* 14: 943-51

Bailer SM, Siniossoglou S, Podtelejnikov A, Hellwig A, Mann M & Hurt E **1998** Nup116p and nup100p are interchangeable through a conserved motif which constitutes a docking site for the mRNA transport factor gle2p *EMBO J* 17: 1107-19

Baker DJ, Jeganathan KB, Cameron JD, Thompson M, Juneja S, Kopecka A, Kumar R, Jenkins RB, de Groen PC, Roche P & van Deursen JM **2004** BubR1 insufficiency causes early onset of aging-associated phenotypes and infertility in mice *Nat Genet* 36: 744-9

Baker DJ, Chen J & van Deursen JM **2005** The mitotic checkpoint in cancer and aging: what have mice taught us? *Curr Opin Cell Biol* 17: 583-9

Baker DJ, Jeganathan KB, Malureanu L, Perez-Terzic C, Terzic A & van Deursen JM **2006** Early aging-associated phenotypes in Bub3/Rae1 haploinsufficient mice *J Cell Biol* 172: 529-40

Baker DJ, Jin F, Jeganathan KB & van Deursen JM **2009** Whole chromosome instability caused by Bub1 insufficiency drives tumorigenesis through tumor suppressor gene loss of heterozygosity *Cancer Cell* 16: 475-86

Baker NA, Sept D, Joseph S, Holst MJ & McCammon JA **2001** Electrostatics of nanosystems: application to microtubules and the ribosome *Proceedings of the National Academy of Sciences of the United States of America* 98: 10037-41

Barford D **2011** Structural insights into anaphase-promoting complex function and mechanism *Philosophical transactions of the Royal Society of London. Series B, Biological sciences* 366: 3605-24

Barisic M & Geley S **2011** Spindly switch controls anaphase: spindly and RZZ functions in chromosome attachment and mitotic checkpoint control *Cell Cycle* 10: 449-56

Barlow JH, Lisby M & Rothstein R **2008** Differential regulation of the cellular response to DNA double-strand breaks in G1 *Molecular cell* 30: 73-85

Bartek J & Lukas J **2001** Mammalian G1- and S-phase checkpoints in response to DNA damage *Current opinion in cell biology* 13: 738-47

Bartek J, Lukas C & Lukas J **2004** Checking on DNA damage in S phase *Nat Rev Mol Cell Biol* 5: 792-804

Bartholomew CR, Woo SH, Chung YS, Jones C & Hardy CF **2001** Cdc5 interacts with the Wee1 kinase in budding yeast *Molecular and cellular biology* 21: 4949-59

Basto R, Scaerou F, Mische S, Wojcik E, Lefebvre C, Gomes R, Hays T & Karess R **2004** In vivo dynamics of the rough deal checkpoint protein during Drosophila mitosis *Curr Biol* 14: 56-61

Belotserkovskaya R, Oh S, Bondarenko VA, Orphanides G, Studitsky VM & Reinberg D **2003** FACT facilitates transcription-dependent nucleosome alteration *Science* 301: 1090-3

Belotserkovskaya R, Saunders A, Lis JT & Reinberg D **2004** Transcription through chromatin: understanding a complex FACT *Biochimica et biophysica acta* 1677: 87-99

Ben-Efraim I, Frosst PD & Gerace L **2009** Karyopherin binding interactions and nuclear import mechanism of nuclear pore complex protein Tpr *BMC Cell Biol* 10: 74

Berman HM, Westbrook J, Feng Z, Gilliland G, Bhat TN, Weissig H, Shindyalov IN & Bourne PE **2000** The Protein Data Bank *Nucleic acids research* 28: 235-42

Bermudez VP, Lindsey-Boltz LA, Cesare AJ, Maniwa Y, Griffith JD, Hurwitz J & Sancar A **2003** Loading of the human 9-1-1 checkpoint complex onto DNA by the checkpoint clamp loader hRad17-replication factor C complex in vitro *Proc Natl Acad Sci U S A* 100: 1633-8

Biggins S, Severin FF, Bhalla N, Sassoon I, Hyman AA & Murray AW **1999** The conserved protein kinase Ipl1 regulates microtubule binding to kinetochores in budding yeast *Genes Dev* 13: 532-44

Bihani T & Hinds PW **2011** Mitosis hit with an ATM transaction fee: aurora B-mediated activation of ATM during mitosis *Mol Cell* 44: 513-4

Birnboim HC & Doty J **1979** A rapid alkaline extraction procedure for screening recombinant plasmid DNA *Nucleic acids research* 7: 1513-23

Blagosklonny MV **2003** Cell senescence and hypermitogenic arrest *EMBO reports* 4: 358-62

Bloecher A, Venturi GM & Tatchell K **2000** Anaphase spindle position is monitored by the BUB2 checkpoint *Nat Cell Biol* 2: 556-8

Bloom J & Cross FR **2007** Multiple levels of cyclin specificity in cell-cycle control *Nat Rev Mol Cell Biol* 8: 149-60

Bohn S, Beck F, Sakata E, Walzthoeni T, Beck M, Aebersold R, Forster F, Baumeister W & Nickell S **2010** Structure of the 26S proteasome from Schizosaccharomyces pombe at subnanometer resolution *Proceedings of the National Academy of Sciences of the United States of America* 107: 20992-7

Boiteux S & Guillet M **2006** Use of yeast for detection of endogenous abasic lesions, their source, and their repair *Methods in enzymology* 408: 79-91

Bolanos-Garcia VM, Kiyomitsu T, D'Arcy S, Chirgadze DY, Grossmann JG, Matak-Vinkovic D, Venkitaraman AR, Yanagida M, Robinson CV & Blundell TL **2009** The crystal structure of the N-terminal region of BUB1 provides insight into the mechanism of BUB1 recruitment to kinetochores *Structure* 17: 105-16

Bolanos-Garcia VM & Blundell TL **2011** BUB1 and BUBR1: multifaceted kinases of the cell cycle *Trends Biochem Sci* 36: 141-50

Bolanos-Garcia VM, Lischetti T, Matak-Vinkovic D, Cota E, Simpson PJ, Chirgadze DY, Spring DR, Robinson CV, Nilsson J & Blundell TL **2011** Structure of a Blinkin-BUBR1 complex reveals an interaction crucial for kinetochore-mitotic checkpoint regulation via an unanticipated binding Site *Structure* 19: 1691-700

Bolanos-Garcia VM, Nilsson J & Blundell TL **2012** The architecture of the BubR1 tetratricopeptide tandem repeat defines a protein motif underlying mitotic checkpoint-kinetochore communication *Bioarchitecture* 2: 23-7

Borges HL, Linden R & Wang JY **2008** DNA damage-induced cell death: lessons from the central nervous system *Cell research* 18: 17-26

Brady DM & Hardwick KG **2000** Complex formation between Mad1p, Bub1p and Bub3p is crucial for spindle checkpoint function *Curr Biol* 10: 675-8

Branzei D & Foiani M **2005** The DNA damage response during DNA replication *Curr Opin Cell Biol* 17: 568-75

Branzei D & Foiani M **2007** Interplay of replication checkpoints and repair proteins at stalled replication forks *DNA Repair (Amst)* 6: 994-1003

Breitkreutz A, Choi H, Sharom JR, Boucher L, Neduva V, Larsen B, Lin ZY, Breitkreutz BJ, Stark C, Liu G, Ahn J, Dewar-Darch D, Reguly T, Tang X, Almeida R, Qin ZS, Pawson T, Gingras AC, Nesvizhskii AI & Tyers M **2010** A global protein kinase and phosphatase interaction network in yeast *Science* 328: 1043-6

Britton DM **1974** Significance of Chromosome-Numbers in Ferns *Annals of the Missouri Botanical Garden* 61: 310-7

Brune C, Munchel SE, Fischer N, Podtelejnikov AV & Weis K **2005** Yeast poly(A)-binding protein Pab1 shuttles between the nucleus and the cytoplasm and functions in mRNA export *Rna* 11: 517-31

Budhidarmo R, Nakatani Y & Day CL **2012** RINGs hold the key to ubiquitin transfer *Trends in biochemical sciences* 37: 58-65

Burton JL & Solomon MJ **2007** Mad3p, a pseudosubstrate inhibitor of APCCdc20 in the spindle assembly checkpoint *Genes Dev* 21: 655-67

Buttrick GJ, Lancaster TC, Meadows JC & Millar JB **2012** Plo1 phosphorylates Dam1 to promote chromosome bi-orientation in fission yeast *Journal of cell science* 125: 1645-51

Byrne KP & Wolfe KH **2005** The Yeast Gene Order Browser: combining curated homology and syntenic context reveals gene fate in polyploid species *Genome Res* 15: 1456-61

Cairo LV, Ptak C & Wozniak RW **2013** Mitosis-specific regulation of nuclear transport by the spindle assembly checkpoint protein mad1p *Molecular cell* 49: 109-20

Caldecott KW **2003** XRCC1 and DNA strand break repair *DNA Repair (Amst)* 2: 955-69

Caldecott KW **2008** Single-strand break repair and genetic disease *Nat Rev Genet* 9: 619-31

Camasses A, Bogdanova A, Shevchenko A & Zachariae W **2003** The CCT chaperonin promotes activation of the anaphase-promoting complex through the generation of functional Cdc20 *Mol Cell* 12: 87-100

Campbell MS, Chan GK & Yen TJ **2001** Mitotic checkpoint proteins HsMAD1 and HsMAD2 are associated with nuclear pore complexes in interphase *J Cell Sci* 114: 953-63

Canman CE, Lim DS, Cimprich KA, Taya Y, Tamai K, Sakaguchi K, Appella E, Kastan MB & Siliciano JD **1998** Activation of the ATM kinase by ionizing radiation and phosphorylation of p53 *Science* 281: 1677-9

Caron C, Lestrat C, Marsal S, Escoffier E, Curtet S, Virolle V, Barbry P, Debernardi A, Brambilla C, Brambilla E, Rousseaux S & Khochbin S **2010** Functional characterization of ATAD2 as a new cancer/testis factor and a predictor of poor prognosis in breast and lung cancers *Oncogene* 29: 5171-81

Caron P, Aymard F, Iacovoni JS, Briois S, Canitrot Y, Bugler B, Massip L, Losada A & Legube G **2012** Cohesin protects genes against gammaH2AX Induced by DNA double-strand breaks *PLoS genetics* 8: e1002460

Carter SD & Sjogren C **2012** The SMC complexes, DNA and chromosome topology: right or knot? *Crit Rev Biochem Mol Biol* 47: 1-16

Carvunis AR, Rolland T, Wapinski I, Calderwood MA, Yildirim MA, Simonis N, Charloteaux B, Hidalgo CA, Barbette J, Santhanam B, Brar GA, Weissman JS, Regev A, Thierry-Mieg N, Cusick ME & Vidal M **2012** Proto-genes and de novo gene birth *Nature* 487: 370-4

Castro A, Vigneron S, Bernis C, Labbe JC & Lorca T **2003** Xkid is degraded in a D-box, KEN-box, and A-box-independent pathway *Mol Cell Biol* 23: 4126-38

Castro A, Bernis C, Vigneron S, Labbe JC & Lorca T **2005** The anaphase-promoting complex: a key factor in the regulation of cell cycle *Oncogene* 24: 314-25

Catlett MG & Forsburg SL **2003** Schizosaccharomyces pombe Rdh54 (TID1) acts with Rhp54 (RAD54) to repair meiotic double-strand breaks *Molecular biology of the cell* 14: 4707-20

Chabes A, Georgieva B, Domkin V, Zhao X, Rothstein R & Thelander L **2003** Survival of DNA damage in yeast directly depends on increased dNTP levels allowed by relaxed feedback inhibition of ribonucleotide reductase *Cell* 112: 391-401

Chan GK, Schaar BT & Yen TJ **1998** Characterization of the kinetochore binding domain of CENP-E reveals interactions with the kinetochore proteins CENP-F and hBUBR1 *J Cell Biol* 143: 49-63

Chan YW, Fava LL, Uldschmid A, Schmitz MH, Gerlich DW, Nigg EA & Santamaria A **2009** Mitotic control of kinetochore-associated dynein and spindle orientation by human Spindly *J Cell Biol* 185: 859-74

Chan YW, Jeyaprakash AA, Nigg EA & Santamaria A **2012** Aurora B controls kinetochore-microtubule attachments by inhibiting Ska complex-KMN network interaction *The Journal of cell biology* 196: 563-71

Chao WC, Kulkarni K, Zhang Z, Kong EH & Barford D **2012** Structure of the mitotic checkpoint complex *Nature* 484: 208-13

Cheeseman IM, Anderson S, Jwa M, Green EM, Kang J, Yates JR, 3rd, Chan CS, Drubin DG & Barnes G **2002** Phospho-regulation of kinetochore-microtubule attachments by the Aurora kinase Ipl1p *Cell* 111: 163-72

Chen RH, Waters JC, Salmon ED & Murray AW **1996** Association of spindle assembly checkpoint component XMAD2 with unattached kinetochores *Science* 274: 242-6

Chen RH, Brady DM, Smith D, Murray AW & Hardwick KG **1999** The spindle checkpoint of budding yeast depends on a tight complex between the Mad1 and Mad2 proteins *Mol Biol Cell* 10: 2607-18

Chen RH **2002** BubR1 is essential for kinetochore localization of other spindle checkpoint proteins and its phosphorylation requires Mad1 *J Cell Biol* 158: 487-96

Chen RH **2004** Phosphorylation and activation of Bub1 on unattached chromosomes facilitate the spindle checkpoint *EMBO J* 23: 3113-21

Chen SH, Albuquerque CP, Liang J, Suhandynata RT & Zhou H **2010a** A proteome-wide analysis of kinase-substrate network in the DNA damage response *The Journal of biological chemistry* 285: 12803-12

Chen ZA, Jawhari A, Fischer L, Buchen C, Tahir S, Kamenski T, Rasmussen M, Lariviere L, Bukowski-Wills JC, Nilges M, Cramer P & Rappsilber J **2010b** Architecture of the RNA polymerase II-TFIIF complex revealed by cross-linking and mass spectrometry *EMBO J* 29: 717-26

Cheung HW, Jin DY, Ling MT, Wong YC, Wang Q, Tsao SW & Wang X **2005** Mitotic arrest deficient 2 expression induces chemosensitization to a DNA-damaging agent, cisplatin, in nasopharyngeal carcinoma cells *Cancer research* 65: 1450-8

Chi YH, Haller K, Ward MD, Semmes OJ, Li Y & Jeang KT **2008** Requirements for protein phosphorylation and the kinase activity of polo-like kinase 1 (Plk1) for the kinetochore function of mitotic arrest deficiency protein 1 (Mad1) *J Biol Chem* 283: 35834-44

Chila R, Celenza C, Lupi M, Damia G & Carrassa L **2013** Chk1-Mad2 interaction: A crosslink between the DNA damage checkpoint and the mitotic spindle checkpoint *Cell Cycle* 12:

Choi E & Lee H **2008** Chromosome damage in mitosis induces BubR1 activation and prometaphase arrest *FEBS Lett* 582: 1700-6

Chow JP, Siu WY, Fung TK, Chan WM, Lau A, Arooz T, Ng CP, Yamashita K & Poon RY **2003** DNA damage during the spindle-assembly checkpoint degrades CDC25A, inhibits cyclin-CDC2 complexes, and reverses cells to interphase *Mol Biol Cell* 14: 3989-4002

Chung E & Chen RH **2003** Phosphorylation of Cdc20 is required for its inhibition by the spindle checkpoint *Nat Cell Biol* 5: 748-53

Ciccia A & Elledge SJ **2010** The DNA damage response: making it safe to play with knives *Mol Cell* 40: 179-204

Ciferri C, Musacchio A & Petrovic A **2007** The Ndc80 complex: hub of kinetochore activity *FEBS Lett* 581: 2862-9

Ciferri C, Pasqualato S, Screpanti E, Varetti G, Santaguida S, Dos Reis G, Maiolica A, Polka J, De Luca JG, De Wulf P, Salek M, Rappsilber J, Moores CA, Salmon ED & Musacchio A **2008** Implications for kinetochore-microtubule attachment from the structure of an engineered Ndc80 complex *Cell* 133: 427-39

Cimini D & Degrassi F **2005** Aneuploidy: a matter of bad connections *Trends Cell Biol* 15: 442-51

Ciro M, Prosperini E, Quarto M, Grazini U, Walfridsson J, McBlane F, Nucifero P, Pacchiana G, Capra M, Christensen J & Helin K **2009** ATAD2 is a novel cofactor for MYC, overexpressed and amplified in aggressive tumors *Cancer Res* 69: 8491-8

Clark AM **1976** Naturally occuring mutagens *Mutation research* 32: 361-74

Clemenson C & Marsolier-Kergoat MC **2006** The spindle assembly checkpoint regulates the phosphorylation state of a subset of DNA checkpoint proteins in Saccharomyces cerevisiae *Mol Cell Biol* 26: 9149-61

Clemenson C & Marsolier-Kergoat MC **2009** DNA damage checkpoint inactivation: adaptation and recovery *DNA repair* 8: 1101-9

Clerici M, Baldo V, Mantiero D, Lottersberger F, Lucchini G & Longhese MP **2004** A Tel1/MRX-dependent checkpoint inhibits the metaphase-to-anaphase transition after UV irradiation in the absence of Mec1 *Mol Cell Biol* 24: 10126-44

Cociorva D, D LT & Yates JR **2007** Validation of tandem mass spectrometry database search results using DTASelect *Curr Protoc Bioinformatics* Chapter 13: Unit 13 4

Cohen-Fix O & Koshland D **1997** The anaphase inhibitor of Saccharomyces cerevisiae Pds1p is a target of the DNA damage checkpoint pathway *Proc Natl Acad Sci U S A* 94: 14361-6

Collura A, Blaisonneau J, Baldacci G & Francesconi S **2005** The fission yeast Crb2/Chk1 pathway coordinates the DNA damage and spindle checkpoint in response to replication stress induced by topoisomerase I inhibitor *Mol Cell Biol* 25: 7889-99

Cotsiki M, Lock RL, Cheng Y, Williams GL, Zhao J, Perera D, Freire R, Entwistle A, Golemis EA, Roberts TM, Jat PS & Gjoerup OV **2004** Simian virus 40 large T antigen targets the spindle assembly checkpoint protein Bub1 *Proceedings of the National Academy of Sciences of the United States of America* 101: 947-52

Cox J & Mann M **2008** MaxQuant enables high peptide identification rates, individualized p.p.b.-range mass accuracies and proteome-wide protein quantification *Nature biotechnology* 26: 1367-72

Crosland MW & Crozier RH **1986** Myrmecia pilosula, an Ant with Only One Pair of Chromosomes *Science* 231: 1278

Cuadrado M, Martinez-Pastor B, Murga M, Toledo LI, Gutierrez-Martinez P, Lopez E & Fernandez-Capetillo O **2006** ATM regulates ATR chromatin loading in response to DNA double-strand breaks *J Exp Med* 203: 297-303

d'Adda di Fagagna F **2008** Living on a break: cellular senescence as a DNA-damage response *Nature reviews. Cancer* 8: 512-22

D'Angiolella V, Mari C, Nocera D, Rametti L & Grieco D **2003** The spindle checkpoint requires cyclin-dependent kinase activity *Genes Dev* 17: 2520-5

D'Arcy S, Davies OR, Blundell TL & Bolanos-Garcia VM **2010** Defining the molecular basis of BubR1 kinetochore interactions and APC/C-CDC20 inhibition *J Biol Chem* 285: 14764-76

da Fonseca PC, Kong EH, Zhang Z, Schreiber A, Williams MA, Morris EP & Barford D **2011** Structures of APC/C(Cdh1) with substrates identify Cdh1 and Apc10 as the D-box co-receptor *Nature* 470: 274-8

Dalgaard JZ **2012** Causes and consequences of ribonucleotide incorporation into nuclear DNA *Trends in genetics : TIG* 28: 592-7

Daum JR, Wren JD, Daniel JJ, Sivakumar S, McAvoy JN, Potapova TA & Gorbsky GJ **2009** Ska3 Is Required for Spindle Checkpoint Silencing and the Maintenance of Chromosome Cohesion in Mitosis *Curr Biol*

Dawkins R **1976** *The selfish gene* Oxford University Press, Oxford

De Antoni A, Pearson CG, Cimini D, Canman JC, Sala V, Nezi L, Mapelli M, Sironi L, Faretta M, Salmon ED & Musacchio A **2005** The Mad1/Mad2 complex as a template for Mad2 activation in the spindle assembly checkpoint *Curr Biol* 15: 214-25

De Souza CP & Osmani SA **2007** Mitosis, not just open or closed *Eukaryot Cell* 6: 1521-7

De Souza CP, Hashmi SB, Nayak T, Oakley B & Osmani SA **2009** Mlp1 acts as a mitotic scaffold to spatially regulate spindle assembly checkpoint proteins in Aspergillus nidulans *Mol Biol Cell* 20: 2146-59

de Voer RM, Hoogerbrugge N & Kuiper RP **2011** Spindle-assembly checkpoint and gastrointestinal cancer *The New England journal of medicine* 364: 1279-80

DeLuca JG, Gall WE, Ciferri C, Cimini D, Musacchio A & Salmon ED **2006** Kinetochore microtubule dynamics and attachment stability are regulated by Hec1 *Cell* 127: 969-82

DeLuca KF, Lens SM & DeLuca JG **2011** Temporal changes in Hec1 phosphorylation control kinetochore-microtubule attachment stability during mitosis *Journal of cell science* 124: 622-34

Den Haese GJ, Walworth N, Carr AM & Gould KL **1995** The Wee1 protein kinase regulates T14 phosphorylation of fission yeast Cdc2 *Molecular biology of the cell* 6: 371-85

Denarier E, Fourest-Lieuvin A, Bosc C, Pirollet F, Chapel A, Margolis RL & Job D **1998** Nonneuronal isoforms of STOP protein are responsible for microtubule cold stability in mammalian fibroblasts *Proc Natl Acad Sci U S A* 95: 6055-60

Denning D, Mykytka B, Allen NP, Huang L, Al B & Rexach M **2001** The nucleoporin Nup60p functions as a Gsp1p-GTP-sensitive tether for Nup2p at the nuclear pore complex *J Cell Biol* 154: 937-50

Desiraju GR **2011** A Bond by Any Other Name *Angewandte Chemie International Edition* 50: 52-9

Diamant N, Hendel A, Vered I, Carell T, Reissner T, de Wind N, Geacinov N & Livneh Z **2012** DNA damage bypass operates in the S and G2 phases of the cell cycle and exhibits differential mutagenicity *Nucleic acids research* 40: 170-80

Dikic I, Wakatsuki S & Walters KJ **2009** Ubiquitin-binding domains - from structures to functions *Nature reviews. Molecular cell biology* 10: 659-71

Dinant C, Houtsmuller AB & Vermeulen W **2008** Chromatin structure and DNA damage repair *Epigenetics Chromatin* 1: 9

Ding D, Muthuswamy S & Meier I **2012** Functional interaction between the Arabidopsis orthologs of spindle assembly checkpoint proteins MAD1 and MAD2 and the nucleoporin NUA *Plant Mol Biol* 79: 203-16

Ding R, West RR, Morphew DM, Oakley BR & McIntosh JR **1997** The spindle pole body of Schizosaccharomyces pombe enters and leaves the nuclear envelope as the cell cycle proceeds *Mol Biol Cell* 8: 1461-79

Diop SB, Bertaux K, Vasanthi D, Sarkeshik A, Goirand B, Aragnol D, Tolwinski NS, Cole MD, Pradel J, Yates JR, 3rd, Mishra RK, Graba Y & Saurin AJ **2008** Reptin and Pontin function antagonistically with PcG and TrxG complexes to mediate Hox gene control *EMBO Rep* 9: 260-6

Dobles M, Liberal V, Scott ML, Benezra R & Sorger PK **2000** Chromosome missegregation and apoptosis in mice lacking the mitotic checkpoint protein Mad2 *Cell* 101: 635-45

Dotiwala F, Harrison JC, Jain S, Sugawara N & Haber JE **2010** Mad2 prolongs DNA damage checkpoint arrest caused by a double-strand break via a centromere-dependent mechanism *Curr Biol* 20: 328-32

Dou Z, von Schubert C, Korner R, Santamaria A, Elowe S & Nigg EA **2011** Quantitative mass spectrometry analysis reveals similar substrate consensus motif for human Mps1 kinase and Plk1 *PLoS ONE* 6: e18793

Duan Z, Zou JX, Yang P, Wang Y, Borowsky AD, Gao AC & Chen HW **2012** Developmental and androgenic regulation of chromatin regulators EZH2 and ANCCA/ATAD2 in the prostate Via MLL histone methylase complex *The Prostate*

Duensing A, Teng X, Liu Y, Tseng M, Spardy N & Duensing S **2006** A role of the mitotic spindle checkpoint in the cellular response to DNA replication stress *J Cell Biochem* 99: 759-69

Durr H, Flaus A, Owen-Hughes T & Hopfner KP **2006** Snf2 family ATPases and DExx box helicases: differences and unifying concepts from high-resolution crystal structures *Nucleic Acids Res* 34: 4160-7

Durr H & Hopfner KP **2006** Structure-function analysis of SWI2/SNF2 enzymes *Methods Enzymol* 409: 375-88

Eichinger CS & Jentsch S **2011** 9-1-1: PCNA's specialized cousin *Trends Biochem Sci* 36: 563-8

Elowe S, Hummer S, Uldschmid A, Li X & Nigg EA **2007** Tension-sensitive Plk1 phosphorylation on BubR1 regulates the stability of kinetochore microtubule interactions *Genes Dev* 21: 2205-19

Elowe S, Dulla K, Uldschmid A, Li X, Dou Z & Nigg EA **2010** Uncoupling of the spindle-checkpoint and chromosome-congression functions of BubR1 *Journal of cell science* 123: 84-94

Eng JK, Mccormack AL & Yates JR **1994** An Approach to Correlate Tandem Mass-Spectral Data of Peptides with Amino-Acid-Sequences in a Protein Database *Journal of the American Society for Mass Spectrometry* 5: 976-89

Erickson HP **2009** Size and shape of protein molecules at the nanometer level determined by sedimentation, gel filtration, and electron microscopy *Biol Proced Online* 11: 32-51

Erlich RL, Fry RC, Begley TJ, Daee DL, Lahue RS & Samson LD **2008** Anc1, a protein associated with multiple transcription complexes, is involved in postreplication repair pathway in S. cerevisiae *PLoS ONE* 3: e3717

Erzberger JP & Berger JM **2006** Evolutionary relationships and structural mechanisms of AAA+ proteins *Annu Rev Biophys Biomol Struct* 35: 93-114

Essen LO & Klar T **2006** Light-driven DNA repair by photolyases *Cellular and molecular life sciences : CMLS* 63: 1266-77

Evans MD, Dizdaroglu M & Cooke MS **2004** Oxidative DNA damage and disease: induction, repair and significance *Mutation research* 567: 1-61

Evans T, Rosenthal ET, Youngblom J, Distel D & Hunt T **1983** Cyclin: a protein specified by maternal mRNA in sea urchin eggs that is destroyed at each cleavage division *Cell* 33: 389-96

Fang G **2002** Checkpoint protein BubR1 acts synergistically with Mad2 to inhibit anaphase-promoting complex *Mol Biol Cell* 13: 755-66

Fang Y, Liu T, Wang X, Yang YM, Deng H, Kunicki J, Traganos F, Darzynkiewicz Z, Lu L & Dai W **2006** BubR1 is involved in regulation of DNA damage responses *Oncogene* 25: 3598-605

Fankhauser C, Marks J, Reymond A & Simanis V **1993** The S. pombe cdc16 gene is required both for maintenance of p34cdc2 kinase activity and regulation of septum formation: a link between mitosis and cytokinesis? *EMBO J* 12: 2697-704

Fava LL, Kaulich M, Nigg EA & Santamaria A **2011** Probing the in vivo function of Mad1:C-Mad2 in the spindle assembly checkpoint *The EMBO journal* 30: 3322-36

Felix MA, Labbe JC, Doree M, Hunt T & Karsenti E **1990** Triggering of cyclin degradation in interphase extracts of amphibian eggs by cdc2 kinase *Nature* 346: 379-82

Feng W, Di Rienzi SC, Raghuraman MK & Brewer BJ **2011** Replication stress-induced chromosome breakage is correlated with replication fork progression and is preceded by single-stranded DNA formation *G3 (Bethesda)* 1: 327-35

Fernius J & Hardwick KG **2007** Bub1 kinase targets Sgo1 to ensure efficient chromosome biorientation in budding yeast mitosis *PLoS Genet* 3: e213

Ferrand A, Chevrier V, Chauvin JP & Birnbaum D **2009** Ajuba: a new microtubule-associated protein that interacts with BUBR1 and Aurora B at kinetochores in metaphase *Biol Cell* 101: 221-35

Fillingham J, Kainth P, Lambert JP, van Bakel H, Tsui K, Pena-Castillo L, Nislow C, Figeys D, Hughes TR, Greenblatt J & Andrews BJ **2009** Two-color cell array screen reveals interdependent roles for histone chaperones and a chromatin boundary regulator in histone gene repression *Mol Cell* 35: 340-51

Finkel T & Holbrook NJ **2000** Oxidants, oxidative stress and the biology of ageing *Nature* 408: 239-47

Finn K, Lowndes NF & Grenon M **2012** Eukaryotic DNA damage checkpoint activation in response to double-strand breaks *Cell Mol Life Sci* 69: 1447-73

Fischer PM & Lane DP **2000** Inhibitors of cyclin-dependent kinases as anti-cancer therapeutics *Curr Med Chem* 7: 1213-45

FitzGerald GB, Rosowsky A & Wick MM **1984** Inhibition of ribonucleotide reductase by naturally occurring quinols from spores of Agaricus bisporus *Biochemical and biophysical research communications* 120: 1008-14

Fojo T & Giannakakou P **2000** Taxol and other microtubule-interactive agents *Current Opinion in Oncologic, Endocrine and Metabolic Investigational Drugs* 2: 293-304

Forsburg SL & Nurse P **1991** Cell cycle regulation in the yeasts Saccharomyces cerevisiae and Schizosaccharomyces pombe *Annu Rev Cell Biol* 7: 227-56

Forsburg SL **2003** Growth and manipulation of S. pombe *Curr Protoc Mol Biol* Chapter 13: Unit 13 6

Forsburg SL & Rhind N **2006** Basic methods for fission yeast *Yeast* 23: 173-83

Foster SA & Morgan DO **2012** The APC/C Subunit Mnd2/Apc15 Promotes Cdc20 Autoubiquitination and Spindle Assembly Checkpoint Inactivation *Molecular cell* 47: 921-32

Fraschini R, Formenti E, Lucchini G & Piatti S **1999** Budding yeast Bub2 is localized at spindle pole bodies and activates the mitotic checkpoint via a different pathway from Mad2 *J Cell Biol* 145: 979-91

Fung MK, Han HY, Leung SC, Cheung HW, Cheung AL, Wong YC, Ling MT & Wang X **2008** MAD2 interacts with DNA repair proteins and negatively regulates DNA damage repair *Journal of molecular biology* 381: 24-34

Furnari B, Rhind N & Russell P **1997** Cdc25 mitotic inducer targeted by chk1 DNA damage checkpoint kinase *Science* 277: 1495-7

Furnari B, Blasina A, Boddy MN, McGowan CH & Russell P **1999** Cdc25 inhibited in vivo and in vitro by checkpoint kinases Cds1 and Chk1 *Molecular biology of the cell* 10: 833-45

Fuss JO & Cooper PK **2006** DNA repair: dynamic defenders against cancer and aging *PLoS biology* 4: e203

Galaktionov K & Beach D **1991** Specific activation of cdc25 tyrosine phosphatases by B-type cyclins: evidence for multiple roles of mitotic cyclins *Cell* 67: 1181-94

Ganmore I, Smooha G & Izraeli S **2009** Constitutional aneuploidy and cancer predisposition *Hum Mol Genet* 18: R84-93

Gao Q, Courtheoux T, Gachet Y, Tournier S & He X **2010** A non-ring-like form of the Dam1 complex modulates microtubule dynamics in fission yeast *Proc Natl Acad Sci U S A* 107: 13330-5

Gao YF, Li T, Chang Y, Wang YB, Zhang WN, Li WH, He K, Mu R, Zhen C, Man JH, Pan X, Chen L, Yu M, Liang B, Chen Y, Xia Q, Zhou T, Gong WL, Li AL, Li HY & Zhang XM **2011** Cdk1-phosphorylated CUEDC2 promotes spindle checkpoint inactivation and chromosomal instability *Nature cell biology* 13: 924-33

Garber PM & Rine J **2002** Overlapping roles of the spindle assembly and DNA damage checkpoints in the cell-cycle response to altered chromosomes in Saccharomyces cerevisiae *Genetics* 161: 521-34

Garber PM, Vidanes GM & Toczyski DP **2005** Damage in transition *Trends Biochem Sci* 30: 63-6

Garcia MA, Koonrugsa N & Toda T **2002** Spindle-kinetochore attachment requires the combined action of Kin I-like Klp5/6 and Alp14/Dis1-MAPs in fission yeast *EMBO J* 21: 6015-24

Garnett MJ, Mansfeld J, Godwin C, Matsusaka T, Wu J, Russell P, Pines J & Venkitaraman AR **2009** UBE2S elongates ubiquitin chains on APC/C substrates to promote mitotic exit *Nature cell biology* 11: 1363-9

Gautier J, Minshull J, Lohka M, Glotzer M, Hunt T & Maller JL **1990** Cyclin is a component of maturation-promoting factor from Xenopus *Cell* 60: 487-94

Gemma A, Hosoya Y, Seike M, Uematsu K, Kurimoto F, Hibino S, Yoshimura A, Shibuya M, Kudoh S & Emi M **2001** Genomic structure of the human MAD2 gene and mutation analysis in human lung and breast cancers *Lung Cancer* 32: 289-95

Gerson SL **2004** MGMT: its role in cancer aetiology and cancer therapeutics *Nat Rev Cancer* 4: 296-307

Gestaut DR, Graczyk B, Cooper J, Widlund PO, Zelter A, Wordeman L, Asbury CL & Davis TN **2008** Phosphoregulation and depolymerization-driven movement of the Dam1 complex do not require ring formation *Nat Cell Biol* 10: 407-14

Gillet LC & Scharer OD **2006** Molecular mechanisms of mammalian global genome nucleotide excision repair *Chem Rev* 106: 253-76

Gomez EB & Forsburg SL **2004** Analysis of the fission yeast Schizosaccharomyces pombe cell cycle *Methods in molecular biology* 241: 93-111

Gorbsky GJ, Chen RH & Murray AW **1998** Microinjection of antibody to Mad2 protein into mammalian cells in mitosis induces premature anaphase *J Cell Biol* 141: 1193-205

Goujon M, McWilliam H, Li W, Valentin F, Squizzato S, Paern J & Lopez R **2010** A new bioinformatics analysis tools framework at EMBL-EBI *Nucleic acids research* 38: W695-9

Gould KL & Nurse P **1989** Tyrosine phosphorylation of the fission yeast cdc2+ protein kinase regulates entry into mitosis *Nature* 342: 39-45

Grabsch H, Takeno S, Parsons WJ, Pomjanski N, Boecking A, Gabbert HE & Mueller W **2003** Overexpression of the mitotic checkpoint genes BUB1, BUBR1, and BUB3 in gastric cancer--association with tumour cell proliferation *The Journal of pathology* 200: 16-22

Gradolatto A, Rogers RS, Lavender H, Taverna SD, Allis CD, Aitchison JD & Tackett AJ **2008** Saccharomyces cerevisiae Yta7 regulates histone gene expression *Genetics* 179: 291-304

Gradolatto A, Smart SK, Byrum S, Blair LP, Rogers RS, Kolar EA, Lavender H, Larson SK, Aitchison JD, Taverna SD & Tackett AJ **2009** A noncanonical bromodomain in the AAA ATPase protein Yta7 directs chromosomal positioning and barrier chromatin activity *Mol Cell Biol* 29: 4604-11

Green RA, Paluch E & Oegema K **2012** Cytokinesis in animal cells *Annual review of cell and developmental biology* 28: 29-58

Grishchuk EL, Spiridonov IS & McIntosh JR **2007** Mitotic chromosome biorientation in fission yeast is enhanced by dynein and a minus-end-directed, kinesin-like protein *Molecular biology of the cell* 18: 2216-25

Grissom PM, Fiedler T, Grishchuk EL, Nicastro D, West RR & McIntosh JR **2009** Kinesin-8 from fission yeast: a heterodimeric, plus-end-directed motor that can couple microtubule depolymerization to cargo movement *Molecular biology of the cell* 20: 963-72

Haase J, Stephens A, Verdaasdonk J, Yeh E & Bloom K **2012** Bub1 kinase and Sgo1 modulate pericentric chromatin in response to altered microtubule dynamics *Current biology : CB* 22: 471-81

Habu T, Kim SH, Weinstein J & Matsumoto T **2002** Identification of a MAD2-binding protein, CMT2, and its role in mitosis *EMBO J* 21: 6419-28

Hagan RS, Manak MS, Buch HK, Meier MG, Meraldi P, Shah JV & Sorger PK **2011** p31(comet) acts to ensure timely spindle checkpoint silencing subsequent to kinetochore attachment *Molecular biology of the cell* 22: 4236-46

Hammet A, Magill C, Heierhorst J & Jackson SP **2007** Rad9 BRCT domain interaction with phosphorylated H2AX regulates the G1 checkpoint in budding yeast *EMBO Rep* 8: 851-7

Han JS, Holland AJ, Fachinetti D, Kulukian A, Cetin B & Cleveland DW **2013** Catalytic assembly of the mitotic checkpoint inhibitor BubR1-Cdc20 by a Mad2-induced functional switch in Cdc20 *Molecular cell* 51: 92-104

Hanisch A, Sillje HH & Nigg EA **2006** Timely anaphase onset requires a novel spindle and kinetochore complex comprising Ska1 and Ska2 *EMBO J* 25: 5504-15

Hanks S, Coleman K, Reid S, Plaja A, Firth H, Fitzpatrick D, Kidd A, Mehes K, Nash R, Robin N, Shannon N, Tolmie J, Swansbury J, Irrthum A, Douglas J & Rahman N **2004** Constitutional aneuploidy and cancer predisposition caused by biallelic mutations in BUB1B *Nature genetics* 36: 1159-61

Hanson PI & Whiteheart SW **2005** AAA+ proteins: have engine, will work *Nat Rev Mol Cell Biol* 6: 519-29

Hardwick KG, Weiss E, Luca FC, Winey M & Murray AW **1996** Activation of the budding yeast spindle assembly checkpoint without mitotic spindle disruption *Science* 273: 953-6

Hardwick KG **1998** The spindle checkpoint *Trends Genet* 14: 1-4

Hardwick KG, Johnston RC, Smith DL & Murray AW **2000** MAD3 encodes a novel component of the spindle checkpoint which interacts with Bub3p, Cdc20p, and Mad2p *J Cell Biol* 148: 871-82

Hardwick KG & Shah JV **2010** Spindle checkpoint silencing: ensuring rapid and concerted anaphase onset *F1000 Biol Rep* 2: 55

Harris L, Davenport J, Neale G & Goorha R **2005** The mitotic checkpoint gene BubR1 has two distinct functions in mitosis *Experimental cell research* 308: 85-100

Harrison JC & Haber JE **2006** Surviving the breakup: the DNA damage checkpoint *Annu Rev Genet* 40: 209-35

Hartlerode AJ & Scully R **2009** Mechanisms of double-strand break repair in somatic mammalian cells *The Biochemical journal* 423: 157-68

Hartwell LH, Culotti J, Pringle JR & Reid BJ **1974** Genetic control of the cell division cycle in yeast *Science* 183: 46-51

Hartwell LH & Weinert TA **1989** Checkpoints: controls that ensure the order of cell cycle events *Science* 246: 629-34

He X, Patterson TE & Sazer S **1997** The Schizosaccharomyces pombe spindle checkpoint protein mad2p blocks anaphase and genetically interacts with the anaphase-promoting complex *Proceedings of the National Academy of Sciences of the United States of America* 94: 7965-70

He X, Jones MH, Winey M & Sazer S **1998** Mph1, a member of the Mps1-like family of dual specificity protein kinases, is required for the spindle checkpoint in S. pombe *J Cell Sci* 111 (Pt 12): 1635-47

Heckman DS, Geiser DM, Eidell BR, Stauffer RL, Kardos NL & Hedges SB **2001** Molecular evidence for the early colonization of land by fungi and plants *Science* 293: 1129-33

Hedges SB **2002** The origin and evolution of model organisms *Nat Rev Genet* 3: 838-49

Hein J, Boichuk S, Wu J, Cheng Y, Freire R, Jat PS, Roberts TM & Gjoerup OV **2009** Simian virus 40 large T antigen disrupts genome integrity and activates a DNA damage response via Bub1 binding *J Virol* 83: 117-27

Heinrich S, Windecker H, Hustedt N & Hauf S **2012** Mph1 kinetochore localization is crucial and upstream in the hierarchy of spindle assembly checkpoint protein recruitment to kinetochores *Journal of cell science*

Helston RM, Box JA, Tang W & Baumann P **2010** Schizosaccharomyces cryophilus sp. nov., a new species of fission yeast *FEMS Yeast Res* 10: 779-86

Henry NL, Campbell AM, Feaver WJ, Poon D, Weil PA & Kornberg RD **1994** TFIIF-TAF-RNA polymerase II connection *Genes Dev* 8: 2868-78

Hentges P, Van Driessche B, Tafforeau L, Vandenhaute J & Carr AM **2005** Three novel antibiotic marker cassettes for gene disruption and marker switching in Schizosaccharomyces pombe *Yeast* 22: 1013-9

Hershko A, Ganoth D, Sudakin V, Dahan A, Cohen LH, Luca FC, Ruderman JV & Eytan E **1994** Components of a system that ligates cyclin to ubiquitin and their regulation by the protein kinase cdc2 *The Journal of biological chemistry* 269: 4940-6

Herzog F, Primorac I, Dube P, Lenart P, Sander B, Mechtler K, Stark H & Peters JM **2009** Structure of the anaphase-promoting complex/cyclosome interacting with a mitotic checkpoint complex *Science* 323: 1477-81

Hewitt L, Tighe A, Santaguida S, White AM, Jones CD, Musacchio A, Green S & Taylor SS **2010** Sustained Mps1 activity is required in mitosis to recruit O-Mad2 to the Mad1-C-Mad2 core complex *The Journal of cell biology* 190: 25-34

Higgins JM **2010** Haspin: a newly discovered regulator of mitotic chromosome behavior *Chromosoma* 119: 137-47

Hiraoka Y, Toda T & Yanagida M **1984** The NDA3 gene of fission yeast encodes beta-tubulin: a cold-sensitive nda3 mutation reversibly blocks spindle formation and chromosome movement in mitosis *Cell* 39: 349-58

Hoeijmakers JH **2009** DNA damage, aging, and cancer *N Engl J Med* 361: 1475-85

Hofer A, Crona M, Logan DT & Sjoberg BM **2012** DNA building blocks: keeping control of manufacture *Crit Rev Biochem Mol Biol* 47: 50-63

Hogan CJ, Aligianni S, Durand-Dubief M, Persson J, Will WR, Webster J, Wheeler L, Mathews CK, Elderkin S, Oxley D, Ekwall K & Varga-Weisz PD **2010** Fission yeast Iec1-ino80-mediated nucleosome eviction regulates nucleotide and phosphate metabolism *Molecular and cellular biology* 30: 657-74

Holland AJ & Cleveland DW **2009** Boveri revisited: chromosomal instability, aneuploidy and tumorigenesis *Nat Rev Mol Cell Biol* 10: 478-87

Hou H, Zhou Z, Wang Y, Wang J, Kallgren SP, Kurchuk T, Miller EA, Chang F & Jia S **2012** Csi1 links centromeres to the nuclear envelope for centromere clustering *The Journal of cell biology* 199: 735-44

Howell AS & Lew DJ **2012** Morphogenesis and the cell cycle *Genetics* 190: 51-77

Howell BJ, McEwen BF, Canman JC, Hoffman DB, Farrar EM, Rieder CL & Salmon ED **2001** Cytoplasmic dynein/dynactin drives kinetochore protein transport to the spindle poles and has a role in mitotic spindle checkpoint inactivation *J Cell Biol* 155: 1159-72

Howell BJ, Moree B, Farrar EM, Stewart S, Fang G & Salmon ED **2004** Spindle checkpoint protein dynamics at kinetochores in living cells *Curr Biol* 14: 953-64

Hoyt MA, Totis L & Roberts BT **1991** S. cerevisiae genes required for cell cycle arrest in response to loss of microtubule function *Cell* 66: 507-17

Hsia EY, Kalashnikova EV, Revenko AS, Zou JX, Borowsky AD & Chen HW **2010** Deregulated E2F and the AAA+ coregulator ANCCA drive proto-oncogene ACTR/AIB1 overexpression in breast cancer *Molecular cancer research : MCR* 8: 183-93

Hsiang YH, Hertzberg R, Hecht S & Liu LF **1985** Camptothecin induces protein-linked DNA breaks via mammalian DNA topoisomerase I *J Biol Chem* 260: 14873-8

Huang H, Hittle J, Zappacosta F, Annan RS, Hershko A & Yen TJ **2008** Phosphorylation sites in BubR1 that regulate kinetochore attachment, tension, and mitotic exit *The Journal of cell biology* 183: 667-80

Huang X, Tran T, Zhang L, Hatcher R & Zhang P **2005** DNA damage-induced mitotic catastrophe is mediated by the Chk1-dependent mitotic exit DNA damage checkpoint *Proc Natl Acad Sci U S A* 102: 1065-70

Huerta-Cepas J, Capella-Gutierrez S, Pryszcz LP, Denisov I, Kormes D, Marcet-Houben M & Gabaldon T **2011** PhylomeDB v3.0: an expanding repository of genome-wide collections of trees, alignments and phylogeny-based orthology and paralogy predictions *Nucleic acids research* 39: D556-60

Huffaker TC, Thomas JH & Botstein D **1988** Diverse effects of beta-tubulin mutations on microtubule formation and function *The Journal of cell biology* 106: 1997-2010

Humphrey T **2000** DNA damage and cell cycle control in Schizosaccharomyces pombe *Mutat Res* 451: 211-26

Humphrey T & Pearce A **2005** Cell cycle molecules and mechanisms of the budding and fission yeasts *Methods Mol Biol* 296: 3-29

Hurley PJ & Bunz F **2007** ATM and ATR: components of an integrated circuit *Cell Cycle* 6: 414-7

Hwang LH, Lau LF, Smith DL, Mistrot CA, Hardwick KG, Hwang ES, Amon A & Murray AW **1998** Budding yeast Cdc20: a target of the spindle checkpoint *Science* 279: 1041-4

Hyun SY, Rosen EM & Jang YJ **2012** Novel DNA damage checkpoint in mitosis: Mitotic DNA damage induces re-replication without cell division in various cancer cells *Biochem Biophys Res Commun*

Ikui AE, Furuya K, Yanagida M & Matsumoto T **2002** Control of localization of a spindle checkpoint protein, Mad2, in fission yeast *J Cell Sci* 115: 1603-10

Indjeian VB, Stern BM & Murray AW **2005** The centromeric protein Sgo1 is required to sense lack of tension on mitotic chromosomes *Science* 307: 130-3

Iouk T, Kerscher O, Scott RJ, Basrai MA & Wozniak RW **2002** The yeast nuclear pore complex functionally interacts with components of the spindle assembly checkpoint *J Cell Biol* 159: 807-19

Ira G, Pellicioli A, Balijja A, Wang X, Fiorani S, Carotenuto W, Liberi G, Bressan D, Wan L, Hollingsworth NM, Haber JE & Foiani M **2004** DNA end resection, homologous recombination and DNA damage checkpoint activation require CDK1 *Nature* 431: 1011-7

Ishihama Y, Rappsilber J & Mann M **2006** Modular stop and go extraction tips with stacked disks for parallel and multidimensional Peptide fractionation in proteomics *Journal of proteome research* 5: 988-94

Ito D, Saito Y & Matsumoto T **2012** Centromere-tethered Mps1 pombe homolog (Mph1) kinase is a sufficient marker for recruitment of the spindle checkpoint protein Bub1, but not Mad1 *Proceedings of the National Academy of Sciences of the United States of America* 109: 209-14

Iwanaga Y, Chi YH, Miyazato A, Sheleg S, Haller K, Peloponese JM, Jr., Li Y, Ward JM, Benezra R & Jeang KT **2007** Heterozygous deletion of mitotic arrest-deficient protein 1 (MAD1) increases the incidence of tumors in mice *Cancer Res* 67: 160-6

Jackson PK **2008** The hunt for cyclin *Cell* 134: 199-202

Jackson SP & Bartek J **2009** The DNA-damage response in human biology and disease *Nature* 461: 1071-8

Jambunathan N, Martinez AW, Robert EC, Agochukwu NB, Ibos ME, Dugas SL & Donze D **2005** Multiple bromodomain genes are involved in restricting the spread of heterochromatic silencing at the Saccharomyces cerevisiae HMR-tRNA boundary *Genetics* 171: 913-22

James P, Halladay J & Craig EA **1996** Genomic libraries and a host strain designed for highly efficient two-hybrid selection in yeast *Genetics* 144: 1425-36

Jang YJ, Ji JH, Choi YC, Ryu CJ & Ko SY **2007** Regulation of Polo-like kinase 1 by DNA damage in mitosis. Inhibition of mitotic PLK-1 by protein phosphatase 2A *J Biol Chem* 282: 2473-82

Jeganathan K, Malureanu L, Baker DJ, Abraham SC & van Deursen JM **2007** Bub1 mediates cell death in response to chromosome missegregation and acts to suppress spontaneous tumorigenesis *J Cell Biol* 179: 255-67

Jeggo PA & Lobrich M **2006** Contribution of DNA repair and cell cycle checkpoint arrest to the maintenance of genomic stability *DNA Repair (Amst)* 5: 1192-8

Jelluma N, Brenkman AB, van den Broek NJ, Cruijsen CW, van Osch MH, Lens SM, Medema RH & Kops GJ **2008** Mps1 phosphorylates Borealin to control Aurora B activity and chromosome alignment *Cell* 132: 233-46

Jelluma N, Dansen TB, Sliedrecht T, Kwiatkowski NP & Kops GJ **2010** Release of Mps1 from kinetochores is crucial for timely anaphase onset *The Journal of cell biology* 191: 281-90

Jeyaprakash AA, Santamaria A, Jayachandran U, Chan YW, Benda C, Nigg EA & Conti E **2012** Structural and functional organization of the Ska complex, a key component of the kinetochore-microtubule interface *Molecular cell* 46: 274-86

Jia L, Li B, Warrington RT, Hao X, Wang S & Yu H **2011** Defining pathways of spindle checkpoint silencing: functional redundancy between Cdc20 ubiquitination and p31(comet) *Molecular biology of the cell* 22: 4227-35

Jimenez G, Yucel J, Rowley R & Subramani S **1992** The rad3+ gene of Schizosaccharomyces pombe is involved in multiple checkpoint functions and in DNA repair *Proceedings of the National Academy of Sciences of the United States of America* 89: 4952-6

Joglekar AP, Bouck DC, Molk JN, Bloom KS & Salmon ED **2006** Molecular architecture of a kinetochore-microtubule attachment site *Nat Cell Biol* 8: 581-5

Joglekar AP, Bloom KS & Salmon ED **2010** Mechanisms of force generation by end-on kinetochore-microtubule attachments *Curr Opin Cell Biol* 22: 57-67

John S, Howe L, Tafrov ST, Grant PA, Sternglanz R & Workman JL **2000** The something about silencing protein, Sas3, is the catalytic subunit of NuA3, a yTAF(II)30-containing HAT complex that interacts with the Spt16 subunit of the yeast CP (Cdc68/Pob3)-FACT complex *Genes Dev* 14: 1196-208

Jones MH, Huneycutt BJ, Pearson CG, Zhang C, Morgan G, Shokat K, Bloom K & Winey M **2005** Chemical genetics reveals a role for Mps1 kinase in kinetochore attachment during mitosis *Curr Biol* 15: 160-5

Jorgensen PM, Brundell E, Starborg M & Hoog C **1998** A subunit of the anaphase-promoting complex is a centromere-associated protein in mammalian cells *Mol Cell Biol* 18: 468-76

Jullien D, Vagnarelli P, Earnshaw WC & Adachi Y **2002** Kinetochore localisation of the DNA damage response component 53BP1 during mitosis *J Cell Sci* 115: 71-9

Kabani M, Michot K, Boschiero C & Werner M **2005** Anc1 interacts with the catalytic subunits of the general transcription factors TFIID and TFIIF, the chromatin remodeling complexes RSC and INO80, and the histone acetyltransferase complex NuA3 *Biochem Biophys Res Commun* 332: 398-403

Kadura S, He X, Vanoosthuyse V, Hardwick KG & Sazer S **2005** The A78V mutation in the Mad3-like domain of Schizosaccharomyces pombe Bub1p perturbs nuclear accumulation and kinetochore targeting of Bub1p, Bub3p, and Mad3p and spindle assembly checkpoint function *Mol Biol Cell* 16: 385-95

Kadyk LC & Hartwell LH **1992** Sister chromatids are preferred over homologs as substrates for recombinational repair in Saccharomyces cerevisiae *Genetics* 132: 387-402

Kalashnikova EV, Revenko AS, Gemo AT, Andrews NP, Tepper CG, Zou JX, Cardiff RD, Borowsky AD & Chen HW **2010** ANCCA/ATAD2 overexpression identifies breast cancer patients with poor prognosis, acting to drive proliferation and survival of triple-negative cells through control of B-Myb and EZH2 *Cancer research* 70: 9402-12

Kaldis P **1999** The cdk-activating kinase (CAK): from yeast to mammals *Cellular and molecular life sciences : CMLS* 55: 284-96

Kalitsis P, Earle E, Fowler KJ & Choo KH **2000** Bub3 gene disruption in mice reveals essential mitotic spindle checkpoint function during early embryogenesis *Genes Dev* 14: 2277-82

Kang RS, Daniels CM, Francis SA, Shih SC, Salerno WJ, Hicke L & Radhakrishnan I **2003** Solution structure of a CUE-ubiquitin complex reveals a conserved mode of ubiquitin binding *Cell* 113: 621-30

Karess R **2005** Rod-Zw10-Zwilch: a key player in the spindle checkpoint *Trends Cell Biol* 15: 386-92

Karlsson-Rosenthal C & Millar JB **2006** Cdc25: mechanisms of checkpoint inhibition and recovery *Trends in cell biology* 16: 285-92

Kasparek TR & Humphrey TC **2011** DNA double-strand break repair pathways, chromosomal rearrangements and cancer *Semin Cell Dev Biol* 22: 886-97

Kastritis PL, Moal IH, Hwang H, Weng Z, Bates PA, Bonvin AM & Janin J **2011** A structure-based benchmark for protein-protein binding affinity *Protein science : a publication of the Protein Society* 20: 482-91

Kawashima SA, Yamagishi Y, Honda T, Ishiguro K & Watanabe Y **2010** Phosphorylation of H2A by Bub1 prevents chromosomal instability through localizing shugoshin *Science* 327: 172-7

Keating P, Rachidi N, Tanaka TU & Stark MJ **2009** Ipl1-dependent phosphorylation of Dam1 is reduced by tension applied on kinetochores *J Cell Sci* 122: 4375-82

Kellis M, Birren BW & Lander ES **2004** Proof and evolutionary analysis of ancient genome duplication in the yeast Saccharomyces cerevisiae *Nature* 428: 617-24

Kemmler S, Stach M, Knapp M, Ortiz J, Pfannstiel J, Ruppert T & Lechner J **2009** Mimicking Ndc80 phosphorylation triggers spindle assembly checkpoint signalling *EMBO J* 28: 1099-110

Kerr GP & Carter JV **1990** Relationship between Freezing Tolerance of Root-Tip Cells and Cold Stability of Microtubules in Rye (Secale cereale L. cv Puma) *Plant Physiol* 93: 77-82

Kim EM & Burke DJ **2008** DNA damage activates the SAC in an ATM/ATR-dependent manner, independently of the kinetochore *PLoS Genet* 4: e1000015

Kim HS, Park KH, Kim SA, Wen J, Park SW, Park B, Gham CW, Hyung WJ, Noh SH, Kim HK & Song SY **2005** Frequent mutations of human Mad2, but not Bub1, in gastric cancers cause defective mitotic spindle checkpoint *Mutation research* 578: 187-201

Kim S, Sun H, Ball HL, Wassmann K, Luo X & Yu H **2010** Phosphorylation of the spindle checkpoint protein Mad2 regulates its conformational transition *Proceedings of the National Academy of Sciences of the United States of America* 107: 19772-7

Kim S, Sun H, Tomchick DR, Yu H & Luo X **2012** Structure of human Mad1 C-terminal domain reveals its involvement in kinetochore targeting *Proceedings of the National Academy of Sciences of the United States of America* 109: 6549-54

Kim SH, Lin DP, Matsumoto S, Kitazono A & Matsumoto T **1998** Fission yeast Slp1: an effector of the Mad2-dependent spindle checkpoint *Science* 279: 1045-7

Kim WJ, Lee S, Park MS, Jang YK, Kim JB & Park SD **2000** Rad22 protein, a rad52 homologue in Schizosaccharomyces pombe, binds to DNA double-strand breaks *The Journal of biological chemistry* 275: 35607-11

Kimura M & Ishihama A **2004** Tfg3, a subunit of the general transcription factor TFIIF in Schizosaccharomyces pombe, functions under stress conditions *Nucleic Acids Res* 32: 6706-15

King EM, Rachidi N, Morrice N, Hardwick KG & Stark MJ **2007a** Ipl1p-dependent phosphorylation of Mad3p is required for the spindle checkpoint response to lack of tension at kinetochores *Genes Dev* 21: 1163-8

King EM, van der Sar SJ & Hardwick KG **2007b** Mad3 KEN boxes mediate both Cdc20 and Mad3 turnover, and are critical for the spindle checkpoint *PLoS ONE* 2: e342

Kireeva ML, Walter W, Tchernajenko V, Bondarenko V, Kashlev M & Studitsky VM **2002** Nucleosome remodeling induced by RNA polymerase II: loss of the H2A/H2B dimer during transcription *Mol Cell* 9: 541-52

Kitagawa K, Abdulle R, Bansal PK, Cagney G, Fields S & Hieter P **2003** Requirement of Skp1-Bub1 interaction for kinetochore-mediated activation of the spindle checkpoint *Mol Cell* 11: 1201-13

Kitamura E, Tanaka K, Kitamura Y & Tanaka TU **2007** Kinetochore microtubule interaction during S phase in Saccharomyces cerevisiae *Genes Dev* 21: 3319-30

Kiyomitsu T, Obuse C & Yanagida M **2007** Human Blinkin/AF15q14 is required for chromosome alignment and the mitotic checkpoint through direct interaction with Bub1 and BubR1 *Dev Cell* 13: 663-76

Kiyomitsu T, Murakami H & Yanagida M **2011** Protein interaction domain mapping of human kinetochore protein Blinkin reveals a consensus motif for binding of spindle assembly checkpoint proteins Bub1 and BubR1 *Mol Cell Biol*

Kondo N, Takahashi A, Ono K & Ohnishi T **2010** DNA damage induced by alkylating agents and repair pathways *J Nucleic Acids* 2010: 543531

Kops GJ, Weaver BA & Cleveland DW **2005** On the road to cancer: aneuploidy and the mitotic checkpoint *Nat Rev Cancer* 5: 773-85

Kops GJ & Shah JV **2012** Connecting up and clearing out: how kinetochore attachment silences the spindle assembly checkpoint *Chromosoma* 121: 509-25

Kotani S, Tugendreich S, Fujii M, Jorgensen PM, Watanabe N, Hoog C, Hieter P & Todokoro K **1998** PKA and MPF-activated polo-like kinase regulate anaphase-promoting complex activity and mitosis progression *Mol Cell* 1: 371-80

Kotani S, Tanaka H, Yasuda H & Todokoro K **1999** Regulation of APC activity by phosphorylation and regulatory factors *J Cell Biol* 146: 791-800

Kraft C, Herzog F, Gieffers C, Mechtler K, Hagting A, Pines J & Peters JM **2003** Mitotic regulation of the human anaphase-promoting complex by phosphorylation *EMBO J* 22: 6598-609

Krenn V, Wehenkel A, Li X, Santaguida S & Musacchio A **2012** Structural analysis reveals features of the spindle checkpoint kinase Bub1-kinetochore subunit Knl1 interaction *The Journal of cell biology* 196: 451-67

Krissinel E & Henrick K **2007** Inference of macromolecular assemblies from crystalline state *Journal of molecular biology* 372: 774-97

Krogh BO & Symington LS **2004** Recombination proteins in yeast *Annu Rev Genet* 38: 233-71

Krohn M, Skjolberg HC, Soltani H, Grallert B & Boye E **2008** The G1-S checkpoint in fission yeast is not a general DNA damage checkpoint *Journal of cell science* 121: 4047-54

Kulukian A, Han JS & Cleveland DW **2009** Unattached kinetochores catalyze production of an anaphase inhibitor that requires a Mad2 template to prime Cdc20 for BubR1 binding *Dev Cell* 16: 105-17

Kumagai A & Dunphy WG **1992** Regulation of the cdc25 protein during the cell cycle in Xenopus extracts *Cell* 70: 139-51

Kumagai A & Dunphy WG **1996** Purification and molecular cloning of Plx1, a Cdc25-regulatory kinase from Xenopus egg extracts *Science* 273: 1377-80

Kumar S & Huberman JA **2009** Checkpoint-dependent regulation of origin firing and replication fork movement in response to DNA damage in fission yeast *Molecular and cellular biology* 29: 602-11

Kurat CF, Lambert JP, van Dyk D, Tsui K, van Bakel H, Kaluarachchi S, Friesen H, Kainth P, Nislow C, Figeys D, Fillingham J & Andrews BJ **2011** Restriction of histone gene transcription to S phase by phosphorylation of a chromatin boundary protein *Genes & development* 25: 2489-501

Labib K & De Piccoli G **2011** Surviving chromosome replication: the many roles of the S-phase checkpoint pathway *Philos Trans R Soc Lond B Biol Sci* 366: 3554-61

Lagerwerf S, Vrouwe MG, Overmeer RM, Fousteri MI & Mullenders LH **2011** DNA damage response and transcription *DNA Repair (Amst)* 10: 743-50

Lambert JP, Mitchell L, Rudner A, Baetz K & Figeys D **2009** A novel proteomics approach for the discovery of chromatin-associated protein networks *Mol Cell Proteomics* 8: 870-82

Langerak P & Russell P **2011** Regulatory networks integrating cell cycle control with DNA damage checkpoints and double-strand break repair *Philos Trans R Soc Lond B Biol Sci* 366: 3562-71

Lara-Gonzalez P, Scott MI, Diez M, Sen O & Taylor SS **2011** BubR1 blocks substrate recruitment to the APC/C in a KEN-box-dependent manner *Journal of cell science* 124: 4332-45

Larsen NA & Harrison SC **2004** Crystal structure of the spindle assembly checkpoint protein Bub3 *J Mol Biol* 344: 885-92

Larsen NA, Al-Bassam J, Wei RR & Harrison SC **2007** Structural analysis of Bub3 interactions in the mitotic spindle checkpoint *Proc Natl Acad Sci U S A* 104: 1201-6

Lau DT & Murray AW **2012** Mad2 and Mad3 cooperate to arrest budding yeast in mitosis *Current biology : CB* 22: 180-90

Lavin MF & Shiloh Y **1997** The genetic defect in ataxia-telangiectasia *Annu Rev Immunol* 15: 177-202

Lee HJ, Hwang HI & Jang YJ **2010** Mitotic DNA damage response: Polo-like kinase-1 is dephosphorylated through ATM-Chk1 pathway *Cell Cycle* 9: 2389-98

Lee HW, Dominy BN & Cao W **2011** New family of deamination repair enzymes in uracil-DNA glycosylase superfamily *The Journal of biological chemistry* 286: 31282-7

Lee J, Gold DA, Shevchenko A & Dunphy WG **2005** Roles of replication fork-interacting and Chk1-activating domains from Claspin in a DNA replication checkpoint response *Mol Biol Cell* 16: 5269-82

Lee JH & Paull TT **2005** ATM activation by DNA double-strand breaks through the Mre11-Rad50-Nbs1 complex *Science* 308: 551-4

Lee KY & Myung K **2008** PCNA modifications for regulation of post-replication repair pathways *Mol Cells* 26: 5-11

Lee MG & Nurse P **1987** Complementation used to clone a human homologue of the fission yeast cell cycle control gene cdc2 *Nature* 327: 31-5

Lee S, Thebault P, Freschi L, Beaufils S, Blundell TL, Landry CR, Bolanos-Garcia VM & Elowe S **2012** Characterization of spindle checkpoint kinase Mps1 reveals domain with functional and structural similarities to tetratricopeptide repeat motifs of Bub1 and BubR1 checkpoint kinases *The Journal of biological chemistry* 287: 5988-6001

Lee SH, Sterling H, Burlingame A & McCormick F **2008** Tpr directly binds to Mad1 and Mad2 and is important for the Mad1-Mad2-mediated mitotic spindle checkpoint *Genes Dev* 22: 2926-31

Lehmann AR & Fuchs RP **2006** Gaps and forks in DNA replication: Rediscovering old models *DNA repair* 5: 1495-8

Lejeune E, Bortfeld M, White SA, Pidoux AL, Ekwall K, Allshire RC & Ladurner AG **2007** The chromatin-remodeling factor FACT contributes to centromeric heterochromatin independently of RNAi *Curr Biol* 17: 1219-24

Leng M, Chan DW, Luo H, Zhu C, Qin J & Wang Y **2006** MPS1-dependent mitotic BLM phosphorylation is important for chromosome stability *Proceedings of the National Academy of Sciences of the United States of America* 103: 11485-90

Letunic I & Bork P **2011** Interactive Tree Of Life v2: online annotation and display of phylogenetic trees made easy *Nucleic acids research* 39: W475-8

Li M & Zhang P **2009** Spindle assembly checkpoint, aneuploidy and tumorigenesis *Cell Cycle* 8: 3440

Li R & Murray AW **1991** Feedback control of mitosis in budding yeast *Cell* 66: 519-31

Li Y & Benezra R **1996** Identification of a human mitotic checkpoint gene: hsMAD2 *Science* 274: 246-8

Lince-Faria M, Maffini S, Orr B, Ding Y, Claudia F, Sunkel CE, Tavares A, Johansen J, Johansen KM & Maiato H **2009** Spatiotemporal control of mitosis by the conserved spindle matrix protein Megator *J Cell Biol* 184: 647-57

Lindahl T **1993** Instability and decay of the primary structure of DNA *Nature* 362: 709-15

Lindahl T & Barnes DE **2000** Repair of endogenous DNA damage *Cold Spring Harb Symp Quant Biol* 65: 127-33

Liou AK & Willison KR **1997** Elucidation of the subunit orientation in CCT (chaperonin containing TCP1) from the subunit composition of CCT micro-complexes *EMBO J* 16: 4311-6

Lipkowitz S & Weissman AM **2011** RINGs of good and evil: RING finger ubiquitin ligases at the crossroads of tumour suppression and oncogenesis *Nature reviews. Cancer* 11: 629-43

Liti G & Louis EJ **2005** Yeast evolution and comparative genomics *Annu Rev Microbiol* 59: 135-53

Littlepage LE & Ruderman JV **2002** Identification of a new APC/C recognition domain, the A box, which is required for the Cdh1-dependent destruction of the kinase Aurora-A during mitotic exit *Genes Dev* 16: 2274-85

Liu D, Vader G, Vromans MJ, Lampson MA & Lens SM **2009** Sensing chromosome bi-orientation by spatial separation of aurora B kinase from kinetochore substrates *Science* 323: 1350-3

Liu D, Vleugel M, Backer CB, Hori T, Fukagawa T, Cheeseman IM & Lampson MA **2010a** Regulated targeting of protein phosphatase 1 to the outer kinetochore by KNL1 opposes Aurora B kinase *J Cell Biol* 188: 809-20

Liu D, Davydenko O & Lampson MA **2012a** Polo-like kinase-1 regulates kinetochore-microtubule dynamics and spindle checkpoint silencing *The Journal of cell biology* 198: 491-9

Liu H, Liang F, Jin F & Wang Y **2008** The coordination of centromere replication, spindle formation, and kinetochore-microtubule interaction in budding yeast *PLoS Genet* 4: e1000262

Liu J & Kipreos ET **2000** Evolution of cyclin-dependent kinases (CDKs) and CDK-activating kinases (CAKs): differential conservation of CAKs in yeast and metazoa *Mol Biol Evol* 17: 1061-74

Liu Q, Hirohashi Y, Du X, Greene MI & Wang Q **2010b** Nek2 targets the mitotic checkpoint proteins Mad2 and Cdc20: a mechanism for aneuploidy in cancer *Exp Mol Pathol* 88: 225-33

Liu S, Song N & Zou L **2012b** The conserved C terminus of Claspin interacts with Rad9 and promotes rapid activation of Chk1 *Cell Cycle* 11:

Lo KW, Kogoy JM & Pfister KK **2007** The DYNLT3 light chain directly links cytoplasmic dynein to a spindle checkpoint protein, Bub3 *J Biol Chem* 282: 11205-12

Logarinho E & Bousbaa H **2008** Kinetochore-microtubule interactions "in check" by Bub1, Bub3 and BubR1: The dual task of attaching and signalling *Cell Cycle* 7: 1763-8

Lohka MJ, Hayes MK & Maller JL **1988** Purification of maturation-promoting factor, an intracellular regulator of early mitotic events *Proc Natl Acad Sci U S A* 85: 3009-13

Lombardi LM, Ellahi A & Rine J **2011** Direct regulation of nucleosome density by the conserved AAA-ATPase Yta7 *Proceedings of the National Academy of Sciences of the United States of America* 108: E1302-11

London N, Ceto S, Ranish JA & Biggins S **2012** Phosphoregulation of Spc105 by Mps1 and PP1 regulates Bub1 localization to kinetochores *Current biology : CB* 22: 900-6

Longtine MS, McKenzie A, 3rd, Demarini DJ, Shah NG, Wach A, Brachat A, Philippsen P & Pringle JR **1998** Additional modules for versatile and economical PCR-based gene deletion and modification in Saccharomyces cerevisiae *Yeast* 14: 953-61

Lou Y, Yao J, Zereshki A, Dou Z, Ahmed K, Wang H, Hu J, Wang Y & Yao X **2004** NEK2A interacts with MAD1 and possibly functions as a novel integrator of the spindle checkpoint signaling *J Biol Chem* 279: 20049-57

Lu B, Ruse C, Xu T, Park SK & Yates J, 3rd **2007** Automatic validation of phosphopeptide identifications from tandem mass spectra *Analytical chemistry* 79: 1301-10

Luijsterburg MS & van Attikum H **2011** Chromatin and the DNA damage response: the cancer connection *Mol Oncol* 5: 349-67

Luo X, Fang G, Coldiron M, Lin Y, Yu H, Kirschner MW & Wagner G **2000** Structure of the Mad2 spindle assembly checkpoint protein and its interaction with Cdc20 *Nat Struct Biol* 7: 224-9

Luo X, Tang Z, Xia G, Wassmann K, Matsumoto T, Rizo J & Yu H **2004** The Mad2 spindle checkpoint protein has two distinct natively folded states *Nat Struct Mol Biol* 11: 338-45

Lussi YC, Shumaker DK, Shimi T & Fahrenkrog B **2010** The nucleoporin Nup153 affects spindle checkpoint activity due to an association with Mad1 *Nucleus* 1: 71-84

Ma HT & Poon RY **2011** Orderly inactivation of the key checkpoint protein mitotic arrest deficient 2 (MAD2) during mitotic progression *The Journal of biological chemistry* 286: 13052-9

MacCoss MJ, Wu CC & Yates JR, 3rd **2002** Probability-based validation of protein identifications using a modified SEQUEST algorithm *Anal Chem* 74: 5593-9

Magrane M & Consortium U **2011** UniProt Knowledgebase: a hub of integrated protein data *Database (Oxford)* 2011: bar009

Maiato H, DeLuca J, Salmon ED & Earnshaw WC **2004** The dynamic kinetochore-microtubule interface *Journal of cell science* 117: 5461-77

Maiolica A, Cittaro D, Borsotti D, Sennels L, Ciferri C, Tarricone C, Musacchio A & Rappsilber J **2007** Structural analysis of multiprotein complexes by cross-linking, mass spectrometry, and database searching *Mol Cell Proteomics* 6: 2200-11

Mannuss A, Trapp O & Puchta H **2012** Gene regulation in response to DNA damage *Biochimica et biophysica acta* 1819: 154-65

Mansfeld J, Collin P, Collins MO, Choudhary JS & Pines J **2011** APC15 drives the turnover of MCC-CDC20 to make the spindle assembly checkpoint responsive to kinetochore attachment *Nature cell biology* 13: 1234-43

Mansour WY, Schumacher S, Rosskopf R, Rhein T, Schmidt-Petersen F, Gatzemeier F, Haag F, Borgmann K, Willers H & Dahm-Daphi J **2008** Hierarchy of nonhomologous end-joining, single-strand annealing and gene conversion at site-directed DNA double-strand breaks *Nucleic acids research* 36: 4088-98

Mapelli M, Filipp FV, Rancati G, Massimiliano L, Nezi L, Stier G, Hagan RS, Confalonieri S, Piatti S, Sattler M & Musacchio A **2006** Determinants of conformational dimerization of Mad2 and its inhibition by p31comet *The EMBO journal* 25: 1273-84

Mapelli M, Massimiliano L, Santaguida S & Musacchio A **2007** The Mad2 conformational dimer: structure and implications for the spindle assembly checkpoint *Cell* 131: 730-43

Marchetti MA, Kumar S, Hartsuiker E, Maftahi M, Carr AM, Freyer GA, Burhans WC & Huberman JA **2002** A single unbranched S-phase DNA damage and replication fork blockage checkpoint pathway *Proc Natl Acad Sci U S A* 99: 7472-7

Marchler-Bauer A, Lu S, Anderson JB, Chitsaz F, Derbyshire MK, DeWeese-Scott C, Fong JH, Geer LY, Geer RC, Gonzales NR, Gwadz M, Hurwitz DI, Jackson JD, Ke Z, Lanczycki CJ, Lu F, Marchler GH, Mullokandov M, Omelchenko MV, Robertson CL, Song JS, Thanki N, Yamashita RA, Zhang D, Zhang N, Zheng C & Bryant SH **2011** CDD: a Conserved Domain Database for the functional annotation of proteins *Nucleic acids research* 39: D225-9

Maresca TJ & Salmon ED **2009** Intrakinetochore stretch is associated with changes in kinetochore phosphorylation and spindle assembly checkpoint activity *J Cell Biol* 184: 373-81

Mariani L, Chiroli E, Nezi L, Muller H, Piatti S, Musacchio A & Ciliberto A **2012** Role of the mad2 dimerization interface in the spindle assembly checkpoint independent of kinetochores *Current biology : CB* 22: 1900-8

Maringele L & Lydall D **2002** EXO1-dependent single-stranded DNA at telomeres activates subsets of DNA damage and spindle checkpoint pathways in budding yeast yku70Delta mutants *Genes Dev* 16: 1919-33

Martin-Lluesma S, Stucke VM & Nigg EA **2002** Role of Hec1 in spindle checkpoint signaling and kinetochore recruitment of Mad1/Mad2 *Science* 297: 2267-70

Martinho RG, Lindsay HD, Flaggs G, DeMaggio AJ, Hoekstra MF, Carr AM & Bentley NJ **1998** Analysis of Rad3 and Chk1 protein kinases defines different checkpoint responses *The EMBO journal* 17: 7239-49

Masson JY & West SC **2001** The Rad51 and Dmc1 recombinases: a non-identical twin relationship *Trends Biochem Sci* 26: 131-6

Masui Y & Markert CL **1971** Cytoplasmic control of nuclear behavior during meiotic maturation of frog oocytes *J Exp Zool* 177: 129-45

Matsumura S, Toyoshima F & Nishida E **2007** Polo-like kinase 1 facilitates chromosome alignment during prometaphase through BubR1 *The Journal of biological chemistry* 282: 15217-27

Matsuoka S, Ballif BA, Smogorzewska A, McDonald ER, 3rd, Hurov KE, Luo J, Bakalarski CE, Zhao Z, Solimini N, Lerenthal Y, Shiloh Y, Gygi SP & Elledge SJ **2007** ATM and ATR substrate analysis reveals extensive protein networks responsive to DNA damage *Science* 316: 1160-6

Matyskiela ME & Morgan DO **2009** Analysis of activator-binding sites on the APC/C supports a cooperative substrate-binding mechanism *Molecular cell* 34: 68-80

Maure JF, Kitamura E & Tanaka TU **2007** Mps1 kinase promotes sister-kinetochore bi-orientation by a tension-dependent mechanism *Curr Biol* 17: 2175-82

Maure JF, Komoto S, Oku Y, Mino A, Pasqualato S, Natsume K, Clayton L, Musacchio A & Tanaka TU **2011** The Ndc80 loop region facilitates formation of kinetochore attachment to the dynamic microtubule plus end *Current biology : CB* 21: 207-13

May KM, Reynolds N, Cullen CF, Yanagida M & Ohkura H **2002** Polo boxes and Cut23 (Apc8) mediate an interaction between polo kinase and the anaphase-promoting complex for fission yeast mitosis *The Journal of cell biology* 156: 23-8

May KM & Hardwick KG **2006** The spindle checkpoint *J Cell Sci* 119: 4139-42

McCready SJ, Osman F & Yasui A **2000** Repair of UV damage in the fission yeast Schizosaccharomyces pombe *Mutation research* 451: 197-210

McCulley JL & Petes TD **2010** Chromosome rearrangements and aneuploidy in yeast strains lacking both Tel1p and Mec1p reflect deficiencies in two different mechanisms *Proc Natl Acad Sci U S A* 107: 11465-70

McSherry TD, Kitazono AA, Javaheri A, Kron SJ & Mueller PR **2007** Non-catalytic function for ATR in the checkpoint response *Cell Cycle* 6: 2019-30

Meadows JC, Shepperd LA, Vanoosthuyse V, Lancaster TC, Sochaj AM, Buttrick GJ, Hardwick KG & Millar JB **2011** Spindle checkpoint silencing requires association of PP1 to both Spc7 and kinesin-8 motors *Developmental cell* 20: 739-50

Meek DW **2004** The p53 response to DNA damage *DNA Repair (Amst)* 3: 1049-56

Meister P, Taddei A, Vernis L, Poidevin M, Gasser SM & Baldacci G **2005** Temporal separation of replication and recombination requires the intra-S checkpoint *The Journal of cell biology* 168: 537-44

Melo J & Toczyski D **2002** A unified view of the DNA-damage checkpoint *Curr Opin Cell Biol* 14: 237-45

Meraldi P, Draviam VM & Sorger PK **2004** Timing and checkpoints in the regulation of mitotic progression *Dev Cell* 7: 45-60

Meyer RE, Kim S, Obeso D, Straight PD, Winey M & Dawson DS **2013** Mps1 and Ipl1/Aurora B act sequentially to correctly orient chromosomes on the meiotic spindle of budding yeast *Science* 339: 1071-4

Michor F, Iwasa Y, Vogelstein B, Lengauer C & Nowak MA **2005** Can chromosomal instability initiate tumorigenesis? *Semin Cancer Biol* 15: 43-9

Miernyk JA & Thelen JJ **2008** Biochemical approaches for discovering protein-protein interactions *Plant J* 53: 597-609

Mikhailov A, Cole RW & Rieder CL **2002** DNA damage during mitosis in human cells delays the metaphase/anaphase transition via the spindle-assembly checkpoint *Curr Biol* 12: 1797-806

Millar JB & Russell P **1992** The cdc25 M-phase inducer: an unconventional protein phosphatase *Cell* 68: 407-10

Millband DN & Hardwick KG **2002** Fission yeast Mad3p is required for Mad2p to inhibit the anaphase-promoting complex and localizes to kinetochores in a Bub1p-, Bub3p-, and Mph1p-dependent manner *Mol Cell Biol* 22: 2728-42

Miller KM & Cooper JP **2003** The telomere protein Taz1 is required to prevent and repair genomic DNA breaks *Mol Cell* 11: 303-13

Miniowitz-Shemtov S, Eytan E, Ganoth D, Sitry-Shevah D, Dumin E & Hershko A **2012** Role of phosphorylation of Cdc20 in p31(comet)-stimulated disassembly of the mitotic checkpoint complex *Proceedings of the National Academy of Sciences of the United States of America* 109: 8056-60

Miranda JJ, King DS & Harrison SC **2007** Protein arms in the kinetochore-microtubule interface of the yeast DASH complex *Mol Biol Cell* 18: 2503-10

Mitchell JB, Thornton JM, Singh J & Price SL **1992** Towards an understanding of the arginine-aspartate interaction *Journal of molecular biology* 226: 251-62

Miura T, Yamana Y, Usui T, Ogawa HI, Yamamoto MT & Kusano K **2012** Homologous recombination via synthesis-dependent strand annealing in yeast requires the Irc20 and Srs2 DNA helicases *Genetics* 191: 65-78

Mochida S, Esashi F, Aono N, Tamai K, O'Connell MJ & Yanagida M **2004** Regulation of checkpoint kinases through dynamic interaction with Crb2 *The EMBO journal* 23: 418-28

Mogni ME, Costa A, Ioannou C & Bell SD **2009** The glutamate switch is present in all seven clades of AAA+ protein *Biochemistry* 48: 8774-5

Moreno S, Klar A & Nurse P **1991** Molecular genetic analysis of fission yeast Schizosaccharomyces pombe *Methods in enzymology* 194: 795-823

Morgan DO **2006** *The cell cycle : principles of control* New Science Press, London

Morris MC, Kaiser P, Rudyak S, Baskerville C, Watson MH & Reed SI **2003** Cks1-dependent proteasome recruitment and activation of CDC20 transcription in budding yeast *Nature* 423: 1009-13

Morrow CJ, Tighe A, Johnson VL, Scott MI, Ditchfield C & Taylor SS **2005** Bub1 and aurora B cooperate to maintain BubR1-mediated inhibition of APC/CCdc20 *J Cell Sci* 118: 3639-52

Moss J, Tinline-Purvis H, Walker CA, Folkes LK, Stratford MR, Hayles J, Hoe KL, Kim DU, Park HO, Kearsey SE, Fleck O, Holmberg C, Nielsen O & Humphrey TC **2010** Break-induced ATR and Ddb1-Cul4(Cdt)(2) ubiquitin ligase-dependent nucleotide synthesis promotes homologous recombination repair in fission yeast *Genes & development* 24: 2705-16

Motorin Y, Lyko F & Helm M **2010** 5-methylcytosine in RNA: detection, enzymatic formation and biological functions *Nucleic acids research* 38: 1415-30

Murray AW & Kirschner MW **1989** Dominoes and clocks: the union of two views of the cell cycle *Science* 246: 614-21

Murray AW, Solomon MJ & Kirschner MW **1989** The role of cyclin synthesis and degradation in the control of maturation promoting factor activity *Nature* 339: 280-6

Murray AW & Marks D **2001** Can sequencing shed light on cell cycling? *Nature* 409: 844-6

Murray JM & Carr AM **2008** Smc5/6: a link between DNA repair and unidirectional replication? *Nature reviews. Molecular cell biology* 9: 177-82

Nakamura TM, Du LL, Redon C & Russell P **2004** Histone H2A phosphorylation controls Crb2 recruitment at DNA breaks, maintains checkpoint arrest, and influences DNA repair in fission yeast *Molecular and cellular biology* 24: 6215-30

Nakano H & Omura S **2009** Chemical biology of natural indolocarbazole products: 30 years since the discovery of staurosporine *J Antibiot (Tokyo)* 62: 17-26

Nasmyth K **1999** Separating sister chromatids *Trends in biochemical sciences* 24: 98-104

Nestoras K, Mohammed AH, Schreurs AS, Fleck O, Watson AT, Poitelea M, O'Shea C, Chahwan C, Holmberg C, Kragelund BB, Nielsen O, Osborne M, Carr AM & Liu C **2010** Regulation of ribonucleotide reductase by Spd1 involves multiple mechanisms *Genes & development* 24: 1145-59

Newman JR, Wolf E & Kim PS **2000** A computationally directed screen identifying interacting coiled coils from Saccharomyces cerevisiae *Proc Natl Acad Sci U S A* 97: 13203-8

Nezi L & Musacchio A **2009** Sister chromatid tension and the spindle assembly checkpoint *Current opinion in cell biology* 21: 785-95

Niida H & Nakanishi M **2006** DNA damage checkpoints in mammals *Mutagenesis* 21: 3-9

Niikura Y, Ogi H, Kikuchi K & Kitagawa K **2010** BUB3 that dissociates from BUB1 activates caspase-independent mitotic death (CIMD) *Cell Death Differ* 17: 1011-24

Nijenhuis W, von Castelmur E, Littler D, De Marco V, Tromer E, Vleugel M, van Osch MH, Snel B, Perrakis A & Kops GJ **2013** A TPR domain-containing N-terminal module of MPS1 is required for its kinetochore localization by Aurora B *The Journal of cell biology* 201: 217-31

Nilsson J, Yekezare M, Minshull J & Pines J **2008** The APC/C maintains the spindle assembly checkpoint by targeting Cdc20 for destruction *Nat Cell Biol* 10: 1411-20

Nitta M, Kobayashi O, Honda S, Hirota T, Kuninaka S, Marumoto T, Ushio Y & Saya H **2004** Spindle checkpoint function is required for mitotic catastrophe induced by DNA-damaging agents *Oncogene* 23: 6548-58

Niwa O, Matsumoto T, Chikashige Y & Yanagida M **1989** Characterization of Schizosaccharomyces pombe minichromosome deletion derivatives and a functional allocation of their centromere *EMBO J* 8: 3045-52

Nurse P & Thuriaux P **1980** Regulatory genes controlling mitosis in the fission yeast Schizosaccharomyces pombe *Genetics* 96: 627-37

O'Connell MJ & Cimprich KA **2005** G2 damage checkpoints: what is the turn-on? *Journal of cell science* 118: 1-6

Ors A, Grimaldi M, Kimata Y, Wilkinson CR, Jones N & Yamano H **2009** The transcription factor Atf1 binds and activates the APC/C ubiquitin ligase in fission yeast *The Journal of biological chemistry* 284: 23989-94

Ouspenski, II, Elledge SJ & Brinkley BR **1999** New yeast genes important for chromosome integrity and segregation identified by dosage effects on genome stability *Nucleic Acids Res* 27: 3001-8

Overmeer RM, Gourdin AM, Giglia-Mari A, Kool H, Houtsmuller AB, Siegal G, Fousteri MI, Mullenders LH & Vermeulen W **2010** Replication factor C recruits DNA polymerase delta to sites of nucleotide excision repair but is not required for PCNA recruitment *Molecular and cellular biology* 30: 4828-39

Pan J & Chen RH **2004** Spindle checkpoint regulates Cdc20p stability in Saccharomyces cerevisiae *Genes Dev* 18: 1439-51

Pan X, Lei B, Zhou N, Feng B, Yao W, Zhao X, Yu Y & Lu H **2012** Identification of novel genes involved in DNA damage response by screening a genome-wide Schizosaccharomyces pombe deletion library *BMC Genomics* 13: 662

Pang B, McFaline JL, Burgis NE, Dong M, Taghizadeh K, Sullivan MR, Elmquist CE, Cunningham RP & Dedon PC **2012** Defects in purine nucleotide metabolism lead to substantial incorporation of xanthine and hypoxanthine into DNA and RNA *Proceedings of the National Academy of Sciences of the United States of America* 109: 2319-24

Passmore LA, Barford D & Harper JW **2005** Purification and assay of the budding yeast anaphase-promoting complex *Methods Enzymol* 398: 195-219

Patra D & Dunphy WG **1998** Xe-p9, a Xenopus Suc1/Cks protein, is essential for the Cdc2-dependent phosphorylation of the anaphase- promoting complex at mitosis *Genes Dev* 12: 2549-59

Pavletich NP **1999** Mechanisms of cyclin-dependent kinase regulation: structures of Cdks, their cyclin activators, and Cip and INK4 inhibitors *Journal of molecular biology* 287: 821-8

Peddibhotla S, Lam MH, Gonzalez-Rimbau M & Rosen JM **2009** The DNA-damage effector checkpoint kinase 1 is essential for chromosome segregation and cytokinesis *Proc Natl Acad Sci U S A* 106: 5159-64

Peng J, Elias JE, Thoreen CC, Licklider LJ & Gygi SP **2003** Evaluation of multidimensional chromatography coupled with tandem mass spectrometry (LC/LC-MS/MS) for large-scale protein analysis: the yeast proteome *J Proteome Res* 2: 43-50

Pereira G, Hofken T, Grindlay J, Manson C & Schiebel E **2000** The Bub2p spindle checkpoint links nuclear migration with mitotic exit *Mol Cell* 6: 1-10

Perillo B, Ombra MN, Bertoni A, Cuozzo C, Sacchetti S, Sasso A, Chiariotti L, Malorni A, Abbondanza C & Avvedimento EV **2008** DNA oxidation as triggered by H3K9me2 demethylation drives estrogen-induced gene expression *Science* 319: 202-6

Petermann E, Orta ML, Issaeva N, Schultz N & Helleday T **2010** Hydroxyurea-stalled replication forks become progressively inactivated and require two different RAD51-mediated pathways for restart and repair *Molecular cell* 37: 492-502

Peters JM **2002** The anaphase-promoting complex: proteolysis in mitosis and beyond *Mol Cell* 9: 931-43

Peters JM **2006** The anaphase promoting complex/cyclosome: a machine designed to destroy *Nat Rev Mol Cell Biol* 7: 644-56

Pfleger CM & Kirschner MW **2000** The KEN box: an APC recognition signal distinct from the D box targeted by Cdh1 *Genes Dev* 14: 655-65

Pfleger CM, Lee E & Kirschner MW **2001** Substrate recognition by the Cdc20 and Cdh1 components of the anaphase-promoting complex *Genes Dev* 15: 2396-407

Pines J & Rieder CL **2001** Re-staging mitosis: a contemporary view of mitotic progression *Nat Cell Biol* 3: E3-6

Pinsky BA, Kotwaliwale CV, Tatsutani SY, Breed CA & Biggins S **2006a** Glc7/protein phosphatase 1 regulatory subunits can oppose the Ipl1/aurora protein kinase by redistributing Glc7 *Mol Cell Biol* 26: 2648-60

Pinsky BA, Kung C, Shokat KM & Biggins S **2006b** The Ipl1-Aurora protein kinase activates the spindle checkpoint by creating unattached kinetochores *Nat Cell Biol* 8: 78-83

Poddar A, Stukenberg PT & Burke DJ **2005** Two complexes of spindle checkpoint proteins containing Cdc20 and Mad2 assemble during mitosis independently of the kinetochore in Saccharomyces cerevisiae *Eukaryot Cell* 4: 867-78

Pomerening JR, Sontag ED & Ferrell JE, Jr. **2003** Building a cell cycle oscillator: hysteresis and bistability in the activation of Cdc2 *Nat Cell Biol* 5: 346-51

Pommier Y, Redon C, Rao VA, Seiler JA, Sordet O, Takemura H, Antony S, Meng L, Liao Z, Kohlhagen G, Zhang H & Kohn KW **2003** Repair of and checkpoint response to topoisomerase I-mediated DNA damage *Mutat Res* 532: 173-203

Prag G, Misra S, Jones EA, Ghirlando R, Davies BA, Horazdovsky BF & Hurley JH **2003** Mechanism of ubiquitin recognition by the CUE domain of Vps9p *Cell* 113: 609-20

Privette LM, Weier JF, Nguyen HN, Yu X & Petty EM **2008** Loss of CHFR in human mammary epithelial cells causes genomic instability by disrupting the mitotic spindle assembly checkpoint *Neoplasia* 10: 643-52

Prudden J, Evans JS, Hussey SP, Deans B, O'Neill P, Thacker J & Humphrey T **2003** Pathway utilization in response to a site-specific DNA double-strand break in fission yeast *EMBO J* 22: 1419-30

Puddu F, Piergiovanni G, Plevani P & Muzi-Falconi M **2011** Sensing of replication stress and Mec1 activation act through two independent pathways involving the 9-1-1 complex and DNA polymerase epsilon *PLoS genetics* 7: e1002022

Qi W, Tang Z & Yu H **2006** Phosphorylation- and polo-box-dependent binding of Plk1 to Bub1 is required for the kinetochore localization of Plk1 *Molecular biology of the cell* 17: 3705-16

Qu M, Yang B, Tao L, Yates JR, 3rd, Russell P, Dong MQ & Du LL **2012** Phosphorylation-dependent interactions between Crb2 and Chk1 are essential for DNA damage checkpoint *PLoS genetics* 8: e1002817

Quevillon E, Silventoinen V, Pillai S, Harte N, Mulder N, Apweiler R & Lopez R **2005** InterProScan: protein domains identifier *Nucleic acids research* 33: W116-20

Quimby BB, Arnaoutov A & Dasso M **2005** Ran GTPase regulates Mad2 localization to the nuclear pore complex *Eukaryot Cell* 4: 274-80

Quinlan RA, Pogson CI & Gull K **1980** The influence of the microtubule inhibitor, methyl benzimidazol-2-yl-carbamate (MBC) on nuclear division and the cell cycle in Saccharomyces cerevisiae *Journal of cell science* 46: 341-52

Raji H & Hartsuiker E **2006** Double-strand break repair and homologous recombination in Schizosaccharomyces pombe *Yeast* 23: 963-76

Ramachandran S, Kota P, Ding F & Dokholyan NV **2011** Automated minimization of steric clashes in protein structures *Proteins* 79: 261-70

Rancati G, Crispo V, Lucchini G & Piatti S **2005** Mad3/BubR1 phosphorylation during spindle checkpoint activation depends on both Polo and Aurora kinases in budding yeast *Cell Cycle* 4: 972-80

Rao CV, Yang YM, Swamy MV, Liu T, Fang Y, Mahmood R, Jhanwar-Uniyal M & Dai W **2005** Colonic tumorigenesis in BubR1+/-ApcMin/+ compound mutant mice is linked to premature separation of sister chromatids and enhanced genomic instability *Proceedings of the National Academy of Sciences of the United States of America* 102: 4365-70

Rape M, Reddy SK & Kirschner MW **2006** The processivity of multiubiquitination by the APC determines the order of substrate degradation *Cell* 124: 89-103

Rappsilber J, Siniossoglou S, Hurt EC & Mann M **2000** A generic strategy to analyze the spatial organization of multi-protein complexes by cross-linking and mass spectrometry *Anal Chem* 72: 267-75

Rappsilber J, Ishihama Y & Mann M **2003** Stop and go extraction tips for matrix-assisted laser desorption/ionization, nanoelectrospray, and LC/MS sample pretreatment in proteomics *Analytical chemistry* 75: 663-70

Rappsilber J, Mann M & Ishihama Y **2007** Protocol for micro-purification, enrichment, pre-fractionation and storage of peptides for proteomics using StageTips *Nat Protoc* 2: 1896-906

Reddy SK, Rape M, Margansky WA & Kirschner MW **2007** Ubiquitination by the anaphase-promoting complex drives spindle checkpoint inactivation *Nature* 446: 921-5

Reichard P **1988** Interactions between deoxyribonucleotide and DNA synthesis *Annual review of biochemistry* 57: 349-74

Reinberg D & Sims RJ, 3rd **2006** de FACTo nucleosome dynamics *J Biol Chem* 281: 23297-301

Reinhardt HC, Cannell IG, Morandell S & Yaffe MB **2011** Is post-transcriptional stabilization, splicing and translation of selective mRNAs a key to the DNA damage response? *Cell Cycle* 10: 23-7

Resnick MA & Martin P **1976** The repair of double-strand breaks in the nuclear DNA of Saccharomyces cerevisiae and its genetic control *Molecular & general genetics : MGG* 143: 119-29

Revenko AS, Kalashnikova EV, Gemo AT, Zou JX & Chen HW **2010** Chromatin loading of E2F-MLL complex by cancer-associated coregulator ANCCA via reading a specific histone mark *Mol Cell Biol* 30: 5260-72

Rhind N, Furnari B & Russell P **1997** Cdc2 tyrosine phosphorylation is required for the DNA damage checkpoint in fission yeast *Genes & development* 11: 504-11

Rhind N & Russell P **2000** Chk1 and Cds1: linchpins of the DNA damage and replication checkpoint pathways *Journal of cell science* 113 (Pt 22): 3889-96

Rhind N, Chen Z, Yassour M, Thompson DA, Haas BJ, Habib N, Wapinski I, Roy S, Lin MF, Heiman DI, Young SK, Furuya K, Guo Y, Pidoux A, Chen HM, Robbertse B, Goldberg JM, Aoki K, Bayne EH, Berlin AM, Desjardins CA, Dobbs E, Dukaj L, Fan L, FitzGerald MG, French C, Gujja S, Hansen K, Keifenheim D, Levin JZ, Mosher RA, Muller CA, Pfiffner J, Priest M, Russ C, Smialowska A, Swoboda P, Sykes SM, Vaughn M, Vengrova S, Yoder R, Zeng Q, Allshire R, Baulcombe D, Birren BW, Brown W, Ekwall K, Kellis M, Leatherwood J, Levin H, Margalit H, Martienssen R, Nieduszynski CA, Spatafora JW, Friedman N, Dalgaard JZ, Baumann P, Niki H, Regev A & Nusbaum C **2011** Comparative functional genomics of the fission yeasts *Science* 332: 930-6

Rieder CL, Schultz A, Cole R & Sluder G **1994** Anaphase onset in vertebrate somatic cells is controlled by a checkpoint that monitors sister kinetochore attachment to the spindle *J Cell Biol* 127: 1301-10

Rieder CL, Cole RW, Khodjakov A & Sluder G **1995** The checkpoint delaying anaphase in response to chromosome monoorientation is mediated by an inhibitory signal produced by unattached kinetochores *J Cell Biol* 130: 941-8

Rieger KE & Chu G **2004** Portrait of transcriptional responses to ultraviolet and ionizing radiation in human cells *Nucleic acids research* 32: 4786-803

Rigaut G, Shevchenko A, Rutz B, Wilm M, Mann M & Seraphin B **1999** A generic protein purification method for protein complex characterization and proteome exploration *Nat Biotechnol* 17: 1030-2

Roberts BT, Farr KA & Hoyt MA **1994** The Saccharomyces cerevisiae checkpoint gene BUB1 encodes a novel protein kinase *Mol Cell Biol* 14: 8282-91

Robertson AB, Klungland A, Rognes T & Leiros I **2009** DNA repair in mammalian cells: Base excision repair: the long and short of it *Cellular and molecular life sciences : CMLS* 66: 981-93

Rodenas E, Gonzalez-Aguilera C, Ayuso C & Askjaer P **2012** Dissection of the NUP107 nuclear pore subcomplex reveals a novel interaction with spindle assembly checkpoint protein MAD1 in Caenorhabditis elegans *Molecular biology of the cell* 23: 930-44

Roy A, Kucukural A & Zhang Y **2010** I-TASSER: a unified platform for automated protein structure and function prediction *Nat Protoc* 5: 725-38

Royou A, Macias H & Sullivan W **2005** The Drosophila Grp/Chk1 DNA damage checkpoint controls entry into anaphase *Curr Biol* 15: 334-9

Rozier L, Guo Y, Peterson S, Sato M, Baer R, Gautier J & Mao Y **2013** The MRN-CtIP pathway is required for metaphase chromosome alignment *Molecular cell* 49: 1097-107

Ruan J, Li H, Chen Z, Coghlan A, Coin LJ, Guo Y, Heriche JK, Hu Y, Kristiansen K, Li R, Liu T, Moses A, Qin J, Vang S, Vilella AJ, Ureta-Vidal A, Bolund L, Wang J & Durbin R **2008** TreeFam: 2008 Update *Nucleic acids research* 36: D735-40

Rudner AD & Murray AW **2000** Phosphorylation by Cdc28 activates the Cdc20-dependent activity of the anaphase-promoting complex *J Cell Biol* 149: 1377-90

Russell P & Nurse P **1986a** cdc25+ functions as an inducer in the mitotic control of fission yeast *Cell* 45: 145-53

Russell P & Nurse P **1986b** Schizosaccharomyces pombe and Saccharomyces cerevisiae: a look at yeasts divided *Cell* 45: 781-2

Ryan SD, Britigan EM, Zasadil LM, Witte K, Audhya A, Roopra A & Weaver BA **2012** Up-regulation of the mitotic checkpoint component Mad1 causes chromosomal instability and resistance to microtubule poisons *Proceedings of the National Academy of Sciences of the United States of America* 109: E2205-14

Sabourin M & Zakian VA **2008** ATM-like kinases and regulation of telomerase: lessons from yeast and mammals *Trends in cell biology* 18: 337-46

Sadygov RG, Eng J, Durr E, Saraf A, McDonald H, MacCoss MJ & Yates JR, 3rd **2002** Code developments to improve the efficiency of automated MS/MS spectra interpretation *J Proteome Res* 1: 211-5

Saitoh S, Kobayashi Y, Ogiyama Y & Takahashi K **2008** Dual regulation of Mad2 localization on kinetochores by Bub1 and Dam1/DASH that ensure proper spindle interaction *Mol Biol Cell* 19: 3885-97

Saka Y, Esashi F, Matsusaka T, Mochida S & Yanagida M **1997** Damage and replication checkpoint control in fission yeast is ensured by interactions of Crb2, a protein with BRCT motif, with Cut5 and Chk1 *Genes & development* 11: 3387-400

Sancar A, Lindsey-Boltz LA, Unsal-Kacmaz K & Linn S **2004** Molecular mechanisms of mammalian DNA repair and the DNA damage checkpoints *Annu Rev Biochem* 73: 39-85

Sanchez-Perez I, Renwick SJ, Crawley K, Karig I, Buck V, Meadows JC, Franco-Sanchez A, Fleig U, Toda T & Millar JB **2005** The DASH complex and Klp5/Klp6 kinesin coordinate bipolar chromosome attachment in fission yeast *The EMBO journal* 24: 2931-43

Sanchez Y, Wong C, Thoma RS, Richman R, Wu Z, Piwnica-Worms H & Elledge SJ **1997** Conservation of the Chk1 checkpoint pathway in mammals: linkage of DNA damage to Cdk regulation through Cdc25 *Science* 277: 1497-501

Santocanale C & Diffley JF **1998** A Mec1- and Rad53-dependent checkpoint controls late-firing origins of DNA replication *Nature* 395: 615-8

Sarker AH, Tsutakawa SE, Kostek S, Ng C, Shin DS, Peris M, Campeau E, Tainer JA, Nogales E & Cooper PK **2005** Recognition of RNA polymerase II and transcription bubbles by XPG, CSB, and TFIIH: insights for transcription-coupled repair and Cockayne Syndrome *Molecular cell* 20: 187-98

Sawin KE & Tran PT **2006** Cytoplasmic microtubule organization in fission yeast *Yeast* 23: 1001-14

Sawin KE, Bicho CC & Snaith HA **2010** Inexpensive synthetic-based matrix for both conventional and rapid purification of protein A- and tandem affinity purification-tagged proteins *Analytical biochemistry* 397: 241-3

Saxena A, Saffery R, Wong LH, Kalitsis P & Choo KH **2002** Centromere proteins Cenpa, Cenpb, and Bub3 interact with poly(ADP-ribose) polymerase-1 protein and are poly(ADP-ribosyl)ated *J Biol Chem* 277: 26921-6

Schmidt M & Bastians H **2007** Mitotic drug targets and the development of novel anti-mitotic anticancer drugs *Drug Resist Updat* 10: 162-81

Schnall R, Mannhaupt G, Stucka R, Tauer R, Ehnle S, Schwarzlose C, Vetter I & Feldmann H **1994** Identification of a set of yeast genes coding for a novel family of putative ATPases with high similarity to constituents of the 26S protease complex *Yeast* 10: 1141-55

Schreiber A, Stengel F, Zhang Z, Enchev RI, Kong EH, Morris EP, Robinson CV, da Fonseca PC & Barford D **2011** Structural basis for the subunit assembly of the anaphase-promoting complex *Nature* 470: 227-32

Schulze JM, Wang AY & Kobor MS **2009** YEATS domain proteins: a diverse family with many links to chromatin modification and transcription *Biochem Cell Biol* 87: 65-75

Schulze JM, Kane CM & Ruiz-Manzano A **2010** The YEATS domain of Taf14 in Saccharomyces cerevisiae has a negative impact on cell growth *Mol Genet Genomics* 283: 365-80

Schuyler SC & Pellman D **2002** Analysis of the size and shape of protein complexes from yeast *Methods Enzymol* 351: 150-68

Schuyler SC & Murray AW **2009** An in vitro assay for Cdc20-dependent mitotic anaphase-promoting complex activity from budding yeast *Methods Mol Biol* 545: 271-85

Schwab MS, Roberts BT, Gross SD, Tunquist BJ, Taieb FE, Lewellyn AL & Maller JL **2001** Bub1 is activated by the protein kinase p90(Rsk) during Xenopus oocyte maturation *Current biology : CB* 11: 141-50

Scott KL & Plon SE **2003** Loss of Sin3/Rpd3 histone deacetylase restores the DNA damage response in checkpoint-deficient strains of Saccharomyces cerevisiae *Mol Cell Biol* 23: 4522-31

Scott RJ, Lusk CP, Dilworth DJ, Aitchison JD & Wozniak RW **2005** Interactions between Mad1p and the nuclear transport machinery in the yeast Saccharomyces cerevisiae *Mol Biol Cell* 16: 4362-74

Sczaniecka M, Feoktistova A, May KM, Chen JS, Blyth J, Gould KL & Hardwick KG **2008** The spindle checkpoint functions of Mad3 and Mad2 depend on a Mad3 KEN box-mediated interaction with Cdc20-APC/C *J Biol Chem*

Searle JS, Schollaert KL, Wilkins BJ & Sanchez Y **2004** The DNA damage checkpoint and PKA pathways converge on APC substrates and Cdc20 to regulate mitotic progression *Nat Cell Biol* 6: 138-45

Seeley TW, Wang L & Zhen JY **1999** Phosphorylation of human MAD1 by the BUB1 kinase in vitro *Biochem Biophys Res Commun* 257: 589-95

Shah JV, Botvinick E, Bonday Z, Furnari F, Berns M & Cleveland DW **2004** Dynamics of centromere and kinetochore proteins; implications for checkpoint signaling and silencing *Curr Biol* 14: 942-52

Shang C, Hazbun TR, Cheeseman IM, Aranda J, Fields S, Drubin DG & Barnes G **2003** Kinetochore protein interactions and their regulation by the Aurora kinase Ipl1p *Mol Biol Cell* 14: 3342-55

Shepperd LA, Meadows JC, Sochaj AM, Lancaster TC, Zou J, Buttrick GJ, Rappsilber J, Hardwick KG & Millar JB **2012** Phosphodependent recruitment of Bub1 and Bub3 to Spc7/KNL1 by Mph1 kinase maintains the spindle checkpoint *Current biology : CB* 22: 891-9

Shiloh Y **2003** ATM and related protein kinases: safeguarding genome integrity *Nat Rev Cancer* 3: 155-68

Sievers F, Wilm A, Dineen D, Gibson TJ, Karplus K, Li W, Lopez R, McWilliam H, Remmert M, Soding J, Thompson JD & Higgins DG **2011** Fast, scalable generation of high-quality protein multiple sequence alignments using Clustal Omega *Mol Syst Biol* 7: 539

Simonetta M, Manzoni R, Mosca R, Mapelli M, Massimiliano L, Vink M, Novak B, Musacchio A & Ciliberto A **2009** The influence of catalysis on mad2 activation dynamics *PLoS Biol* 7: e10

Sinz A **2006** Chemical cross-linking and mass spectrometry to map three-dimensional protein structures and protein-protein interactions *Mass Spectrom Rev* 25: 663-82

Sipiczki M **2000** Where does fission yeast sit on the tree of life? *Genome Biol* 1: REVIEWS1011

Sironi L, Mapelli M, Knapp S, De Antoni A, Jeang KT & Musacchio A **2002** Crystal structure of the tetrameric Mad1-Mad2 core complex: implications of a 'safety belt' binding mechanism for the spindle checkpoint *EMBO J* 21: 2496-506

Skoufias DA, Lacroix FB, Andreassen PR, Wilson L & Margolis RL **2004** Inhibition of DNA decatenation, but not DNA damage, arrests cells at metaphase *Mol Cell* 15: 977-90

Smith J, Tho LM, Xu N & Gillespie DA **2010** The ATM-Chk2 and ATR-Chk1 pathways in DNA damage signaling and cancer *Adv Cancer Res* 108: 73-112

Smits VA, Klompmaker R, Arnaud L, Rijksen G, Nigg EA & Medema RH **2000** Polo-like kinase-1 is a target of the DNA damage checkpoint *Nat Cell Biol* 2: 672-6

Smolka MB, Albuquerque CP, Chen SH, Schmidt KH, Wei XX, Kolodner RD & Zhou H **2005** Dynamic changes in protein-protein interaction and protein phosphorylation probed with amine-reactive isotope tag *Molecular & cellular proteomics : MCP* 4: 1358-69

Snider J & Houry WA **2008** AAA+ proteins: diversity in function, similarity in structure *Biochem Soc Trans* 36: 72-7

Snider J, Thibault G & Houry WA **2008** The AAA+ superfamily of functionally diverse proteins *Genome Biol* 9: 216

Solomon MJ, Glotzer M, Lee TH, Philippe M & Kirschner MW **1990** Cyclin activation of p34cdc2 *Cell* 63: 1013-24

Steen JA, Steen H, Georgi A, Parker K, Springer M, Kirchner M, Hamprecht F & Kirschner MW **2008** Different phosphorylation states of the anaphase promoting complex in response to antimitotic drugs: a quantitative proteomic analysis *Proc Natl Acad Sci U S A* 105: 6069-74

Stegmeier F, Rape M, Draviam VM, Nalepa G, Sowa ME, Ang XL, McDonald ER, 3rd, Li MZ, Hannon GJ, Sorger PK, Kirschner MW, Harper JW & Elledge SJ **2007** Anaphase initiation is regulated by antagonistic ubiquitination and deubiquitination activities *Nature* 446: 876-81

Stewart E & Enoch T **1996** S-phase and DNA-damage checkpoints: a tale of two yeasts *Current opinion in cell biology* 8: 781-7

Stolz A, Ertych N & Bastians H **2011** Tumor suppressor CHK2: regulator of DNA damage response and mediator of chromosomal stability *Clin Cancer Res* 17: 401-5

Studitsky VM, Kassavetis GA, Geiduschek EP & Felsenfeld G **1997** Mechanism of transcription through the nucleosome by eukaryotic RNA polymerase *Science* 278: 1960-3

Su TT **2006** Cellular responses to DNA damage: one signal, multiple choices *Annu Rev Genet* 40: 187-208

Sudakin V & Yen TJ **2004** Purification of the mitotic checkpoint complex, an inhibitor of the APC/C from HeLa cells *Methods Mol Biol* 281: 199-212

Sugimoto I, Murakami H, Tonami Y, Moriyama A & Nakanishi M **2004** DNA replication checkpoint control mediated by the spindle checkpoint protein Mad2p in fission yeast *J Biol Chem* 279: 47372-8

Suijkerbuijk SJ, van Osch MH, Bos FL, Hanks S, Rahman N & Kops GJ **2010** Molecular causes for BUBR1 dysfunction in the human cancer predisposition syndrome mosaic variegated aneuploidy *Cancer research* 70: 4891-900

Suijkerbuijk SJ, van Dam TJ, Karagoz GE, von Castelmur E, Hubner NC, Duarte AM, Vleugel M, Perrakis A, Rudiger SG, Snel B & Kops GJ **2012a** The vertebrate mitotic checkpoint protein BUBR1 is an unusual pseudokinase *Developmental cell* 22: 1321-9

Suijkerbuijk SJ, Vleugel M, Teixeira A & Kops GJ **2012b** Integration of Kinase and Phosphatase Activities by BUBR1 Ensures Formation of Stable Kinetochore-Microtubule Attachments *Developmental cell* 23: 745-55

Symington LS & Gautier J **2011** Double-strand break end resection and repair pathway choice *Annual review of genetics* 45: 247-71

Tabb DL, McDonald WH & Yates JR, 3rd **2002** DTASelect and Contrast: tools for assembling and comparing protein identifications from shotgun proteomics *J Proteome Res* 1: 21-6

Tackett AJ, Dilworth DJ, Davey MJ, O'Donnell M, Aitchison JD, Rout MP & Chait BT **2005** Proteomic and genomic characterization of chromatin complexes at a boundary *J Cell Biol* 169: 35-47

Tamm T, Grallert A, Grossman EP, Alvarez-Tabares I, Stevens FE & Hagan IM **2011** Brr6 drives the Schizosaccharomyces pombe spindle pole body nuclear envelope insertion/extrusion cycle *The Journal of cell biology* 195: 467-84

Tanaka K & Russell P **2004** Cds1 phosphorylation by Rad3-Rad26 kinase is mediated by forkhead-associated domain interaction with Mrc1 *The Journal of biological chemistry* 279: 32079-86

Tanaka K, Mukae N, Dewar H, van Breugel M, James EK, Prescott AR, Antony C & Tanaka TU **2005a** Molecular mechanisms of kinetochore capture by spindle microtubules *Nature* 434: 987-94

Tanaka TU **2005** Chromosome bi-orientation on the mitotic spindle *Philos Trans R Soc Lond B Biol Sci* 360: 581-9

Tanaka TU, Stark MJ & Tanaka K **2005b** Kinetochore capture and bi-orientation on the mitotic spindle *Nat Rev Mol Cell Biol* 6: 929-42

Tang J, Erikson RL & Liu X **2006** Checkpoint kinase 1 (Chk1) is required for mitotic progression through negative regulation of polo-like kinase 1 (Plk1) *Proc Natl Acad Sci U S A* 103: 11964-9

Tang Z, Coleman TR & Dunphy WG **1993a** Two distinct mechanisms for negative regulation of the Wee1 protein kinase *The EMBO journal* 12: 3427-36

Tang Z, Coleman TR & Dunphy WG **1993b** Two distinct mechanisms for negative regulation of the Wee1 protein kinase *EMBO J* 12: 3427-36

Tang Z, Shu H, Oncel D, Chen S & Yu H **2004** Phosphorylation of Cdc20 by Bub1 provides a catalytic mechanism for APC/C inhibition by the spindle checkpoint *Mol Cell* 16: 387-97

Tange Y & Niwa O **2008** Schizosaccharomyces pombe Bub3 Is Dispensable for Mitotic Arrest Following Perturbed Spindle Formation *Genetics* 179: 785-92

Taylor SS, Ha E & McKeon F **1998** The human homologue of Bub3 is required for kinetochore localization of Bub1 and a Mad3/Bub1-related protein kinase *J Cell Biol* 142: 1-11

Taylor SS, Hussein D, Wang Y, Elderkin S & Morrow CJ **2001** Kinetochore localisation and phosphorylation of the mitotic checkpoint components Bub1 and BubR1 are differentially regulated by spindle events in human cells *J Cell Sci* 114: 4385-95

Taylor SS, Scott MI & Holland AJ **2004** The spindle checkpoint: a quality control mechanism which ensures accurate chromosome segregation *Chromosome Res* 12: 599-616

Teichner A, Eytan E, Sitry-Shevah D, Miniowitz-Shemtov S, Dumin E, Gromis J & Hershko A **2011** p31comet promotes disassembly of the mitotic checkpoint complex in an ATP-dependent process *Proc Natl Acad Sci U S A* 108: 3187-92

Thebault P, Chirgadze DY, Dou Z, Blundell TL, Elowe S & Bolanos-Garcia VM **2012** Structural and functional insights into the role of the N-terminal Mps1 TPR domain in the spindle assembly checkpoint (SAC) *The Biochemical journal*

Tholander F & Sjoberg BM **2012** Discovery of antimicrobial ribonucleotide reductase inhibitors by screening in microwell format *Proceedings of the National Academy of Sciences of the United States of America* 109: 9798-803

Thron CD **1996** A model for a bistable biochemical trigger of mitosis *Biophys Chem* 57: 239-51

Thulasiraman V, Yang CF & Frydman J **1999** In vivo newly translated polypeptides are sequestered in a protected folding environment *EMBO J* 18: 85-95

Tomasini R, Tsuchihara K, Tsuda C, Lau SK, Wilhelm M, Ruffini A, Tsao MS, Iovanna JL, Jurisicova A, Melino G & Mak TW **2009** TAp73 regulates the spindle assembly checkpoint by modulating BubR1 activity *Proceedings of the National Academy of Sciences of the United States of America* 106: 797-802

Tooley J & Stukenberg PT **2011** The Ndc80 complex: integrating the kinetochore's many movements *Chromosome research : an international journal on the molecular, supramolecular and evolutionary aspects of chromosome biology* 19: 377-91

Toyoda Y & Yanagida M **2006** Coordinated requirements of human topo II and cohesin for metaphase centromere alignment under Mad2-dependent spindle checkpoint surveillance *Mol Biol Cell* 17: 2287-302

Tseng RJ, Armstrong KR, Wang X & Chamberlin HM **2007** The bromodomain protein LEX-1 acts with TAM-1 to modulate gene expression in C. elegans *Mol Genet Genomics* 278: 507-18

Tsukasaki K, Miller CW, Greenspun E, Eshaghian S, Kawabata H, Fujimoto T, Tomonaga M, Sawyers C, Said JW & Koeffler HP **2001** Mutations in the mitotic check point gene, MAD1L1, in human cancers *Oncogene* 20: 3301-5

Turner JJ, Ewald JC & Skotheim JM **2012** Cell size control in yeast *Current biology : CB* 22: R350-9

Tyson JJ & Novak B **2008** Temporal organization of the cell cycle *Curr Biol* 18: R759-R68

Ubersax JA, Woodbury EL, Quang PN, Paraz M, Blethrow JD, Shah K, Shokat KM & Morgan DO **2003** Targets of the cyclin-dependent kinase Cdk1 *Nature* 425: 859-64

Uchida KS, Takagaki K, Kumada K, Hirayama Y, Noda T & Hirota T **2009** Kinetochore stretching inactivates the spindle assembly checkpoint *J Cell Biol* 184: 383-90

Uetz P, Giot L, Cagney G, Mansfield TA, Judson RS, Knight JR, Lockshon D, Narayan V, Srinivasan M, Pochart P, Qureshi-Emili A, Li Y, Godwin B, Conover D, Kalbfleisch T, Vijayadamodar G, Yang M, Johnston M, Fields S & Rothberg JM **2000** A comprehensive analysis of protein-protein interactions in Saccharomyces cerevisiae *Nature* 403: 623-7

Uhlmann F **2003** Chromosome cohesion and separation: from men and molecules *Curr Biol* 13: R104-14

Umbreit NT, Gestaut DR, Tien JF, Vollmar BS, Gonen T, Asbury CL & Davis TN **2012** The Ndc80 kinetochore complex directly modulates microtubule dynamics *Proceedings of the National Academy of Sciences of the United States of America* 109: 16113-8

Uzawa S, Li F, Jin Y, McDonald KL, Braunfeld MB, Agard DA & Cande WZ **2004** Spindle pole body duplication in fission yeast occurs at the G1/S boundary but maturation is blocked until exit from S by an event downstream of cdc10+ *Mol Biol Cell* 15: 5219-30

Uzunova K, Dye BT, Schutz H, Ladurner R, Petzold G, Toyoda Y, Jarvis MA, Brown NG, Poser I, Novatchkova M, Mechtler K, Hyman AA, Stark H, Schulman BA & Peters JM **2012** APC15 mediates CDC20 autoubiquitylation by APC/C(MCC) and disassembly of the mitotic checkpoint complex *Nature structural & molecular biology*

van der Waal MS, Saurin AT, Vromans MJ, Vleugel M, Wurzenberger C, Gerlich DW, Medema RH, Kops GJ & Lens SM **2012** Mps1 promotes rapid centromere accumulation of Aurora B *EMBO reports* 13: 847-54

van Vugt MA, Smits VA, Klompmaker R & Medema RH **2001** Inhibition of Polo-like kinase-1 by DNA damage occurs in an ATM- or ATR-dependent fashion *J Biol Chem* 276: 41656-60

van Vugt MA & Medema RH **2005** Getting in and out of mitosis with Polo-like kinase-1 *Oncogene* 24: 2844-59

Vanoosthuyse V, Valsdottir R, Javerzat JP & Hardwick KG **2004** Kinetochore targeting of fission yeast Mad and Bub proteins is essential for spindle checkpoint function but not for all chromosome segregation roles of Bub1p *Mol Cell Biol* 24: 9786-801

Vanoosthuyse V & Hardwick KG **2009a** A novel protein phosphatase 1-dependent spindle checkpoint silencing mechanism *Curr Biol* 19: 1176-81

Vanoosthuyse V & Hardwick KG **2009b** Overcoming inhibition in the spindle checkpoint *Genes Dev* 23: 2799-805

Vanoosthuyse V, Meadows JC, van der Sar SJ, Millar JB & Hardwick KG **2009** Bub3p facilitates spindle checkpoint silencing in fission yeast *Mol Biol Cell* 20: 5096-105

Varetti G, Guida C, Santaguida S, Chiroli E & Musacchio A **2011** Homeostatic control of mitotic arrest *Molecular cell* 44: 710-20

Verdaasdonk JS, Gardner R, Stephens AD, Yeh E & Bloom K **2012** Tension-dependent nucleosome remodeling at the pericentromere in yeast *Molecular biology of the cell* 23: 2560-70

Vigneron S, Prieto S, Bernis C, Labbe JC, Castro A & Lorca T **2004** Kinetochore localization of spindle checkpoint proteins: who controls whom? *Mol Biol Cell* 15: 4584-96

Vink M, Simonetta M, Transidico P, Ferrari K, Mapelli M, De Antoni A, Massimiliano L, Ciliberto A, Faretta M, Salmon ED & Musacchio A **2006** In vitro FRAP identifies the minimal requirements for Mad2 kinetochore dynamics *Curr Biol* 16: 755-66

Visconti R, Palazzo L & Grieco D **2010** Requirement for proteolysis in spindle assembly checkpoint silencing *Cell Cycle* 9: 564-9

Visintin R, Prinz S & Amon A **1997** CDC20 and CDH1: a family of substrate-specific activators of APC-dependent proteolysis *Science* 278: 460-3

Vleugel M, Hoogendoorn E, Snel B & Kops GJ **2012** Evolution and function of the mitotic checkpoint *Developmental cell* 23: 239-50

Vodermaier HC **2004** APC/C and SCF: controlling each other and the cell cycle *Current biology : CB* 14: R787-96

Vogel C, Kienitz A, Hofmann I, Muller R & Bastians H **2004** Crosstalk of the mitotic spindle assembly checkpoint with p53 to prevent polyploidy *Oncogene* 23: 6845-53

Walworth N, Davey S & Beach D **1993** Fission yeast chk1 protein kinase links the rad checkpoint pathway to cdc2 *Nature* 363: 368-71

Wang HW, Long S, Ciferri C, Westermann S, Drubin D, Barnes G & Nogales E **2008** Architecture and flexibility of the yeast Ndc80 kinetochore complex *J Mol Biol* 383: 894-903

Wang Q, Liu T, Fang Y, Xie S, Huang X, Mahmood R, Ramaswamy G, Sakamoto KM, Darzynkiewicz Z, Xu M & Dai W **2004** BUBR1 deficiency results in abnormal megakaryopoiesis *Blood* 103: 1278-85

Wang X, Babu JR, Harden JM, Jablonski SA, Gazi MH, Lingle WL, de Groen PC, Yen TJ & van Deursen JM **2001** The mitotic checkpoint protein hBUB3 and the mRNA export factor hRAE1 interact with GLE2p-binding sequence (GLEBS)-containing proteins *J Biol Chem* 276: 26559-67

Warren CD, Brady DM, Johnston RC, Hanna JS, Hardwick KG & Spencer FA **2002** Distinct chromosome segregation roles for spindle checkpoint proteins *Mol Biol Cell* 13: 3029-41

Wassmann K, Liberal V & Benezra R **2003** Mad2 phosphorylation regulates its association with Mad1 and the APC/C *The EMBO journal* 22: 797-806

Waterhouse RM, Tegenfeldt F, Li J, Zdobnov EM & Kriventseva EV **2013** OrthoDB: a hierarchical catalog of animal, fungal and bacterial orthologs *Nucleic acids research* 41: D358-65

Waters JC, Chen RH, Murray AW & Salmon ED **1998** Localization of Mad2 to kinetochores depends on microtubule attachment, not tension *J Cell Biol* 141: 1181-91

Wei JH, Chou YF, Ou YH, Yeh YH, Tyan SW, Sun TP, Shen CY & Shieh SY **2005** TTK/hMps1 participates in the regulation of DNA damage checkpoint response by phosphorylating CHK2 on threonine 68 *J Biol Chem* 280: 7748-57

Wei R, Ngo B, Wu G & Lee WH **2011** Phosphorylation of the Ndc80 complex protein, HEC1, by Nek2 kinase modulates chromosome alignment and signaling of the spindle assembly checkpoint *Molecular biology of the cell* 22: 3584-94

Weinert TA & Hartwell LH **1988** The RAD9 gene controls the cell cycle response to DNA damage in Saccharomyces cerevisiae *Science* 241: 317-22

Weiss E & Winey M **1996** The Saccharomyces cerevisiae spindle pole body duplication gene MPS1 is part of a mitotic checkpoint *J Cell Biol* 132: 111-23

Welburn JP, Grishchuk EL, Backer CB, Wilson-Kubalek EM, Yates JR, 3rd & Cheeseman IM **2009** The human kinetochore Ska1 complex facilitates microtubule depolymerization-coupled motility *Dev Cell* 16: 374-85

Westermann S, Avila-Sakar A, Wang HW, Niederstrasser H, Wong J, Drubin DG, Nogales E & Barnes G **2005** Formation of a dynamic kinetochore- microtubule interface through assembly of the Dam1 ring complex *Molecular cell* 17: 277-90

Westhorpe FG, Tighe A, Lara-Gonzalez P & Taylor SS **2011** p31comet-mediated extraction of Mad2 from the MCC promotes efficient mitotic exit *Journal of cell science* 124: 3905-16

Willis N & Rhind N **2009** Regulation of DNA replication by the S-phase DNA damage checkpoint *Cell division* 4: 13

Willis N & Rhind N **2011** Studying G2 DNA damage checkpoints using the fission yeast Schizosaccharomyces pombe *Methods in molecular biology* 782: 1-12

Wilson KA & Stern DF **2008** NFBD1/MDC1, 53BP1 and BRCA1 have both redundant and unique roles in the ATM pathway *Cell Cycle* 7: 3584-94

Windecker H, Langegger M, Heinrich S & Hauf S **2009** Bub1 and Bub3 promote the conversion from monopolar to bipolar chromosome attachment independently of shugoshin *EMBO Rep* 10: 1022-8

Winey M, Goetsch L, Baum P & Byers B **1991** MPS1 and MPS2: novel yeast genes defining distinct steps of spindle pole body duplication *J Cell Biol* 114: 745-54

Winey M & O'Toole ET **2001** The spindle cycle in budding yeast *Nat Cell Biol* 3: E23-7

Wolthuis R, Clay-Farrace L, van Zon W, Yekezare M, Koop L, Ogink J, Medema R & Pines J **2008** Cdc20 and Cks direct the spindle checkpoint-independent destruction of cyclin A *Mol Cell* 30: 290-302

Wong J, Nakajima Y, Westermann S, Shang C, Kang JS, Goodner C, Houshmand P, Fields S, Chan CS, Drubin D, Barnes G & Hazbun T **2007** A protein interaction map of the mitotic spindle *Mol Biol Cell* 18: 3800-9

Wong OK & Fang G **2007** Cdk1 phosphorylation of BubR1 controls spindle checkpoint arrest and Plk1-mediated formation of the 3F3/2 epitope *J Cell Biol* 179: 611-7

Wood V, Harris MA, McDowall MD, Rutherford K, Vaughan BW, Staines DM, Aslett M, Lock A, Bahler J, Kersey PJ & Oliver SG **2012** PomBase: a comprehensive online resource for fission yeast *Nucleic acids research* 40: D695-9

Wu N & Yu H **2012** The Smc complexes in DNA damage response *Cell Biosci* 2: 5

Wyman C, Ristic D & Kanaar R **2004** Homologous recombination-mediated double-strand break repair *DNA Repair (Amst)* 3: 827-33

Xia G, Luo X, Habu T, Rizo J, Matsumoto T & Yu H **2004** Conformation-specific binding of p31(comet) antagonizes the function of Mad2 in the spindle checkpoint *EMBO J* 23: 3133-43

Yamagishi Y, Honda T, Tanno Y & Watanabe Y **2010** Two histone marks establish the inner centromere and chromosome bi-orientation *Science* 330: 239-43

Yamagishi Y, Yang CH, Tanno Y & Watanabe Y **2012** MPS1/Mph1 phosphorylates the kinetochore protein KNL1/Spc7 to recruit SAC components *Nature cell biology* 14: 746-52

Yamaguchi S, Decottignies A & Nurse P **2003** Function of Cdc2p-dependent Bub1p phosphorylation and Bub1p kinase activity in the mitotic and meiotic spindle checkpoint *EMBO J* 22: 1075-87

Yamamoto A, Guacci V & Koshland D **1996** Pds1p, an inhibitor of anaphase in budding yeast, plays a critical role in the APC and checkpoint pathway(s) *The Journal of cell biology* 133: 99-110

Yang C, Tang X, Guo X, Niikura Y, Kitagawa K, Cui K, Wong ST, Fu L & Xu B **2011** Aurora-B mediated ATM serine 1403 phosphorylation is required for mitotic ATM activation and the spindle checkpoint *Mol Cell* 44: 597-608

Yang C, Wang H, Xu Y, Brinkman KL, Ishiyama H, Wong ST & Xu B **2012** The kinetochore protein Bub1 participates in the DNA damage response *DNA Repair (Amst)* 11: 185-91

Yang M, Li B, Tomchick DR, Machius M, Rizo J, Yu H & Luo X **2007** p31comet blocks Mad2 activation through structural mimicry *Cell* 131: 744-55

Yang M, Li B, Liu CJ, Tomchick DR, Machius M, Rizo J, Yu H & Luo X **2008** Insights into mad2 regulation in the spindle checkpoint revealed by the crystal structure of the symmetric mad2 dimer *PLoS Biol* 6: e50

Yeh PC, Yeh CC, Chen YC & Juang YL **2012** RED, a spindle pole-associated protein, is required for kinetochore localization of MAD1, mitotic progression, and activation of the spindle assembly checkpoint *The Journal of biological chemistry* 287: 11704-16

Yeh YH, Huang YF, Lin TY & Shieh SY **2009** The cell cycle checkpoint kinase CHK2 mediates DNA damage-induced stabilization of TTK/hMps1 *Oncogene* 28: 1366-78

Yi C & He C **2013** DNA repair by reversal of DNA damage *Cold Spring Harb Perspect Biol* 5:

Yoon HJ, Feoktistova A, Wolfe BA, Jennings JL, Link AJ & Gould KL **2002** Proteomics analysis identifies new components of the fission and budding yeast anaphase-promoting complexes *Current biology : CB* 12: 2048-54

Yudkovsky Y, Shteinberg M, Listovsky T, Brandeis M & Hershko A **2000** Phosphorylation of Cdc20/fizzy negatively regulates the mammalian cyclosome/APC in the mitotic checkpoint *Biochem Biophys Res Commun* 271: 299-304

Zachariae W & Nasmyth K **1999** Whose end is destruction: cell division and the anaphase-promoting complex *Genes Dev* 13: 2039-58

Zachos G, Black EJ, Walker M, Scott MT, Vagnarelli P, Earnshaw WC & Gillespie DA **2007** Chk1 is required for spindle checkpoint function *Dev Cell* 12: 247-60

Zakian VA **1995** ATM-related genes: what do they tell us about functions of the human gene? *Cell* 82: 685-7

Zeisig DT, Bittner CB, Zeisig BB, Garcia-Cuellar MP, Hess JL & Slany RK **2005** The eleven-nineteen-leukemia protein ENL connects nuclear MLL fusion partners with chromatin *Oncogene* 24: 5525-32

Zeng X, Sigoillot F, Gaur S, Choi S, Pfaff KL, Oh DC, Hathaway N, Dimova N, Cuny GD & King RW **2010** Pharmacologic inhibition of the anaphase-promoting complex induces a spindle checkpoint-dependent mitotic arrest in the absence of spindle damage *Cancer Cell* 18: 382-95

Zhang H & Lawrence CW **2005** The error-free component of the RAD6/RAD18 DNA damage tolerance pathway of budding yeast employs sister-strand recombination *Proceedings of the National Academy of Sciences of the United States of America* 102: 15954-9

Zhang T, Nirantar S, Lim HH, Sinha I & Surana U **2009** DNA damage checkpoint maintains CDH1 in an active state to inhibit anaphase progression *Dev Cell* 17: 541-51

Zhang X & Wigley DB **2008** The 'glutamate switch' provides a link between ATPase activity and ligand binding in AAA+ proteins *Nat Struct Mol Biol* 15: 1223-7

Zhang X, Ling Y, Wang W, Zhang Y, Ma Q, Tan P, Song T, Wei C, Li P, Liu X, Ma RZ, Zhong H, Cao C & Xu Q **2013** UV-C irradiation delays mitotic progression by recruiting Mps1 to kinetochores *Cell Cycle* 12:

Zhang Z, Yang J, Kong EH, Chao WC, Morris EP, da Fonseca PC & Barford D **2012** Recombinant expression, reconstitution and structure of human Anaphase Promoting Complex (APC/C) *The Biochemical journal*

Zhao Y & Chen RH **2006** Mps1 phosphorylation by MAP kinase is required for kinetochore localization of spindle-checkpoint proteins *Curr Biol* 16: 1764-9

Zich J & Hardwick KG **2010** Getting down to the phosphorylated 'nuts and bolts' of spindle checkpoint signalling *Trends Biochem Sci* 35: 18-27

Zich J, Sochaj AM, Syred HM, Milne L, Cook AG, Ohkura H, Rappsilber J & Hardwick KG **2012** Kinase activity of fission yeast Mph1 is required for Mad2 and Mad3 to stably bind the anaphase promoting complex *Current biology : CB* 22: 296-301

Zou JX, Revenko AS, Li LB, Gemo AT & Chen HW **2007** ANCCA, an estrogen-regulated AAA+ ATPase coactivator for ERalpha, is required for coregulator occupancy and chromatin modification *Proc Natl Acad Sci U S A* 104: 18067-72

Zou JX, Guo L, Revenko AS, Tepper CG, Gemo AT, Kung HJ & Chen HW **2009** Androgen-induced coactivator ANCCA mediates specific androgen receptor signaling in prostate cancer *Cancer Res* 69: 3339-46

Zou L & Elledge SJ **2003** Sensing DNA damage through ATRIP recognition of RPA-ssDNA complexes *Science* 300: 1542-8

Zunder RM & Rine J **2012** Direct Interplay among Histones, Histone Chaperones, and a Chromatin Boundary Protein in the Control of Histone Gene Expression *Molecular and cellular biology* 32: 4337-49